Characterisation of Vascular Dysfunction in a Murine Model of Rheumatoid Arthritis

A thesis submitted in candidature for the degree of Doctor of Philosophy

By

Jessica Olivia Williams

September 2016

Infection and Immunity

School of Medicine

Cardiff University

Cardiff

CF14 4XN

Table of Contents

Publications Arising

Exacerbated inflammatory arthritis in response to hyperactive gp130 signaling is independent of IL-17A. G W Jones, C J Greenhill, **J O Williams**, M A Nowell, A S Williams, B J Jenkins, S A Jones; Ann Rheum Dis doi:10.1136/annrheumdis-2013-203771

Death Receptor 3 (TNFRSF25) Increases Mineral Apposition by Osteoblasts and Region Specific New Bone Formation in the Axial Skeleton of Male DBA/1 Mice. F L. Collins, **J O. Williams**, A C. Bloom, M D. Stone, E Choy, E C. Y. Wang and A S. Williams; J Immunol Res. 2015; 2015: 901679

Characterisation of Death Receptor 3 dependent aortic changes during inflammatory arthritis **J O Williams**, E C Y. Wang, D Lang, A S Williams; Pharmacology Research and Perspectives, *2016* doi: 10.1002/prp2.240

CCL3 and MMP-9 are Downstream Effectors of DR3/TL1A Pathway-Dependent Osteoclast Function and Systemic Bone Loss. F L Collins, **J O Williams**, A C Bloom, L Jordan, M D Stone, E Choy, L R McCabe, E C Y Wang and A S Williams. *Accepted Bone January 2017*

Prizes Presentations and Posters

I have had many opportunities to present my data on both a University, National and International scale during my PhD project:

Poster Presentation "*Death Receptor 3 Drives Vascular Dysfunction in a Murine Model of Rheumatoid Arthritis*" at the American College of Rheumatology Annual Meeting, Boston; November 2014.

Prize Winning Poster Presentation "*Death Receptor 3 Drives Vascular Dysfunction in a Murine Model of Rheumatoid Arthritis*" at Cardiff University Post Graduate Research Day, January 2015.

Oral Presentation "*Chronic mCIA Drives Dysregulation of Collagen and Elastin Fibres within the Aortic Vessel Wall*", at the British Society of Matrix Biology annual meeting, Chester, April 2016.

List of Tables

List of Figures

Abbreviations

ADRF – Adipocyte Derived Relaxing Factor

AIM2- Absent in Melanoma 2

AIA – Antigen Induced Arthritis

ATF4-Activating Transcription Factor 2

CFA – Complete Freunds Adjuvant

CRP – C Reactive Protein

CV- Cardiovascular

CVD – Cardiovascular Disease

DR3 – Death Receptor 3

$DR3^{-/-}$- Death Receptor 3 Knock Out

DR3 WT – Death Receptor 3 Wild Type

ECM- Extracellular Matrix

EDTA- Ethylenediaminetetraacetic acid

ESR – Erythrocyte Sedimentation Rate

H&E- Haematoxylin and Eosin

I.D – Intradermal

IFNϒ- Interferon Gamma

IL-1 – Interleukin 1

IL-6 – Interleukin 6

IL-8 – Interleukin 8

Interleukin 12 – IL-12

IL-18 – Interleukin 18

mBSA- Methylated Bovine Serum Albumin

mCIA- Murine Collagen Induced Arthritis

MGP- Matrix GLA Protein

mM – MilliMolar

MMP - Matrix Metalloproteinase

mN – MilliNewtons

NF-κβ – Nuclear Factor κβ

NLR – Nod like Receptors/ Nucleotide Binding Domain, Leucine Rich Repeat Containing Protein

NO-Nitric Oxide

OPG -Osteoprotegerin

OPN- Osteopontin

OSX-Osterix

PBS- Phosphate Buffered Saline

PVAT – Perivascular Fat

RA – Rheumatoid Arthritis

RANK – Receptor Activator NF-κβ

RANKL- Receptor Activator NF-κβ ligand

RT-qPCR – Real Time Quantitative Polymerase Chain Reaction

RQ- Relative Quantification

RUNX2 – Runt Related Transcription Factor 2

TBS- Tris Buffered Saline

TIMP- Tissue Inhibitor of Metalloproteinase

TL1A – TNF like Protein 1A

TNF-α – Tumour Necrosis Factor α

TRADD-TNFR1 Associated Death Domain

TRAP- Tartate Resistant Acid Phosphatase

Vascular Adhesion Molecule 1 – VCAM1

VSMCs – Vascular Smooth Muscle Cells

WT- Wild Type

5-HT- Serotonin

Acknowledgements

The work carried out in this thesis would not have been possible without the help, support and guidance of numerous people in both the Tenovus building and Wales Heart Research Institute, whom I would like to thank, as well as the financial support from The British Heart Foundation.

Firstly, I would like to deeply thank my supervisors, Dr Derek Lang and Dr Anwen Williams. Your support in finding me a PhD project, your patience, your guidance has been greatly appreciated and has made me the scientist I am today. Thank you for being my work mum and dad! Special thanks also go to Eddie Wang for your unquestionable help during my DR3 work. Also, Gareth Jones for your hands on advice, letting me pick your brain and always being there when things weren't going quite right!

I'd like to thank my friends here in the Tenovus building, your popping in and questionably long lunch breaks have definitely helped! To Lauren, Katie, Ruth, Charlie, Rav, Anne and Saydul, without you it just wouldn't have been the same! Thanks for all your love, gossip and laughs over the last 3 years, you've always managed to put the smile back on my face and for that I will be forever grateful. Special thanks to my PhD sister Lauren, for being there from day 1, we did it girl!

Special thanks to all of my family. Mum, Dad, Elaine for your unconditional support and love, for picking me up and never letting me give up and for always trying to help even though you don't really know what I do. To my friends at home who always help me to see the bigger picture and remind me how to relax now and again, thank you for the distractions. Your WhatsApp messages have kept me going!

To Ryan, thank you for your love, for always being there and having faith in me, the little things in life have helped me through. And finally, Ella and Sienna, thank you for being my little rays of sunshine, you've made it all worthwhile!

Candidate's Declaration

This work has not been submitted in substance for any other degree or award at this or any other university or place of learning, nor is being submitted concurrently in candidature for any degree or other award.

Signed …… (Jessica Williams) Date ……

STATEMENT 1

This thesis is being submitted in partial fulfillment of the requirements for the degree of PhD

Signed …… (Jessica Williams) Date ……

STATEMENT 2

This thesis is the result of my own independent work/investigation, except where otherwise stated.

Other sources are acknowledged by explicit references. The views expressed are my own.

Signed …… (Jessica Williams) Date ……

STATEMENT 3

I hereby give consent for my thesis, if accepted, to be available for photocopying and for inter-library loan, and for the title and summary to be made available to outside organisations.

Signed …… (Jessica Williams) Date ……

STATEMENT 4

I hereby give consent for my thesis, if accepted, to be available for photocopying and for inter-library loans **after expiry of a bar on access previously approved by the Academic Standards & Quality Committee.**

Signed …… (Jessica Williams) Date ……

Abstract

Background

RA patients have an increased prevalence of CVD independently of traditional risk factors. Studies using a mouse model of inflammatory arthritis – mCIA have shown decreased vascular constriction response of the thoracic aorta to 5HT, associated with increased MMP-9 production. The source of the latter, inflammatory content and impact on the structural proteins of the vessel wall remains elusive.

Methods

Myography was used to determine vascular constriction response in mCIA animals. Immunohistochemistry determined presence of F4/80+ macrophages, Ly6G+ neutrophils, DR3 and MMP-9. DR3 was assessed in the healthy and arthritic constriction response using $DR3^{-/-}$ and DR3WTs. Vascular calcification was determined in short and long term mCIA using RT-qPCR. Protein levels were quantified using immunohistochemistry. Collagen and elastin were determined using Van Geisson and Ver Hoeffs staining. The role of the AIM2 inflammasome in mCIA associated vascular dysfunction was also determined using CRID3 therapy.

Results

Increased macrophages with complimentary DR3 staining were observed in the aorta and PVAT.$DR3^{-/-}$ had normal constriction response despite increased cells and MMP-9 in the PVAT. DR3 ablation decreased arthritis onset and severity, however, worsened the vascular function. DR3 PVAT was protective to the constriction response. Calcification mediators remained constant following the onset of mCIA. Long term mCIA showed exciting trends of increase to calcification mediators. Collagen and elastin both become deregulated during mCIA and showed a fibrosis like phenotype. Blocking the AIM2 inflammasome had no impact on mCIA onset but partially restored vascular constriction response.

Discussion

Systemic inflammation is key in explaining the vascular dysfunction associated with the mCIA model. mCIA allows us to determine very early changes in the vasculature associated with systemic inflammation as opposed to long term changes. Macrophages specifically are early inflammatory cells implicated in the aorta and are associated with both DR3 and AIM2, suggesting them as key players contributing to vascular dysfunction in this model. Successful AIM2 blocking therapy has potential to be used in human RA patients to reduce CV co-morbidity.

Chapter 1 – General Introduction

This general introduction provides an overview of the main topics explored during this thesis. Each subsequent results chapter is accompanied by its own in depth introduction to the appropriate pathways and mediators under investigation.

1.1 Rheumatoid Arthritis

Rheumatoid Arthritis (RA) is a common, chronic, inflammation-driven auto immune disease. It is the second most common type of arthritis, the most common inflammatory joint disease and affects 1% of the world's population (Firestein, 2002), equating to approximately 400,000 people in the UK. RA impacts approximately three times more women than men, and while it is thought of as a disease of the aging population, in 80% of cases initial onset occurs between the ages of 35 and 60 (Kavanaugh and Lipsky, 1996). The health related quality of life for RA patients is significantly reduced by the burden of chronic joint pain, persistent synovitis, swelling, fatigue and decline in bodily function. Importantly RA is also associated with systemic inflammation and the production of auto-antibodies, commonly rheumatoid factor and anti-citrullinated proteins (Scott *et al*, 2010). Despite some cases of RA being mild and self-limiting, many patients experience severe joint destruction, physical disability and multiple co-morbidities (Plenge, 2009). It is therefore no surprise that RA is a huge burden to the economy, costing the UK approximately £8 billion per year (NRAS, 2010), with current mortality rates at twice that of the general population (Kelly *et al*, 2007). Existing treatment options focus on the symptoms of RA and do not focus on disease progression or symptom reversal. In reality they largely slow down the onset of RA, thus promoting remission.

1.1.1 RA pathogenesis

Longitudinal studies have assessed the pathogenesis of RA and suggest it to be a serious, long term disease with dominant features, limited treatment options and poor outcomes (Scott *et al*, 1987). RA is a polyarthritis, initiating primarily in the small joints of the hands and feet, often presenting as morning stiffness (Suresh, 2004). A healthy synovial joint has a synovial membrane that coats the joint capsule and produces synovial fluid to lubricate the joint. The initial onset of joint damage begins at the synovial membrane where synovitis is driven by the local activation and recruitment of primary immune cells including; T and B cells, macrophages, mast cells and dendritic cells. Consequently, the synovial membrane thickens due to increased cellular populations and eventually becomes hyperplasic (Smolen and Steiner, 2003). During this time an osteoclast (cells that break down bone) rich region of the synovial membrane forms the pannus and eventually leads to pathological bone erosion. At the same time inflammatory cells such as neutrophils, along with synoviocytes and chondrocytes secrete enzymes capable of degrading cartilage into the joint cavity (Smolen and Steiner,

2003). These changes create severe pain and ultimately disability for the RA patient (Figure 1.1). Many of the RA cohort also experience extra-articular manifestations and recent data suggest that in the first four years following a rheumatoid diagnosis 47.5% of patients are affected by at least one of these (Hochberg *et al*, 2008). The most common included; rheumatoid nodules, vasculitis, pericarditis, uveitis and rheumatoid lung disease, while other studies have also shown the increased prevalence of systemic manifestations such as anaemia, cardiovascular disease (CVD), fatigue and depression (Hochberg *et al*, 2008).

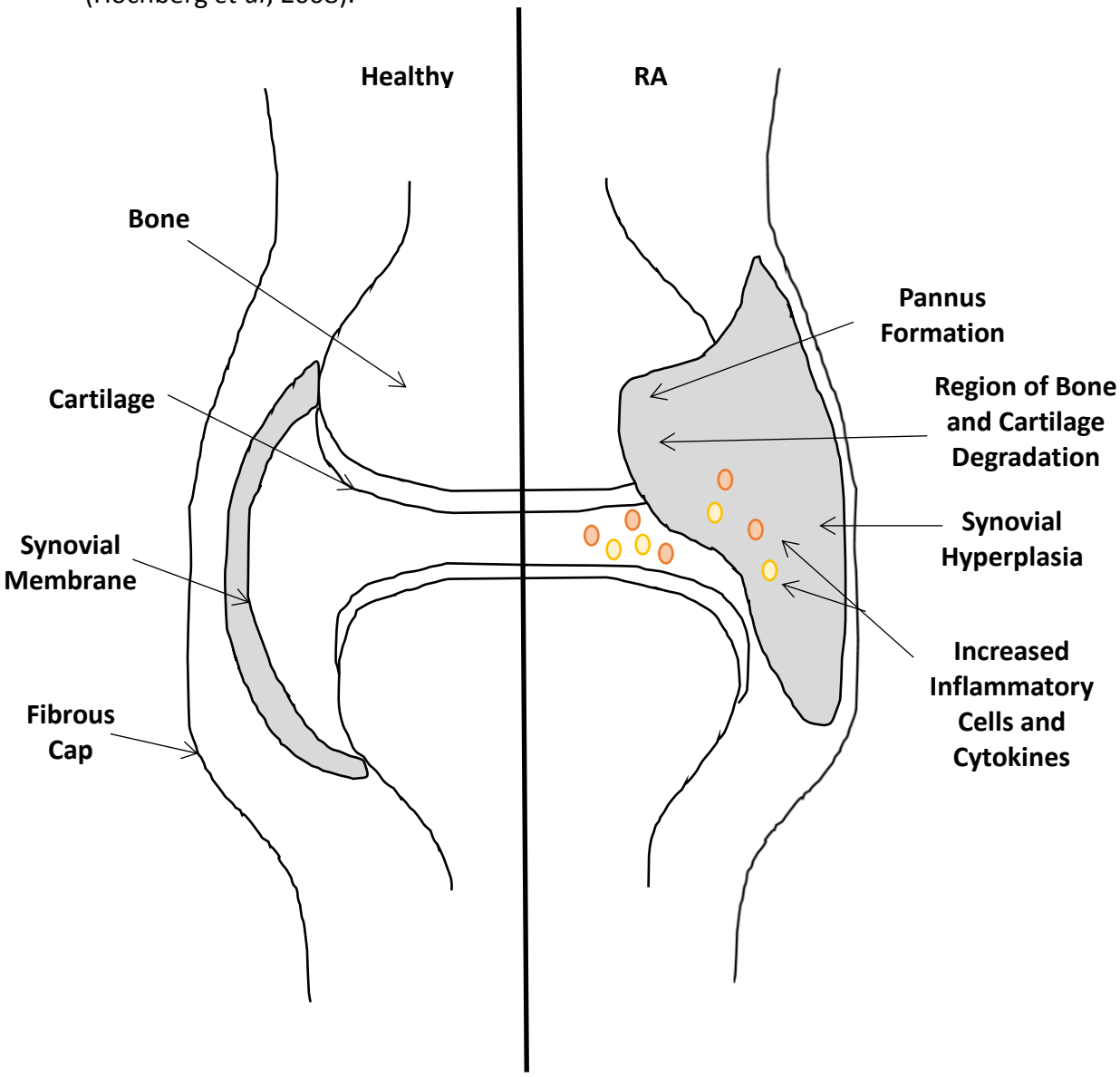

Figure 1.1 – The pathogenesis of RA – The healthy joint is compared with the arthritic joint. During arthritis common pathological features present including: pannus formation, synovial hyperplasia, increased trafficking of immune cells and production of their cytokines. This ultimately leads to the destruction of cartilage and bone.

1.2 RA and CVD – The Associated Co-Morbidity

Currently CVD is the leading cause of death worldwide (WHO, 2016). In 2012, CVD accounted for over 30% of all deaths, approximately 17.5 million people in one year. The biggest killer of all CVDs is coronary heart disease, closely followed by stroke. Alarmingly, the majority of CV deaths are preventable. This is caused by the common association of CVD with traditional risk factors. Activities such as smoking, unhealthy diet, obesity and physical inactivity are all behaviours likely to increase the risk of heart disease (WHO, 2016). The impact of such unhealthy activities can often be determined by high blood pressure, high lipid profile, high blood glucose and body mass index. Changes to these behaviours such as stopping smoking or treatment of high blood pressure have been positively shown to reduce CV risk. It is imperative that health policies drive a healthy lifestyle in the population in order to reduce overall CV risk.

CVD is a common co-morbidity experienced by RA patients. In fact, CVD has now been identified as the leading cause of mortality in this cohort, accounting for almost 40% of all deaths. RA patients have a twofold greater risk of CVD, rising to threefold with over ten years of disease, than someone of the general population (Solomon *et al*, 2006). This represents a similarly elevated risk experienced by individuals with diabetes mellitus (Peters *et al*, 2009). Importantly, increased risk in affected individuals remains unexplained and is not associated with the traditional CV risk factors, such as age, gender and smoking status. The only currently known association with risk factors in this cohort is that a lower body mass index is associated with increased mortality. This is likely explained by individuals with more severe arthritis experiencing a higher inflammatory burden and thus a higher cytokine -mediated catabolic state leading to weight loss (Escalante *et al*, 2005). Interestingly, in some patients CVD is evident often before the RA diagnosis, possibly due to the long diagnosis time often seen in rheumatoid clinics (Iafolla, 2013). That patients can have increased systemic levels of inflammation, as dictated by their C-reactive protein and Erythrocyte Sedimentation Rate, before the onset of articular symptoms is very relevant to the early presentation of CVD.

As traditional risk factors are not the driving force for increasing CV risk in RA patients, a number of studies have been conducted to determine the underlying mechanisms. The majority of these have focused on the role of a systemically increased inflammatory profile. Particularly relevant to rheumatoid joint pathology are the cytokines, including Tumour Necrosis Factor-α (TNF-α), Interleukin-1 (IL-1) and Interleukin-6 (IL-6) that are detectable systemically. The latter means that these signalling proteins have the potential to affect the normal function and homeostasis of many tissues including adipose tissue, skeletal muscle, liver and more specifically regarding CVD, the wider vasculature (Sattar *et al*, 2003). It is therefore imperative that the earliest changes in the vasculature system during RA are examined. This will identify the priming events and factors driving cardiovascular (CV) dysfunction in this disease.

1.3 Normal Vascular Function

The cardiovascular system comprises of the heart and vasculature. The latter is a complex network of vessels responsible for the delivery of oxygen and nutrients around the body whilst removing waste products. Importantly it also acts as a trafficking system for inflammatory cells and cytokines, critical to auto immune disease pathology. Normal artery structure comprises of a three-layered wall, encompassing the tunica intima, the thick elastin and muscle cell layer the tunica media and the outer most tunica adventitia (see Figure 1.2) with an endothelium lining the lumen of the vessel.

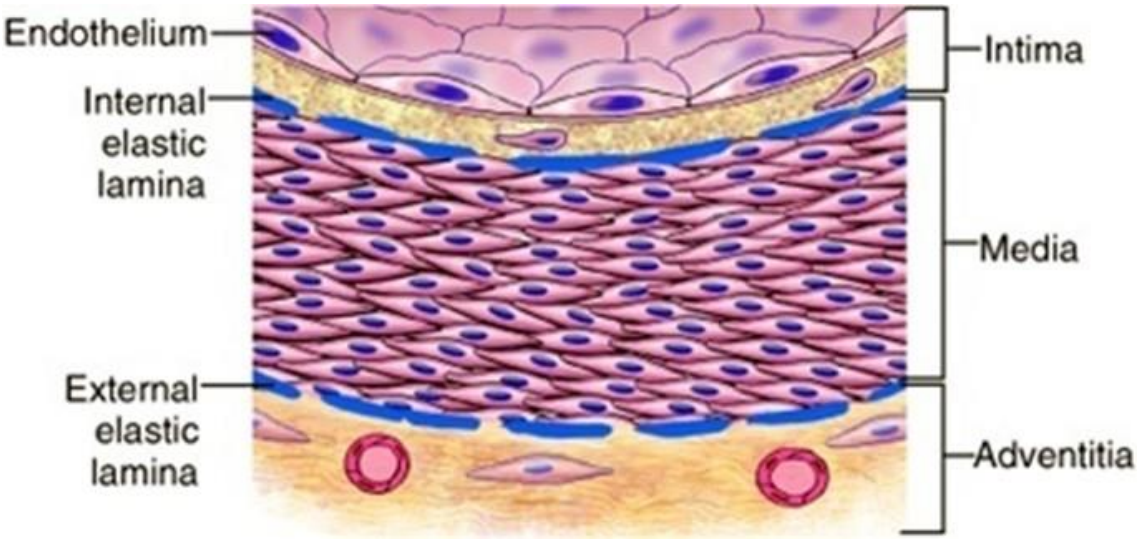

Figure 1.2 – The Arterial Vessel Wall (Shawky, 2015). The normal vessel wall is lined by an endothelial layer in contact with the lumen of the vessel. The vessel wall is made up of three layers, inner most the tunica intima, the middle tunica media containing both internal and external elastic lamina and the outermost tunica adventitia.

Nitric oxide (NO) and cyclic guanosine monophosphate (cGMP) and are key mediators in vasorelaxation. An extensive body of evidence has shown that NO produced by the endothelium is involved in both normal and pathological blood pressure regulation (for review see Nava and Llorens, 2016). Stimulation of soluble guanylate cyclase by endothelium-derived NO causes an increase in cGMP within the vascular smooth muscle. Subsequent activation of cGMP-dependent protein kinase (PKG) then mediates the actions of NO to lower vascular tone and maintain a healthy vasculature (Sausbier et al, 2000).

The healthy vascular constriction response is well documented (for review see Benoit and Taylor, 1997). Briefly, the binding of agonists such as, angiotensin II, norepinephrine and serotonin to their appropriate membrane bound receptors activates phospholipase C. This leads to an increase in inositol trisphosphate production, and the release of calcium from the sarcoplasmic reticulum. The increase in intracellular calcium then

mediates a pathway of processes, including further influx of extracellular calcium, and leads to vascular smooth muscle contraction.

1.4 Perivascular Adipose Tissue

PVAT surrounds all blood vessels and is thought to increase in line with an individual's adiposity (Lehman *et al*, 2010). It is continuous with the adventitial layer of the blood vessel wall (Chatterjee *et al*, 2009), demonstrating the potential cross talk between the two entities and that PVAT may play an important role in normal and diseased vascular function. This tissue was historically considered to only play a mechanical support role in the vascular system, acting as a scaffold to support the vessel itself. However, more recently the PVAT has emerged as a metabolically active organ, capable of producing many signalling moieties that have important effects on the vasculature (Szasz and Webb, 2012). For example, active hormones and cytokines, collectively termed adipokines, are now thought to be essential for normal vascular function (Chatterjee *et al*, 2009). These mediators were first discovered following the incidental observation that rat vascular constriction responses in isolated tissues were reduced in the presence of PVAT (Soltis and Cassis, 1991). This adipocyte-derived relaxing factor (ADRF) was later shown to be transferable and independent of NO release (Lohn *et al* 2002). The ability of PVAT to produce such factors in close proximity to the vessel wall shows how important it is in both health and disease.

The makeup of PVAT is also important when determining its function, and this is dependent on the type of vessel that the PVAT surrounds. For example, smaller resistance vessels are surrounded by PVAT that is predominantly made up of white adipocytes (Gao, 2007). Conversely, larger vessels are surrounded by a mixture of both brown and white adipocytes (Gao, 2007). Whether changes to these cell types occur in the face of inflammation is an interesting question.

Importantly, roles for PVAT in the pathology of cardiovascular disease (CVD) are emerging (Lee *et al*, 2013). Recent studies have demonstrated an increase in PVAT-derived adipokines in human stenotic arteries (Verhagen *et al*, 2014). Moreover, the Framingham heart study has shown that increased amounts of thoracic PVAT are positively correlated with a higher prevalence of CVD. What contribution PVAT makes to the vascular dysfunction seen in RA is unknown. An animal model would provide an ideal tool to investigate this further.

1.5 Vascular Calcification

Interestingly, it would appear that the majority of the over 60s population have some type of calcium deposit within their major arteries (Allison *et al*, 2004). With regards to the aetiology of CVD, the propensity of arteries to quite literally turn to bone is a major issue. These calcium deposits are harmful in many ways to CV health and affect homeostasis within the vessel itself. Ultimately, the presence of mineral deposits increases morbidity and mortality (Wayhs *et al*, 2002). The main outcomes of calcium

deposits within the major arteries include; hypertension, congestive heart failure and compromised structural integrity. Over the years the description of vascular calcification has changed dramatically. Originally it was considered to be both passive and degenerative; however, recently it has been described as an active process with many similarities to bone formation (Mizobuchi *et al*, 2009).

1.5.1 Vascular Calcification in RA

A condition widely recognised as a complication in renal disease (Moe and Chen, 2008), early onset and diffuse vascular calcification is now clearly associated with RA (Paccou *et al*, 2012). However, the pathogenesis driving this increased risk is poorly understood despite many potential explanations in the literature. Recent studies have shown that coronary artery calcification is significantly higher in men than women with RA (Giles *et al,* 2009), although both male and female RA patients had increased coronary artery calcification in comparison to a "normal" population. Moreover, it has also been shown that prevalence and extent of coronary artery calcification is associated with worsened RA severity at all ages (Giles *et al* 2009). Notably the biggest difference between RA patients and "normals" occurred in the youngest age category (Giles *et al* 2009). This suggests that vascular calcification could well be a significant issue for a young RA population in the absence of traditional risk factors for CVD.

Vascular calcification in RA patients is not specific to one region, though its prevalence would seem to be higher in the aorta in comparison to other sites such as the coronary and carotid arteries (Wang *et al,* 2009). Conversely, in age-matched non-RA, the highest levels are seen within the coronary artery (Wang et al, 2009). This highlights the aorta as a potential early region of calcification, and suggests that RA-associated increased systemic inflammation may contribute to the differences described (Wang *et al*, 2009).

1.5.2 Importance of Vascular Smooth Muscle Cells and Phenotypic Switching.

Vascular smooth muscle cells (VSMCs) are crucial cells within the vascular wall and have been deemed the main cellular determinant of arterial wall pathology (Lacolley *et al*, 2012). Due to the VSMC association with myosin and actin interactions they are crucial within the vasoconstriction response. This implicated them in the regulation of blood pressure and blood flow. Phenotypically VSMCs differ dependent on their location within the arterial tree (Michel *et al*, 2012). However, they also differ depending on their organ microenvironment and can react to changes therein. The role of VSMCs also goes beyond the vascular constriction response and they are now recognized to play a role in the synthesis and secretion of extracellular matrix, comprising the vessel wall (Forsyth *et al*, 1997). As a consequence of their constant exposure to circulating plasma molecules, over time VSMCs can become damaged (Michel *et al*, 2012). Indeed, they can respond in a number of ways to their local environment, including undergoing

apoptosis, and perhaps more interesting, modification of their phenotype. During pathological conditions the plasticity of VSMC is key and broad changes in phenotypes between migratory, proliferative, synthetic, endocytic, phagocytic or osteoblastic can occur (Lacolley *et al*, 2012). Hypertension, as an example can both directly, via blood pressure and indirectly by sheer flow influence the VSMC phenotype. Ultimately in this circumstance the change in VSMC phenotype leads to increased rigidity in the vessel wall (Michel *et al*, 2012). Similar effects are seen during aging.

1.5.3 VSMC Switching and Vascular Calcification

As described above ectopic vascular calcifications constitute a huge risk to life. The current underlying mechanisms by which this occurs is not well defined and therefore potential lifesaving treatments are few and far between. One possible mechanism, the prospect of VSMC to calcify, has been described in depth in the literature. It has been suggested that medial calcification is a process with many similarities to bone mineralization and is caused by VSMCs that have switched to an osteoblastic-like phenotype (Persy and D'Haese, 2009). The expression of bone transcription factors within the vasculature suggests that the differentiation of VSMCs to osteogenic phenotype is similar to that differentiation seen in osteoblasts (Bostrom *et al*, 1993). However, the exact mechanism underlying this transition remains unknown.

1.6 Matrix Metalloproteinases

Gelatinases are proteolytic enzymes that catalyse the breakdown of gelatin. In humans, the gelatinases are matrix metalloproteinases 2 and 9 (MMP-2/MMP-9). The majority of MMPs, including MMP-2 and MMP-9, are produced as pro-enzymes and require proteolytic cleavage via a proteinase enzyme in order to be activated (Woessner, 1991). The enzymes within the MMP family are highly conserved and share similar characteristics including mode of activation, amino acid sequences and regulation by tissue inhibitors of metalloproteinases (TIMPs) (Edwards *et al*, 1996). They are involved in the breakdown of the extracellular matrix, and as such are important in vascular remodelling and cellular migration. This process occurs during normal tissue homeostasis, for example in embryonic development, but also happens during diseases such as cancer metastasis and arthritis.

1.6.1 MMP-9 Association with RA

An associated between MMP-9 and RA has been well documented. Indeed, RA patients are characterised by elevated serum and synovial fluid MMP-9 levels in comparison with

healthy controls (Gruber *et al*, 1998). Furthermore, immunohistochemistry has identified MMP-9 expression in synovial specimens, and particularly associated with both fibroblasts and macrophages within vascular walls (Gruber *et al*, 1998). More recently, the role of MMP-9 in RA progression has been highlighted. When MMP-9 was supressed in isolated RA synovial fibroblasts, concurrent decreases were seen in key cytokines such as IL-1β, IL-6, IL-8 and TNF-α (Xue *et al*, 2014). Importantly, the inhibition of MMP-9 was also associated with decreased RA synovial fibroblast-mediated cartilage degradation (Xue *et al*, 2014). A further study has identified pro-MMP-9 expression by both monocytes-macrophages and neutrophils, and indeed osteoclasts within the lining of the rheumatoid joint (Seki *et al*, 1997). Whether there is a role for the MMP's in RA-associated CVD is less clear.

1.6.2 MMP-9 Association with CVD

Increasing evidence demonstrates that MMPs have pathology-associated effects within the vasculature that have now been shown to involve both the endothelium and VSMCs (Chen *et al*, 2013). In healthy tissue MMP production and activation is tightly controlled at the level of transcription, post-translational proteolytic activation and by the presence of TIMPs (Brew and Nagase, 2010). It is in fact the balance between active MMPs and TIMPs that determine the role of MMPs in the vasculature, a switch in favour of MMPs being likely to drive pathological changes (Raffetto and Khalil, 2008).

MMP-9 is one of the most widely investigated MMPs in CVD. It acts to degrade the ECM and activate both cytokines and chemokines, and as such plays a key role in pathological remodelling during both inflammation and fibrosis. Indeed, both the deletion and inhibition of MMP-9 has proven to be therapeutically beneficial in CVD (Yabluchanskiy *et al*, 2013). A previous study published by our group suggested a role for MMP-9 in the contractile dysfunction phenotype observed in a mouse model of inflammatory arthritis (Reynolds *et al*, 2012). However, the source of the increased MMP-9 in this model has not been identified. Such information is imperative should this gelatinase be considered as a therapeutic agent in RA-associated CVD.

1.7 Death Receptors

Death Receptors are essential in tissue homeostasis as they are key regulators of both cell death and cell survival. However, recent studies have highlighted the importance of the death receptor family beyond these roles. The signalling from death receptors is now considered dynamic and further studies are required to determine the alternative consequences of death receptor signalling.

1.7.1. Death Receptor Superfamily

Death receptors are members of the tumour necrosis factor (TNF) superfamily and are characterised by the presence of a highly conserved 80 amino acid cytoplasmic region known as a “death domain” (Guicciardi and Gores, 2009). This death domain is required to initiate apoptosis and allows the binding of specific ligands (Nagata, 1997). The latter are defined by the presence of up to six cysteine rich domains and are capable of driving cytotoxic pathways (Guicciardi and Gores, 2009). All members of the death receptor family are type 1 transmembrane proteins, and all have an intracellular C terminal domain, a membrane spanning region and an extracellular N terminal domain (Guicciardi and Gores, 2009).

The ligands that bind to the death receptors are complementary cytokines that also belong to the TNF family. The majority of these “death ligands” are type 2 transmembrane proteins comprising of an intracellular N terminus, membrane spanning region and extracellular C terminus domain (Guicciardi and Gores, 2009). Importantly, not all of the death ligands are membrane bound, some following proteolytic cleavage become soluble. However, it has been reported that these soluble forms are less potent in comparison to their membrane-bound counterparts. (Schneider *et al*, 1998)

Death receptors have a general initiation pathway that is similar throughout the family, and includes three main steps. Firstly, an appropriate ligand binds to the membrane-bound portion and mediates trimerization of the receptor. This leads to the recruitment of adaptor proteins, allowing the initiation of a caspase complex. Consequently, initiator caspase 8 and 10 drive the formation of effector caspase complexes, including caspases 3, 6 and 7 (Guicciardi and Gores, 2009). Conversely, more recent studies have shown the capability of death receptor activation to mediate non-cytotoxic pathways via the activation of nuclear factor- κβ (NF-κβ) and mitogen-activated protein kinases (Migone *et al*, 2002). However, the roles of such signalling pathways are yet to be determined.

1.7.2. DR3

Death Receptor 3 (DR3) has been shown to play a major role in immunity, inflammation and inflammatory disease, being implicated in many auto-immune diseases including RA (Wang *et al*, 2014). It was discovered in 1996 by various groups of researchers and was originally known by different names, including Apo3, LARD, TR3, TRAMP and WSL-1 (Kitson *et al*, 1996; Chinnaiyan *et al*, 1996; Marsters *et al*, 1996). The wide variety of DR3-mediated roles that have now been identified suggest that in fact driving apoptosis is a minor part of the puzzle, rather DR3 having more significant actions in cell survival, expansion and differentiation (Wang, 2012).

DR3 has close sequence homology to TNF superfamily member TNF Receptor 1 and is predominantly expressed on lymphocytes such as T cells (Aiba and Nakamura, 2013), B cells (Cavallini *et al*, 2013) and Natural Killer cells (Screaton *et al*, 1997). More recently expression has also been identified on osteoblasts (Borysenko *et al*, 2006), macrophages

(McLaren *et al,* 2012), fibroblasts (Ge *et al*, 2011) and possibly adipocytes (GeneCards.com). That DR3 expression on both osteoblasts and macrophages is associated with vascular inflammation (Borysenko *et al*, 2006; McLaren *et al*, 2010), further investigations regarding its role in vascular inflammation associated with inflammatory arthritis is of great interest. The impact of such DR3 ligand binding and pathway activations will be further discussed in chapter 3 of this thesis.

1.8. The Inflammasome

Inflammasomes are a broad group of initiating proteins that act as innate immune system receptors and sensors and ultimately control the activation of caspase-1 as part of the host inflammatory response (Vladimer *et al*, 2013). Importantly they have recently been implicated in immune diseases and their mechanisms of action have been well characterised (Shaw *et al*, 2011). As a consequence of this increased attention, a number of potential therapeutics have been developed with a high potential for use in a number of currently poorly treated diseases (Guo *et al*, 2015).

A number of pattern recognition receptors are involved in the initiation of inflammasome complexing. These include "nucleotide binding domain, leucine-rich repeat containing proteins" (NOD-like Receptors, NLRs) and "absent in melanoma 2-like receptors" (AIM2) (Takeuchi and Akira, 2010). Depending on the stimuli, the appropriate receptor oligomerizes allowing the recruitment and activation of pro-caspase-1 (Netea *et al*, 2015). Further downstream caspase-1 is able to trigger cytokines pro-interleukin-1 and pro-interleukin-18 into their active forms interleukin-1 (IL-1) and interleukin-18 (IL-18) respectivel (Netea *et al*, 2015). Ultimately the activation of any inflammasome leads to a specific type of cell death known as pyroptosis (Guo *et al,* 2015).

1.8.1 The AIM2 Inflammasome

The AIM2 inflammasome will be a particular focus in this thesis, firstly regarding a role in RA-associated CVD and secondly its potential as a therapeutic target.

AIM2 is unique within the inflammasome family. The first major difference between AIM2 and other inflammasomes, such as NLRs, is that AIM2 is IFN-inducible (Burckstrummer et al, 2009). Both IFNβ and IFNϒ have been shown to upregulate AIM2 activation and this is important given that IFNϒ is a key cytokine implicated in the progression of RA. Secondly the composition of AIM2 is also different in that it has a pyrin (PYD) domain and a hematopoietic interferon-inducible nuclear antigen with 200 amino acid repeats (HIN200) domain (Guo et al, 2015). These have key functions that aid the activation of the AIM2 pathway; in particular HIN-200 being involved in the recruitment of the AIM2 substrate, cytosolic double stranded DNA (Hornung et al, 2009). The presence of HIN-200 makes AIM2 the only inflammasome complex that is able to directly bind its substrate. The HIN-200 domain recognises double stranded DNA that is over 80 amino acids in length, but independently of its specific amino acid sequence (Jin

et al, 2012). On DNA binding PYD domain is displaced and allows the recruitment of adapter protein apoptosis speck containing protein (ASC) (Hornung et al, 2009). The latter is common to all inflammasome pathways and is the recruitment protein for inactive zymogram pro-caspase-1. The interaction of ASC and AIM2 triggers the assembly of a large protein containing mulitmers of ASC dimers (Fernandes-Alnemri et al, 2007). Upon the recruitment of pro-caspase 1 it is able to self-cleave and form the active heterotetrameric caspase 1. When caspase 1 is proteolytically active, it cleaves a number of inactive proteins, including pro-IL-1β and pro-IL18 into their active forms (Thornberry et al, 1992).

The AIM2 inflammasome is active mainly in macrophages following host infection. Within these cells a caspase-1 mediated inflammatory response is initiated and results ultimately in macrophage cell death (Burckstrummer et al, 2009). The production and activation of pro-inflammatory cytokines IL1 and IL18 within the macrophage are also cruicial for innate immunity. This shows the importance of AIM2 in clearing bacterial infections within the host. However, inappropriate recognition of cytoplasmic self-DNA by the AIM2 complex can contribute to a number of auto immune diseases. Inappropriate AIM2 activation has been linked with the development of psoriasis, dermatitis, systemic lupus, inflammatory bowel disease, and importantly for this study, arthritis (Man et al, 2016). Under normal circumstances, DNA is contained within the cell nucleus or mitochondria. It is when host DNA appears in the cytosol, for example from impairment of DNA degradation or clearance that inflammation is initiated (Dombrowski et al, 2011).

1.9 Animal Models of RA

To investigate the nature of CV pathology caused by inflammatory arthritis, *in vivo* animal models are essential, particularly with regard to the very earliest changes. This is not possible in human patients due to obvious ethical issues and the fact that the varied time before diagnosis often means the critical early time points are missed. Animal models of inflammatory autoimmune arthritis have proved to be invaluable in the study of RA pathogenesis and potential therapeutics. As such there are several well established mouse models that are in routine use, namely Antigen or Collagen-induced arthritis, Streplococcal cell wall arthritis, Oil-induced arthritis, or spontaneous models such as the TNF-α transgenic mouse and the K/BxN T-cell Receptor transgenic mouse (Brand, 2007).

The transgenic models of RA were developed and established many years ago. For example, the TNF-α transgenic mouse expresses both wild-type and 3'-modified human TNF-α and is a chronic model where mice develop erosive poly arthritis (Keffer *et al*, 1991). Importantly it has aided the understanding of TNF-α's role in RA progression and been intrinsically involved in the establishment of anti-TNF-α treatment in humans (Asquith *et al*, 2009).

Antigen-Induced Arthritis (AIA) is another commonly used model of inflammatory arthritis that can be initiated in a variety of animal species, including mice (Brackertz *et*

al, 1977), rabbits (Henderson *et al*, 1991) and guinea pigs (Bendele, 2001). In particular mouse models of AIA have been extensively used to study the biology of many cytokines in disease pathogenesis (Oshima *et al*, 1998). Regardless of the species, the protocol of induction in AIA is standard, comprising of two subcutaneous injections of methylated bovine serum albumin (m-BSA) a week apart. This antigen traffics to the joint where it binds to negatively charged cartilage. Subsequently m-BSA is injected intra-articullarly into the knee joint (Van der Berg *et al*, 2007) and provides an acute inflammatory reaction leading to rapid joint destruction. One benefit of the AIA model is that disease only impacts the local knee joint, so the contralateral can be used as an internal control. However, despite the disease locally showing similar pathological joint changes, RA is a systemic disease and this is not mirrored in this model. For this reason, the systemic murine collagen-induced arthritis (mCIA) model now represents the gold standard for arthritis research and is discussed in more detail below.

1.10 mCIA

Whilst all the above described mouse models of RA have advantages and disadvantages for research, the mCIA model is both reproducible and well defined, and is now the most commonly used (Brand, 2007). It is induced via intradermal injections of an emulsion containing type II collagen and complete Freund's adjuvant (CFA). Importantly this model shares many pathological features with human RA and its main target, type II collagen is a major constituent of cartilage. Similarities between mCIA and RA include characteristic pathological hallmarks such as synovial hyperplasia, mononuclear cell infiltration, cartilage degradation and the potential to express specific MHC class II genes (Brand, 2007). However, there are some phenotypic features of mCIA that differ to RA. These include the absence of Rheumatoid Factor, little sex bias between male and female mice and the fact that mCIA is a monophasic disease in comparison to the relapsing and remitting phases seen in RA. A further advantage of mCIA over the other antigen-induced protocol is the short time frame of approximately 7 days between immunization and disease manifestation. The mCIA model has been used extensively allowing the identification of common inflammatory cells and their mediators that drive disease pathology and indeed potential therapeutics.

1.10.1 Susceptibility

Induction of mCIA in DBA/1 mice is often quoted as the gold standard model for researching RA. The main reason for this is due to the DBA/1's susceptibility to mCIA, with arthritis incidence falling between 80 and 100%. Susceptibility to mCIA is strongly related to the major histocompatibility complex (Wooley *et al*, 1981). However, more recently studies have shown that several mouse genotypes are also susceptible to mCIA

and can be used successfully in the study of RA. These mice are known as HLA-DR models and have established transgenic expression of the HLA-DR1 or DR4 class II genes. Data show that the DR molecules are necessary for mCIA susceptibility and are involved some way in the immune response to collagen II.

1.10.2 Pathogenesis

An orchestrated response of both B and T cells to type II collagen II underlies the pathology of mCIA. The B-cell populations produce anti-Collagen II antibodies (Terato *et al*, 1992), the significance of which is starkly evidenced by the fact that B-cell deficient mice are protected from mCIA onset (Svensson *et al*, 1998). While T-cells are also instrumental in the production of anti-Collagen II antibodies, they also play a secondary role in the joint where they can induce activation of other inflammatory cells, such as macrophages (Kinne *et al*, 2000). A number of cytokines are also involved in the progression of mCIA, and these include IFN-Ɣ, TNF-α, IL-6, IL-12, IL-17 and IL-22 (Lubberts and van der berg, 2000). Interestingly some of these agents are involved in pro-inflammatory disease progression, while others act in an anti-inflammatory manor (McInnes and Schett, 2007). The differentiation of naïve T-cells allows the production of IL-1β, TNF-α, IL-6, RANKL, MMPs and chemokines that are vital in both local and systemic inflammation (Billiau and Matthys, 2011). The role of some of these mediators will be discussed later in this thesis and their role within vascular dysfunction during mCIA will be investigated.

1.11 Project Summary

In RA patients the increased prevalence of CVD is apparent and studies suggest that the CVD predictors are present in this cohort prior to RA diagnosis. Few studies exist that examine the early changes in the RA vasculature meaning the underlying mechanisms of the RA-associated vascular pathology remain elusive. mCIA was therefore chosen as an appropriate murine model of inflammatory arthritis, as it has distinct advantages enabling the very earliest vascular changes to be examined. Although a dysfunctional vascular contractile phenotype has been previously observed in the mCIA model (Reynolds *et al*, 2012), the underlying mechanism(s) of this pathology remain unclear. While the systemic inflammation associated with RA is thought to contribute, the inflammatory context of the arthritic blood vessel remains unknown.

DR3 has been implicated in many inflammatory disorders and specifically linked with both RA and vascular disease. However, no study has investigated the role of DR3 in vascular dysfunction in mCIA or the RA patient cohort. As a consequence of its expression profile, and previously reported associated with inflammatory disease, the potential for DR3 to play an important role in the interplay between RA and CVD is highly likely. For the first time in this thesis the role of DR3 in both the healthy and arthritic constriction responses to serotonin in isolated tissues, and its impact on the inflammatory context of the thoracic aorta, are reported. As an adjunct to these studies, the onset of vascular calcification will also be determined.

Since RA is a bone-associated condition, it is postulated that decreased bone formation in the joints and increased bone metabolism may drive ectopic calcification of the vasculature. Finally, due to the association of calcification systemic inflammation, inflammatory activation pathways will also be discussed. The AIM2 inflammasome has previously been implicated in vascular disease and here a relationship with vascular dysfunction will be examined. The therapeutic potential of inhibiting these inflammatory pathways will also be analysed later in this thesis.

1.12 Hypothesis, Aim and Objectives

Data reported within this thesis will answer the hypothesis that vascular dysfunction in mCIA occurs in a DR3-dependent manor and is driven by increased inflammasome activation which may contribute to aortic calcification. The hypothesis was investigated using the following aim; to determine the role of systemic inflammation associated with inflammatory arthritis in driving cardiovascular pathology and to postulate potential mechanisms responsible for vascular dysfunction in a murine model of inflammatory arthritis. This aim will be achieved using the following five objectives:

1. To determine the inflammatory context of the thoracic aorta during mCIA and to analyse the relationship between inflammation and vascular dysfunction in this model.

2. To analyse the role of DR3 in both the healthy and arthritic vascular constriction response.

3. To investigate whether vascular calcification is initiated in the mCIA model, potentially explaining the apparent dysfunction observed.

4. To establish the relationship between time with mCIA and vascular calcification onset.

5. To mechanistically evaluate increased AIM2 inflammasome activation in the thoracic aorta during mCIA and to determine the therapeutic potential of inhibiting AIM2 activation in terms of inflammatory arthritis and vascular dysfunction.

Chapter 2 – Characterisation of the Vascular Constriction Response in Arthritic Thoracic Aortae.

2.1 Introduction

RA patients have high levels of systemic inflammation, as reflected by increased C Reactive Protein (CRP) and Erythrocyte Sedimentation Rate (ESR) (Rashid *et al*, 2007). This high inflammatory burden can often affect regions outside of the joints and causes damage, for example to the vasculature. The extent of this issue means that clinical arthritis is now associated with a double in risk of heart attack and stroke, compared with the general population (Mayo Clinic Study, 2013). Despite this co-morbidity being well recognized, few studies have investigated the early impact of systemic inflammation on the normal function of the vasculature.

Investigating the effect of systemic inflammation upon vascular function is challenging and experiments of this nature are difficult, if not impossible, to conduct in humans or indeed in human tissues. It is for this reason that the gold standard animal model for inflammatory arthritis –mCIA was employed in this project. Previous studies using mCIA showed decreased vascular constriction response by thoracic aorta to cumulative concentrations of 5-Hydroxytriptamine (5-HT) following arthritis induction (Reynolds *et al*, 2012). Reynolds *et al* showed no effect on endothelium-dependent relaxation responses which suggested that the constriction impairment was due to a change in the contractile phenotype of the aorta. Here for the first time, the inflammatory profile of the thoracic aorta was examined. The main cell types present in control and arthritic vasculature and surrounding PVAT were determined. In doing so, the aim was to achieve insight cellular and molecular characteristics of the vasculature that were attributable to experimental inflammatory arthritis and to establish phenotypic alterations of potential therapeutic and/or diagnostic importance.

For many years the PVAT was thought to act as an inert physically protective barrier against vascular damage. Therefore most studies looking at isolated vascular function, including those using the mCIA model, were carried out in the absence of PVAT. We now know that PVAT is an important modulator of vascular constriction responses and removing it may alter the physiological response of the aorta. The presence of PVAT modulates the constriction response by more than one mechanism: it is capable of releasing a relaxation factor which can act on the endothelium, inducing relaxation via nitric oxide release while also producing hydrogen peroxide (Gao *et al*, 2007) which has a negative effect on relaxation. However, it is important to consider that PVAT has more recently been associated with the production of leptin and angiotensin II, which are known to promote vasoconstriction (Chang *et al*, 2012). The impact of the PVAT on vascular function following arthritis induction is unknown and will be investigated in this thesis.

Very few studies have attempted to determine the cellular makeup of the aortic vessel wall during arthritis-associated vascular dysfunction. Therefore this Chapter will interrogate the very earliest changes seen within the vessel wall, following arthritis induction, in the absence of any overt cardiovascular disease. Previously, the focus of vessel inflammation has been linked with atherosclerosis, where immune cells such as macrophages populate the vessel wall from an early stage (Ley *et al*, 2011) (Bennett, 2013).

It has previously been shown that the presence of inflammatory cells, such as macrophages, in the vasculature during overt CVD is related the increased expression of the TNF family cytokine – TL1A (McLaren *et al*, 2010). TL1A is the only known ligand which directly binds to DR3. The presence of macrophages and increased TL1A has been shown in foam cells of the atherosclerotic plaque *in vitro* (McLaren *et al*, 2010). DR3 has a well characterised "death domain", in which when activated via its ligand TL1A, can initiate apoptosis. However, DR3 is also known for its capability to signal via NF-κβ, in which plays a role in cell survival, driving differentiation and proliferation (Kitson *et al*, 1996). This work outlines the relationship of the inflammatory cells present in the vasculature following systemic inflammation and how they are impacted by DR3 expression for a number of reasons. TL1A itself has been implicated in overt CVD; where *in vitro* it drives increased uptake of low density lipoprotein (McLaren *et al*, 2010). Moreover, DR3 is involved in the modulation of immune cells (Fang *et al*, 2008) and its role has been shown in a number of inflammatory diseases, including, inflammatory bowel disease (Takedatsu *et al*, 2008) and RA (Bull *et al*, 2008). Furthering this DR3 has been shown to be explicitly expressed on the osteoblast – a major regulator in bone formation, important within the RA cohort (Borysenko *et al*, 2006). Given the importance of DR3 and its potential to be involved in vascular inflammation, its expression in the vasculature of healthy and arthritic mice will be a significant driver in the present studies.

When considering changes to vascular function in our model, it is suggested that the early phenotypic changes may prime the vessel for vascular disease. To this regard it has previously been shown that vascular dysfunction is potentially linked with increased levels of MMP-9 in mCIA (Reynolds *et al*, 2012). As a type IV collagenase enzyme, the addition of MMP-9 to an environment made up of extracellular matrix has potential to cause serious damage, especially when active MMP-9 levels are greatly increased (Cho and Reidy, 2002). While the Reynolds *et al*, study concluded that the source of MMP-9 was the aortic tissue itself, it did not explore the identity of cells capable of making MMP-9 nor their presence within this tissue. As such this Chapter explores the possible cellular sources of MMP-9, including macrophages and neutrophils.

This chapter describes the experiments used to determine whether the systemic inflammation associated with mCIA was driving an inflammatory change within the aortic vessel wall and surrounding PVAT. The constriction response was determined in the absence and presence of PVAT, in order to demonstrate the role of the latter in health and disease. The cell types and soluble factors produced within the aortic vessel wall and PVAT were studied in order to identify potential relevance to changes in vascular constriction. This Chapter details methodology, results and discussion under the following hypothesis and objectives:

Hypothesis: mCIA associated systemic inflammation drives vascular dysfunction, attributable to increased inflammatory cell ingress into the vasculature and surrounding PVAT.

- To validate the vascular constriction response to 5-HT seen previously in the mCIA model and to determine the impact of the PVAT on this response
- To identify and measure early changes in the cells, namely macrophages and neutrophils and soluble mediators, such as MMP-9, in both the aortic vessel wall and surrounding PVAT that potentially underlie the vascular dysfunction observed following the onset of arthritis.

2.2 Materials and Methods

All chemicals were purchased from Sigma-Aldrich (unless stated otherwise). Solvents were supplied by Fisher Scientific (unless stated otherwise). A Millipore Milli-Q system produced dH_2O that was used to prepare buffers, reagents and stains. Phosphate Buffered Saline (PBS) pH7.2 was supplied by Life Technologies Ltd. All plastic-ware was obtained from Greiner Bio-One Ltd.

2.2.1 Materials

Male mice (8 weeks old) were used for all experiments. Wild Type (WT) DBA/1 mice were acquired from Harlan, UK. All experiments were carried out with age and sex matched non-immunized controls. All animal care and experimental procedures complied with the United Kingdom Animals (Scientific Procedures) Act 1986 and were under the authority of Home Office Project Licence (30/2928).

2.2.1.1 Preparation of Collagen Induced Arthritis Reagents

1M Acetic Acid

To make 100mls of a 1M acetic acid stock solution, 5.74 mls of glacial acetic acid was added to 94.26mls of dH_2O, in a glass bottle, in a class II fume hood.

Complete Freund's Adjuvant

To prepare a complete adjuvant, 100mg of *Mycobacterium tuberculosis* (*M. tuberculosis*) (Difco, H37 RA, 231141) was ground into a fine powder using a pestle and mortar, in a fume hood. This was then added to 20ml of incomplete Freund's adjuvant (Sigma, F5506), providing a final bacterium concentration of 5mg/ml. The CFA was then stored at -20^{o}C.

Type II Collagen Solution

The type II chick collagen (Sigma, C9301) solution was prepared by dissolving 10mg in 2.5mls of 10mM acetic acid (the latter made by adding 2.5µl of 1M acetic acid stock to 2475 µl of dH_2O). Collagen was dissolved by stirring overnight at 4^{o}C.

Type II collagen Immunization Emulsion

The immunization emulsion to initiate mCIA was made by combining equal volumes of the type II collagen and CFA solutions. Double the volume required for immunization was prepared (to account for loss of emulsion, for example in the space between needle and syringe). The mixture was made in a glass syringe and emulsified by passing through a 19-gauge needle 20 times. All emulsions were made fresh prior to immunization.

2.2.1.2 Myography Reagents

All buffers and reagents were made up using dH_2O.

Table 2.1 - Krebs Buffer Composition

Reagent	mM
NaCl	109.17
KCl	2.68
KH_2PO_4	1.18
$MgSO_4.7H_2O$	1.22
$NaHCO_3$	25.00
Glucose	10.99
$CaCl_2.H_2O$	1.71

Table 2.2 - High Potassium Krebs Buffer (60mM) Composition

Reagent	mM
NaCl	39.36
KCl	59.99
KH_2PO_4	1.18
$MgSO_4.7H_2O$	1.22
$NaHCO_3$	25.00
Glucose	10.99
$CaCl_2.H_2O$	1.71

10mM 5-HT solution

To make a 10mM solution of 5-HT (Sigma) 2.13mg was weighed and dissolved in 1ml of dH_2O.

2.2.1.3. Histological Reagents

Industrial Methylated Spirit (IMS) was required at 90% and was diluted with dH_2O. Harris Haematoxylin and Eosin were purchased from Fisher Scientific. DPX Mountant was purchased from Sigma.

2.2.1.4 General Immunohistochemistry Reagents

All reagents for immunohistochemistry were made up and used as per manufacturer's instructions.

Table 2.3 – Immunohistochemistry Reagents

Product	Supplier
Pap Pen	Pyramid
H_2O_2 Block (3%)	Life Technologies
Goat Serum	Vector Laboratories
Avidin/ Biotin Blocking kit	Vector Laboratories
TBS	Sigma
High Sensitivity Horse Radish Peroxidase	Vector Laboratories
DAB kit	Vector Laboratories

Table 2.4 – Immunohistochemistry Antibodies

Antibody	Supplier
F4/80	Abd Serotech
Ly6G	BD Pharmigen
MMP-9	R and D Systems
DR3	R and D Systems

2.2.2 Induction of mCIA

Following arrival all animals received a settling in period of at least one week before experimental procedures were initiated. To induce mCIA mice were anaesthetised (isoflurane (4L/min) and oxygen (2-4L/min)) and immunized using the intra-dermal route with a total of 100 µl of immunization emulsion (as described above, section 2.2.1.1). Immunizations of 50 µl were administered at multiple adjacent sites right laterally at the base of the tail (see Figure 2.1). This was termed day 0.

For the next 20 days mice were inspected on a regular basis, to ensure good health status was retained. On day 20 mice received temgesic (400 micrograms/L) in their drinking water, which was later changed on a daily basis. On day 21 a booster immunization, identical to that given on day 0, was administered at multiple adjacent sites left laterally at the base of the tail (see Figure 2.1). Concurrently from day 21 mice were also weighed daily and hind paw diameters were measured using a micrometer, to deduce arthritis induction. This was accompanied by manually scoring each paw (Table 2.5) to produce an Arthritis Index, a measure of disease activity (Table 2.6). During this time health monitoring sheets were filled in daily.

Table 2.5 – Paw Scoring System

Paw Score	Pathological Features
0	Normal
1	Mild/ Moderate erythema and Swelling (single toes effected with no other swelling)
2	Severe swelling encompassing whole paw
3	Severe swelling encompassing the whole paw, and toes beginning to become effected
4	Whole paw/ankle/ toes swollen.
5	Deformed paw / ankylosis

Table 2.6 – Paw Scores Used to Determine Arthritis Index

Total Paw Score	Arthritis Severity
0	No Arthritis
1-5	Mild
6-10	Moderate
11-15	Severe

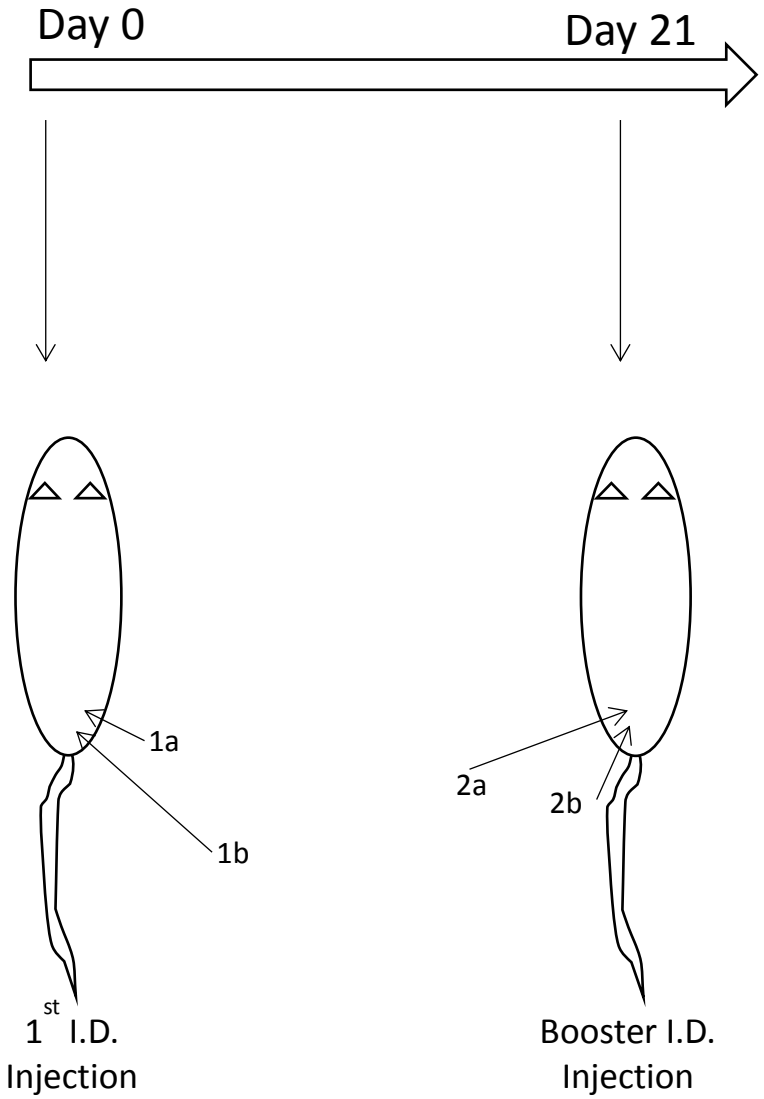

Figure 2.1 – Intradermal Injection Sites. During mCIA intradermal injections were given at the above shown sites on day 0 and then on day 21.

2.2.3 Experimental Sample Collection

When the experimental end point was reached (the onset of mild arthritis), mice were killed by a Schedule 1 method. Each mouse was placed in a rising concentration of CO_2 until breathing ceased. Palpitation of the heart was then carried out to ensure circulation was terminated and the mouse was dead.

2.2.3.1 Isolating Blood Plasma – Cardiac Puncture

Blood samples were collected from all mice via cardiac puncture immediately following the procedure described above. Using a 25 gauge needle, between 600µl and 1ml of whole blood was obtained from each animal and transferred promptly into 3ml vacutainers coated with EDTA and stored on ice. Samples were then centrifuged at

16000 g for 20 minutes at 4^{o}C. The resulting plasma was then isolated and stored at -20^{o}C for later analysis.

2.2.3.2 Tissue Preparation for Histology

All tissue samples that were collected for histological analysis were fixed in 70% (v/v) ethanol for no less than one week prior to processing. If aortas were required for myography they were removed into fresh physiological Krebs solution and kept on ice.

Following cardiac puncture, the skin and ribcage was removed from each mouse, exposing the heart. The abdominal aorta was vented (Figure 2.2) and the heart was flushed using an injection of physiological Krebs solution into the right ventricle. The heart was then removed with a small portion of aortic arch still intact. The thoracic aorta was revealed by removing the ribs, diaphragm and lungs and then carefully dissected out without impacting on the elasticity of the vessel. The hind limbs were finally removed by cutting up the spine to the hip bone and were fixed for histology as above.

2.2.3.3. Bone Specific Preparations

Hind limbs were fixed for a minimum of 6 weeks in 70% Ethanol before being processed for histology. Following the fixation period all bones were subject to a decalcification process for a minimum of 2 weeks, or until bone was evidently decalcified. Decalcification solution consisted of 70g of Ethylenediaminetetraacetic acid (EDTA) in 900ml of PBS (pH 7) and was changed twice weekly. In order to ensure all bone was fully decalcified, legs were imaged by X-RAY using a Kodak FX-Pro.

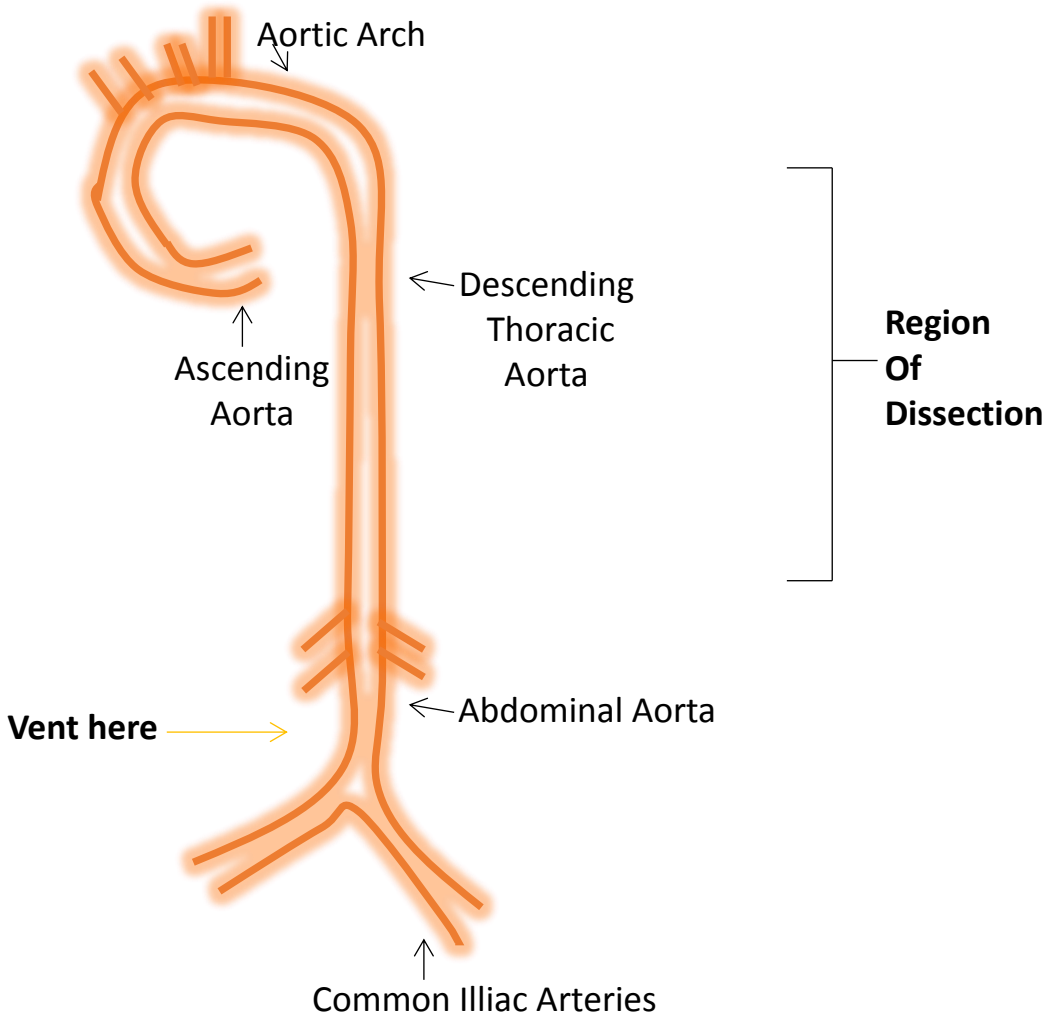

Figure 2.2 - The Anatomy of the Murine Aorta. During experimental tissue collection the region of the descending thoracic aorta highlighted was taken for sample preparation.

1.2.4 Tissue Processing

Following tissue fixation, thoracic aortic sections were processed for histology. A Shandon Tissue processor was used on a 21 hour cycle to prepare each sample for the embedding process. Each sample was exposed to a series of washes; 1 70% ethanol, 1 90 % ethanol, 5 100% ethanol and 3 100% xylene, before being infiltrated with 4 cycles of wax. Samples were then transferred to a histocentre, where each was embedded within a wax block.

A microtome was used to trim all excess wax from each block before 8µm sections were cut using a specialised S35 soft tissue blade. A minimum of 12 sections were cut and mounted onto Superfrost+ slides (2 sections per slide) and stored at 56^{o}C overnight. Slides were then stored at room temperature until staining was initiated.

2.2.5 Histology

In order to gauge the general structure and to count total cells within the thoracic aorta and surrounding PVAT a Haematoxylin and Eosin (H&E) stain was carried out (Table 2.7) in all control and mild arthritic samples. Images of staining were taken on a Leica Microscope at x10, x20 or x40 magnification.

Table 2.7 – General Histology Protocol

Step	Time	Reason
3 x Xylene Washes	3 x 5 minutes	Rehydration Step
2 x 100% IMS Washes	2 x 3 minutes	
90% IMS Wash	3 minutes	
dH_2O Wash	3 minutes	
Haematoxylin Stain	90 seconds	Identify Cell Nuclei
Running Tap Water	Until Clear	Remove Excess Stain
Eosin Stain	30 seconds	Identify Eosinophilic Structures
Running Tap Water	Until Clear	Remove Excess Stain
90% IMS Wash	3 minutes	Dehydration Step
2x 100% IMS Washes	2 x 3 minutes	
3 x Xylene Washes	3 x 5 minutes	
Mount in DPX	-	Preservation of Staining

Corel Paint Shop Pro was used to separate each image into two separate images – one of the aortic vessel and one of the surrounding PVAT. From this point the images were analysed separately. A Carestream package was used to identify specific regions of interest within each image. This programme works by identifying an edge gradient thus allowing each cell nuclei to be counted as a single region of interest. Total area of either the aortic vessel wall or the PVAT was then determined using Image J. This information was used to calculate the number of cells per mm^2.

2.2.5.2 Determining Arthritis Index – Histological Assessment

The protocol detailed above (Table 2.7) was also used to stain non-immunized and arthritic ankle joints in order to determine an arthritis index. Following H&E staining, images were taken at x20 magnification using a Leica Microscope. Each joint was scored using the following scoring system (Table 2.8) and was given a total score, termed the Arthritis Index.

Table 2.8 – Histological Assessment of mCIA Joints

Subsynovial Inflammation	
0	Normal
1	Focal Inflammatory Infiltrates, adiposity hardly affected (10% Inflammatory cells : 90% Adipose Tissue cells)
2	Focal Inflammatory Infiltrates equal adiposity (50% Inflammatory cells : 50% Adipose Tissue cells)
3	Random Inflammatory Infiltrates that dominate cellular histology (70% Inflammatory cells : 30% Adipose Tissue cells)
4	Substantial Inflammatory Infiltrates with severe loss of adiposity (90% Inflammatory cells : 10% Adipose Tissue cells)
5	Ablation of adipose tissue due to Inflammatory Infiltrates (100% Inflammatory cells : 0% Adipose Tissue cells)
Synovial Exudate	
0	Normal
1	Evidence of Inflammatory Cells in Joint Space
2	Moderate Numbers of Inflammatory Cells in Joint Space, Fibrin Deposits Evident
3	Substantial Numbers of Inflammatory Cells in Joint Space, Large Fibrin Deposits Evident
Synovial Hyperplasia and Pannus Formation	
0	Normal (1-3 Layers Thick)
1	Synovial Lining >3 Layers Thick, Thickening is Evident and/or Invades the Joint Space
2	Synovial Lining >3 Layers Thick, Approaching Cartilage and/or finger like processes into the Joint Space
3	Synovial Lining >3 Layers Thick, Covering Cartilage, with evident Cartilage Loss
Cartilage and Bone Erosions	
0	Normal
1	Detectable loss of Cartilage – caused by pannus
2	Detectable erosions of underlying bone – caused by pannus
3	Significant erosion of part of the bone

2.2.6 Immunohistochemistry

The following protocol was used generally in all immunohistochemistry (Table 2.9) with optimized steps for individual proteins of interest, for example a different wash buffer was required for each. Identification of macrophages (F4/80+ cells), neutrophils (Ly6G+ cells), DR3 positive cells and the presence of MMP-9 was carried out. Different antibodies, isotypes and therefore serum blocks were also used and details can be found along with the specific antibody concentrations in Table 2.10.

Table 2.9 – General Immunohistochemistry Protocol

Process	Reason	Time
3 Xylene Washes	Rehydration and Wax Clearing	3 x 5 minutes
2 100% Ethanol Washes	Slide Rehydration	2 x 3 minutes
90% Ethanol Wash		3 minutes
Distilled H_2O	Equilibrate	5 minutes
Buffer Rinse		-
3% Hydrogen Peroxidase Block	Quench Hydrogen Peroxidase Activity	30 minutes
PBS wash		5 minutes
Secondary Host Serum Block	Decrease non-specific binding of antibody	20 minutes
Buffer wash		5 minutes
Avidin Block	Decrease non-specific binding of antibody	10 minutes
Buffer wash		5 minutes
Biotin Block	Decrease non-specific binding of antibody	10 minutes
Buffer wash		5 minutes
Addition of primary antibody or Isotype control antibody (4^oC)	Identification of target protein and control IgG staining	Over night
3x Buffer wash	Remove excess antibody	3 x 2 minutes
Addition of secondary antibody	Identification of bound primary antibody	1 hour
3x Buffer wash	Remove excess/unbound antibody	3x2 minutes
High Sensitivity Horse Radish Peroxidase	Identify bound Antibody in sections	30 minutes
PBS wash	Remove excess HRP	5 minutes
DAB	Allows identification of positive staining	3-5 minutes
Running Tap Water	Remove excess DAB staining	5 minutes
Haematoxylin	Counter stain	90 seconds
Running Tap Water	Remove excess counter stain	Until water runs clear
90% Ethanol	Dehydration of slides and Clearing	3 minutes
2 x 100% Ethanol		2 x 3 minutes
3 x Xylene		3 x 5 minutes
Mount with DPX and coverslip	Preservation of staining	

Table 2.10 – Antibody Specific Reagents and Concentrations

Reagent	**F4/80**	**Ly6G**	**DR3**	**MMP-9**
Wash Buffer	TBS Tween	TBS Tween	TBS	PBS
Serum Block	Rabbit	Rabbit	Goat	Goat
Primary Antibody	Rat Anti MouseF480 (2ug/ml)	Rat Anti Mouse Ly6G (5ug/ml)	Biotinylated Goat anti mDR3 (2ug/ml)	Biotinylated Goat anti MMP-9 (15ug/ml)
Isotype	Rat IgG2A (2ug/ml)	Rat IgG2B (5ug/ml)	Normal Goat IgG (2ug/ml)	Normal Goat IgG (15ug/ml)
Secondary Antibody	Rabbit Anti Rat IgG	Rabbit Anti Rat IgG	None	None

Representative high power images (x40) were taken on the Leica microscope, of both the aortic vessel wall and the surrounding PVAT. From this point the aortic vessel wall and the PVAT were analysed separately.

Photoshop was used to determine the total number of pixels in the selected area of the picture (eg, the vessel wall). The number of brown pixels, representative of positive staining, was then calculated. The positive staining was calculated as a percentage of the total region and was corrected for isotype control values.

2.2.7 Myography

In order to determine the baseline vasomotor responses of the descending thoracic aorta and the effect of mCIA and PVAT on this response, myography was carried out on both fat denuded and fat intact aortic rings (see below). Tissues from experimental mCIA and control animals were compared in order to gauge the level of vascular dysfunction present in this model.

2.2.7.1 Determination of Baseline Constriction Responses for Fat Intact and Fat Denuded Aorta

Each well of the myograph was first washed and filled with Krebs solution, gassed at 95% O_2 and 5% CO_2. For each aorta, two PVAT intact rings (2mm wide) were cut with the aid of a dissection microscope and mounted in the myograph (see Figure 2.3). The remaining aorta was then carefully cleaned of PVAT and a further two rings cut and mounted as above. Tissues were left to equilibrate in the bath for 20 minutes at 37^{o}C with the tension of the prongs set at 0 MilliNewtons (mN). A resting tension of 5mN was then applied by increasing the tension by 0.5mN per minute, over a 10 minute period. Subsequently tissues were allowed to equilibrate for a further 20 minutes over which time the resting tension was readjusted to 5mN as appropriate. The MyoDaq programme was used to monitor changes in tension throughout the experiments.

Following removal of the physiological Krebs from each bath, a “wake-up response” was carried out by addition of 60mM Potassium Krebs, for 10 minutes. Baths were then repeatedly washed with physiological Krebs until the vessel tension returned to a resting 5mN. At this point each bath contained 5mls of physiological Krebs.

A serial dilution of 10mM 5-HT was carried out in order to produce a range of concentrations. To produce a cumulative concentration curve, varying volumes of each 5-HT concentration were added in turn to each bath (see Table 2.11).

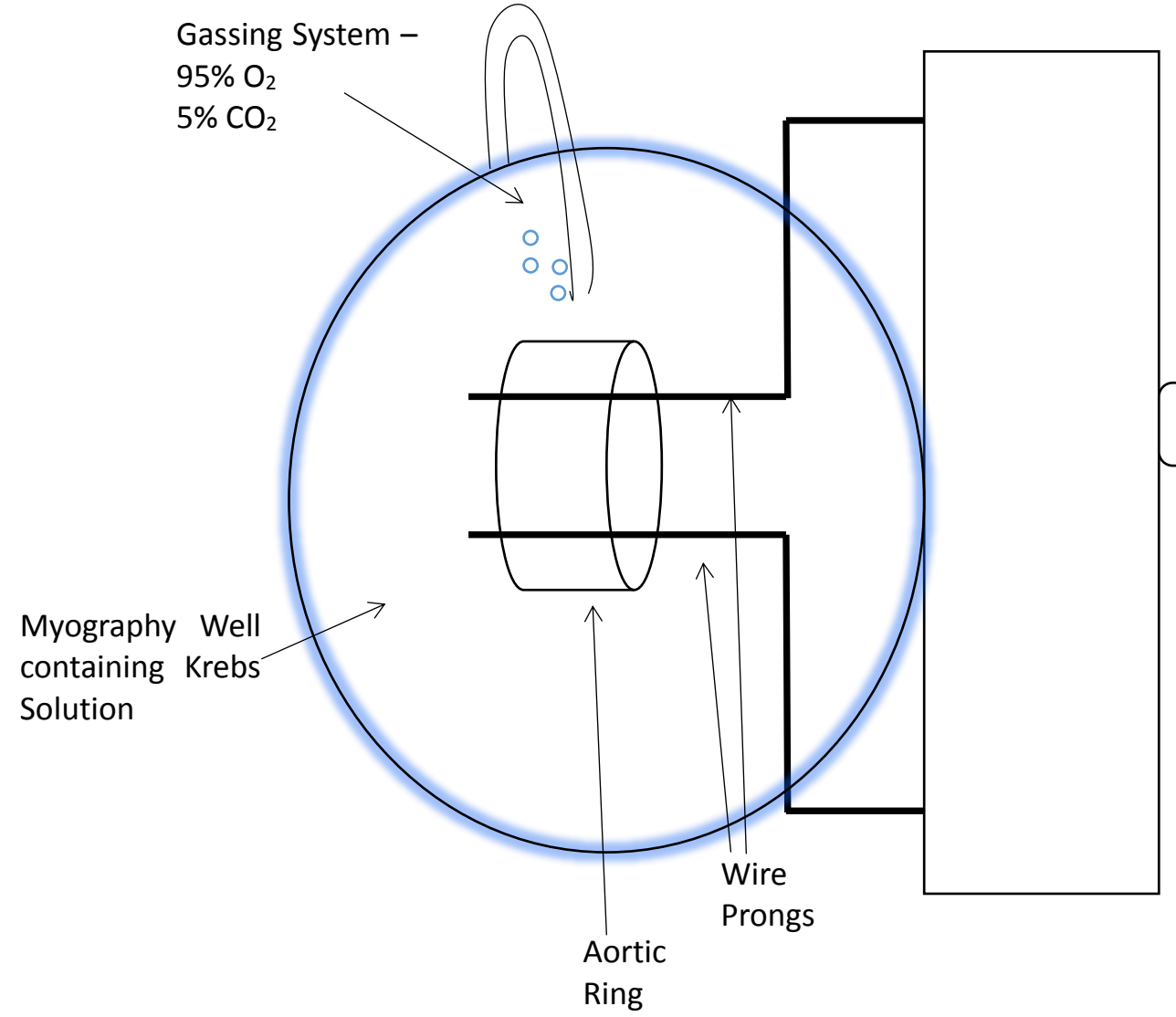

Figure 2.3 - A Single Well of a Myograph. Aortic rings were mounted on two wire prongs as shown above. The well of the myograph allows for addition of different pharmacological agents and determines vascular constrction response.

Table 2.11 – Cumulative Concentration Curve

Volume Added to Bath (µl)	Concentration of 5-HT added to Bath (M)	Final Bath Concentration (M)
50	1×10^{-7}	1×10^{-9}
100	1×10^{-7}	3×10^{-9}
35	1×10^{-6}	1×10^{-8}
100	1×10^{-6}	3×10^{-8}
35	1×10^{-5}	1×10^{-7}
100	1×10^{-5}	3×10^{-7}
35	1×10^{-4}	1×10^{-6}
100	1×10^{-4}	3×10^{-6}
35	1×10^{-3}	1×10^{-5}
100	1×10^{-3}	3×10^{-5}

2.2.7.2 Myography Analysis

In order to analyse constriction responses the MyoData programme was used. Agonist-induced contraction responses were calculated as plateau developed tension to each concentration above the resting tension.

2.2.7.3 Statistics

Statistics used were dependant on the experiments performed. For all histology and immunohistochemical analysis, Students T-Test was used to compare the non-immunized group with the arthritic group. All correlations were plotted using Graph Pad Prism and Spearman's Rank Coefficients were determined. Where appropriate data were averaged for each animal and counted as one n-value. All concentration response data were fitted to sigmoid curves using Graph Pad Prism and resulting Ec50 (half maximal constriction) and RMAX (maximal constriction) values were then compared

using a Students T-Test. Differences that were considered significant were $p<0.05$. Values are all plotted as Mean ± SEM.

2.3 Results

2.3.1 Arthritis Incidence in DBA/1 Mice Over a 45 Day Time Course

Both non-immunized control and arthritic mice were housed together and there was no difference in weight prior to, or at the point of the booster immunization (day21). However, from day 22 onwards it was noted that non-immunized mice weighed significantly ($P<0.001$) more than immunized mice. This was apparent even prior to the steep curve of arthritis onset, seen between days 26 and 30 (Figure 2.4). Despite arthritic mice weighing less than their non-immunized counter parts, no more than 20% weight loss was seen, over the time course, from day 21.

By day 34 mCIA was initiated in 100% of experimental DBA/1mice (Figure 2.5a). Total paw score and hind paw diameter of experimental animals were both significantly ($P<0.0001$) increased in comparison to non-immunized control mice (Figure 2.5b&c). Individual paw score positively and significantly ($p<0.0001$) correlated with paw diameter (Figure 2.5d).

In order to assess the local impact of systemic inflammatory arthritis, the ankle joints were analysed for aspects of inflammation. All such markers were up regulated within joints of arthritic mice compared to non-immunized controls. Sub-synovial inflammation was significantly ($p<0.0001$) increased (0 vs. 2.9 ± 0.23). This was matched by a significant ($p=0.0001$) increase in synovial hyperplasia and panus formation (0 vs. 1.9 ± 0.23). Synovial exudate (0.2 ± 0.2 vs. 0.6 ± 0.18), cartilage and bone erosions (0 vs. 0.9 ± 0.35) were increased, but not significantly. To determine the arthritis index the total of the 4 inflammatory measures was calculated and was significantly ($p<0.0001$) increased in arthritic ankle joints in comparison with controls (0.2 ± 0.2 vs. 6.3 ± 0.62) (Figure 2.6a-e).

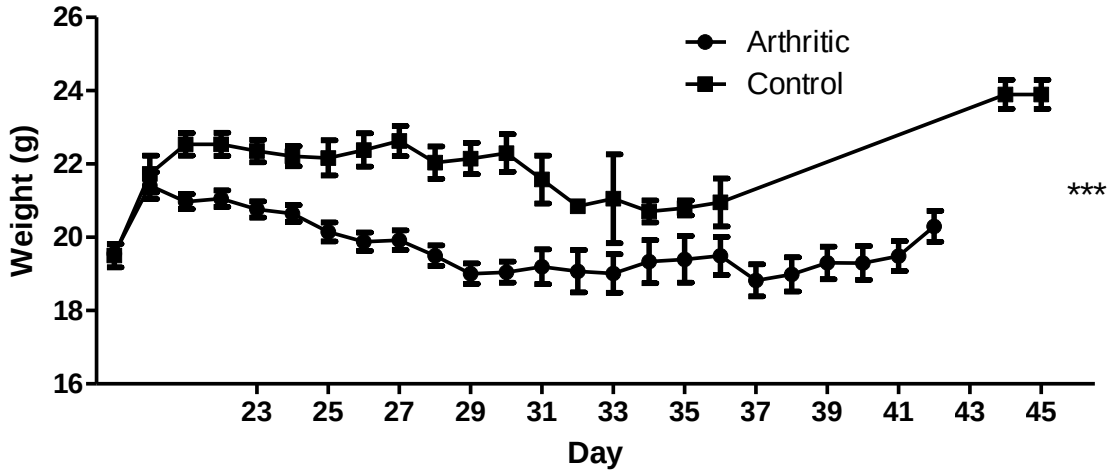

Figure 2.4 – Weight Changes Over the Arthritic Time Course. The weight of a sample of non-immunized controls (N=20) was compared to the weight of immunized arthritic animals (N=48), following the booster injection on day 21, for 24 days. ***=p<0.0001.

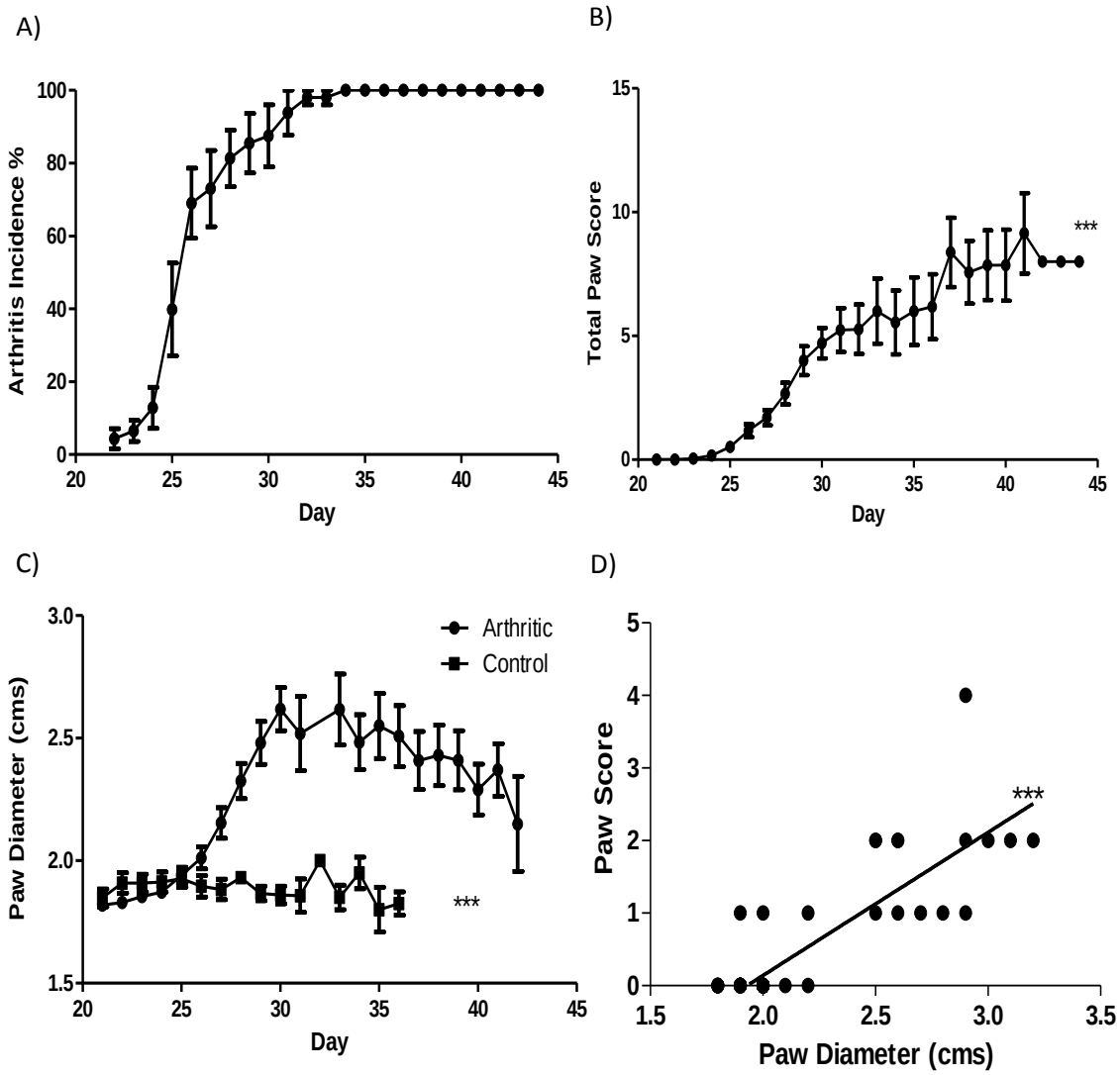

Figure 2.5 - Arthritis Induction in DBA/1 Mice Over a 45 day Time Course. Arthritis Incidence is shown over a sample set of 6 experiments, for a total of 48 experimental mice (A). Total Paw Score is shown over a 45 day time course (N=48) (B). Individual hind paw diameter (including right and left measurements) are shown for arthritic (N=52) vs. non-immunized control paws (N=24) (C). Individual paw score and paw diameter were correlated for 2 experiments (N=16) (D). ***=p<0.0001.

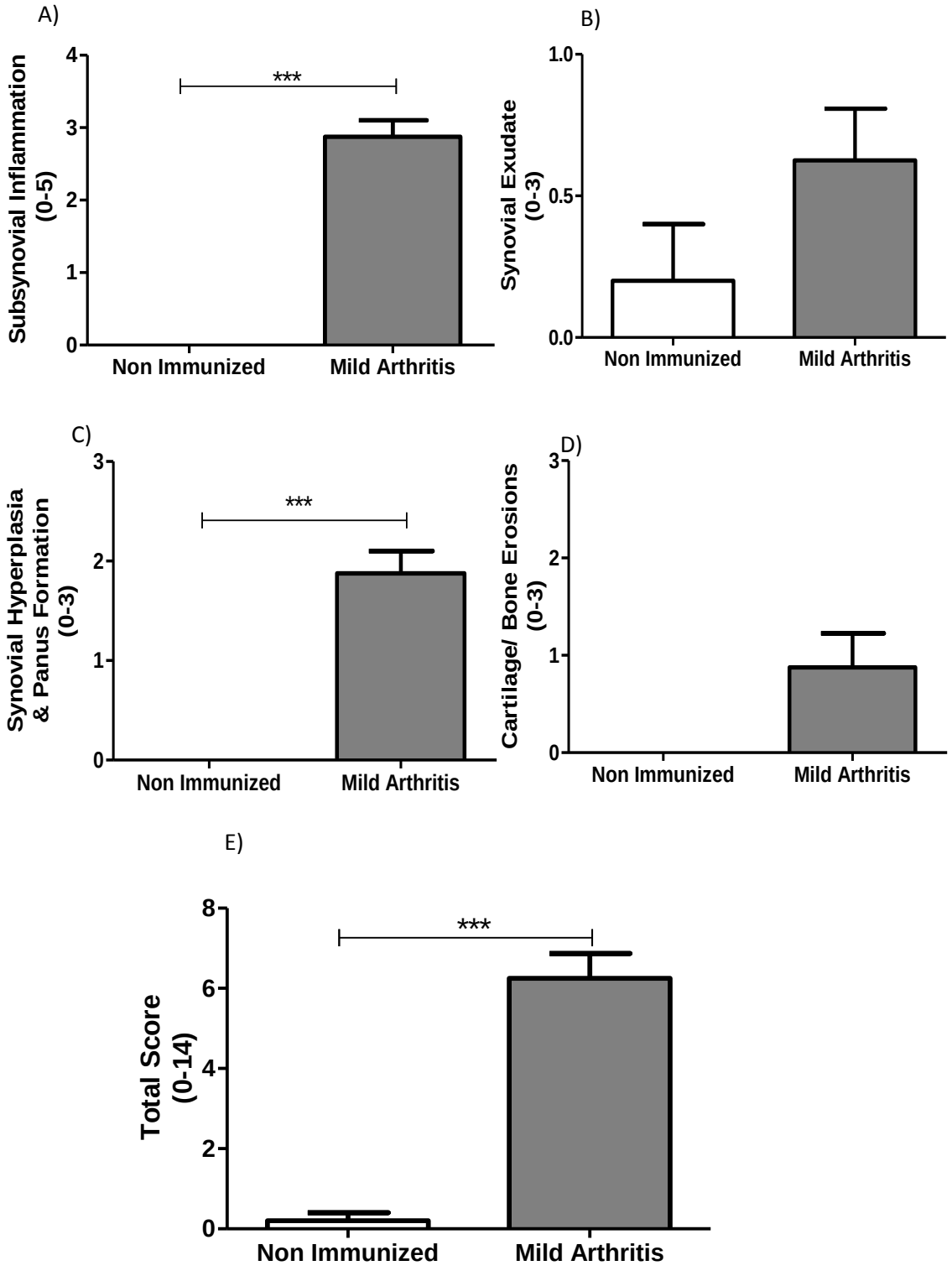

Figure 2.6- Measurement of Arthritis Index. Inflammatory measures were analysed following H&E staining of ankle joints from non-immunized control mice (N=5) and arthritic mice (N=8). These included; subsynovial inflammation (A), synovial exudate (B), synovial hyperplasia and panus formation (C) and cartilage/ bone erosions (D). A final total score of all inflammatory measures makes up the arthritis index (E). ***=p<0.001.

2.3.2 Arthritis Significantly Reduces the Vascular Constriction Response.

Vascular constriction response to 5-HT was measured in PVAT-denuded and -intact tissues from non-immunized control and arthritic mice. In those from non-immunized mice, the presence of PVAT caused a significant (P=0.0009) dextral shift in the constriction response to 5-HT but did not impact the RMAX. (Figure 2.7a) The PVAT altered the constriction responses in tissues from mildly arthritic animals in a similar way, causing a significant (P<0.0001) dextral shift to the curve, without affecting RMAX (Figure 2.7b).

No difference in EC50 values was observed for constriction responses between PVAT-denuded tissues from non-immunized control and mild arthritic animals (-6.22±0.11mN (N=8) vs. -6.11±0.11 (N=14)). However, RMAX responses were significantly (P=0.0003) reduced in arthritic tissues compared to controls (4.40 ± 0.18 mN (N=14) vs 5.56 ± 0.17 (N=8)) (Figure2.7c&d).

The EC50 values for PVAT-intact tissues from non-immunized controls and mildly arthritic rings were comparable (-6.71±0.079 (N=8) vs. -6.80±0.11 (N=14)). However, as described above for PVAT-denuded tissues, the RMAX response of PVAT-intact arthritic rings was significantly (P=0.025) decreased in comparison to non-immunized controls (4.62 ± 0.19 (N=14) vs.5.43 ± 0.29 mN (N=8)).

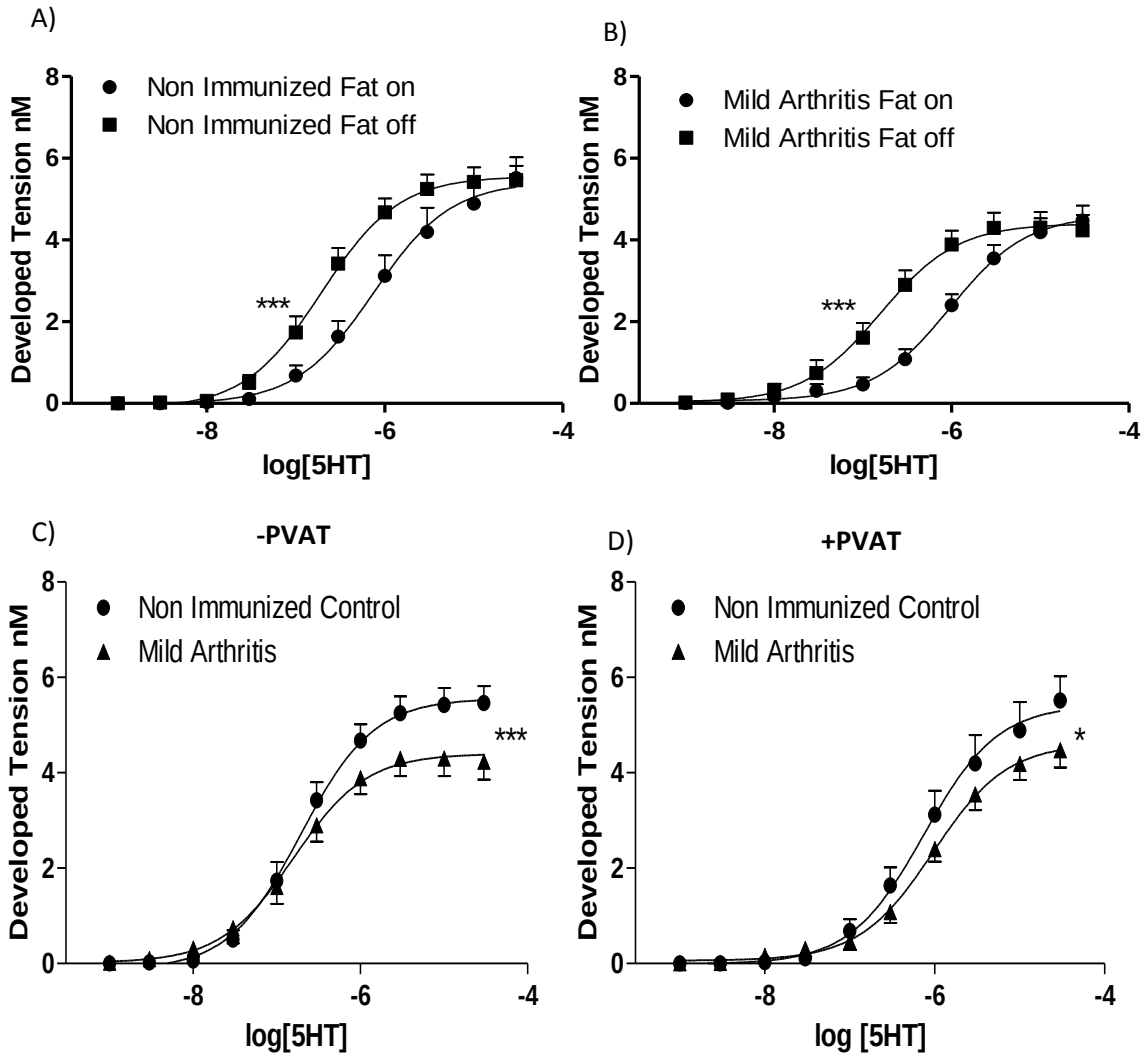

Figure 2.7 - Comparison of Constriction Response Curves in Isolated Rings from Control and Arthritic Mice. Constriction responses to 5-HT were determined for PVAT-intact and -denuded tissues from both non-immunized controls (N=8) (A) and mildly arthritic mice (N=14) (B). The PVAT-denuded (C) and intact (D) constriction responses for non-immunized controls and arthritic rings were also compared *=p<0.05, ***=p<0.001.

2.3.3 Arthritis Does Not Impact on Total Cell Number Within the Aorta or Surrounding PVAT.

Following the onset of mild arthritis, total cell numbers within the aortic vessel wall and the surrounding PVAT were calculated (Figure 2.8). There was no significant difference in total cell number following arthritis onset within the aortic vessel wall (4575 ± 243 (N=21) vs. 4169 ± 531 cells/mm^2 (N=8)). Similar results were seen in the PVAT, with no significant difference in total cell number following arthritis onset (2328 ± 181 vs. 2742 ± 297 cells/mm^2).

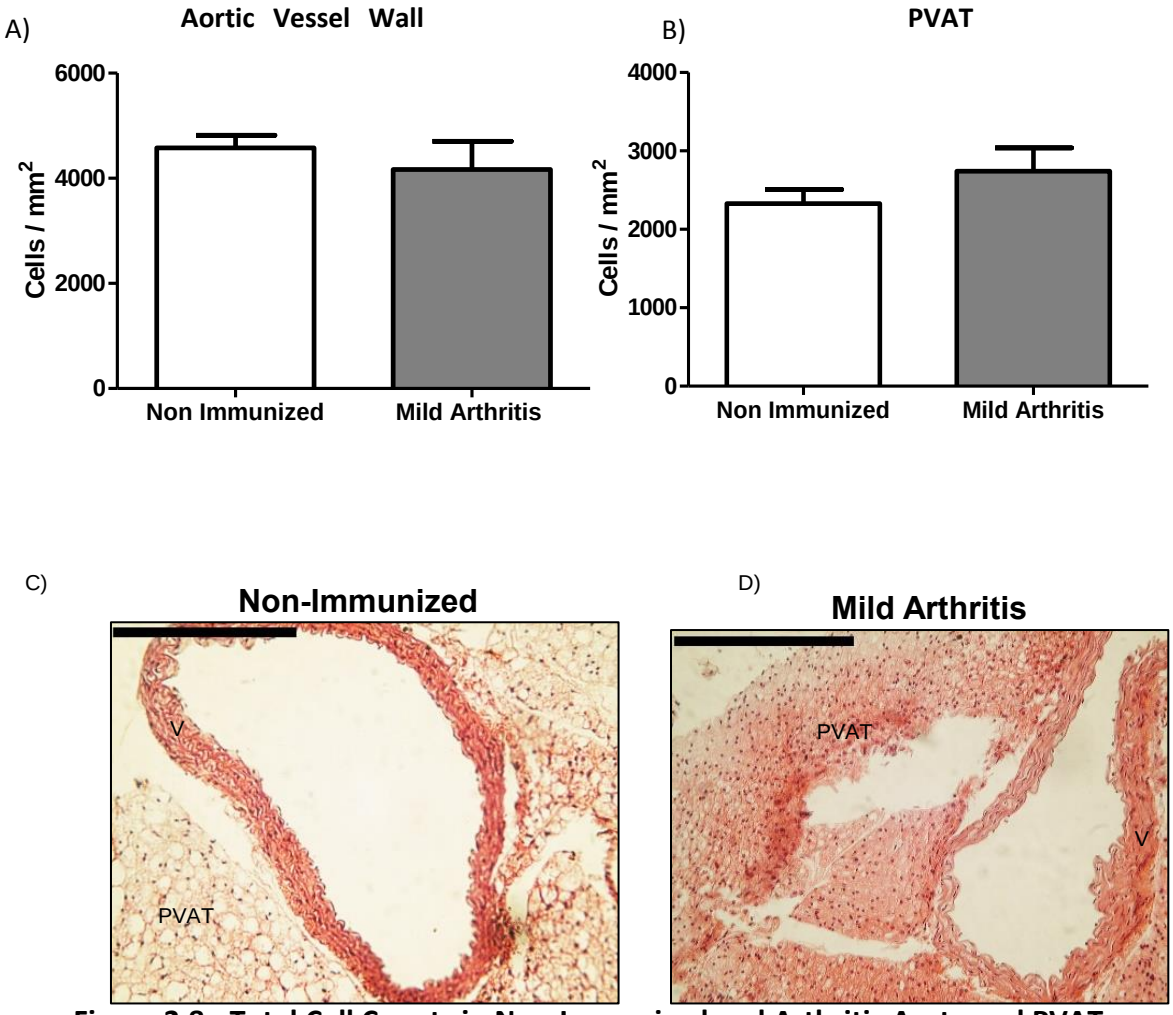

Figure 2.8 - Total Cell Counts in Non-Immunized and Arthritic Aorta and PVAT. Total cell numbers were counted in the aortic vessel wall (A) and the surrounding PVAT (B) for non-immunized (N=21) and arthritic (N=8) mice. Representative images show non-immunized (C) and arthritic (D) vasculature. Images are taken at x20 magnification and scale bars represent 0.25µm. Images are taken at x10 magnification. Scale bars represent 0.2µm.

2.3.4 Onset of Arthritis Significantly Changes the Inflammatory Profile of the Vasculature

Following the onset of mild arthritis increased numbers of macrophages were found within both the aortic vessel wall and the surrounding PVAT. F4/80+ macrophages were identified in both regions in both groups of mice (Figure 2.9) and a significant ($p<0.02$) increase was observed within the aorta (4.83 ± 0.6% (N=21) vs. 11.23 ± 3.2% (N=8)) and PVAT ($p=0.008$) (3.08 ± 0.6% vs. 8.81 ± 2.4%) following arthritis onset.

A small percentage of cells expressed Ly6G in both non-immunized and mildly arthritic tissues (Figure 2.10). In the aortic vessel wall Ly6G expression shows a trend ($p=0.055$) towards decreased expression following arthritis onset (1.87 ± 0.86% (N=4) vs. 0.55 ± 0.22% (N=10)). No difference in Ly6G expression was seen within the PVAT (1.64 ± 0.92% vs. 1.84 ± 1.13%).

Following the onset of arthritis MMP-9 expression in the aorta showed an increasing trend (Figure 2.11), though this was not significant (5.31 ± 3.11% (N=4) vs. 12.45 ± 3.06% (N=12). However, a significant ($p=0.044$) increase in MMP-9 expression in PVAT was observed (7.0 ± 6.57% vs. 27.15 ± 4.86%).

A significant ($p=0.003$) increase in the cellular expression of DR3 was observed within the aortic vessel wall ($p=0.003$) (4.96 ± 0.49% (N=13) vs. 9.84 ± 1.68% (N=8)) and PVAT ($p=0.048$) (5.78 ± 0.78% vs. 10.18 ± 2.45%) following the onset of arthritis (Figure 2.12).

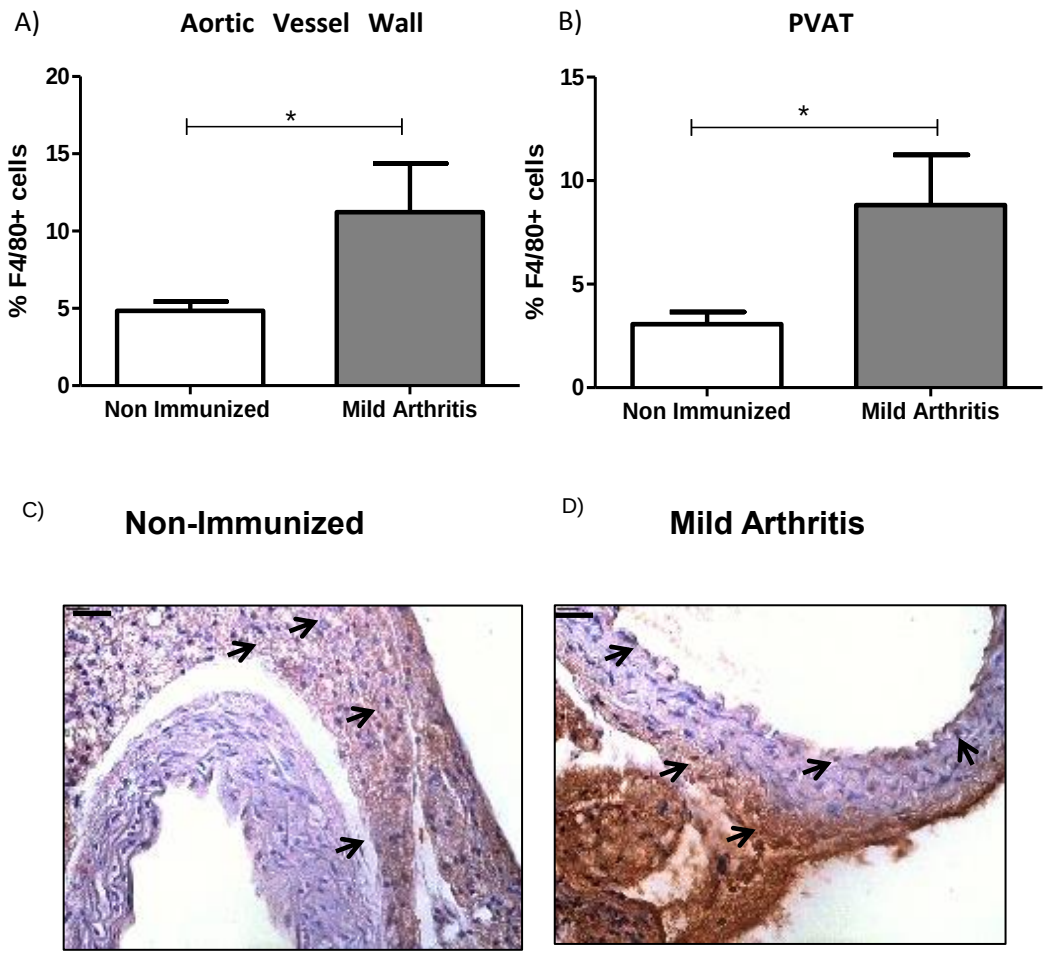

Figure 2.9 – Effect of Arthritis Onset on Macrophage Number in the Vasculature. The % of cells expressing the macrophage marker F4/80 was determined in the aortic vessel wall (A) and surrounding PVAT (B) for non-immunized (N=21) and mildly arthritic (N=8) mice. Representative images show F4/80 positive staining in non-immunized controls (C) and mild arthritic (D) vasculature. *$p<0.05$. Images are taken at x20 magnification. Scale bars represent 0.2µm.

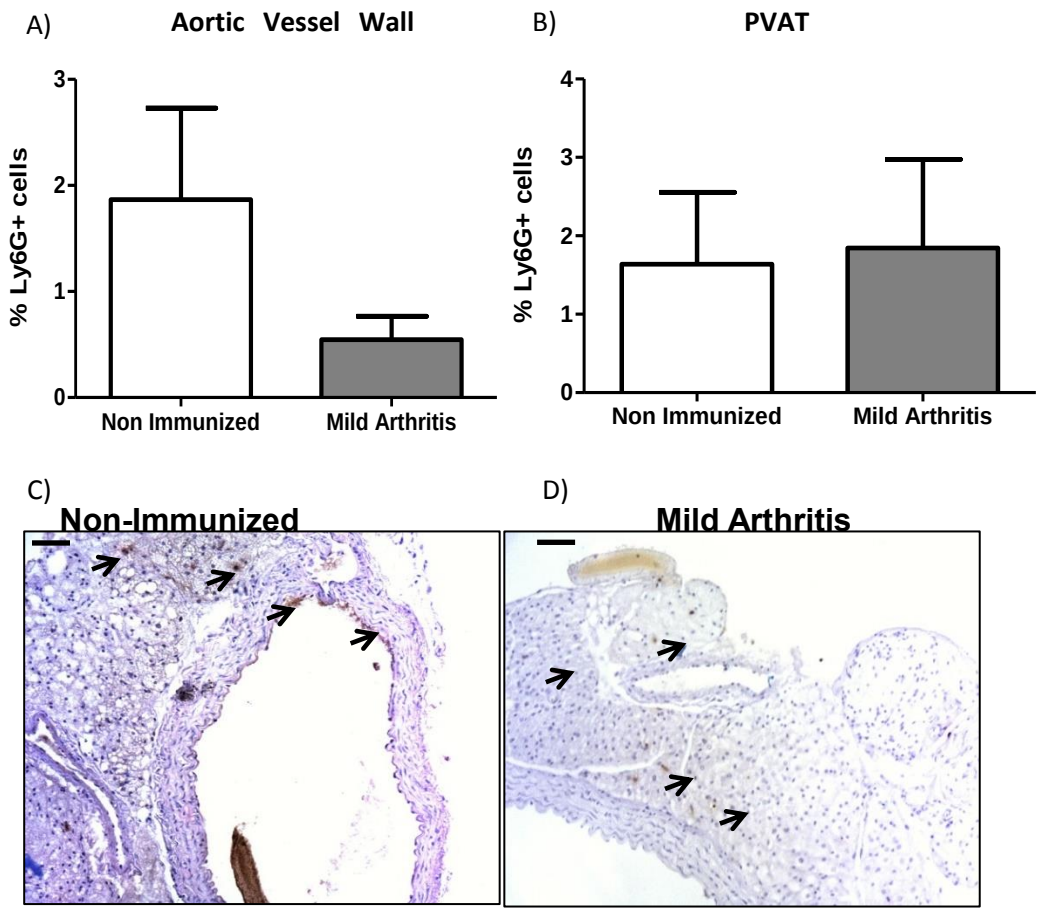

Figure 2.10 – Effect of Arthritis on the Number of Neutrophils in the Vasculature. The % of cells expressing neutrophil marker Ly6G was determined in the aortic vessel wall (A) and surrounding PVAT (B) for non-immunized (N=4) and mildly arthritic (N=10) mice. Representative images show Ly6G positive staining in non-immunized controls (C) and mild arthritic (D) vasculature. Images are taken at x20 magnification. Scale bars represent 0.2µm.

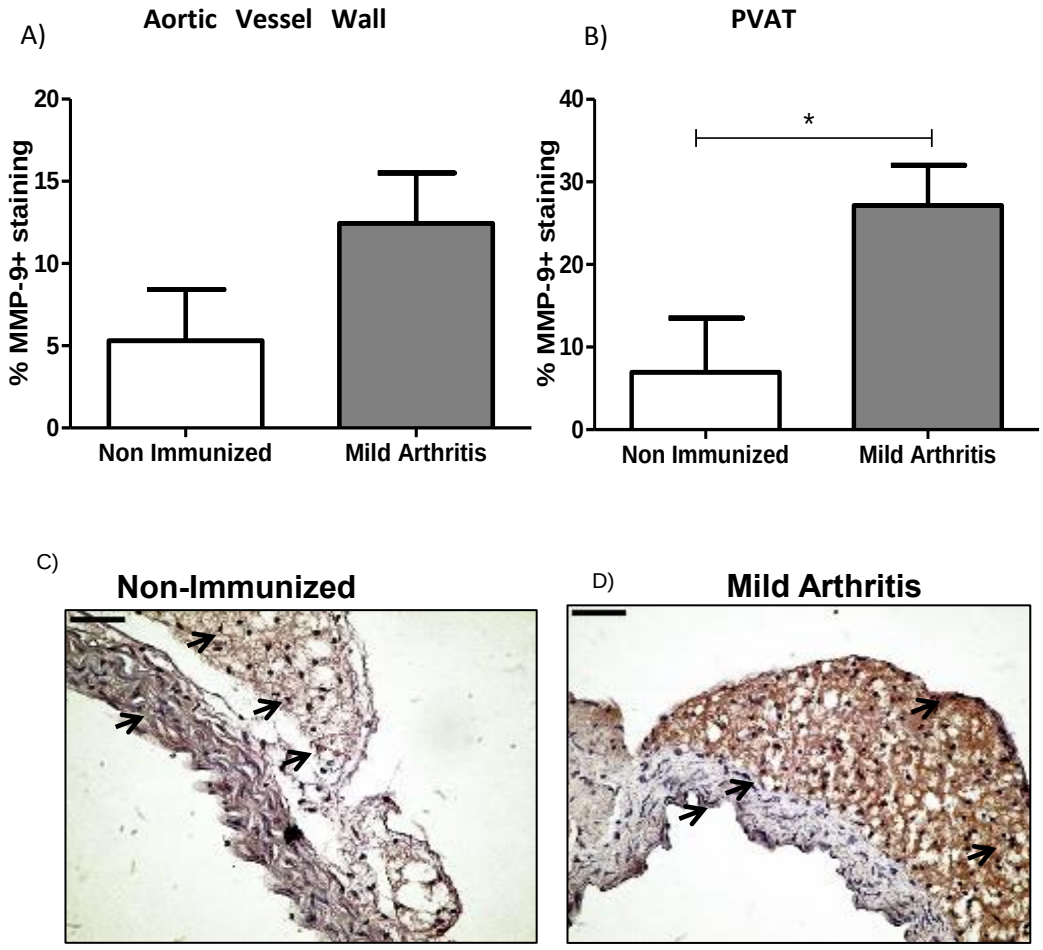

Figure 2.11 – Effect of Arthritis on the Expression of MMP-9 in the Vasculature. The % of MMP-9 staining was determined in the aortic vessel wall (A) and surrounding PVAT (B) for non-immunized (N=4) and mildly arthritic (N=12) mice. Representative images show MMP-9 positive staining in non-immunized controls (C) and mild arthritic (D) vasculature.*$p<0.05$. Images are taken at x20 magnification. Scale bars represent 0.2µm.

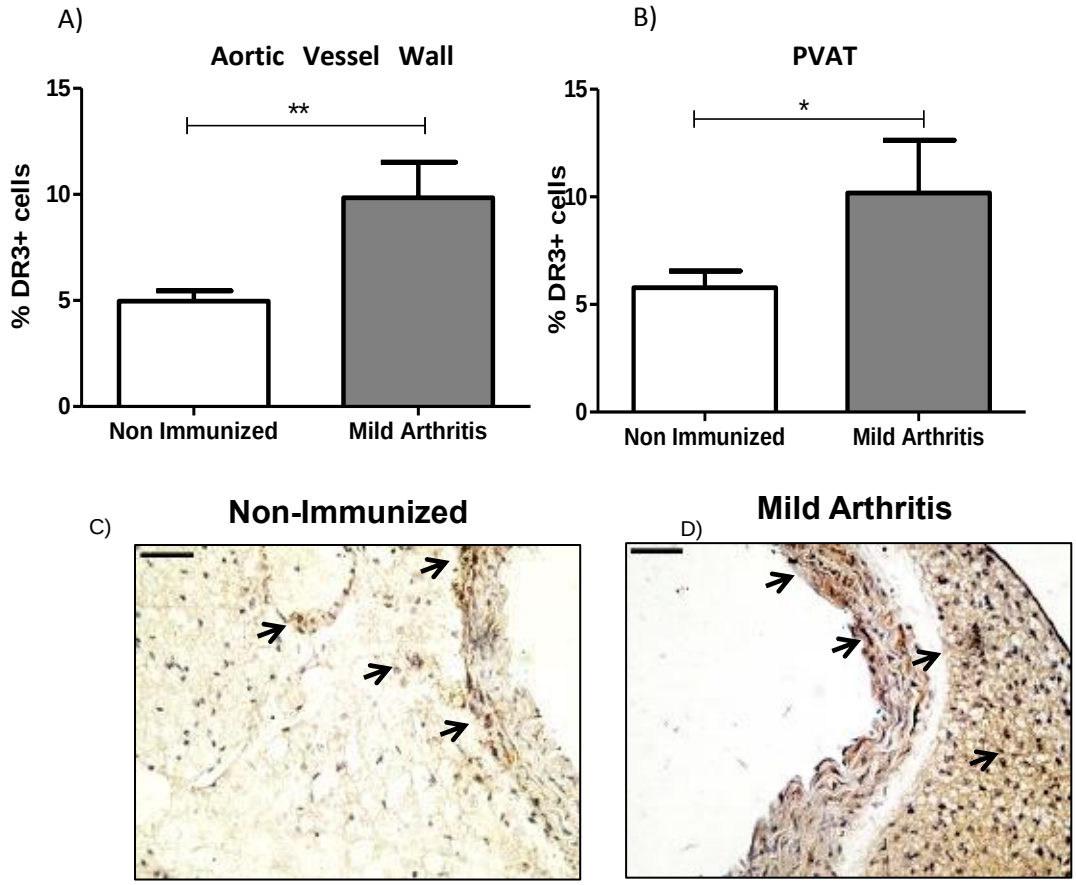

Figure 2.12 – Effect of Arthritis on the Cellular Expression of DR3 in the Vasculature. The % of DR3 expression was determined in the aortic vessel wall (A) and surrounding PVAT (B) for non-immunized (N=13) and mildly arthritic (N=8) mice. Representative images show DR3 positive staining in non-immunized controls (C) and mild arthritic (D) vasculature.*p<0.05, **p<0.001. Images are taken at x20 magnification. Scale bars represent 0.2µm.

2.4 Discussion

The increased risks to health associated with systemic inflammatory diseases such as RA and CVD are well established, however the underlying mechanisms linking these disorders to clinical events is poorly understood. Here, we show that systemic inflammation leads to an impaired vascular constriction response that is impacted by the presence of PVAT. These alterations in constriction responses are associated with increased inflammatory mediators within both the aortic vessel wall and the surrounding PVAT.

Vascular contractile dysfunction in mCIA has been described previously (Reynolds *et al*, 2012). The experiments described herein to determine that the mCIA model worked successfully in our hands. However, the isolated tissue studies described by Reynolds *et al*, were carried out in the absence of PVAT- a tissue that has been shown to modulate vascular constriction response (Lohn *et al*, 2002, Verlohren *et al*, 2004, Owen *et al*, 2013). Importantly, the present study demonstrates for the first time the impact of PVAT on constriction response following the onset of mCIA. To this end PVAT causes a dextral shift in constriction response to 5-HT in both control and mCIA aortas while having no effect on maximum contraction responses. While PVAT does not impact on the maximal constriction potential of the aortic vessel, these findings build on an increasing body of evidence that PVAT is not just an inert fat store providing physical protection to the vasculature, but that it plays a major role in the modulation of vascular tone (Lohn *et al*, 2002), (Verlohren *et al*, 2004), (Owen *et al*, 2013).

The definitive mechanism by which PVAT affects vascular constriction response is currently unknown. There are many potential candidates that have been postulated, all of which are distinct possibilities in this model. Examples of these mechanisms include the release of a transferable relaxing factor which induces endothelium-dependent relaxation (Gao *et al*, 2007). This involves the action of nitric oxide (NO) release and the activation of K_{Ca} channels (Yuan *et al*, 1996). It is important to note, that despite Reynolds *et al* showing dysfunction in fat denuded vessels occurred independently of the endothelium, it was shown that there was no change in endothelium dependant relaxation. This suggests the endothelium was functional and therefore able to react to any factors produced in its proximity (Reynolds *et al*, 2012). For example, it is well known the PVAT can produce a number of vasorelaxant factors that could impact on vascular constriction. Another distinct possibility is that this delayed constriction response occurs independently of the endothelium and involves the activity of H_2O_2, allowing activation of soluble guanylyl cyclase (Krieger-Brauer and Kather, 1992). From our results we would suggest that whichever mechanism is responsible for the dextral shift seen in constriction response to 5-HT, that the mechanism works to the same effect in both control and mCIA aortic tissue. Although we show similarities in health and disease, we continued to analyse both the aortic vessel and PVAT to determine differences that may still exsist at a cellular level.

Interestingly, there is no significant change in total cell number within either the aortic vessel wall or the surrounding PVAT. This is surprising considering the changing populations of both macrophages and neutrophils within these regions. As such this would suggest that the whole dynamic of the vessel wall and surrounding fat is changing as a consequence of systemic inflammation. It is likely that while cells such as macrophages ingress into the vasculature, a change in residential cells is simultaneous.

This novel data have not previously been reported in the absence of any overt CVD. In order for cells to be able to infiltrate into either region there must be a change within the control mechanisms within both tissues. For example, we would likely see an increase in adhesion molecules, such as, Vascular Adhesion Molecule 1 (VCAM-1), which facilitate both recruitment and trans-endothelial migration of both monocytes and macrophages, into the regions (Kaden *et al*, 2005).

Although the total number of cells does not change, an alteration to the cellular population is not ruled out. For instance, it was noted that the structure of the PVAT itself appears to change between non-immunized and arthritic histology images (Figure 2.13). In non-immunized mice the PVAT appears to be phenotypically white. Structurally white adipocytes have a scant ring of cytoplasm surrounding a single lipid droplet. They have nuclei that appear flattened within the cell (Klaus, 1997). This is different to what we see within the PVAT of arthritic mice. The PVAT appears densely packed; suggestive of brown fat. These cells have an increased volume of cytoplasm and contain multiple lipid droplets. The cell nuclei are also a different shape to those in white fat, here they are round and are usually located centrally within the cell (Cypess *et al*, 2009), (Klaus, 1997). Further work would be required in order to determine if these adipocytes express markers specific for white or brown fat. Although the PVAT appears to impact both non-immunized and arthritic constriction response equally, the change in structure may be an important consideration when determining more specific changes, unique to the arthritic PVAT.

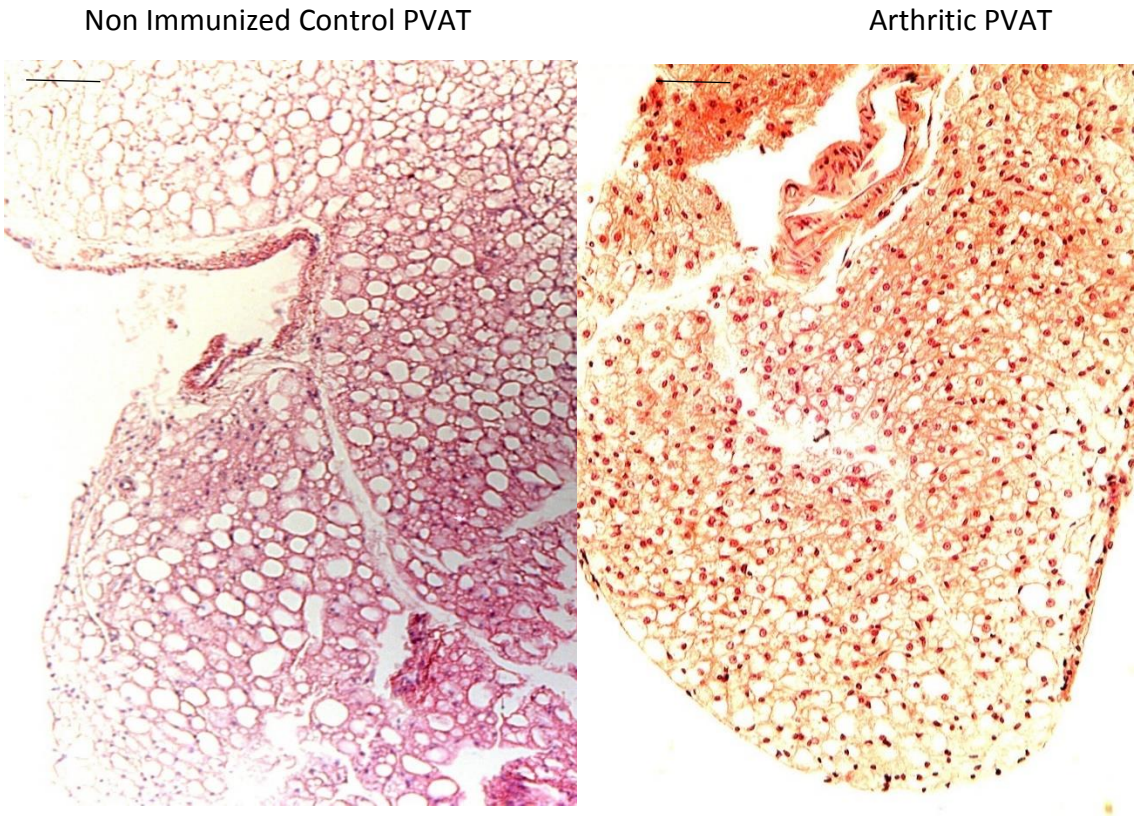

Figure 2.13 The Structural Differences in PVAT Between Controls and Arthritic Mice. A comparison of structural PVAT composition in regions of non-immunized and arthritic PVAT. Images show a change in appearance from typically white fat in non-immunized PVAT to a brown fat like phenotype in arthritic PVAT.

Surprisingly in this study we found no significant difference in the number of neutrophils in the vasculature following the onset of systemic inflammation. The peak in neutrophil ingress into an inflammatory environment occurs prior to the peak in macrophage ingress. This is due to macrophages being recruited to the region to clear out dead neutrophils (Godson *et al,* 2000). Thus our data suggest that our experimental samples were collected post the neutrophil peak (Figure 2.10). This could therefore explain the low percentage of neutrophils found in the aortic vessel wall and surrounding PVAT, in both non-immunized and arthritic aortas. It also goes some way to explain the overall lack of change in cell number, as although one specific cell subset may be increasing, another will be decreasing.

The observation that the numbers of macrophages are increased in both the aortic vessel wall and the surrounding PVAT, in the absence of overt CVD, is indeed novel. Many studies have reported ingress of macrophages into the aorta itself; however, the majority of these studies refer to the onset or development of atherosclerosis (Boisvert *et al,* 2006, Bennett, 2013). Here, we look at the very earliest changes to the vasculature following the onset of mCIA, suggesting that these changes happen prior to any CV development. It is important to note that in the mCIA model the presence of atherosclerotic plaque has never been confirmed. It is well established that F4/80+ macrophages are resident within the "healthy" aorta (Gerrity, 1981). As these cells are a resident population it is suggested that they play a role in "normal" tissue functions and homeostasis, such as, in tissue remodelling and angiogenesis (Fantin *et a*l, 2010). However, it is also known that local inflammation can drive the recruitment of monocytes to the aorta (Butcher and Galkina, 2012). Recent studies have shown that differing populations of macrophages exist within the aorta itself and these vary from M1 (Stanley *et al*, 1978), M2 (Stein *et al*, 1992) macrophages to MOX (Kadl *et al,* 2010) and M4 (Gleissner *et al*, 2010) macrophages. Such differentiation is dependent on the local micro environment these macrophages encounter once resident within the aorta (Italiani and Boraschi, 2014). Further studies are required for us to determine the inflammatory phenotype of these macrophages. However, the expansion we show in the arthritic vasculature is similar to that shown by Moore *et al* (2015) during hypertension. We suggest that this increase in macrophage number is highly likely to impact on vascular constriction. During inflammatory arthritis, it is well established that systemic levels of IFN-ϒ are increased (Kawashima and Miossec 2005). The increase in macrophages, coupled with this increase in such inflammatory mediators, could lead to the production of vasodilatory mediators, such as, nitric oxide (Fang, 2002).

The macrophage plays a critical role within the innate inflammatory response. In order for any inflammatory cell to infiltrate into the aortic vessel wall or the PVAT a change in the local micro environment is essential (Grivennikov *et al*, 2010). The mechanistic pathway that allows this change in local environment is currently unknown. However, we have shown that the number of macrophages does increase in both the aortic vessel wall and the surrounding PVAT, suggesting this change in micro-environment is a reality. It is likely that the resident macrophages present in these tissues act as sentinels during this process and thus act to recruit firstly neutrophils and secondly more macrophages to the regions (Schiwon *et al*, 2014). These resident macrophages produce cytokines that enable the endothelium of the aortic vessel to become "sticky". Expression of

adhesions molecules such as P-selectin (Hume, 2015), allows peripheral blood monocytes to be able to adhere to the vessel wall and cross the endothelial barrier - chemotaxis. Once these macrophages are within the region they can orchestrate the release of a number of pro-inflammatory cytokines to drive the inflammatory response (Dugue *et al*, 2014). This includes the production of Interleukin-12 (IL-12), to activate natural killer cells, IL-8 secretion to recruit neutrophils and TNF-α and IL-1, cytokines that are known hallmarks in RA (Beutler, 1999). Therefore, once the macrophage is recruited to the aortic vessel wall and surrounding tissues the inflammatory response is fully initiated.

It is clear from these data that the constitution of the tissues surrounding the vasculature (PVAT and aortic wall) will likely determine its functional responsiveness. As a potential effector molecule capable of degrading stromal tissue and impacting on contractility through its gelatinase and collagenase activity, we chose to study MMP-9 (Zorina *et al*, 2002). Primarily MMP-9 was chosen because of previous reports that described; firstly, increased levels associated with vascular dysfunction in mCIA (Reynolds *et al*, 2012) and secondly the reduced levels of MMP-9 observed in the absence of DR3 in AIA (Wang *et al*, 2014). MMP-9 is also of interest due to the capacity of DR3 signalling to trigger MMP-9 release from macrophages *in vitro* (Kang *et al*, 2005), (Collins *et al*, 2015). Here we show that the change in constriction response is not simply attributable to increased levels of MMP-9 in the aortic vessel wall, as previously suggested by Reynolds *et al*. There is no increase in total MMP-9 levels in the aorta itself and therefore does not correlate with the decreased response to 5-HT. As we know both macrophages and neutrophils produce MMP-9 (Lepidi *et al,* 2, Lin *et al*, 2005 and Webster *et al*, 2006). In the aorta the total numbers of macrophages are increased in comparison with non-immunized controls. This would suggest that the heightened macrophage population is not producing MMP-9 in this region. As the number of neutrophils in this region does not change, we would suggest this cell type as the potential main producer of MMP-9 in this region. Although neutrophils have not been shown as the main producer of MMP-9 in the vasculature, it has been shown that neutrophils are critical for delivery of pro-MMP9 to tumour sites, in early tumour development (Deryugina *et al*, 2014). This does not rule out the possibility of resident cells being the source of MMP-9 in our model.

Contrastingly in the PVAT we see a significant increase in the total expression of MMP-9. This is accompanied by increased macrophages but a static number of neutrophils. Therefore it is possible that in this region the main cell type producing total MMP-9 is the macrophage and thus is different to that within the aorta. Despite this increase in total MMP-9 we have not determined if this MMP-9 is activated. An excess in MMP-9 production, where the MMP-9 becomes activated would have an impact on the structure of the PVAT and its capability to produce any transferable factors thought to cause the dextral shift in constriction response. The lack of activation of MMP-9 may explain why the function of PVAT is not changed between non-immunized control and arthritic animals.

Of course it is important to consider that macrophages and neutrophils themselves are not the only cell types which are capable of producing MMP-9. Perhaps another cell type, present in both the aortic vessel wall and the surrounding PVAT population changes simultaneously with the changes in MMP-9 production. There are many cell

types in these regions that are capable of this production. For example, fibroblasts (Wang *et al*, 2007), adipocytes (Bouloumie *et al*, 2001), mast cells (Kanbe *et al*, 1999) and mesenchymal stem cells are all capable of MMP-9 production in these regions. Further study would be required to determine if any of these cellular populations would correlate with MMP-9 production in the aortic vessel wall and PVAT. However, from the studies we have already carried out we can show that MMP-9 production does not correlate with the changes seen in constriction response to 5-HT.

The final mediator that we looked at to answer the hypothesis within this chapter was DR3. Here, for the first time we demonstrate a complementary macrophage/DR3 expression profile in the absence of overt CVD, following inflammatory stimulus. Such a profile has been shown previously (McLaren *et al*, 2010) during inflammatory CVD, where DR3 signalling induced an increase in uptake of cholesterol into foam cells *in vitro*. In order to explain static total cell numbers, while the macrophage population is expanding, we postulate a mechanism of apoptosis occurring within our regions. If programmed cell death is occurring to either residential cells or early inflammatory cells, an increase in macrophage population would be concealed, by counting total cell number. If this is occurring it would be expected that markers of apoptosis such as FAS or Caspases would be up regulated. Expression of markers of apoptosis will be determined in the later chapters of this thesis. Therefore, we suggest DR3 as a potential mechanism orchestrating cell death via its "death domain" and therefore as a potential driving force behind the changing cellular populations that we see.

2.5 Conclusion

The work represented in this chapter shows validation of the arthritic vascular constriction response. We also demonstrate how PVAT causes a dextral shift in vascular constriction without impacting on maximal constriction response, in both health and disease. I have shown how total cell number doesn't change in either the aortic vessel wall or surrounding PVAT. This is despite macrophage number being increased in both regions. Macrophage expression is complimented by increased DR3 expression following arthritis onset and MMP-9 expression is increased only in the PVAT. It is suggested that changes in DR3 are integral to changes in the vascular constriction response via its role in increasing macrophage recruitment. Although we show increased macrophage and DR3 expression we have not fully elucidated the role of DR3 in vascular constriction response and how it impacts on the expression of mediators such as MMP-9. Within the next chapter we will fully explore the impact of DR3 in health and disease, determine its impact on vascular constriction and on changing inflammatory cell populations within the aortic vessel wall and PVAT.

Chapter 3 – Does Death Receptor 3 drive inflammatory changes in the vasculature during inflammatory arthritis?

3.1 Introduction

Previous work shown in Chapter 2 demonstrates that DR3 was up regulated in the aorta and PVAT of arthritic mice (Chapter 2). This response was matched by the increased expression profile of macrophages in both regions and correlated with decreased vascular constriction response to cumulative concentrations of 5-HT following arthritis onset. Previous reports suggested that MMP-9 was the driving force behind this impaired vascular function (Reynolds *et al*, 2012). However, the data showed that MMP-9 was only increased in the PVAT of arthritic mice and so was unlikely to cause the dysfunction "single handed". Therefore in this chapter we investigate the impact of DR3 in the vasculature of both healthy and mCIA mice. In particular we determine the impact on vascular constriction response and inflammatory measures in the aorta and surrounding PVAT.

The Death Receptor family is a sub-section of the Tumour Necrosis Factor Receptor (TNFR) superfamily and currently contains eight characterised members (Lavrick *et al*, 2005). DR3 is the closest relative to TNFR-1 having a 47% sequence homology compared to 20 – 30% for other TNFR family members (Cleveland and Ihle, 1995). The main identifying features of the Death Receptor group include the presence of a number of cysteine rich regions, along with an approximately 80 amino acid "death domain". The DR3 death domain is well characterised and is known to initiate apoptosis (Park *et al*, 2007). However, DR3 has a number of diverse roles that are related to its ability to activate NFκβ (Park *et al*, 2007). The activation of NFκβ allows DR3 to play a role in cell survival, along with differentiation and cell proliferation (Kitson *et al*, 1996; Chinnaiyan *et al*, 1996; Marsters *et al*, 1996), with cellular expression and localisation being imperative when determining the impact of DR3 on molecular pathways. Indeed roles for DR3 in numerous locations, including the lung, joints and vasculature are current topics of high interest.

Activation of DR3 occurs via binding of its high affinity ligand, TL1A (Migone *et al*, 2002). TL1A itself is a close relative of TNFα (Bamias *et al*, 2006; Jin *et al*, 2007), a master regulator of inflammation that is up-regulated in RA (Feldman *et al*, 2003). Cellular expression of TL1A is wide and is confirmed on monocytes, macrophages, plasma cells, dendritic cells, T-cells and endothelial cells (Pobezinskaya *et al*, 2011). Such extensive expression demonstrates the plethora of roles in which the DR3/TL1A signalling pathway could be involved. Moreover, cellular expression of TL1A can be induced by a variety of mechanisms, for example, following antigen presenting cell stimulation via the cross linking of FcϒR receptor (Meylan *et al,* 2011), activation of toll-like receptors (Casatella *et al*, 2007) and increased expression of IFN-ϒ (Shih *et al*, 2011). As such TL1A is implicated within the immune response and is further associated with key pro-inflammatory cytokines implicated during inflammatory arthritis.

As previously explained (Chapter 2), the binding of TL1A to DR3 can drive the activation of two different pathways (Figure 3.1). In brief, the binding of TL1A causes trimerisation of the DR3 receptor which then instigates a conformational change in the death domain

itself, allowing the recruitment of adaptor protein TNFR1 Associated Death Domain (TRADD). This is the point in the pathway where recruitment can either lead to apoptosis or conversely promote cell survival. To initiate apoptosis, TRADD recruits downstream proteins, ultimately resulting in the activation of a caspase complex, initiating cell death (Kruidering and Evan, 2000). Alternatively, TRADD can complex to activate a number of cell survival proteins, including NFκβ, ERK, JNK and p38 mitogen activated protein kinase pathways (Orange *et al*, 2005). Once activated NFκβ can pass into the nucleus where it works to up regulate cell survival transcription factors (Wen *et al*, 2003).

It is important to consider that recent studies have found a second ligand capable of binding to DR3 – Progranulin derived Atsttrin. Atsttrin acts as an antagonist of TNF and TNF Receptor signalling via the targeting of multiple TNF Receptors (Liu *et al*, 2014). Atsttrin works to inhibit the action of TL1A binding to DR3 and thus has mediated anti-inflammatory action in models of inflammatory arthritis (Tang *et al*, 2011). The following work does not look at the impact of Atsttrin or TL1A independently but looks at the whole system in a global context. AS DR3 was globally diminished, neither TL1A nor Atsttrin were able to signal. Thus all actions of either ligand through the DR3 receptor were inhibited.

DR3 was studied due to its association with both RA (Bull *et al*, 2008; Wang *et al*, 2014) and CVD (McLaren *et al*, 2010), while expression of its ligand TL1A is observed specifically within the aorta (McLaren et al, 2010). In RA, DR3 is linked with neutrophil accumulation in the arthritic joint (Bull *et al*, 2008) whereas in atherosclerosis, it is associated with macrophage differentiation to foam cells, a process intrinsic to plaque development (McLaren *et al*, 2010). There is also an association between DR3 and the up regulation of MMP-9 production during an inflammatory model of RA (Wang *et al*, 2014). Considering DR3 is implicated in RA and CVD, as well as being associated with increased MMP-9 production, it is suggested that it may play a key role in the vascular changes we see in mCIA. To further elucidate the role of the DR3 pathway we must consider its role physiologically as well as in pathological conditions.

This chapter highlights the experimental approaches used to determine whether DR3 played a role in the vascular dysfunction associated with our model of inflammatory arthritis. DR3 WT and DR3 Knockout ($DR3^{-/-}$) mice were used to determine the impact of DR3 on the constriction response of isolated aortic rings in both health and disease. To further investigate the impact of DR3 ablation, and to identify the relevance of potential changes in vascular constriction responses, the cell type and soluble factors produced within the aortic vessel wall and PVAT were studied. This chapter details methodology, results and discussion under the following objectives:

Hypothesis: DR3 drives arthritis associated vascular changes contributing to vascular dysfunction *in vivo.*

- To investigate the role of DR3 in vascular constriction response in health and disease.

- To identify and measure changes in the cell type and soluble mediators attributable to ablation of DR3 and to establish the role of DR3 specifically in the aorta and PVAT.
- To determine whether cellular ingress and mediator production drives vascular dysfunction in inflammatory arthritis in a DR3 dependent manor.

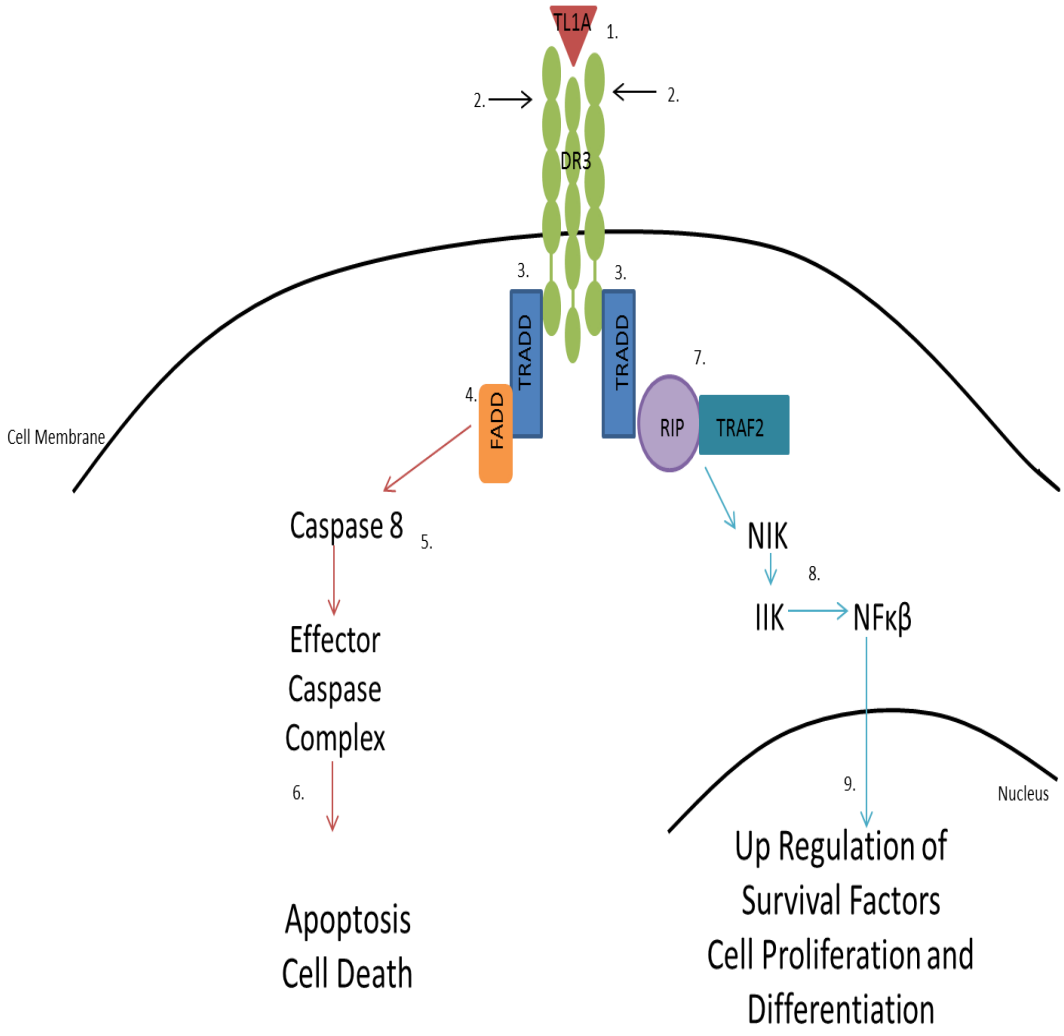

Figure 3.1 –The DR3/TL1A signalling cascade. 1. The binding of high affinity ligand TL1A to DR3 (2) leads to trimerization of the DR3 receptor on the cell membrane. (3) Following receptor activation, TRADD is recruited to the intracellular death domain. This can lead to activation of one of two intracellular signalling cascades. (4) The first of these cascades in driven by effector protein FADD, which is recruited by TRADD to the death domain. (5) Binding of FADD leads to activation of Pro-Caspase 8 and therefore induces an effector Caspase complex within the cell. (6) This protease enzyme complex is the trigger for apoptosis within the vell and ultimately leads to cell death. (7) The second of the possible pathways is driven by receptor interacting protein (RIP), which in turn recruits effector protein TRAF2 to the death domain. (8) The addition of TRAF2 drives the activation of transcription factor NF-κβ, via the NIK, IKK pathways. (9) Activated NF-κβ passes into the cell nucleus where it works to up regulate the transcription of cell survival proteins driving cell proliferation and differentiation.

3.2 Materials and Methods

New methods relevant to the work discussed in this chapter are described below, previous methods detailed in Chapter 3 also apply here.

3.2.1 Animals

Male mice (8 weeks old) were used for all experiments. The DBA DR3$^{-/-}$ colony was produced through backcrossing C57Bl/6^{het} mice with DBA/1 WT mice for 7 generations, allowing the breeding of DBA/1 DR3^{het} mice. DBA/1 DR3 knockout (DR3$^{-/-}$) and appropriately age-matched DBA/1 DR3 WT were then sourced from the in-house breeding colony, generated by DR3^{het} x DR3^{het} crossing. All animal care and experimental procedures complied with the United Kingdom Animals (Scientific Procedures) Act 1986 and were under the authority of Home Office Project Licence (30/2928).

3.2.2 Genotyping

3.2.2.1 Preparation of Cell Lysis Buffer for DNA Extraction

Table 3.1 – Genotyping Materials

Reagent	Description
0.5mM EDTA	
Tris HCl 300mM NaCl	
1% SDS	
Proteinase K	Roche Diagnostics
Isopropanol	Fisher Scientific
70% (v/v) Ethanol	Fisher Scientific
dNTPs	Invitrogen
10 x Buffer	Invitrogen
50mM $MgCl_2$	Invitrogen
Taq Polymerase	Invitrogen
DNA ladder	Invitrogen

Lysis buffer was prepared as a master mix containing the following constituents. The volumes given are those required per sample being lysed.

Table 3.2 – Lysis Buffer Materials

Reagent	Volume Per Sample (mls)
Distilled Water	12.6
0.5 mM EDTA	2
Tris HCl	1
300mM NaCl	0.4
1% (w/v) SDS	2

3.2.2.2 Preparation of Master Mix for Polymerase Chain Reaction

Table 3.3 - Genotyping Primer Sequences

Primer	Sequence
AV1	CAT CGC CTA TCG CCT TC
4F	AGA AGG AGA AAG TCA GTA GGA CCG
2R	GAA AGG ATG CTT GCC TGT TGG

Table 3.4 – Genotyping Reagents

Reagent	Volume Per Sample (µl)
dNTPs	5
10x Buffer	4
50mM $MgCl_2$	1.2
AV1 Primer	0.2
4F Primer	0.6
2R Primer	0.8
Taq	0.5

The reagents for PCR were made as a master mix before adding to each sample.

3.2.2.3 Preparation of a 1.6% (w/v) Agarose Gel

Table 3.5- Genotyping Gel Reagents

Reagent	Manufacturer
Ultra-Pure Agarose	Invitrogen
1x Tris Borate EDTA (TBE)	1 in 10 dilution with dH_2O of 10x TBE purchased from Fisher Scientific
Ethidium Bromide	Sigma

2.4g of ultra pure agarose was added to 150ml of 1xTBE and heated in a microwave for 1 minute 50 seconds, with occasional stirring. 7.5µl of 10mg/ml ethidium bromide was added and the gel was poured into a mould to set.

3.2.2.4 Preparation of Orange G

Orange G was required at a concentration of 2.5mg/ml (v/v) and was prepared in 2x TBE containing 30% (v/v) glycerol.

3.2.2.5 DNA Extraction and Purification for Genotypic Analysis

Ear punches or tail tips were taken from all new animals in the DR3 breeding colony at approximately 4 weeks of age. Each was lysed by adding 750µl of lysis buffer and 20µl of 1.3% Proteinase K (Roche) at 56^0C overnight. Salt extraction of DNA was then carried out by the addition of 310µl of 5M NaCl, vortexing and incubating at room temperature for 30 minutes. Following the formation of a precipitate, samples were centrifuged for 25 minutes at 13250g. 800µl of the DNA containing, clear supernatant from each sample was subsequently used for purification.

In order to purify DNA, 500µl of ice cold isopropanol was added to each sample. Following thorough mixing, samples were centrifuged for 10 minutes at $13250_{g.}$ Following removal of the supernatant, 500µl of 70% (v/v) ethanol was added to each sample and left for 30 minutes at room temperature. After final centrifugation was carried out for 10 minutes at 13250g, all excess liquid was removed and the samples left to dry at 37^oC for 45 minutes. For short term storage (overnight) samples were re-suspended in 50µl of dH_2O.

3.2.2.6 Polymerase Chain Reaction

The PCR required 8µl of extracted DNA (500ng/µl), which was added to a 0.5ml thin walled reaction tube (Star Labs). 12.1µl of master mix (Table 3.4) and 19.9µl of dH_2O was added to each sample. The following cycles were initiated on the Mygene Series Peltier Thermal Cycler.

Table 3.6- PCR Cycles for DR3 Colony Genotyping

Temperature (°C)	Time	Number of Cycles
94	5 minutes	1
60	45 seconds	
72	45 seconds	
94	45 seconds	33
60	45 seconds	
72	45 seconds	
94	45 seconds	1
60	45 seconds	
72	5 minutes	

3.2.2.7 Visualising PCR Products

To visualise PCR products, 4µl of Orange G solution was added to each sample. 20µl of each sample was then loaded into a well of a 1.6% (w/v) agarose gel. A DNA ladder (5µl) was also run in the final well of each gel, to allow identification of product bands. The gel was run at 100V for 90 minutes and then visualised under UV light.

3.3 Results

3.3.1. Ablation of DR3 Does Not Impact On Vascular Constriction Response

Vascular constriction response to 5-HT was measured in PVAT intact and PVAT denuded thoracic aortic rings of DR3 WT and DR3$^{-/-}$ mice in the absence of arthritis. In DR3 WT the presence of PVAT produced a significant ($p<0.0001$) dextral shift (logEC50) in the constriction response curve to 5-HT (-6.65 ± 0.09 vs. - 5.86 ± 0.13 mN) (Figure 3.2 (A)). The presence of PVAT was also associated with a significant ($p<0.0001$) decrease in the maximal constriction response to 5-HT (RMAX) (8.06 ± 0.31 vs. 6.99 ± 0.48 mN). The PVAT impacted DR3$^{-/-}$ vascular constriction responses in the same way, with a significant ($p<0.0001$) dextral shift (logEC50) in the constriction response curve (-6.74 ± 0.12 vs. -6.05 ± 0.15 mN) and significant ($p<0.0001$) decrease in RMAX (7.81 ± 0.42 vs. 6.19 ± 0.49 mN) being observed (Figure 3.2 (B)).

When DR3 WT and DR3$^{-/-}$ vascular constriction responses were compared in both PVAT denuded (Figure 3.2 (C)) and PVAT intact vessels (Figure 3.2 (D)), no differences were observed with regard to either EC50 or RMAX.

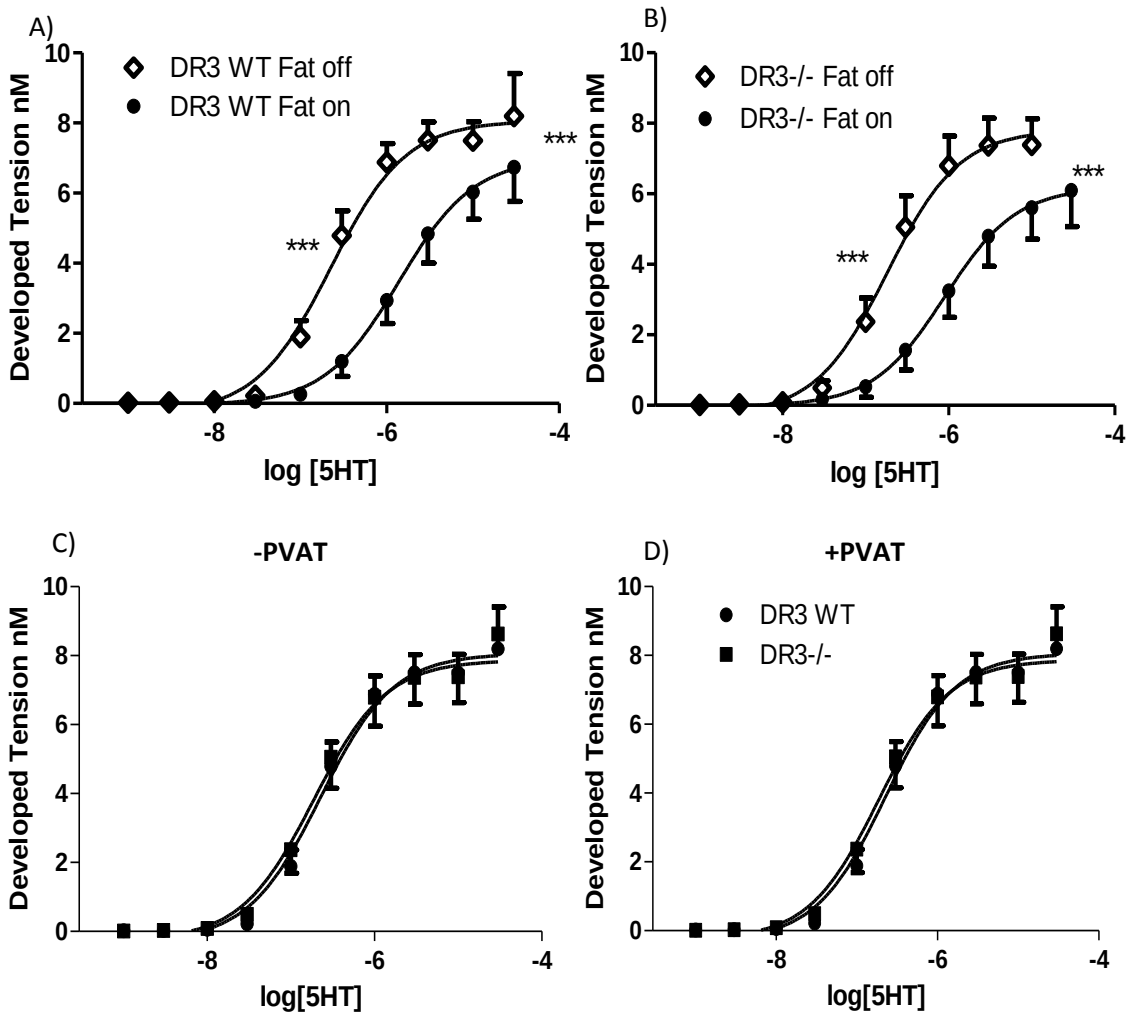

Figure 3.2- Comparison of the DR3 WT and DR3$^{-/-}$ Constriction Response Curves, in the Absence of Arthritis. Constriction response to 5HT was determined for non-arthritic PVAT intact (+PVAT) and PVAT denuded (-PVAT) DR3 WT (N=7) (A) and DR3$^{-/-}$ aortic rings (N=6) (B). The -PVAT (C) and +PVAT (D) constriction responses for DR3 WT and DR3$^{-/-}$ rings were also compared. ***=p<0.0001

3.3.2. The Ablation of DR3 Drives Increased Total Cell Numbers into the PVAT.

Total cell numbers within the aortic vessel wall and the surrounding PVAT were calculated in samples from DR3 WT and DR3$^{-/-}$ mice in the absence of arthritis (Figure 3.3). No difference was observed between groups with regard to the vessel wall (4857 ± 242.3 (N=17) vs. 4387 ± 112.9 cells/mm^2 (N=19) for DR3 WT and DR3$^{-/-}$ respectively). However, within the PVAT, a significant (p=0.003) increase was seen in total cell number following the ablation of DR3 (2278 ± 195.8 (N=17) vs 3031 ± 138.4 cells/mm^2 (N=19)) for DR3 WT and DR3$^{-/-}$ respectively).

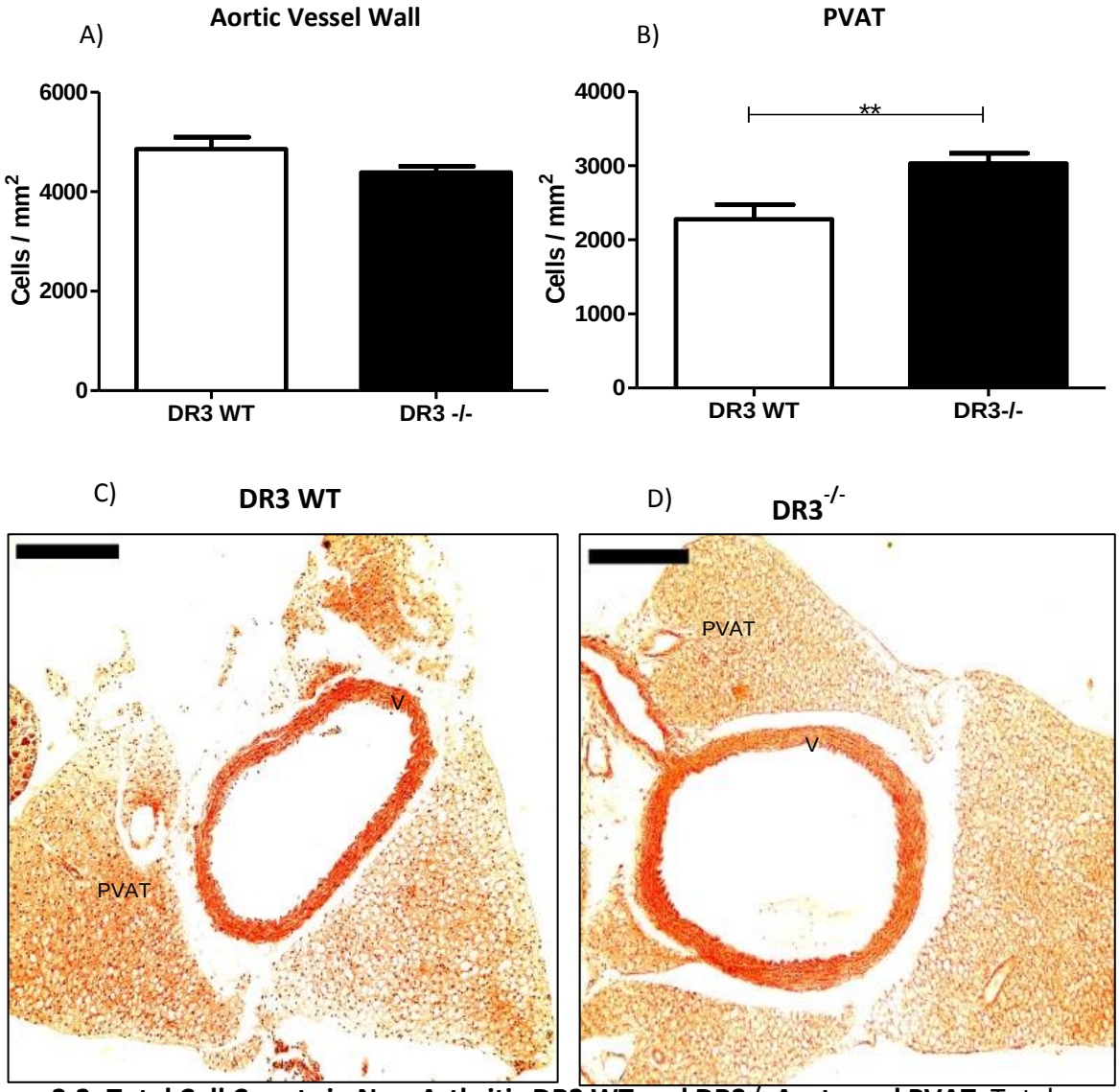

Figure 3.3- Total Cell Counts in Non-Arthritic DR3 WT and DR3$^{-/-}$ Aorta and PVAT. Total cell numbers were counted in the aortic vessel wall (A) and the surrounding PVAT (B) for DR3 WT (N=17) and DR3$^{-/-}$ (N=19) mice. Representative images show DR3 WT (C) and DR3$^{-/-}$ (D) vasculature. Images are taken at x20 magnification and scale bars represent 0.2µm. **=p<0.01.

3.3.3. Ablation of DR3 Impacts on the Inflammatory Profile of the Vasculature

Inflammatory cells and their mediators are found within the aortic vessel wall and the surrounding PVAT of DR3 WT and DR3$^{-/-}$ mice. F4/80+ macrophages were identified (Figure 3.4) though no significant change was seen between DR3 WT and DR3$^{-/-}$ in either the aortic vessel wall (5.22 ± 0.75% (N=11) vs. 3.62 ± 0.75% (N=9)), or surrounding PVAT (2.81 ± 0.61% (N=11) vs. 1.88 ± 0.53% (N=9)).

Conversely Ly6G positive cells (Figure 3.5), indicative of neutrophils, were significantly ($p=0.005$) increased in the vessel wall of DR3$^{-/-}$ compared to DR3 WT mice (19.13 ± 3.0 (N=4) vs. 4.7 ± 2.2 (N=5)). PVAT Ly6G expression is not affected by DR3 ablation (15.9 ± 4.9% (N=4) vs. 7.8 ± 4.6% (N=5)) for DR3 WT and DR3$^{-/-}$ respectively).

Since MMP-9 is a potential underlying cause of vascular dysfunction in the mCIA model, and is further linked to expression of DR3, its levels within the non-arthritic vasculature were determined (Figure 3.6). Expression within the aortic vessel wall of DR3 WT and DR3$^{-/-}$ mice was similar (11.29 ± 2.78% (N=14) vs. 13.58 ± 1.73% (N=16)). However, in the PVAT, a significant ($p=0.0065$) increase in MMP-9 expression was observed following the ablation of DR3 (12.26 ± 2.21% (N=12) vs. 25.67 ± 3.54% (N=16) for DR3 WT and DR3$^{-/-}$ respectively).

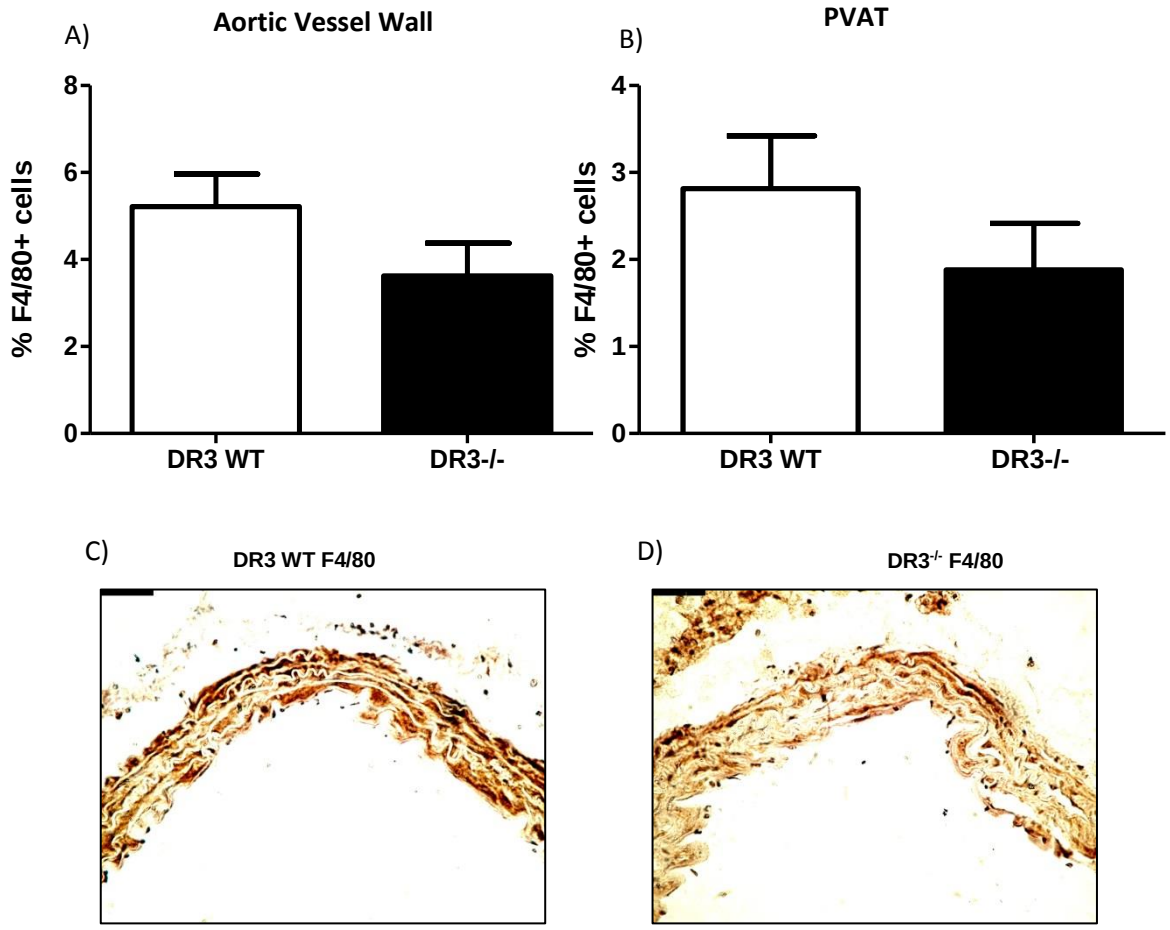

Figure 3.4 – Effect of DR3 Ablation on Macrophage Number in the Vasculature. The % of cells expressing macrophage marker F4/80 was determined in the aortic vessel wall (A) and surrounding PVAT (B) for DR3 WT (N=11) and $DR3^{-/-}$ (N=9) mice. Representative images show F4/80 positive staining (Brown Staining) in non-arthritic DR3 WT (C) and $DR3^{-/-}$ (D) vasculature. Images are taken at x20 magnification and scale bars represent 0.25µm.

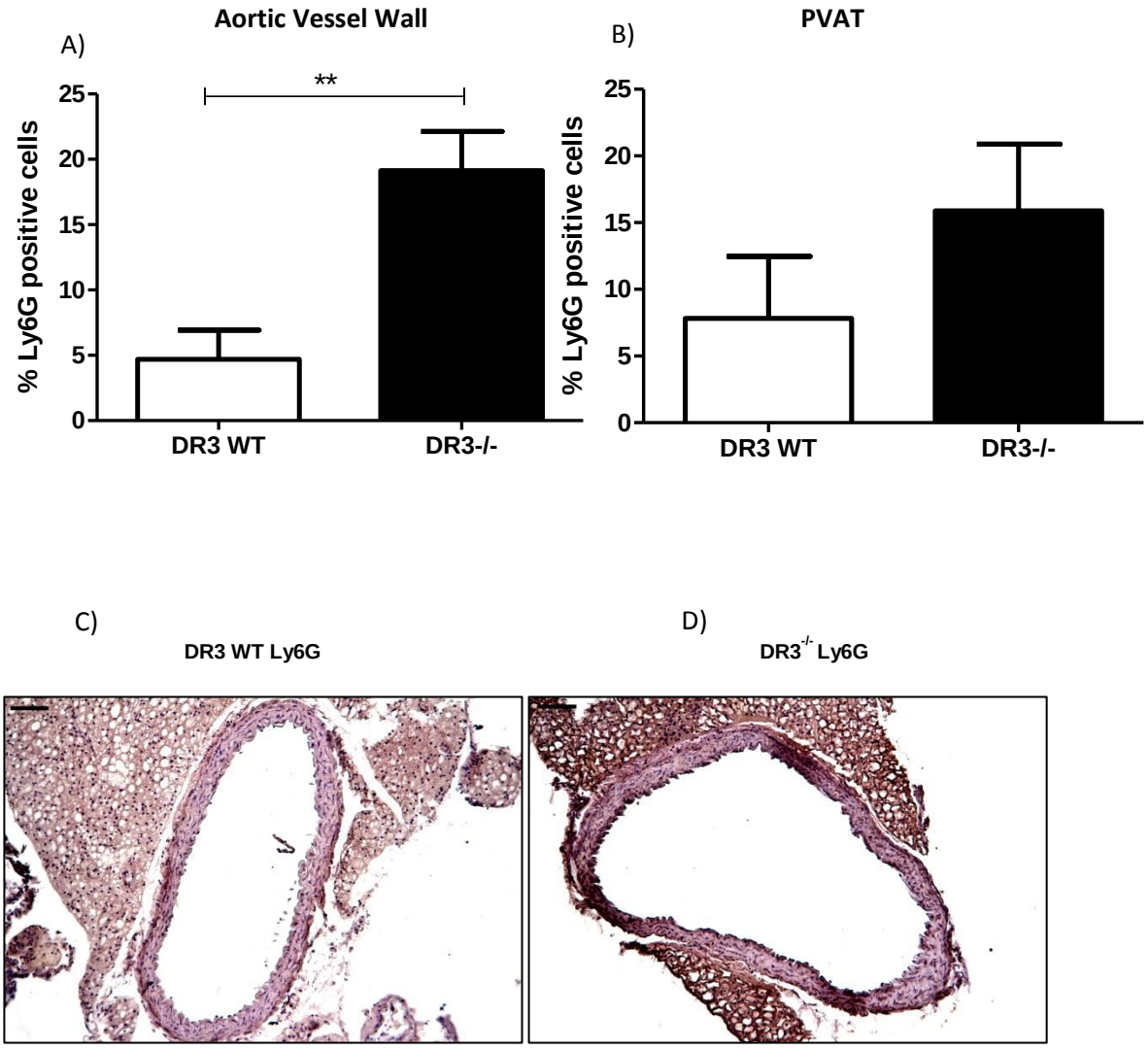

Figure 3.5 – Effect of DR3 Ablation on the Expression of Ly6G in the Vasculature. The % of Ly6G expression was determined in the aortic vessel wall (A) and surrounding PVAT (B) for DR3 WT (N=5) and DR3$^{-/-}$ (N=4) mice. Representative images show Ly6G positive staining (Brown Staining) in non-arthritic DR3 WT (C) and DR3$^{-/-}$ (D) vasculature. Images are taken at x10 magnification and scale bars represent 0.25µm. **p<0.01.

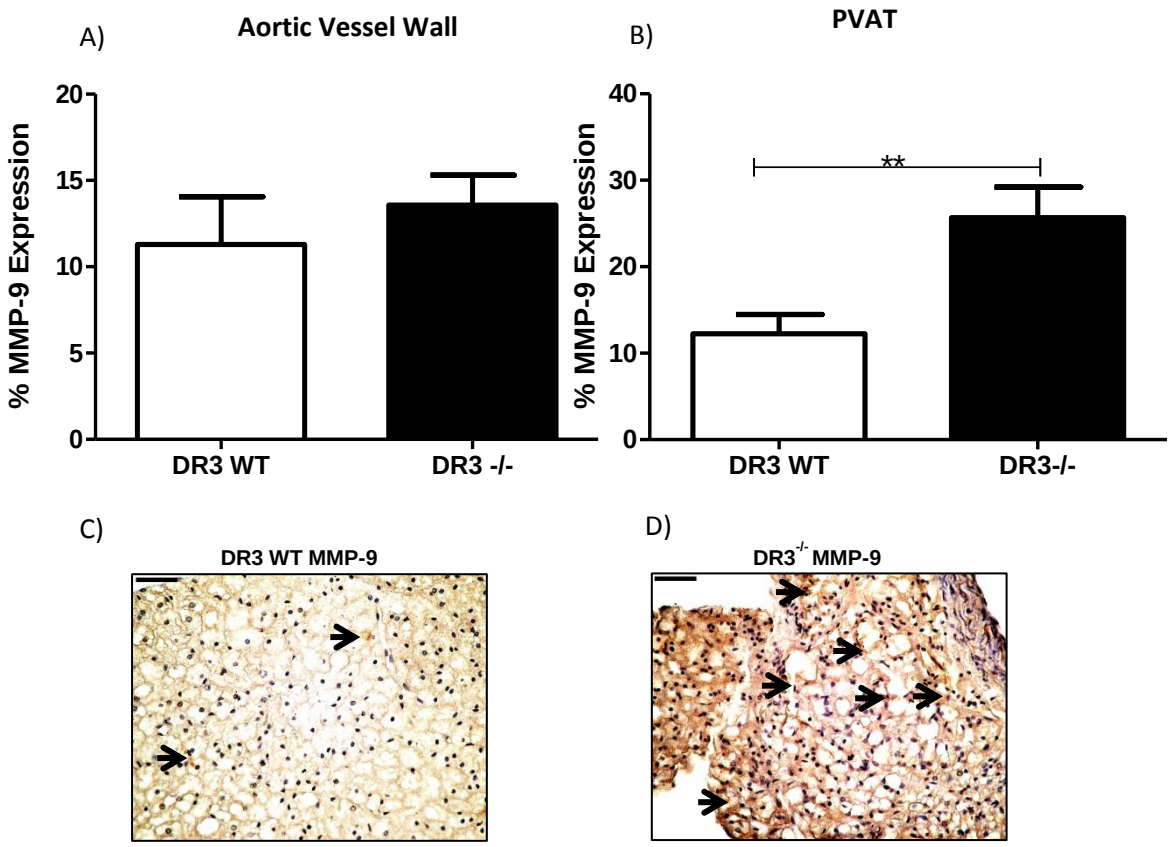

Figure 3.6 – Effect of DR3 Ablation on the Expression of MMP-9 in the Vasculature. The % of MMP-9 expression was determined in the aortic vessel wall (A) and surrounding PVAT (B) for DR3 WT (N=12) and DR3$^{-/-}$ (N=16) mice. Representative images show MMP-9 positive staining (Brown Staining) in non-arthritic DR3 WT (C) and DR3$^{-/-}$ (D) PVAT. Images are taken at x20 magnification and scale bars represent 0.25µm. **=p<0.01.

3.3.4. Ablation of DR3 Does Not Impact on TL1A Expression

As TL1A antibodies are not commercially available, the impact of knocking out DR3 on TL1A expression was determined using RTqPCR. There was no difference in expression of TL1A within the vasculature (aortic vessel and PVAT combined) (0.324 ± 0.75 (N=4) vs. 0.427 ± 0.28 (N=3)).

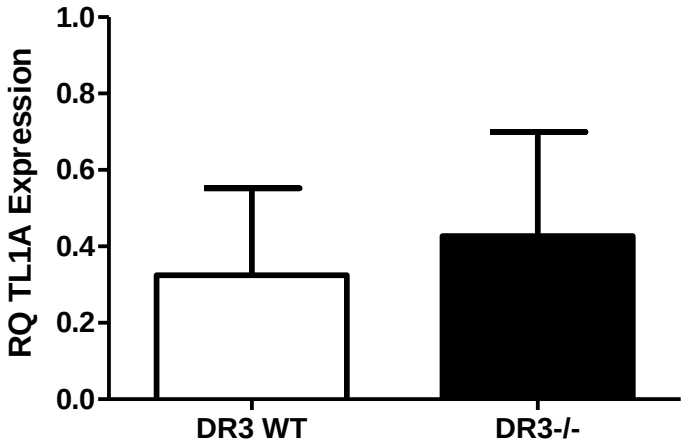

Figure 3.7 – Effect of DR3 Ablation on the Expression of TL1A. Expression of TL1A in the aortic vessel wall and PVAT combined as determined by RTqPCR.

3.3.5 Arthritis Incidence in DR3 WT and DR3$^{-/-}$ Mice

mCIA was initiated in on average 93% of DR3 WT mice by day 34. This was compared with an average of 38% of DR3$^{-/-}$ mice, over three separate experiments (Figure 3.8). The arthritis incidence between DR3 WT and DR3$^{-/-}$ was decreased following ablation of DR3, however, this difference is non-significant, at any time point over the time course. Of those mice that did get arthritis by the experimental end point total paw score significantly ($P<0.05$) reduced in DR3$^{-/-}$ mice in comparison to DR3 WT mice. However, hind paw diameter of experimental animals did not differ significantly between all DR3 WT and DR3$^{-/-}$ mice.

During all experiments, DR3 WT and DR3$^{-/-}$ mice were housed together and had the same *ab libtum* access to food and water. There was no difference in weight prior to, or at the point of the booster immunization (day21). Despite the difference in arthritis incidence between DR3 WT and DR3$^{-/-}$ there was no significant difference in weight at any point throughout the time course.

In order to check locally at the impact of systemic inflammatory arthritis the joints within the feet were analysed for aspects of inflammation. All of the inflammatory markers were down regulated within the joints of DR3$^{-/-}$ mice when compared with DR3 WT. Subsynovial inflammation was significantly ($p<0.0011$) decreased (2.75 ± 0.25 (N=4) vs. 0.5 ± 0.29 (N=4)). This was matched by a significant ($p=0.005$) decrease in synovial hyperplasia and panus formation (1.75 ± 0.25 vs. 0.25 ± 0.25). Synovial exudate (0.50 ± 0.29 vs. 0.25 ± 0.25), cartilage and bone erosions (1.25 ± 0.49 vs. 0) were decreased, but not significantly. To determine the arthritis index the total of the 4 inflammatory measures was calculated and was significantly ($p=0.0015$) decreased in DR3$^{-/-}$ joints in comparison with DR3 WT (6.25 ± 0.75 vs. 1.0 ± 0.58) (Figure 3.9).

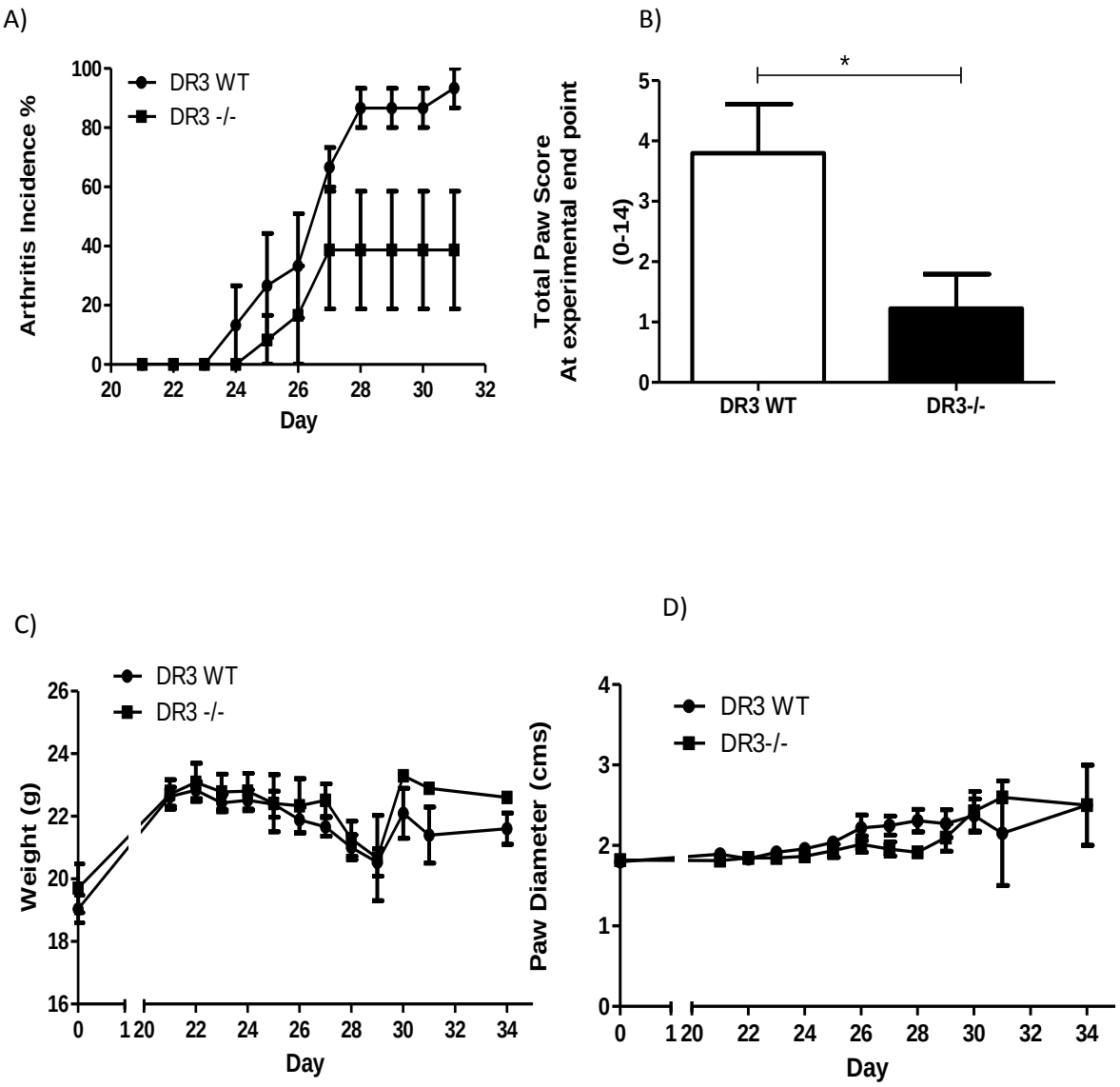

Figure 3.8 - Arthritis Induction in DBA/1 Mice over a 45 Day Time Course. Arthritis Incidence was shown over 6 experiments, for a total of 48 experimental mice (A). Total Paw Score is shown over a 45 day time course (N=48) (B). Individual hind paw diameter (including right and left measurements) are shown for arthritic (N=52) vs. Non-Immunized control paws (N=24) (C). Individual Paw score and Paw diameter were correlated for 2 experiments (N=16) (D). *=$p<0.05$.

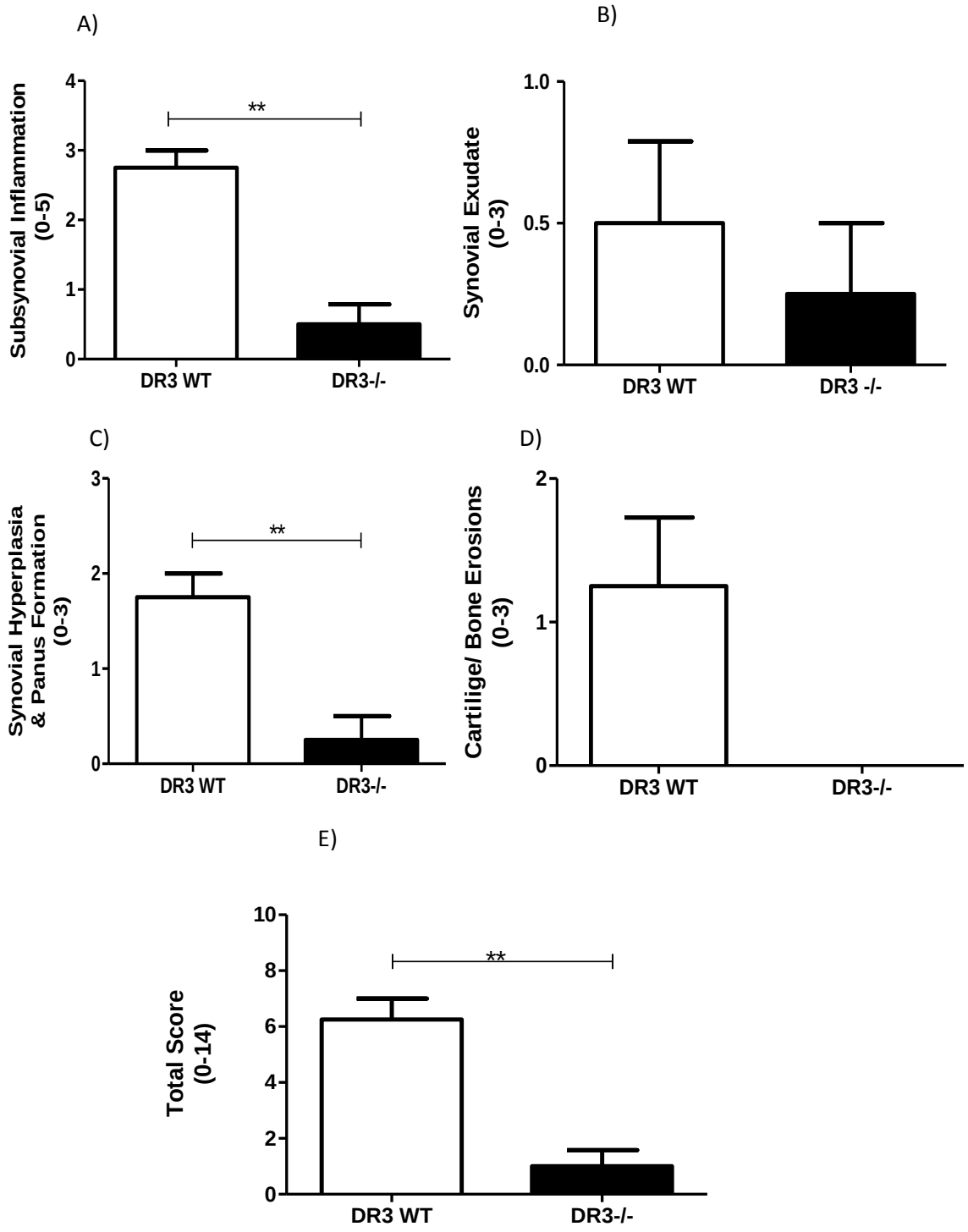

Figure 3.9- Measurement of Arthritis Index. Inflammatory measured were analysed following haematoxylin and eosin staining of ankle joints from DR3 WT (N=4) and DR3$^{-/-}$ (N=4). Inflammatory measures included; subsynovial inflammation (A), synovial exudate (B), synovial hyperplasia and panus formation (C) and cartilage/ bone erosions (D). A final total score of all inflammatory measures makes up the arthritis index (E). **=p<0.01.

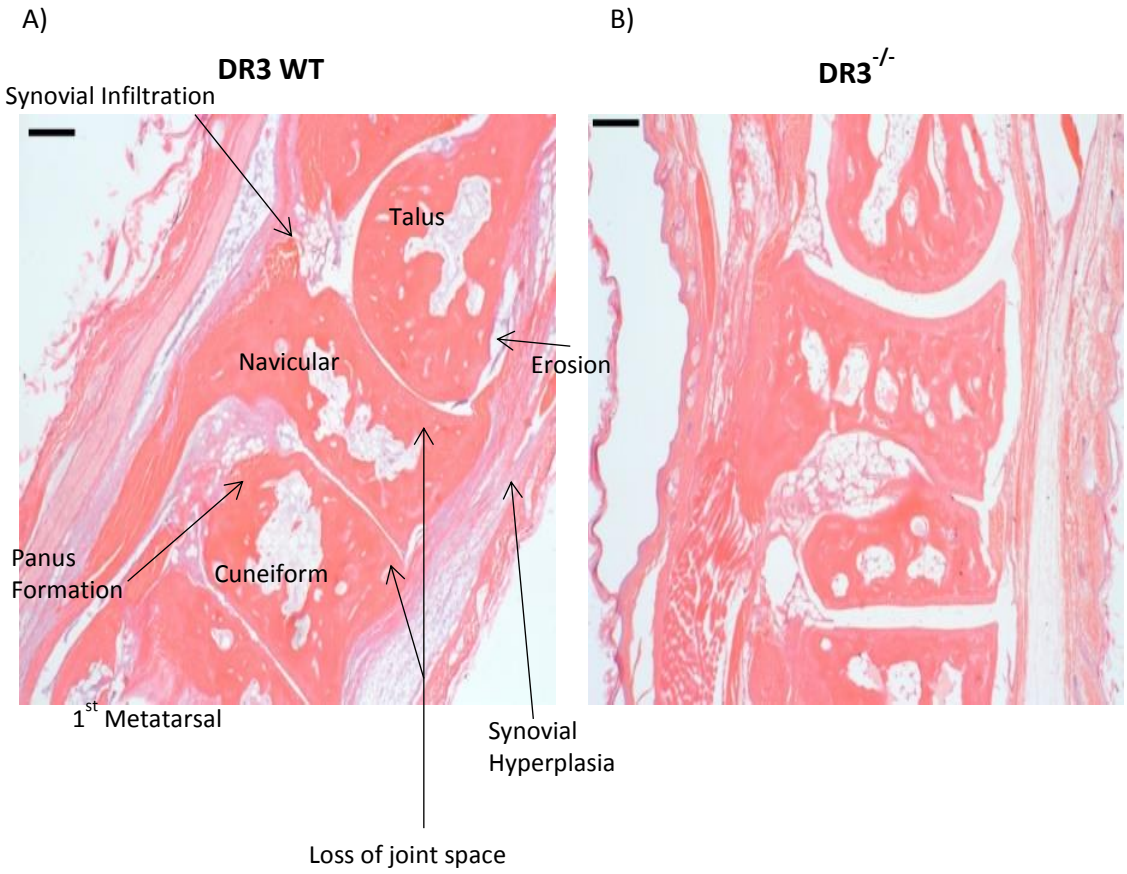

Figure 3.10- Representative Images of Changes in Arthritis Index. The foot joints were assessed for arthritic damage in order to determine arthritis index. Joints from DR3 WT (A) and DR3$^{-/-}$ (B) were assessed.

3.3.6. Arthritis Induction and DR3 Ablation Significantly Alters the Vascular Constriction Response.

Vascular constriction response to 5-HT was measured in arthritic DR3 WT and DR3$^{-/-}$ thoracic aortic rings, PVAT denuded and PVAT intact. When constriction response was determined in DR3 WT thoracic rings the presence of PVAT had no significant impact on either the half maximal or maximal constriction response, determined by EC50 and RMAX measurements respectively. The PVAT, however, did significantly (p=0.014) impact the DR3$^{-/-}$ constriction response, PVAT shifted the curve dextrally, without impacting on maximal constriction.

When the fat denuded constriction response curves for arthritic DR3 WT and DR3$^{-/-}$ rings were compared no difference was seen in the half maximal constriction response. However, the maximal constriction of DR3$^{-/-}$ rings were significantly (P=0.0004) reduced when compared to arthritic DR3 WT rings (4.938 ± 0.21 (N=10) vs. 3.527 ± 0.16 mN (N=6)).

When PVAT remains intact, half maximal constriction for arthritic DR3 WT and DR3$^{-/-}$ rings is comparable. However, unlike in fat denuded tissues the maximal constrictions were also comparable, with no change being seen between DR3 WT and DR3$^{-/-}$.

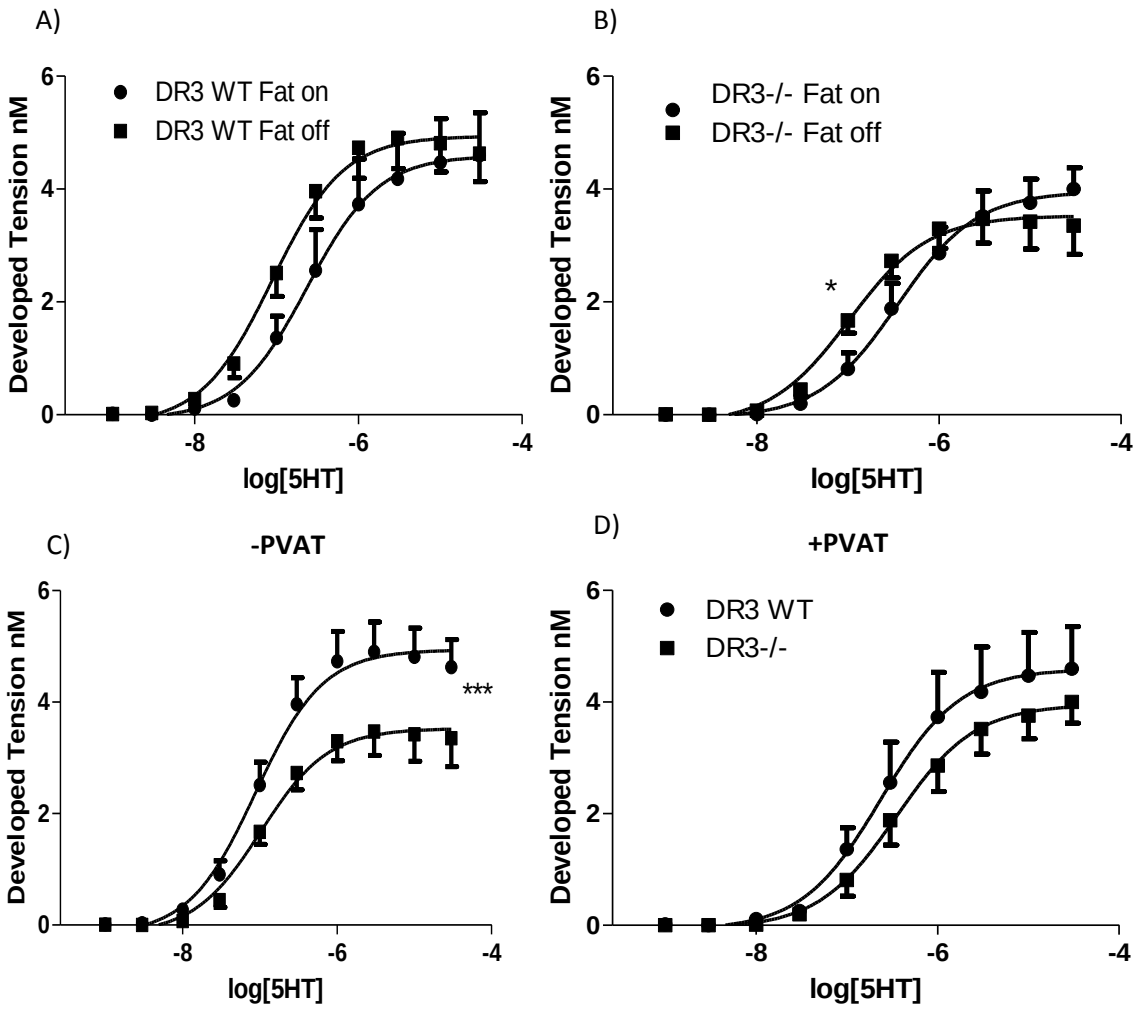

Figure 3.11- Comparison of the Arthritic DR3 WT and DR3$^{-/-}$ Constriction Response Curves. Constriction response to 5HT was determined for PVAT intact vs. PVAT denuded arthritic DR3 WT aortic rings (N=10) (A) and for DR3$^{-/-}$ aortic rings (N=6) (B). The PVAT denuded constriction responses for DR3 WT and DR3$^{-/-}$ rings were compared (C), along with the PVAT intact responses (D). *=p<0. 05, ***=p<0.001.

3.3.7. Arthritis Does Not Impact on Total Cell Number Within the Aorta or Surrounding PVAT Between DR3 WT and DR3$^{-/-}$.

Following the onset of mild arthritis, total cell numbers within the aortic vessel wall and the surrounding PVAT were calculated, in DR3 WT and DR3$^{-/-}$ (Figure 3.12). There was no significant difference in total cell number following arthritis onset within the aortic vessel wall (5096 ± 722.8 (N=8) vs. 3325 ± 571.3 cells/mm^2 (N=6)). Similar results were seen in the PVAT, with no significant difference in total cell number following arthritis onset (2807 ± 269.6 vs. 3035 ± 489.5 cells/mm^2).

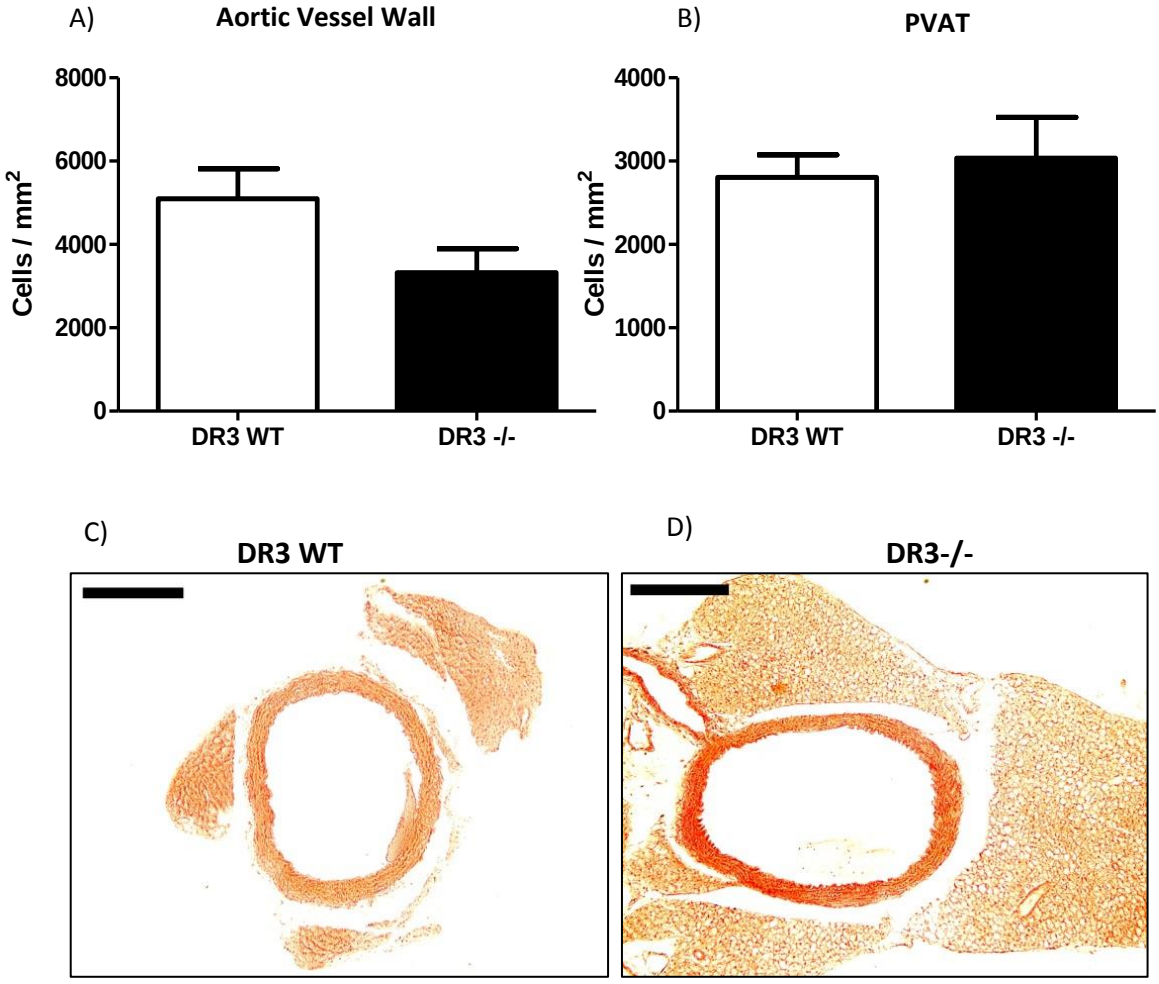

Figure 3.12- Total Cell Counts in Arthritic DR3 WT and DR3$^{-/-}$ Aorta and PVAT. Total cell numbers were counted in the aortic vessel wall (A) and the surrounding PVAT (B) for arthritic DR3 WT (N=8) and DR3$^{-/-}$ (N=6) mice using haematoxylin and eosin staining. Representative images show DR3 WT (C) and DR3$^{-/-}$ (D) vasculature. Images are taken at x10 magnification and scale bars represent 0.2µm.

3.3.8. Onset of Mild Arthritis Significantly Changes the Inflammatory Profile of the Vasculature in a DR3 Dependent Manor.

Following the onset of arthritis increased inflammatory cells are found within both the aortic vessel wall and the surrounding PVAT of $DR3^{-/-}$ mice. Firstly, F4/80+ macrophages were identified in both regions in DR3 WT and $DR3^{-/-}$ vasculature (Figure 3.13). The ablation of DR3 had no significant impact on the presence of F4/80+ cells within the aorta and expression was stable when DR3 WT were compared with $DR3^{-/-}$(7.37 ± 1.73% (N=8) vs. 7.99 ± 2.69% (N=6)). However, a significant (p=0.031) increase was seen within the PVAT when DR3 WT was compared with $DR3^{-/-}$ (14.02 ± 1.86% vs. 23.15 ± 5.40%).

The percentage of cells expressing neutrophil marker Ly6G was also determined (Figure 3.14). A small percentage of cells expressed Ly6G in DR3 WT and $DR3^{-/-}$ arthritic vasculature. In the aortic vessel wall Ly6G expression is significantly (p=0.01) increased, following arthritis induction in $DR3^{-/-}$ (0.372 ± 0.16% (N=5) vs. 1.806 ± 0.48% (N=4)). A similar significant (p=0.01) increase in Ly6G expression is seen within the PVAT of $DR3^{-/-}$ mice (0.467 ± 0.10% vs.1.754 ± 0.35%).

As previously identified as having importance in vascular dysfunction, MMP-9 levels within the vasculature were also determined (Figure 3.15). MMP-9 expression in the aorta is stable following arthritis induction, between DR3 WT and $DR3^{-/-}$ mice (14.38 ± 2.80% (N=7) vs. 11.73 ± 3.24% (N=5). In the PVAT MMP-9 expression is also steady following arthritis induction and DR3 ablation (34.39 ± 2.81% vs. 18.11 ± 6.45%).

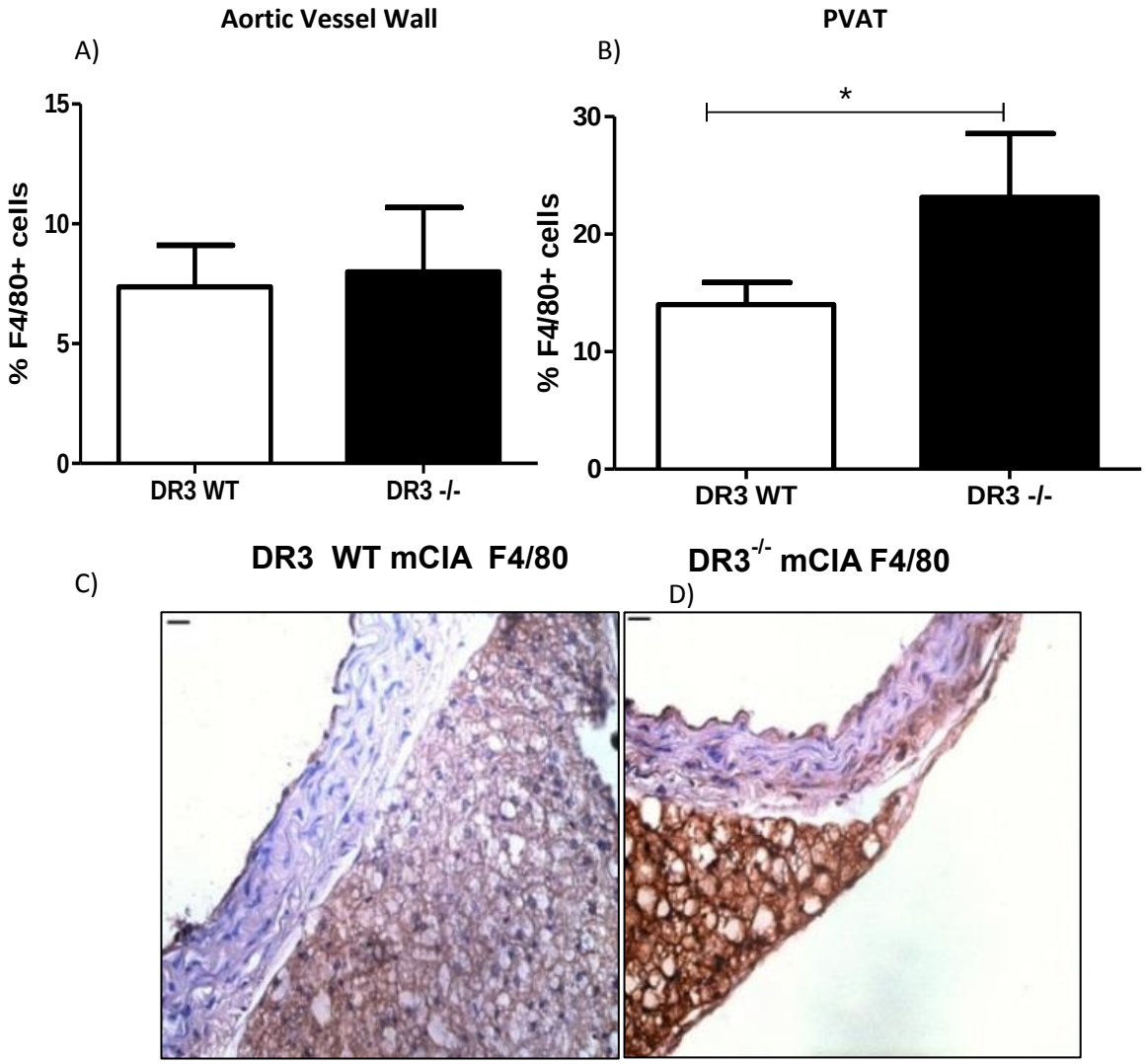

Figure 3.13– Effect of Arthritis Induction and DR3 on Macrophage Number in the Vasculature. The % of cells expressing macrophage marker F4/80 was determined in the aortic vessel wall (A) and surrounding PVAT (B) for arthritic DR3 WT (N=8) and DR3$^{-/-}$ (N=6) mice. Representative images show F4/80 positive staining in DR3 WT (C) and DR3$^{-/-}$ (D) vasculature. Images are taken at x40 magnification and scale bars represent 0.2µm. *=p<0.05.

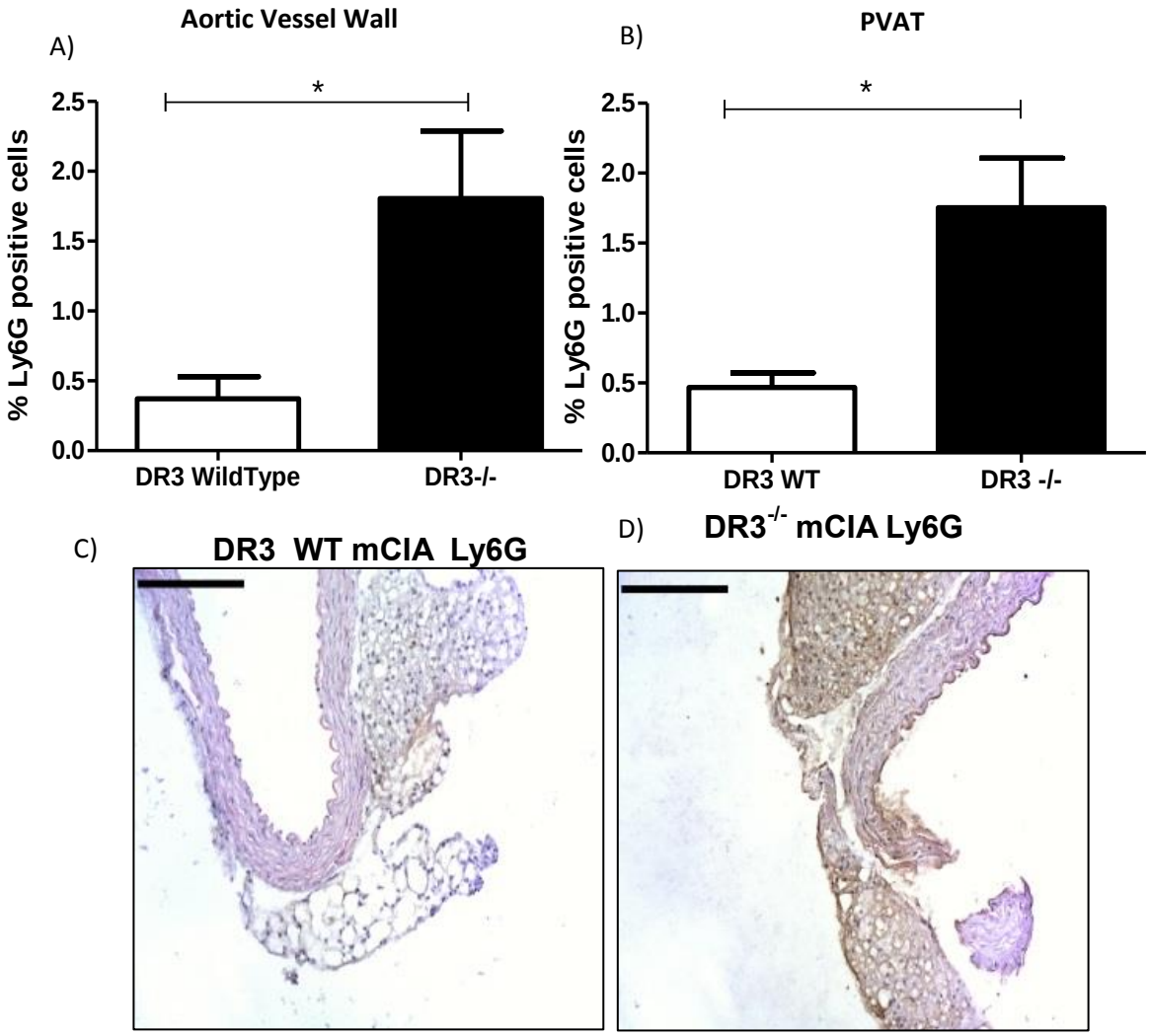

Figure 3.14– Effect of Arthritis Induction and DR3 on Neutrophil Number in the Vasculature. The % of cells expressing neutrophil marker Ly6G was determined in the aortic vessel wall (A) and surrounding PVAT (B) for arthritic DR3 WT (N=5) and DR3$^{-/-}$ (N=4) mice. Representative images show Ly6G positive staining in DR3 WT (C) and DR3$^{-/-}$ (D) vasculature. Images are taken at x20 magnification and scale bars represent 0.25µm.*=p<0.01.

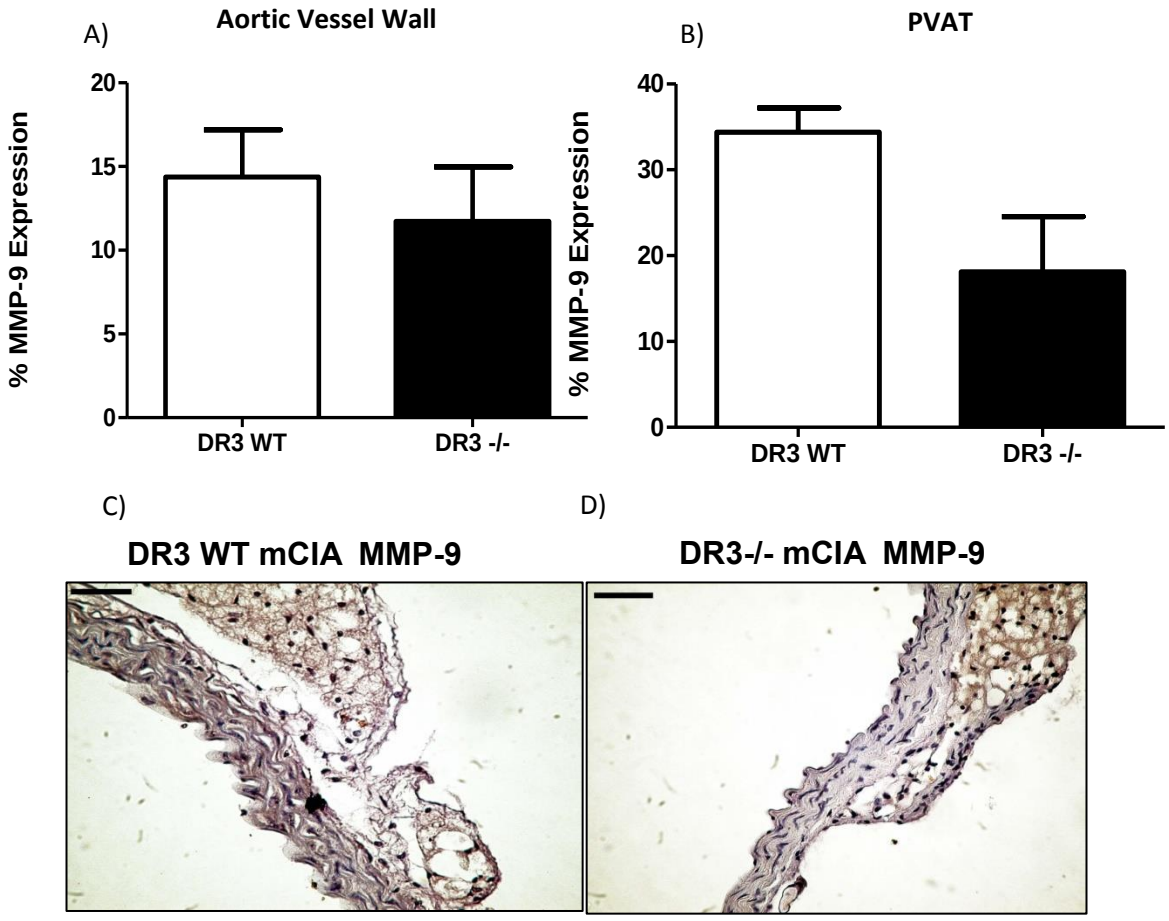

Figure 3.15– Effect of Arthritis Induction and DR3 on MMP-9 Production in the V asculature. The % of MMP-9 expression was determined in the aortic vessel wall (A) and surrounding PVAT (B) for arthritic DR3 WT (N=7) and DR3$^{-/-}$ (N=5) mice. Representative images show MMP-9 positive staining in DR3 WT (C) and DR3$^{-/-}$ (D) vasculature. Images are taken at x20 magnification and scale bars represent 0.25µm.

3.4 Discussion

In unchallenged healthy aorta (+/- PVAT), DR3 ablation does not impact on the vascular constriction response. However, when comparing the same parameters between in house bred DBA/1 DR3 colony mice and Harlan WT, some striking differences were noted. The presence of PVAT decreases the RMAX in unchallenged DR3 colony mice, whereas, it had no impact on the RMAX in unchallenged Harlan WTs. Given that these animals should be genetically very similar, if not identical, the question is why our in house bred DR3 WT and Harlan WTs (described in the previous chapter) differ in their response to PVAT.

Many factors have previously been discussed in the literature regarding divergences between in house and commercially supplied animals (Olfe *et al,* 2010). These include handling and transport within the juvenile period, practices that differ drastically between the two sources. Another example is our in house DR3 colony undergoes genotyping requiring animals to be tail tipped, a procedure likely to induce a stress response in the animals and thus have the potential to alter experimental outcomes. Other environmental stressors that can occur in, and significantly differ between, laboratories include restraint, noise, temperature and the presence of various people. Coupled with alterations in routine laboratory procedures, these factors can also activate the stress response (Besch *et al,* 1971; Brown *et al,* 2000; Balcombe *et al,* 2004). It is impossible to say whether any or all of the above underlie the observed differences between in house bred DBA/1 DR3 WT and Harlan WT. However, this does emphasise the need to use the most appropriate controls, in this case in house DR3 WT mice for the $DR3^{-/-}$ experiments.

Despite the overall constriction response in unchallenged healthy tissues remaining unchanged between DR3 WT and $DR3^{-/-}$, morphological differences are seen in the PVAT between these genotypes. Firstly, $DR3^{-/-}$ have increased total cell numbers in the PVAT compared to DR3 WT. While the underlying mechanism for this difference remains unexplained, a number of potential reasons may be attributable to DR3, for instance its ability to drive apoptosis (Kitson *et al*, 1996; Grimaldo, 2009; Wen *et al*, 2003). Grimaldo (2009) suggests that deleting DR3 in endothelial cells renders protection from a number of apoptotic ligands. Moreover, it may also result in an increase in NF-κβ signalling, and therefore cell survival, via production of anti-apoptotic proteins (Grimaldo, 2009). While we have no direct proof, it is possible that either of these mechanisms may be occurring in the PVAT resulting in the described differences.

That key PVAT cellular residents (Gao, 2007), have been shown to express DR3 (Zhang *et al,* 2009) suggests a potential role for this cell surface receptor in the control of PVAT cellular ingress. If DR3 normally recruits cells to the PVAT, its deletion may allow cells to be freely recruited to the region. DR3's ability to control cellular ingress has been shown previously in inflammatory disease but has not been elucidated in "healthy" murine models. For example, it is known that DR3 controls neutrophil ingress into the knee joint during inflammatory arthritis (Wang *et al*, 2014) and is also involved in cellular

recruitment to the lungs during allergic lung disease (Singh, 2014). These data presented do not identify the specific cell type that is responsible for the increase in cell number within the PVAT; however, it rules out F4/80+ macrophages and Ly6G+ neutrophils.

The "healthy" PVAT consists of a number of cell types, all of which have the ability to change with age, nutrition and environmental conditions and could indeed be changing within our model (Miao and Li, 2012). However, as suggested above, the increase in cell numbers is linked with changing DR3 expression. This would most likely involve fibroblasts, lymphocytes or immune cell populations given they have previously been shown to be associated with DR3 expression (Aiba and Nakamura, 2013). Gene expression profiles from the human gene database suggests DR3 expression on human adipocytes, however, this work has not been validated in the literature (www.genecards.org). Importantly, in the context of our results, this change in cellular populations does not impact on the vascular constriction response.

In our "healthy" mice the increase in cell numbers in $DR3^{-/-}$ PVAT is accompanied by an increase in total MMP-9 levels. Taking into account the static expression of macrophages and neutrophils in this region, there are many potential scenarios that could underlie this observation. Firstly, resident cells could be responsible for both increased cell number and increased total MMP-9 in the absence of DR3. Secondly, the cell type moving into the PVAT could also be capable of producing MMP-9. Alternatively, resident cells could produce increased amounts of MMP-9 to facilitate the ingress of other cells. Indeed, many cells in the PVAT are capable of the latter, adipocytes themselves having been shown to produce MMP-9 (Bouloumie *et al*, 2001). The study showed this increase in adipocyte-derived MMP-9 to correlate positively with both hyperplasia and adipocyte hypertrophy (Bouloumie *et al*, 2001) and could explain both the increase in MMP-9 and the expansion in cell numbers observed above. However, if we take into account two factors; cellular expression of DR3 and ability to produce MMP-9, the potential identities of cell type(s) changing in our model are much reduced. From the current literature it would seem that the only resident cell type in this region that has both these characteristics is the fibroblast (Wang *et al*, 2007; Ospelt and Gay, 2012; Shih *et al*, 2014; Ma *et al*, 2016). We therefore suggest it as a real contender in being responsible for the observed changes. Despite MMP-9 levels being increased in the $DR3^{-/-}$ PVAT, PVAT intact constriction responses are comparable with DR3 WT, suggesting the main driving force of the contractile phenotype seen during arthritis is MMP-9 independent.

When examining the aortic vessel wall of "healthy" $DR3^{-/-}$ an increase in the number of neutrophils was detected. This was surprising considering consistent constriction responses between the genotypes. As this increase in the neutrophil population did not impact on vascular constriction, we suggest that neutrophils do not work independently to drive contractile dysfunction, highlighting the importance of inflammatory cells working together to produce the changes we see in our model.

DR3 ablation was previously investigated in a local inflammatory arthritis model – Antigen Induced Arthritis (AIA) (Bull *et al*, 2008; Wang *et al*, 2014). These studies show that DR3 is increased in arthritic WT mice and that DR3 ablation significantly reduced reduces histological hallmarks of arthritis. More specifically, mice were protected from

cartilage damage (Wang *et al*, 2014) and subchondral bone erosions (Bull *et al*, 2008). For the first time in the present study the impact of DR3 ablation in a systemic inflammatory arthritis model mCIA was determined. Incidence of arthritis in $DR3^{-/-}$ animals remained 50% lower than in DR3 WT animals. This was complimented by a decrease in arthritis severity in the animals that became arthritic, with reductions in total paw score and all histological hallmarks. These data support the current literature in showing DR3 plays a key role in the onset and progression of arthritic disease, both locally and systemically, and warrants further investigations in the future.

Despite improved mCIA in $DR3^{-/-}$ mice, DR3 ablation was associated with decreased vascular constriction in the absence of PVAT in comparison to DR3 WT. This poses a conundrum; DR3 is actively involved in both the onset and progression or arthritis and its ablation is beneficial for joint health. Conversely, DR3 is also involved in the vascular constriction response in arthritic animals and is required for maintaining high constriction potential. If inhibition of DR3 were proposed as a future treatment option, further evaluation of its impact in the vasculature would be required, especially to determine the risk/benefit ratio of such an action.

When the PVAT is intact, the constriction of $DR3^{-/-}$ rings is restored to the same level as DR3 WT (Figure 3.11(D)). These data suggest that PVAT is protective in the arthritic constriction response and for the first time in this study it was established that PVAT has the potential to drive vasoconstriction. Such an effect of PVAT has been shown previously in models of obesity, where there is an increase in both oxidative and inflammatory factors (Agabiti-Rosei *et al*, 2014). It is suggested that changes to the $DR3^{-/-}$ PVAT during mCIA may indeed facilitate the production of vasoconstriction agents. Further experiments, beyond the scope of the current study, are warranted.

In mCIA $DR3^{-/-}$ an increased aortic Ly6G+ neutrophil population was observed. As discussed previously increased neutrophils cannot drive the decreased vascular constriction response independently. Therefore, although this adds to the evidence that DR3 is acting as the cellular control mechanism responsible for neutrophil infiltration to the aorta, it does not explain the decreased constriction potential in this colony. A complimentary change in another mediator, cell type or mechanistic pathway is postulated. One potential mechanism is associated with the increased circulating mineral levels in the RA cohort due to increased bone erosions. That vascular calcification can lead to vascular dysfunction has recently been demonstrated in chronic kidney disease patients (Shanahan *et al*, 2011). These studies show how elevated levels of circulating calcium and phosphate have direct impact on VSMCs and stimulate osteogenic differentiation within the vessel wall, while also driving apoptosis and extracellular matrix degradation. This opens up a wide range of possibilities for the potential mechanisms underlying contractile dysfunction in our model of inflammatory arthritis, some of which will be investigated in the later chapters of this thesis.

During mCIA the $DR3^{-/-}$ PVAT also exhibits morphological changes, specifically an increase in F480+ macrophages. It has previously been established that macrophages

have multiple functions in the vasculature, whether they are resident macrophages in the aorta (Gerrity, 1981) carrying out "normal" functions such as tissue remodelling (Fantin *et al*, 2010), or infiltrating inflammatory macrophages that produce a complex mixture of chemokines and adhesion molecules that induce inflammation (Wellen and Hotamisligil, 2003; Permana *et al*, 2006). Although more work would be required to determine the specific macrophage phenotypes within the PVAT, the impact of both M1 and M2 macrophages are discussed. The protective phenotype of PVAT in $DR3^{-/-}$ suggests an increase in M2 anti-inflammatory macrophages (Murray and Wynn, 2011). While this does not exclude M1 – pro-inflammatory macrophages from being present, it is likely that the ratio tips in favour of M2. The relationship between M1 and M2 macrophages in PVAT has recently been evaluated. Ruan *et al* (2015) showed how a decrease in M1, coupled with an increase in M2 ameliorates vascular injury. Moreover, it is also possible that increased production of IL-10 by M2 macrophages underlies the protective effect of the PVAT (Weisser *et al*, 2013). IL-10 is a potent anti-inflammatory protein, and while knocking out the IL-10 gene has no impact on vascular constriction in healthy mice, following an inflammatory stimuli ablation of IL-10 exacerbates vascular contractile dysfunction (Gunnett *et al*, 1999).

3.5 Conclusion

Within this chapter the importance of DR3 in both inflammatory arthritis and the vascular constriction response has been demonstrated. Firstly, it was established that DR3 was not a regulator of the "healthy" constriction response, despite driving changes at a cellular level. Ablation of DR3 was beneficial in mCIA, decreasing both onset and progression. Despite the benefits in arthritis, ablation mediated vascular dysfunction in the mCIA model. Surprisingly, and for the first time, $DR3^{-/-}$ PVAT has been shown to play an important protective role in the constriction response. It has been established that the presence of either neutrophils or MMP-9 independently does not underlie vascular dysfunction, and other associated mechanisms must be involved in order to drive the observed changes. The role of other apoptotic pathways is postulated in order to explain consistencies in total cell number, despite changes in both neutrophil and macrophage populations, along with changes to resident cells such as VSMC differentiation. Finally, the ability of programmed cell death to instigate vascular calcification is an avenue for exploration with a view to explaining the decreased contractility in the mCIA model. It is postulated that these changes may occur in conjunction with others in the extracellular matrix and will be investigated in the following chapters.

Chapter 4 - Medial Calcification and/or Structural Changes Mediate Early Contractile Dysfunction in mCIA

4.1 Introduction

Vascular calcification was once thought to be a benign sign of aging. However, in recent years the serious implications to the vasculature have become starkly evident. With an alarming number of people aged over 60 having some degree of calcium deposits in their vasculature, and associated outcomes such as stroke and ischaemic heart disease, research in this important area has expanded greatly. Vascular calcification has become well defined and is now divided in to two categories; medial artery calcification and intimal artery calcification, otherwise known as atherosclerosis (Vattikuti and Towler, 2004). The exact underlying mechanisms are currently hot topics for debate, and unique differences between the processes have been identified.

Medial artery calcification is common amongst RA patients and thus is the main focus of the experiments that follow in this Chapter (Davies and Hruska, 2001). RA patients show increasingly early onset diffuse calcification within a number of vascular beds, including the aorta and carotid and coronary arteries, in comparison to "healthy" age matched controls (Giles *et al*, 2009). It would seem that this type of calcification resembles matrix vesicle-mediated intramembranous bone formation, with regions of calcification organized as bone-like structures.

Medial artery calcification is known to impact on vessel elasticity and has the potential to increase vascular stiffness. This is interesting considering the associated contractile dysfunction seen in mCIA (Reynolds *et al*, 2012). Numerous studies have now established the roles of factors such as inflammation and oxidative stress signalling in contributing to the pathogenesis of vascular mineral deposition (Towler, 2008). Importantly this thesis (Chapter 2) demonstrated that contractile dysfunction was coupled with an increase in macrophage numbers in the aortic region. These cells have been associated with impaired vascular function via two mechanisms. Firstly, they are capable of cell-cell interactions and secondly they produce factors such as TNF-α that can indirectly drive vascular calcification (Tinut *et al*, 2000). Given that this cytokine is known to be up regulated in inflammatory arthritis (Bradley, 2008) it is suggested that the macrophage can contribute to the onset of vascular calcification in mCIA.

Once thought to be a passive process, it is now well established that medial artery calcification is tightly regulated by osteoblast-like cells and is similar in mechanism to normal bone formation (Johnson *et al*, 2006). Whether these pathways become dysregulated following the onset of inflammatory arthritis is open to question and will be discussed throughout this chapter. The master osteoblast transcription factor of bone development is Runt Related Transcription Factor 2 (RUNX2) (Schroeder *et al*, 2005). Its expression is seen in medial artery calcification in mice prior to a switch in VSMC phenotype from contractile to osteogenic (Liu *et al*, 2015). The importance of RUNX2 in this process has recently been shown following the creation of a mouse model with specific knockdown of RUNX2 in VSMCs. This work has established the obligatory role RUNX2 expression in medial artery calcification, its depletion completely preventing the transition of VSMCs to an osteogenic phenotype (Liu *et al*, 2015) (Figure 4.1).

Conversely, when RUNX2 expression is forced, osteogenic gene expression was elevated. This is mirrored by the knocking out of RUNX2 driving enhanced VSMC differentiation in human VSMCs (Tanaka *et al*, 2007).

The role of RUNX2 in the pathogenesis of calcification also implicates the involvement of other osteoblast transcription factors such as osterix (OSX) and activating transcription factor 4 (ATF4) (Komori, 2006). As both OSX and ATF4 act downstream of RUNX2, varying expression profiles in relation to changes in RUNX2 are expected, possibly occurring later in the progression of vascular calcification. Indeed, the prominence of these factors in vascular disease progression is evidenced by the up regulation of OSX in the vasculature of diabetic patients (Shao *et al*, 2010). The use of OSX knock out mice shows the importance for any bone formation at all, these mice showing a lack of bone mineral deposition, a process that is essential during vascular calcification (Nakashima *et al*, 2002).

It is well known in bone biology that osteoblasts function in equilibrium with osteoclasts. Taken with that described above, this suggests that an obvious experimental route is to investigate the involvement of both bone cell phenotypes in the vasculature of the mCIA model. The interaction of osteoblasts with osteoclasts works directly through osteoprotegerin (OPG), receptor activator of NF-κβ ligand (RANKL) and its receptor RANK pathway (Boyce and Xing, 2007) (Figure 4.1). OPG is a glycoprotein that acts as a soluble decoy receptor that binds to RANKL, competitively inhibiting the binding of RANKL and RANK thereby preventing excessive bone resorption (Simonet *et al*, 1997). Conversely the binding of RANKL to its receptor RANK promotes the formation of the multinucleated osteoclast from precursor cells, and controls their activation and survival. It is therefore the ratio of inhibitory OPG to RANKL that determines normal bone density in both health and disease (Hofbauer and Schoppet, 2004). However, the exact role of this pathway in vascular calcification remains unclear.

OPG levels are known to be up regulated in RA and vascular calcification (Ziolkowska *et al*, 2002) and it is suggested that this protects arteries from medial calcification. The importance of OPG is shown by knockout studies where rats are characterised by excessive renal and aortic calcification (Bucay *et al*, 1998) and double knock out OPG/apolipoprotein E mice exhibit accelerated atherosclerosis (Bennet *et al*, 2006). Such observations imply that inhibiting RANK-RANKL binding prevents increased osteoclast activation and demonstrates that these TNF superfamily members have important functions outside of bone. Given that described above, and in the previous chapters of this thesis, it is essential that the role of this signalling pathway is investigated in the mCIA model. Moreover, since communication between osteoblasts and osteoclasts is an integral part of mineral deposition, it is appropriate that further osteoclast expression markers, such as tartrate resistant acid phosphatase (TRAP), cathepsin K and calcitonin receptor, are assessed in complementary studies.

Despite a limited number of peer reviewed papers that report the incidence of osteoclasts within the vessel wall, there is evidence to suggest that they, or other osteoclast-like cells, are present and do play an important role in vascular calcification (Massy *et al*, 2008). It is well known that osteoclasts express TRAP and this

metalloprotein enzyme has long been used as a histochemical osteoclast marker (Burstone, 1959). Indeed, the essential role of TRAP in normal mineralization of cartilage and subsequent maintenance of bone integrity is clearly demonstrated in TRAP knock out mice studies (Hayman *et al*, 1996). Previously TRAP has been associated with vascular calcification in the arteries of OPG knock out mice (Bucay *et al*, 1998). While the expression of TRAP in the aorta during RA has not been demonstrated, data now suggests that the mechanism of vascular calcification is similar to that seen in bone, in which both osteoblasts and osteoclasts are essential (Massy et al, 2008). The assessment of TRAP levels is therefore an obvious choice when investigating the presence of vascular osteoclasts in mCIA.

Cathepsin K is a lysosomal cysteine protease which has been shown to be implicated in vascular calcification. Like TRAP, Cathepsin K was also shown to be up regulated in the arteries of OPG knock out mice (Bucay *et al*, 1998). Although Cathepsin K levels have not previously been determined in RA patients, a recent study assessed them in both chronic kidney disease and diabetes mellitus. Notably, increased circulating levels of Cathepsin K were associated with major adverse cardiac and cerebrovascular events (Izumi *et al*, 2016). Further knock out animal studies have provided direct evidence implicating cathepsins in vascular disease. Suggested roles include; matrix protein remodelling, activation, liberation and modification of angiogenic growth factors cytokines and proteases (Cheng *et al*, 2011).

The third marker used to identify the presence of osteoclasts is the calcitonin receptor. Within bone and marrow-type cells this is unique to the osteoclast and studies have shown its expression to correlate with osteoclast-mediated bone resorption (Hattersley and Chambers, 1989). As such it will further provide us with information of osteoclast functionality.

If osteoblast and osteoclast-like cells do reside within the diseased vasculature, questions remain as to the absence or presence of signalling mechanisms that would allow this to occur, and indeed moderate the activity of the cells. One proposed theory is that mineral deposition is not an active pathological process, but rather the result of a diminished protective mechanism that would usually oppose calcification. Despite high systemic circulating concentrations of calcium and phosphate, normal mineralization only occurs in the bone, teeth and cartilage (Schafer *et al*, 2003). This would suggest that undesirable mineralization is inhibited to prevent ectopic calcification. Many animal studies using knock out models have now shown the importance of several non-collagenous proteins in inhibiting vascular calcification (Luo *et al*, 1997; Speer *et al,* 2002). The involvement of two in particular, osteopontin (OPN) and matrix gla protein (MGP) have been widely investigated (Figure 4.1).

OPN is known to inhibit the deposition of a calcified matrix, dependent on its phosphorylation state (Wada *et al*, 1999). It has also been shown to aid osteoclast function by acting as an anchor between mineral and osteoclasts and stimulating the resorption of calcium phosphate crystals (Reinholt *et al*, 1990). Very pertinent to this thesis is the suggestion that OPN is capable of regulating the inflammatory response, including the accumulation of immune cells (Scatena *et al*, 2007). Given the influx of

inflammatory cells to the mCIA aorta and surrounding tissues described in the previous two chapters, assessment of OPN in this module is essential.

A role for MGP in vascular calcification is less well defined, with conflicting data suggesting that both an increase and decrease can contribute to this process (Zebboudj *et al*, 2002), (Brindle, 2001). Importantly MGP expression has been confirmed on VSMC as well as chondrocytes (Murshed *et al*, 2004). While both OPN and MGP have been shown to work in conjunction with OPG, the question remains as to whether they are decreased to allow calcification or increased to reverse calcification. The onset of vascular calcification is likely to occur due to the dysregulation of both inhibitory and activating signals.

Data now also support the notion that initiation of calcification is driven by cell apoptosis (Shroff *et al*, 2013) (Figure 4.1). Since this thesis (Chapters 2 and 3) describes changes in inflammatory cell populations in the face of little change in total cell number, it is possible that apoptosis is actively occurring in the mCIA vasculature. Importantly studies have identified a role for apoptosis prior to calcification in VSMC *in vitro,* inhibition of apoptosis by caspase resulting in a 40% reduction in calcification (Proudfoot *et al*, 2000). For this reason, apoptosis markers will constitute investigative targets allowing us to determine a time line of events contributing to aortic medial calcification in the mCIA model.

FAS ligand is one such marker that is also a member of the TNF superfamily, and like DR3 its receptor signals via a death domain. It was discussed in the previous chapter as a potential driver of changes in the vasculature when DR3 is ablated. The relationship between FAS and FAS ligand, and its ability to induce apoptosis, has been well characterized (Waring and Mullbacher, 1999). Apoptosis via this pathway is important for homeostasis in the immune system while also constituting a role for killing for cytotoxic T cells. Fas receptor is shown to be up regulated following DNA damage and this up regulation is said to be p53 dependent (Waring and Mullbacher, 1999).

Other than its association with FAS ligand, p53, has also been associated with osteogenic differentiation in the vasculature (He *et al*, 2015). It plays a crucial role in bone homeostasis by acting as a negative regulator (Wang, 2006), but more specifically, p53 inhibition is required to induce RUNX2 activation and therefore subsequent osteoblast differentiation (Lengner *et al*, 2006). In the context of vascular disease, p53 prevents trans-differentiation of bone marrow stromal cells to VSMC and protects against apoptosis (Li *et al*, 2012). Whether a decrease in p53 is associated with vascular dysfunction and calcification will be investigated.

Caspases are crucial in programmed cell death; caspase 3 specifically is a frequently activated protein and mediates the cleavage of many key cellular proteins (Porter and Janicke, 1999). It has also been shown to be important in the dismantling of a cell and the formation of apoptotic bodies. In terms of vascular disease, tissue expression of caspase 3 is correlated with apoptosis (TUNEL) staining within atherosclerotic plaques (Akishima *et al*, 2005). Plasma caspase 3 levels have also been associated with traditional

CV risk factors, suggesting both the importance of itself and apoptosis in vascular disease (Matulevicius *et al*, 2008).

In order to determine the presence of any mineral depots within the aortic vessel wall itself, two commonly used markers will be assessed. Osteocalcin (OCN) is a bone gla protein produced by osteoblasts (Lepage *et al*, 1990) and forms part of the bone extracellular matrix following carboxylation and hydroxyapatite binding. Importantly expression of OCN has been associated with calcifying VSMCs (Kapustin and Shanahan, 2011) and suggested as a novel regulator of osteochondrogenic differentiation within these cells (Idelevich *et al*, 2011). The second marker is the enzyme alkaline phosphatase, which appears to act in a number of ways to enhance mineralization; it is known to increase local concentrations of inorganic phosphate (Jones and Shinowara, 1941), it is a mineralization promoter (Golub and Boesze-Battaglia, 2007) and can decrease the high concentration of extracellular pyrophosphate that normally inhibits mineralization (Golub and Boesze-Battaglia, 2007). With specific relevance to this thesis, increased alkaline phosphatase has also been associated with vascular calcification (Schoppet and Shanahan, 2008).

Finally, we must consider the normal structure of the vasculature and how changes to this may impact on the vascular constriction response to an exogenous agonist. The composition of the ECM, produced by the VSMCs, ultimately defines the mechanical properties of the vessel wall. Within the tunica media there are two major ECM components, elastin and collagen, accounting for 50% of the vessel weight (Harkness *et al*, 1957). Elastin comprises a continuous network of lamellae (Dingemans *et al*, 2000), the woven structure forming an elastic reservoir to transfer stress throughout the vessel wall thus imparting vessel dispensability (Berry *et al*, 1997). The importance of elastic lamellar units in distributing tensile strength is evidenced by larger vessels having the greatest number of elastic layers (Berry *et al*, 1972). Studies now suggest that elastin turnover (Ashwini *et al*, 2011) and dysregulation (Ashwini *et al*, 2011) are early markers of phenotypic change, often occurring before the onset of calcification. Importantly elastin dysregulation may aid calcification but is not sufficient to do so single-handed (Ashwini *et al*, 2011) pointing to the multifactorial nature of this process. Changes to the elasticity of the vessel alter arterial compliance, resulting in altered pulse wave velocity, a strong predictor for CVD. Sandwiched between these lamellar layers are bundles of collagen fibres that show no distinct pattern of arrangement. Collagen content is often associated with vascular diseases such as atherosclerosis and is important in determining the stability of atherosclerotic plaque (Miller, 2016). In this thesis we will discuss collagen and elastin content in terms of medial calcification and determine associated changes.

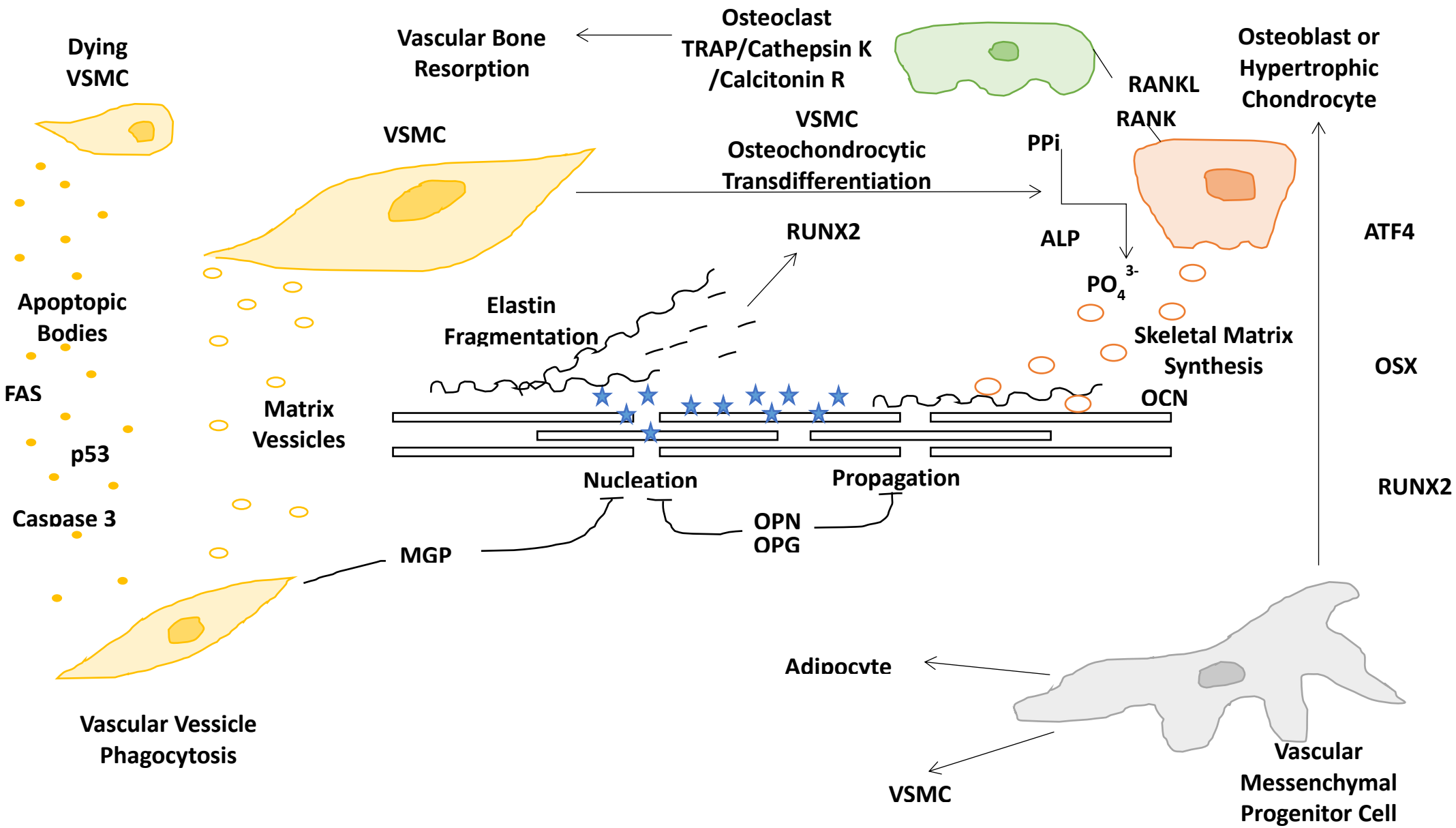

Figure 4.1 – The Association between Mineralization Factors. Mesenchymal progenitor cells can differentiate into VSMcs, adipocytes or osteoblast/ chondrocyte-like cells dependent on environmental conditions. In the presence of osteoblast transcription factors, RUNX2, OSX and ATF4 these cells differentiate towards an osteoblast-like phenotype. These cells express RANK and can interact with RANKL expressed on osteoclasts, along with TRAP, Cathepsin K and Calcitonin Receptor. The binding of RANK and RANKL initiates osteoclastogenesis. VSMCs can also transdifferentiate in the presence of master osteoblast transcription factor RUNX2. This factor can be produced in response to the fragmentation of elastin, which often occurs due the presence of high calcium concentrations within the region. This process allows the production of ALP and initiates the production of skeletal matrix, including bone like proteins such as osteocalcin from the osteoblast like cells. Apoptopic cells, expressing markers such as FAS, p53 and Caspase 3, within the region are thought to produce matrix vesicles which are phagocytosed. This drives increased production of inhibitors such as OPN, MGP and OPG that act to counteract calcification-promoting processes within the vessel wall.

This chapter describes the experiments used top interrogate whether the vascular dysfunction in our model of inflammatory arthritis was attributable to vascular calcification and/or important structural changes. It details methodology, results and discussion under the following objectives:

Hypothesis: Structural changes to the thoracic aorta and surrounding PVAT drive dysregulation of constriction response in the mCIA model.

- To evaluate whether medial calcification is driving vascular dysfunction in mCIA
- To understand the presence of osteoblast/osteoclast-like cells in the thoracic aorta and surrounding PVAT of mCIA mice
- To investigate whether apoptosis occurs prior to calcification in the vasculature
- To ascertain whether mineral is produced in the aortic vessel wall following arthritis onset
- To determine whether changes in density and structure of the ECM components elastin and collagen are effected during mCIA

4.2 Methods

New methods are described below. Methods from Chapter 2 still apply here, including; mCIA induction (2.2.2) and immunohistochemistry (2.2.6).

4.2.1 Molecular Biology

Molecular biology was used to determine the expression of calcification markers within the aortic vessel wall and surrounding PVAT. These include calcification inhibitors, apoptosis markers, osteoblast transcription factors and Osteoclastogenesis factors.

4.2.2 Tissue Isolation

Aortas were isolated with PVAT still intact as previously described (3.2.3.2). Aortas were immediately put into RNA later and stored on ice. The samples were kept at 4^{o}C overnight before being stored at -20^{o}C until later analysis.

4.2.3 RNA Extraction

RNA was extracted from each aorta (with PVAT still intact) on ice using a trizol method. Firstly, each tissue sample was fully homogenized using an ultra-turrax T8 (IKA) in 1ml of tri reagent. The resulting homogenate was then transferred to a 1.5ml Eppendorf tube and 200µl of chloroform added. This was quickly vortex mixed and left at room temperature for 5 minutes before being centrifuged at 1200g for 15 minutes at 4^{o}C. Following this separation technique, the RNA containing top phase was transferred to a new Eppendorf tube. An equal volume of 100% isopropanol was then added and the tube vortex mixed before freezing at -20^{o}C overnight. Subsequently samples were thawed at room temperature before being centrifuged at 1200g for 15 minutes at 4^{o}C. The isopropanol was then carefully removed without disturbing the RNA and 1ml of 100% ethanol added to purify the pellet. Following vortex mixing and centrifugation at 7500g for 5 minutes at 4^{o}C, this process was repeated. All remaining ethanol was then removed and pellets left to air dry for 10 minutes at room temperature, before being re-suspended in 10µl of RNAse/DNAse free water. RNA samples were stored at -80^{o}C for later analysis.

4.2.4 Analysis of RNA Concentration

The RNA concentration in 1µl of each prepared sample was determined using a NanoDrop spectrophotometer (Thermo). Results were expressed in ng/ml and 260/280 and 260/230 ratios were collated.

4.2.5 Analysis of RNA Purity

Each RNA sample was also analysed on the BioAnalyser chip in order to determine any contamination or breakdown of the RNA product. This gave an RNA Integrity Number (RIN) for each sample, which reflected the determination of RNA quality. All samples had a high level of RNA quality.

4.2.6 Production of cDNA – Reverse Transcription

In order to use the same concentration of RNA in each Reverse Transcriptase reaction, RNA samples were appropriately diluted with RNAse/DNAse free water to 500ng/µl.

For the Reverse Transcription reaction, a mastermix of reagents was prepared. This contained 10µl of 2x buffer and 1µl of Reverse Transcriptase enzyme (Applied Biosystems, 4387406). 11µl of this mastermix was added to 2µl of RNA (at 500ng/µl) and 7µl of RNAse/DNAse free water. Two controls were also run; a water control containing no RNA but 2µl extra of RNAse/DNAse free water and a no transcript control containing no enzyme but an extra 1µl of RNAse/DNAse free water. All cDNA samples were stored at -20^{o}C for later analysis.

4.2.7 Primer Design

All primers (Table 4.1) were designed using three software packages. Ensemble was used to determine the exon sequences for the required gene in the correct organism. This was then exported as a FASTA sequence into Primer 3 to determine an appropriate primer sequence with a product range between 80 and 150 base pairs as well as having a 50% guanine-cytosine content. Finally, the designed primers were run through Primer Blast to determine specificity and the likelihood of amplification of an unwanted gene.

Table 4.1 - Genes and Designed Primer Sequences

	Forward Primer	Reverse Primer
RUNX-2	CCCTGAACTCTGCACCAAGT	TGGCTCAGATAGGAGGGGTA
Osterix	TCTCCATCTGCCTGACTCCT	CAGGGGACTGGAGCCATAGT
ATF 4	CCACCATGGCGTATTAGAGG	CAACACTGCTGCTGGATTTC
Matrix Gla Protein	AAGAGAGTCCAGGAACGCAA	TGAAGTAGCGGTTGTAGGCA
Osteopontin	AGCCATGAGTCAAGTCAGCT	TGTGGCTGTGAAACTTGTGG
OPG	TTATACGGACAGCTGGCACA	TCACACTCACACACTCGGTT
RANK	TGAAAGCACCGTGGATTCTG	TTGTCAGGTGCTTTTCAGGG
RANKL	CATGAAACATCGGGAAGCGT	TTCGTGCTCCCTCCTTTCAT
MMP-9	GCATCCGAGCAAGAAGACAA	CTGTCACAAAAGCCAGCTGA
Beta Smooth Muscle Actin	AGCAAGCAGGAGTACGATGA	GGTGTAAAACGCAGCTCAGT
GAPDH	TGGCAAAGTGGAGATTGTTGCC	AAGATGGTGATGGGCTTCCCG
Alpha Smooth Muscle Actin	TGAAAATGAGATGGCCACGG	AGCGTTCGTTTCCAATGGTG

4.2.8 Primer Preparation

Each primer was diluted with RNAse/DNAse free water to make a 100µM stock solution.

4.2.9 Real Time Quantitative Polymerase Chain Reaction (RT-qPCR)

RT-qPCR was used to determine gene expression of early calcification markers in the aortic vessel wall and surrounding PVAT. For each gene analysed by RT-qPCR, a mastermix was prepared to contain 10µl of SYBR green mastermix (Life Technologies), 0.8µl of 10µM specific forward primer, 0.8µl of 10µM specific reverse primer and 4.4µl of RNAse/DNAse free water. Subsequently a 1 in 5 dilution was made of the cDNA resulting from the RT reaction. In a 96-well plate 16µl of mastermix was added to each appropriate well along with 4µl of cDNA (500ng/µL). Three wells were used as controls; the water control from the RT reaction, the no transcript control from the RT reaction and a no transcript control for this reaction containing 4µl of RNAse/DNAse free water. Each plate was sealed with a plastic top and centrifuged at 7500g for 1 minute to ensure thorough mixing of reagents. Each plate also contained cDNA samples with mastermix for one of two housekeeping genes β-actin and GAPDH. For individual samples, each gene was run in triplicate. Each 96 well plate was analysed by the Viia 7 qPCR machine, using 40 cycles of the following method. PCR was initiated with a denaturation step at 95°C for 2 minutes, followed by 40 amplification cycles at 95°C for 1 second and 60°C for 30 seconds to enable the annealing and extension of the primers along the cDNA.

4.3 Alkaline Phosphatase Activity

ALP activity was determined using an assay kit from Abcam (ab83371).

Firstly, buffers and enzymes were prepared as per kit instructions. Briefly, 4-Methylumbelliferyl phosphate (MUP) substrate was dissolved in 1.2mls of assay buffer to produce a 5mM solution. ALP antibody was also diluted in 1ml of assay buffer. A 50µM MUP standard was prepared by diluting 5µl of 5mM MUP solution with 495µl of assay buffer. A standard curve was then produced with 6 points ranging from 0nmol/well to 0.5nmol/well. All standards and samples were run in duplicate.

Aortic samples were first homogenised as described above in 100ml of assay buffer before centrifugation at 13000g for 3 minutes at 4^{o}C. 50µl of the resulting supernatant was then added to the appropriate well of a 96-well plate along with 60µl of assay buffer. For each sample, 20µl of MUP substrate (2µl of 5mM solution and 18µl of assay buffer) was added and 10µl of ALP enzyme added to each well of the standard curve. Subsequently samples were incubated for 30 minutes at room temperature in the dark. After this time 20µl of stop solution was added to each well, the plate gently shaken before analysis using a plate reader at 360/440nm.

To ensure ALP activity was standardised for protein concentrations, the latter was assessed in each sample by use of a concomitant bicinchoninic acid protein assay (BCA) (Thermo, 23225). Briefly, a standard curve was produced from commercial standards with concentrations varying from 0- 2000µg/ml. BCA working reagent was prepared as per manufacture instructions. In a 96-well plate 25µl of each standard or sample was added to appropriate duplicate wells. 200µl of working reagent (a 50:1 ratio of provided reagents A and B) was added to each well and following gentle mixing the plate incubated at 37^{o}C for 30 minutes. Subsequently the plate was analysed using a plate reader at 562nm and protein concentrations determined in relation to the standard curve.

4.4 TRAP Positive Cell Identification

In order to visualise osteoclasts in the aortic vessel wall and surrounding PVAT, TRAP staining was carried out using the protocol detailed below.

70% ethanol fixed samples were rehydrated through xylene and varying concentrations of IMS to water as previously described (Section 2.2.5) before being incubated overnight in preparation buffer (Table 4.2). The following day the pH of the remaining preparation buffer was adjusted to 5 and samples incubated in working TRAP solution (Table 4.3) for 6 hours at 37^{o}C. Subsequently samples were dehydrated and preserved with DPX (as previously described, section 2.2.5).

Table 4.2 - TRAP Preparation Buffer

	Constituents
Preparation Buffer	50ml dH_2O
	0.82g Sodium Acetate
	0.58g Tartaric Acid

Table 4.3- Working TRAP solution

	Constituents
Working TRAP solution	5 ml Preparation Buffer
	0.5mg/ml Napthol
	1.1mg/ml Fast Red

4.5 MGP Immunohistochemistry

Immunohistochemistry was used to identify MGP within the aortic vessel wall and PVAT. The previously described (Table 2.9) general protocol was followed with the inclusion of specific reagents and concentrations (Table 4.4). Positive staining was determined and quantified as previously described (Section 2.2.6).

Table 4.4- MGP staining reagents

Reagent	**F4/80**
Wash Buffer	TBS Tween
Serum Block	Goat
Primary Antibody	Rabbit Anti MouseF480 (4ug/ml)
Isotype	Mouse IgG1 (4ug/ml)
Secondary Antibody	Goat Anti Rabbit

4.6 Elastin Staining

Tissue sections were processed using a Ver Hoeff's stain (Abcam, ab150667) to identify elastin fibre density and structure within the aortic vessel wall using the following protocol (Table 4.5). A working elastin solution was prepared as shown in Table 4.6.

Table 4.5- Ver Hoeff's Staining Protocol

Step	Reason
3 x Xylene Washes (5 minutes)	Wax Clearing
2x100% IMS (3 minutes)	Rehydration
1x90%IMS (3 minutes)	
dH_2O (5 minutes)	
Ver Hoeff's Working Elastin Stain (15 minutes)	Identify Collagen
Running Tap Water	Remove Excess Stain
Differentiation Solution (20 dips)	Differentiation of Stain
Running Tap Water	Clears Excess Solution
Sodium Thiosulphate (1 minute)	Removes Excess Iodine
Running Tap Water	Clears Excess Solution
1x90% IMS (3 minutes)	Clear Excess Stain & Dehydrate
2x100%IMS (3 minutes)	
3xXylene Washes (5 minutes)	
DPX and Coverslip	Preservation of Staining

Table 4.6 - Working Elastin Solution

Reagent	Volume
Haematoxylin (5%)	30ml
Ferric Chloride (10%)	12ml
Lugols Iodine Solution	12ml

4.7 Collagen Staining

Tissue sections collected from mCIA experiments were processed to wax blocks and mounted on superfrost+ slides, as previously described (2.2.3.2). The following protocol (Table 4.7) details the methodology in which Van Geisson (Abcam, ab150667) staining was used to determine collagen density and structure within the aortic vessel wall.

Table 4.7- Van Geison Staining Protocol

Step	Reason
3 x Xylene Washes (5 minutes)	Wax Clearing
2x100% IMS (3 minutes)	Rehydration
1x90%IMS (3 minutes)	
dH_2O (5 minutes)	
Van Geisson Stain (5 minutes)	Identify Collagen
Running Tap Water	Remove Excess Stain
1x90% IMS (3 minutes)	Clear Excess Stain & Dehydrate
2x100%IMS (3 minutes)	
3xXylene Washes (5 minutes)	
DPX and Coverslip	Preservation of Staining

4.7.1 Structural Stain Analysis

Images of elastin and collagen staining were acquired using an Olympus U-TV1 Microscope at x10 magnification. These were then analysed using Photoshop. Areas of positive staining were identified using the colour pick tool. This provides the total number of positively stained pixels in the image. This was calculated as a pixel percentage of the entire vessel. The area of the vessel wall that did not contain elastin and collagen was similarly determined. All staining analysis was carried out blind.

4.8 Statistics

Statistics used in this chapter are the same as those described previously in section 2.2.7.3. All RT-qPCR data were analysed in two ways. Firstly the impact of arthritis severity on factor expression was determined. Secondly, factor expression was compared with time with arthritis by correlation. Comparison of Non-Immunized, Mild and Severe arthritis groups was carried out using a one way ANOVA with a Bon-Ferronni post hoc test. $P<0.05$ was considered significant.

4.3 Results

4.3.1 Arthritis Severity and Time with Disease Contribute to Changes in the Interplay between Osteoblasts and Osteoclasts in the Aorta and PVAT.

Impact of Arthritis Severity

Following the onset of both mild and severe arthritis, there were no changes in the expression of osteoblast transcription factors RUNX2 (Figure 4.2A) (1.10 ± 0.08 (N=12) vs. 1.30 ± 0.19 (N=9) vs. 1.23 ± 0.32 (N=11)), OSX (Figure 4.2B) (0.76 ± 0.13 (N=8) vs. 0.90 ± 0.19 (N=8) vs. 0.46 ± 0.09 (N=5)) and ATF4 (Figure 4.2C) (1.44 ± 0.31 (N=12) vs. 1.68 ± 0.29 (N=9) vs. 1.89 ± 0.47 (N=11)).

Expression of osteoclastogenesis markers; OPG (Figure 4.4A), RANK (Figure 4.4B) and RANKL (Figure 4.4C) were also calculated following the onset of both mild and severe arthritis. No significant change was seen in OPG expression (1.28 ± 0.25 (N=12) vs. 2.49 ± 0.97 (N=9) vs. 1.64 ± 0.37 (N=11)). However, RANK expression (1.10 ± 0.14 (N=12) vs. 2.28 ± 0.49 (N=9) vs. 0.99 ± 0.15 (N=11)) was significantly (p=0.0059) increased in mild arthritis in comparison to both non-immunized control aorta and severely arthritic aorta. No significant changes in RANKL expression were seen (2.19 ± 0.57 (N=12) vs. 1.63 ± 0.41 (N=9) vs. 3.31 ± 0.79 (N=11)).

No significant changes were identified in the expression profiles of the osteoclast markers TRAP (Figure 4.6A) (1.61 ± 0.17 (N=12) vs. 1.52 ± 0.17 (N=9) vs. 1.80 ± 0.17(N=11)), Cathepsin K (Figure 4.6B) (1.28 ± 1.20 (N=12) vs. 0.92 ± 0.13 (N=9) vs. 1.25 ± 0.15 (N=11)) and Calcitonin Receptor (Figure 4.6C) (2.55 ± 1.24 (N=12) vs. 2.30 ± 0.75 (N=9) vs. 1.40 ± 0.46 (N=11)) between non-immunized control, mild and severe arthritis respectively.

Impact of Time with Arthritis

Expression of transcription factors were also correlated against time with arthritis (days) in order to determine whether this is a factor in progression of vascular calcification. RUNX2 (Pearson's R=0.29) and OSX (Pearson's R=0.06) expression did not change, but ATF4 (Pearon's R=0.44) expression significantly (p=0.008) increased (Figures 4.3A, B and C respectively).

Expression of osteoclastogenesis markers, OPG, RANK and RANKL showed no correlation with time with arthritis (Figures 4.5A, B and C respectively).

Similarly, osteoclast markers, TRAP, Cathepsin K and Calcitonin Receptor were not changed over time with arthritis (Figure 4.7A, B and C respectively).

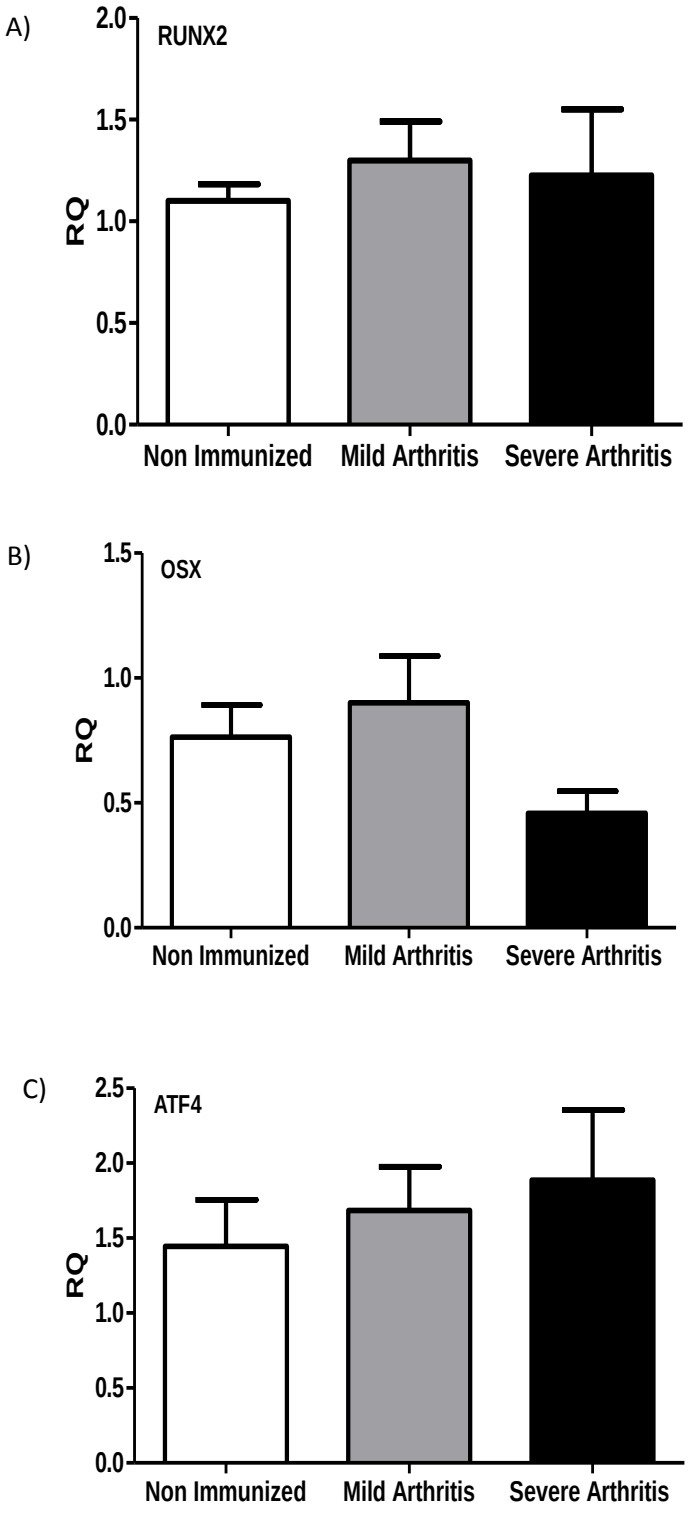

Figure 4.2 - Osteoblast Transcription Factors. Expression of osteoblast transcription factors RUNX2 (A), OSX (B) and ATF4 (C) were determined in non-immunized, mild and severely arthritic aorta and PVAT.

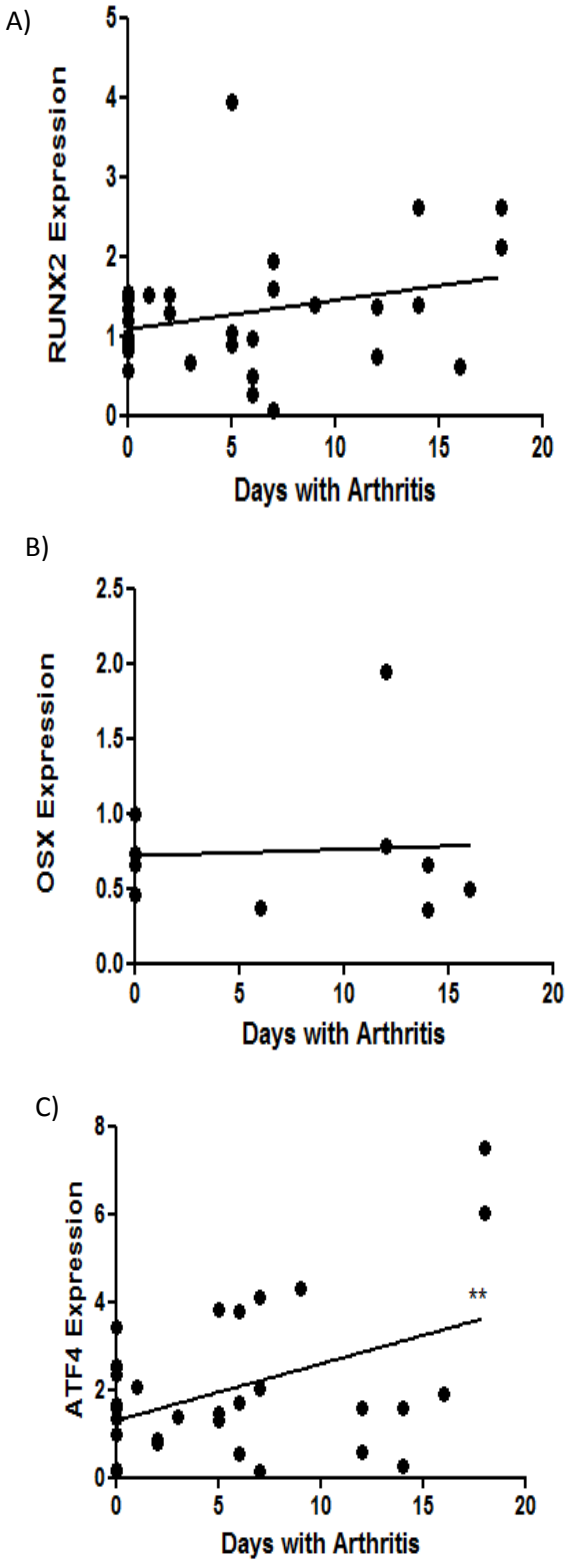

Figure 4.3 – Osteoblast Transcription Factors Over Time. The expression of RUNX2 (A), OSX (B) and ATF4 (C) were also determined over time with arthritis. **=p<0.01

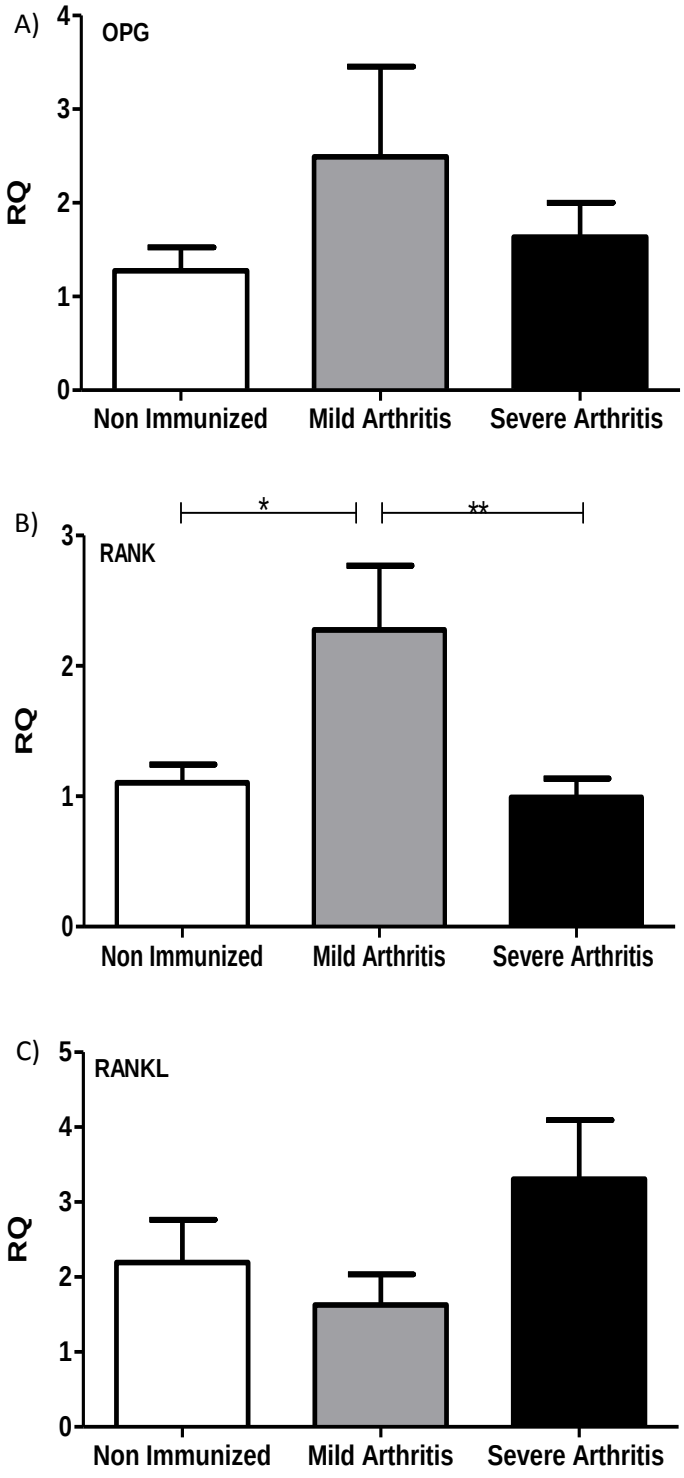

Figure 4.4 - Osteoclastogenesis Markers. Expression of osteoclastogenesis markers OPG (A), RANK (B) and RANKL (C) were determined in non-immunized, mild and severely arthritic aorta and PVAT. *=$p<0.05$,**=$p<0.01$.

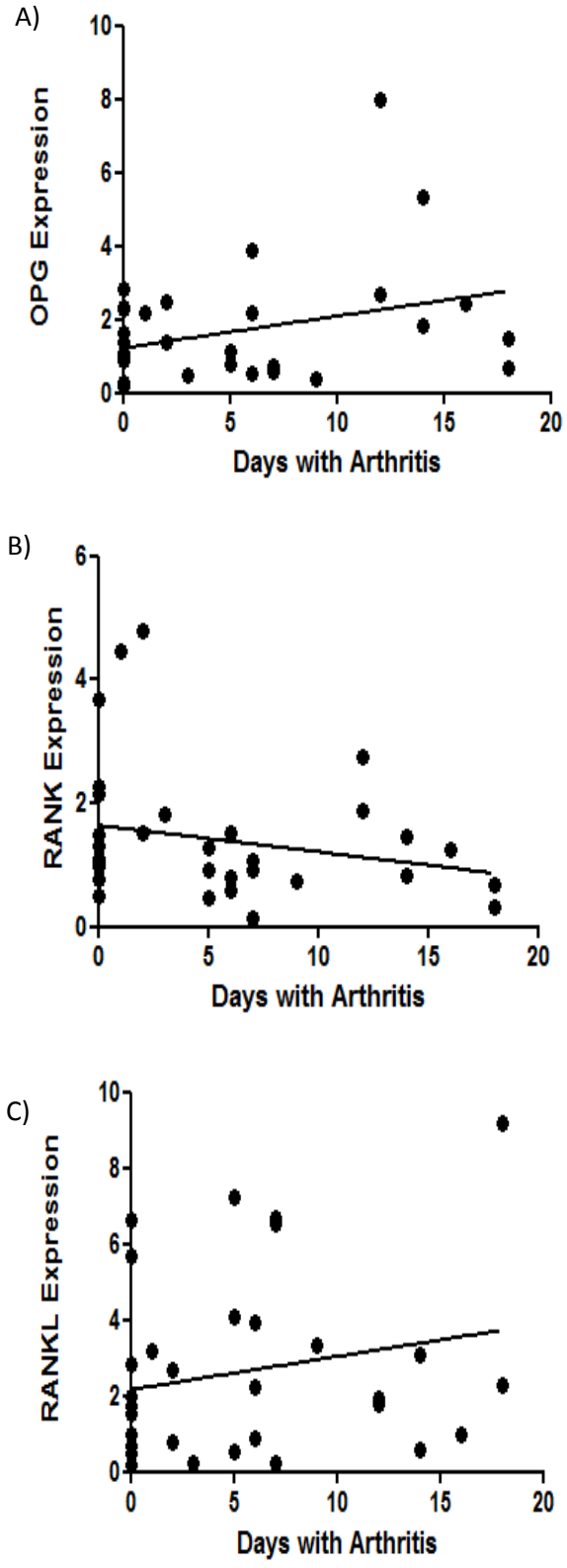

Figure 4.5- Osteoclastogenesis Markers Over Time. The expression of OPG (A), RANK (B) and RANKL (C) were also determined over time with arthritis.

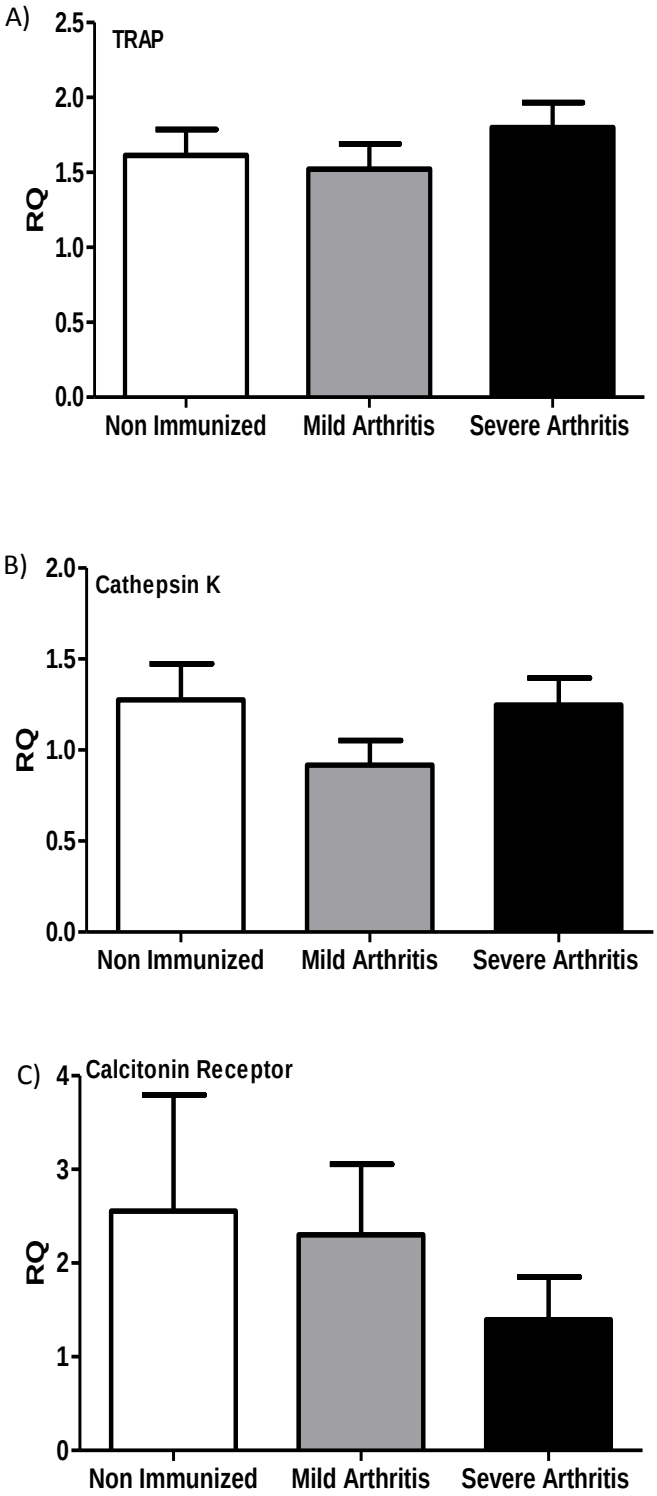

Figure 4.6 - Osteoclast Markers. Expression of osteoclast markers TRAP (A), Cathepsin K (B) and Calcitonin Receptor (C) were determined in non-immunized, mild and severely arthritic aorta and PVAT.

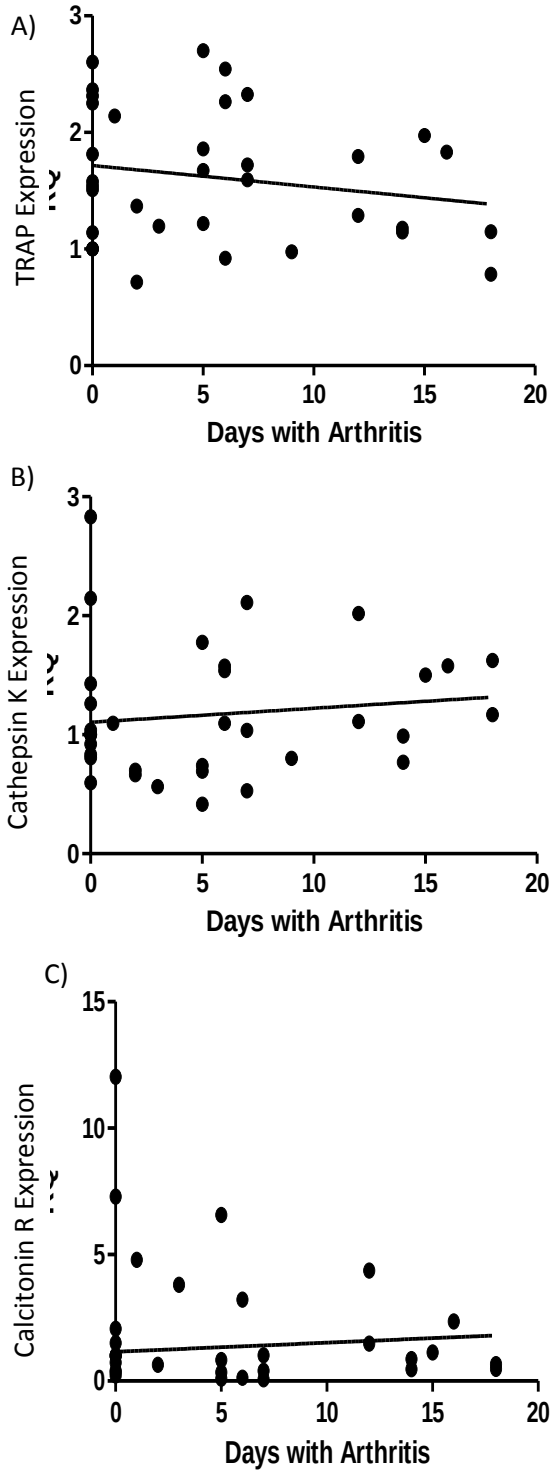

Figure 4.7 – Osteoclast Markers Over Time. The expression of TRAP (A), Cathepsin K (B) and Calcitonin Receptor (C) were also determined over time with arthritis.

4.3.2 Mechanisms for Initiating Mineralization over Time with Arthritis

Impact of Arthritis Severity

There was no change in MGP (Figure 4.8A) (1.09 ± 0.10 (N=12) vs. 1.31 ± 0.17 (N=9) vs. 1.15 ± 0.10 (N=11)) or OPN expression (Figure 4.8B) (3.25 ± 1.32 (N=12) vs. 11.40 ± 6.53 (N=9) vs. 26.62 ± 12.43 (N=11)) between non-immunized control, mild and severe arthritis respectively.

No significant changes were identified in the expression profiles of the apoptosis markers Fas (Figure 4.11A), Caspase 3 (Figure 4.11B) and p53 (Figure 4.11C); Fas (1.17 ± 0.12 (N=12) vs. 1.03 ± 0.15 (N=9) vs. 1.51 ± 0.20 (N=11)), Caspase 3 (1.01 ± 0.09(N=12) vs. 1.09 ± 0.14 (N=9) vs. 0.85 ± 0.08 (N=11)) and p53 (1.25 ± 0.25 (N=12) vs. 1.09 ± 0.16 (N=9) vs. 1.32 ± 0.32 (N=11)) between non-immunized control, mild and severe arthritis respectively.

Impact of Time with Arthritis

MGP showed no significant correlation with time with arthritis (Figure 4.9A). However Figure 4.9B illustrates a significant (p=0.031) correlation (Pearson's R=0.37) between OPN expression and time with arthritis. Moreover, when compared across all mice OPN expression was significantly (P=0.01) higher than MGP expression (Figure 4.10).

When apoptosis markers were analysed in relation to time with arthritis, only Caspase 3 changed significantly (p=0.035), decreasing over time with arthritis (Pearsons R=-0.36) (Figure 4.12B).

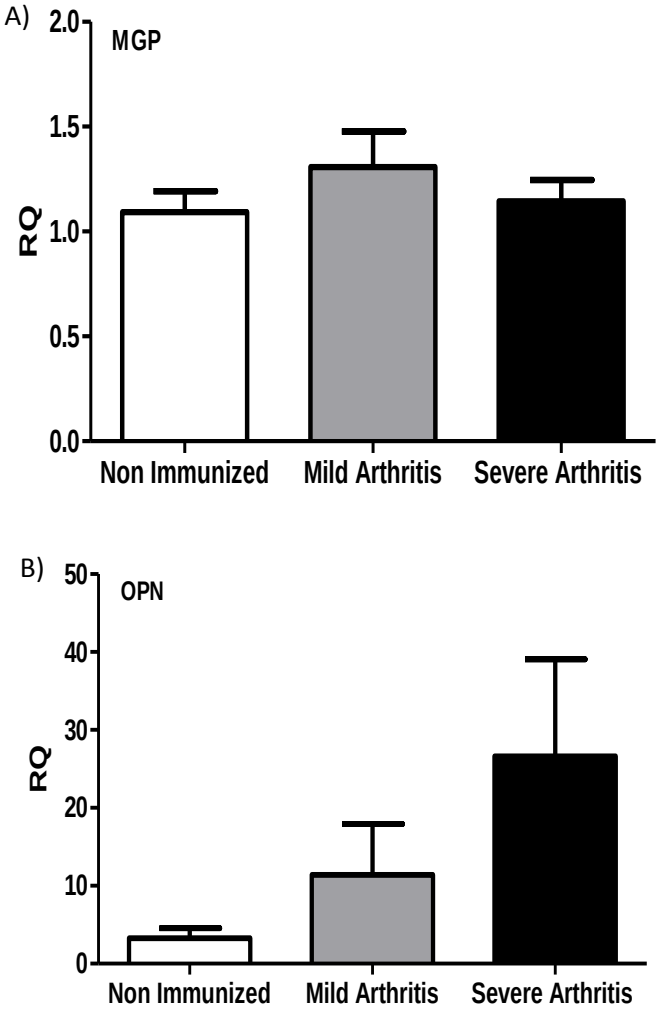

Figure 4.8 - Mineralization Inhibitors. Expression of mineralization inhibitors; MGP (A) and OPN (B) were determined in non-immunized, mild and severely arthritic aorta and PVAT.

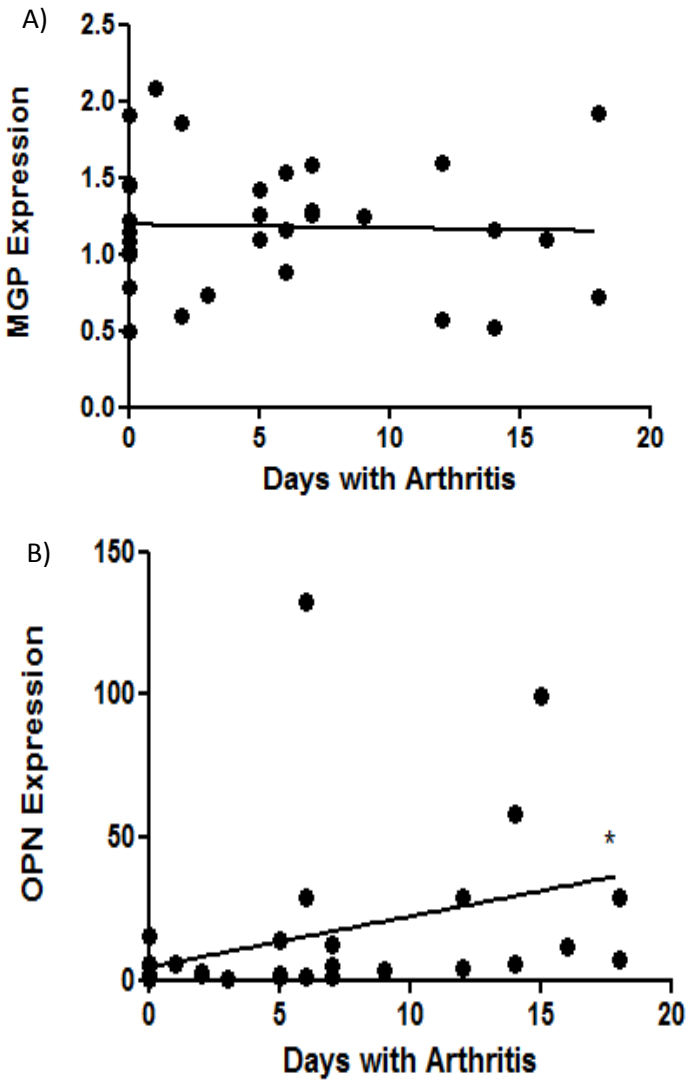

Figure 4.9 – Mineralization Inhibitors Over Time. The expression of MGP (A) and OPN (B) were also determined over time with arthritis. *=p<0.05.

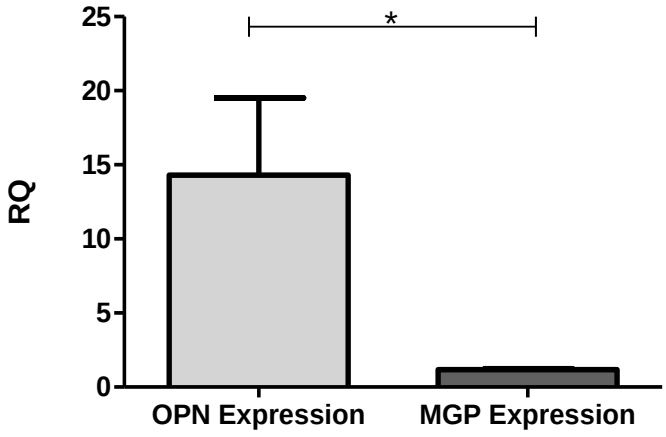

Figure 4.10 - Comparison of Mineralization Inhibitors. Overall expression of OPN and MGP in PVAT intact aorta were compared. *=p<0.05.

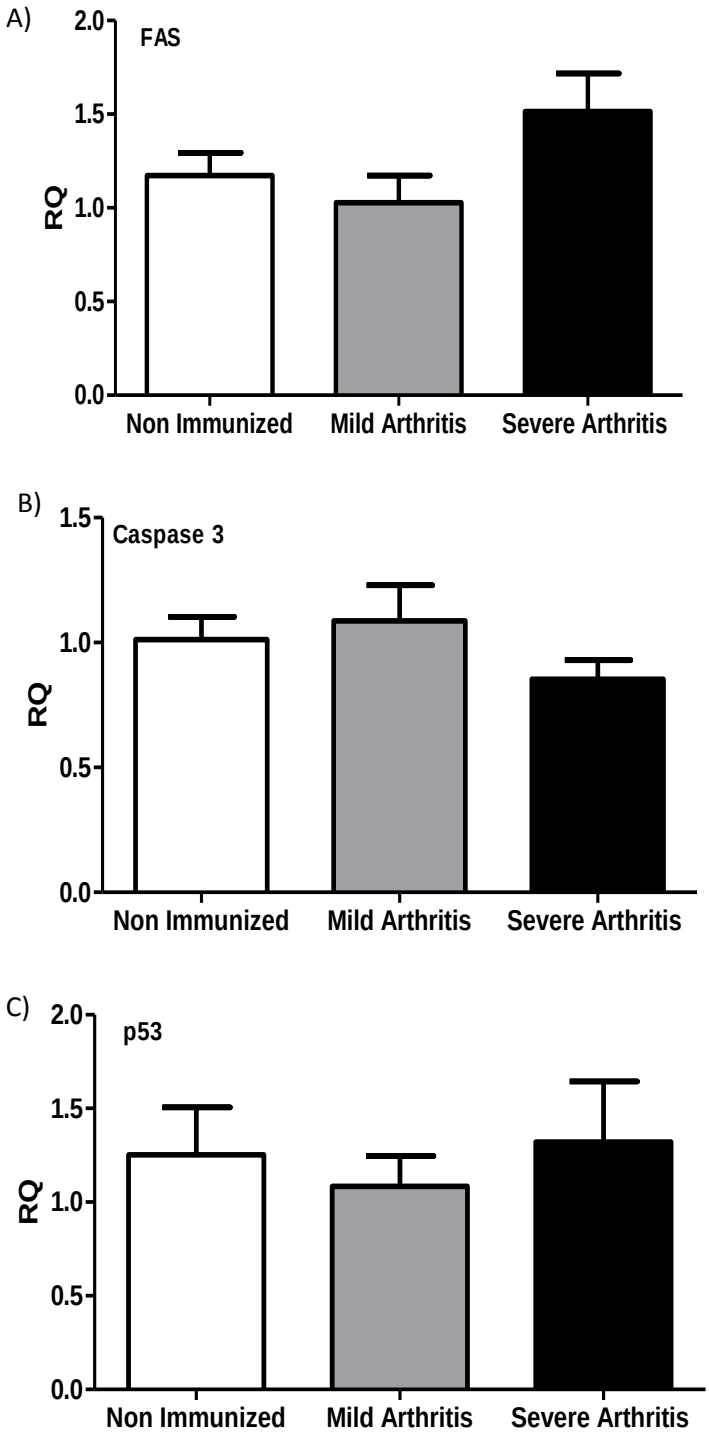

Figure 4.11 - Apoptosis Markers. Expression of apoptosis markers FAS (A), Caspase 3 (B) and p53 (C) were determined in non-immunized, mild and severely arthritic aorta and PVAT.

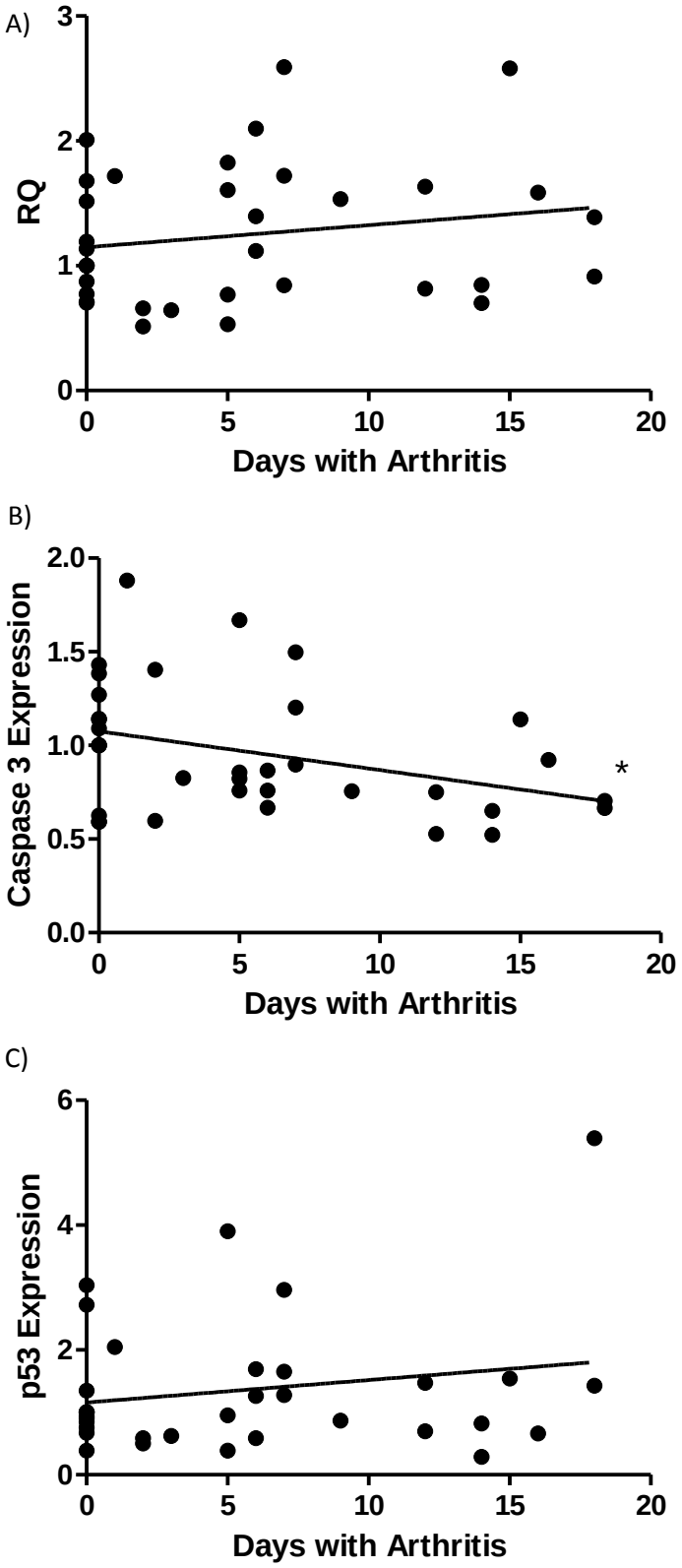

4.12 Apoptosis Markers Over Time. The expression of FAS (A), Caspase 3 (B) and p53 (C) were also determined over time with arthritis. *=p<0.05

4.3.3 Mineralization Markers Remain Constant in the Aorta Following Onset of Arthritic Disease

Impact of Arthritis Severity

There was no significant difference in the expression of OCN, a broad marker of calcification, between non-immunized, mild and severely arthritic tissues (Figure 4.13) (2.74± 0.99 (N=4) vs. 0.98± 0.26 (N=2) vs. 2.31± 0.65 (N=4)).

Levels of the second mineralisation marker ALP were also determined, but only in non-immunized (N=3) and severe arthritis tissues (N=3), due to experimental constraints (Figure 4.15). Again, no change with disease severity was observed.

Impact of Time with Arthritis

No significant correlation with time of disease presence was observed for OCN (Pearson's R=-0.46) (Figure 4.14).

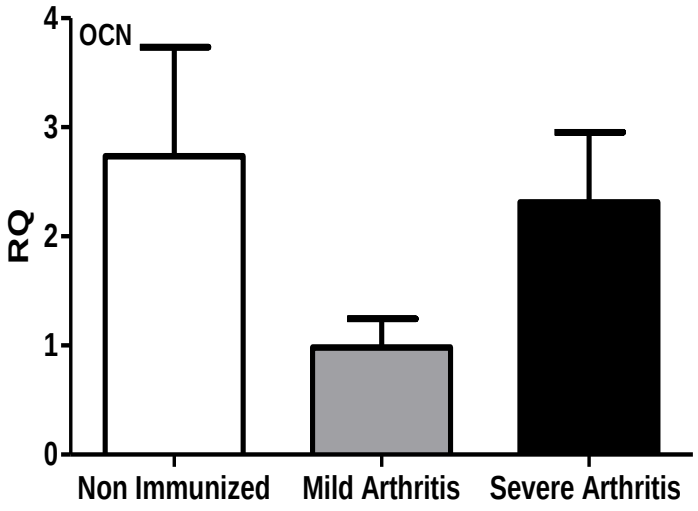

Figure 4.13 - Osteocalcin. Expression of the calcification marker OCN was determined in non-immunized, mild and severely arthritic aorta and PVAT.

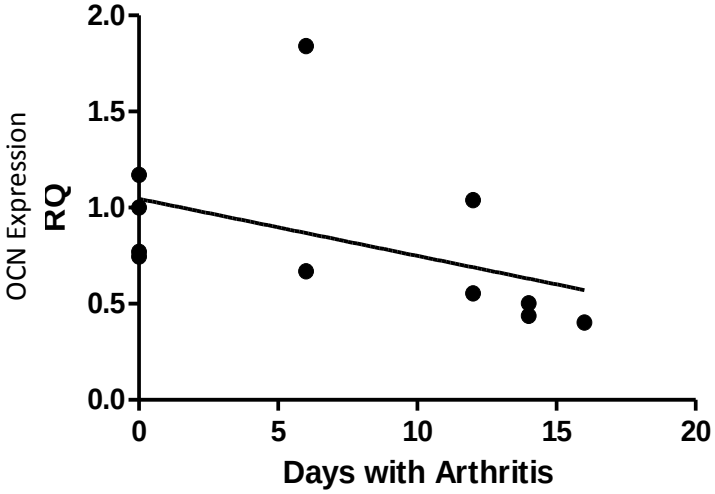

Figure 4.14- Osteocalcin Over Time. The expression of OCN was also determined over time with arthritis.

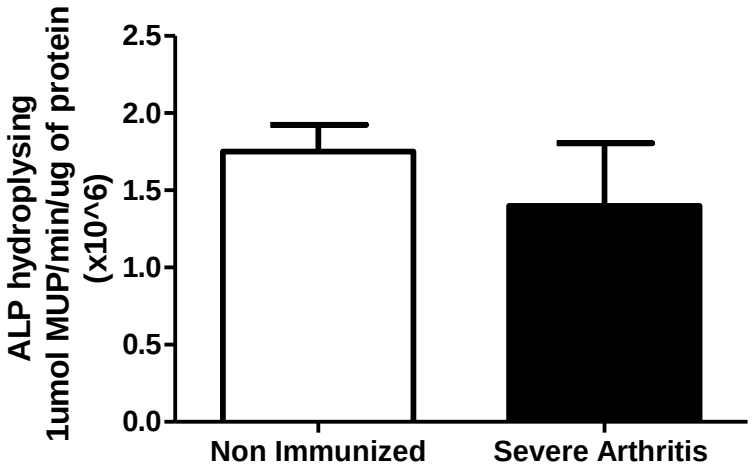

Figure 4.15 - Alkaline Phosphatase. Activity of ALP was determined in non-immunized and severely arthritic PVAT-intact aortic homogenates.

4.3.4 TRAP Positive cell Number Does Not Change in the Aorta or PVAT Following Induction of Arthritis

When the number of TRAP positive cells was counted in both the aorta (Figure 4.16A) and PVAT (Figure 4.16B), no significant differences between non-immunized, mild and severely arthritic tissues were identified (0.5±0.3 (N=4) vs. 1±0.6 (N=4) vs. 0.75±0.3 (N=4) and (6.3±1.5 (N=4) vs. 3.3±1.5 (N=4) vs. 4.5±1.7 (N=4)) respectively.

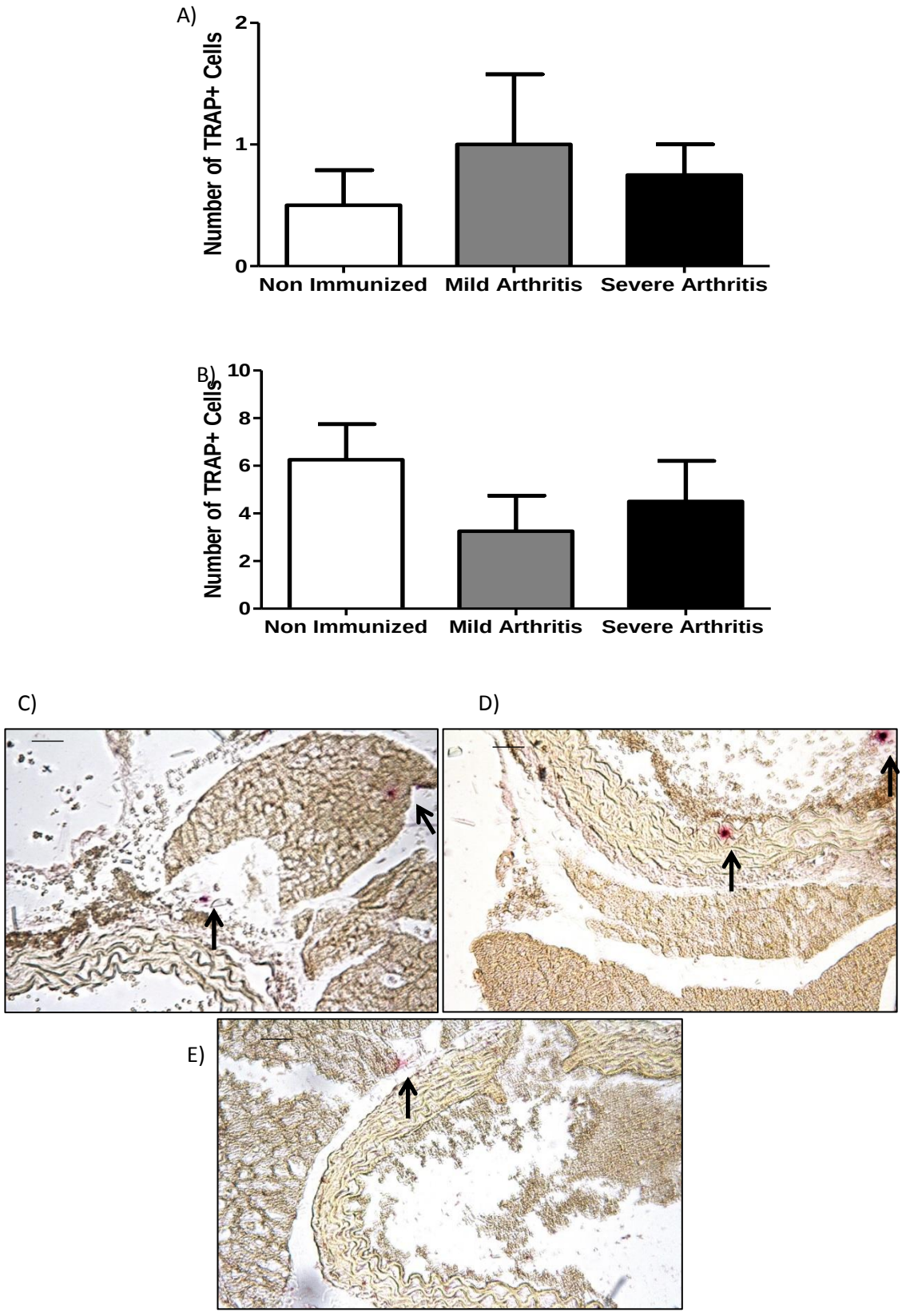

Figure 4.16- TRAP Protein Profile. TRAP expression was determined in the aorta (A) and PVAT (B) of non-immunized, mild and severe arthritic mice. Representative images (x40 magnification) of aorta and PVAT of non-immunized (C) mild (D) and severely arthritic (E) mice are shown. Scale Bars represent 0.25µm. Red staining represents TRAP positive cells.

4.3.5 MGP Protein was not Altered Following Onset of Arthritis

When MGP protein levels were determined in the aorta (Figure 4.17A) and surrounding PVAT (Figure 4.17B), no significant changes between non-immunized, mild and severely arthritic tissues were evident: (15.1±6.1 (N=3) vs. 13.9±2.6 (N=12) vs. 16.0±6.2 (N=5)) and (25.7±6.2 (N=3) vs. 20.3±4.9 (N=12) vs. 16.2±4.7 (N=5)) respectively.

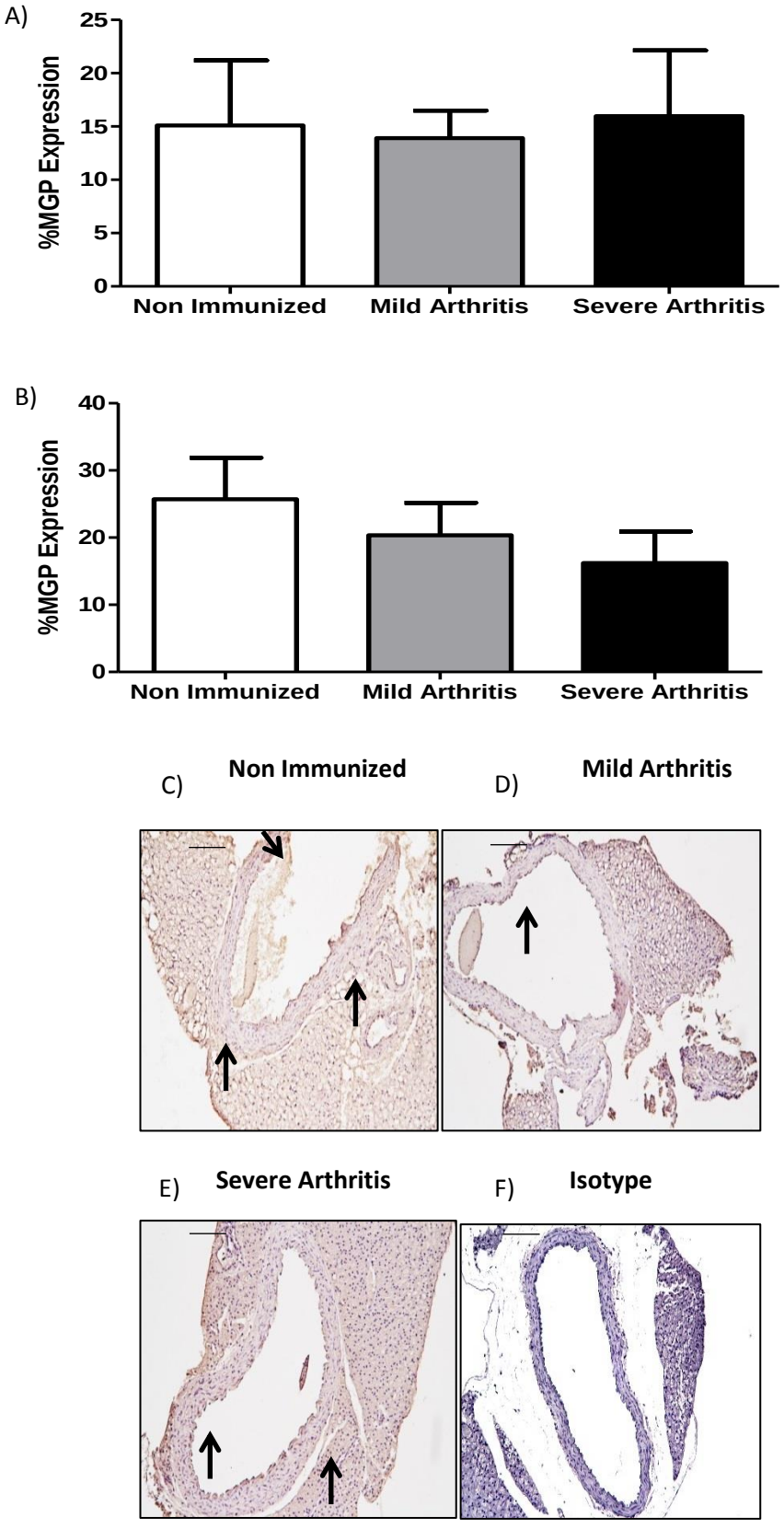

Figure 4.17- MGP Protein Profile. MGP protein levels were determined in the aorta (A) and PVAT (B) of non-immunized, mild and severe arthritic mice. Representative images (x20 magnification) of non-immunized (C), mild (D), severely (E) arthritic mice and Isotype (F) are shown. Scale Bars represent 0.2µm. Brown staining represents MGP positive cells.

4.3.6 OPN Protein was Significantly Increased in the PVAT of Severely Arthritic Mice.

When OPN protein levels were determined in the aorta no significant differences between non-immunized, mild and severely arthritic tissues were identified (Figure 4.18A) (7.5±1.9 (N=4) vs. 8.6±1.6 (N=4) vs. 10.4±1.9 (N=4)). In the PVAT (Figure 4.18B) OPN protein levels were significantly ($p=0.027$) increased in severe disease in comparison to non-immunized controls (9.0±2.1 (N=4) vs. 11.7±3.8 (N=4) vs. 28.2±6.3 (N=4)).

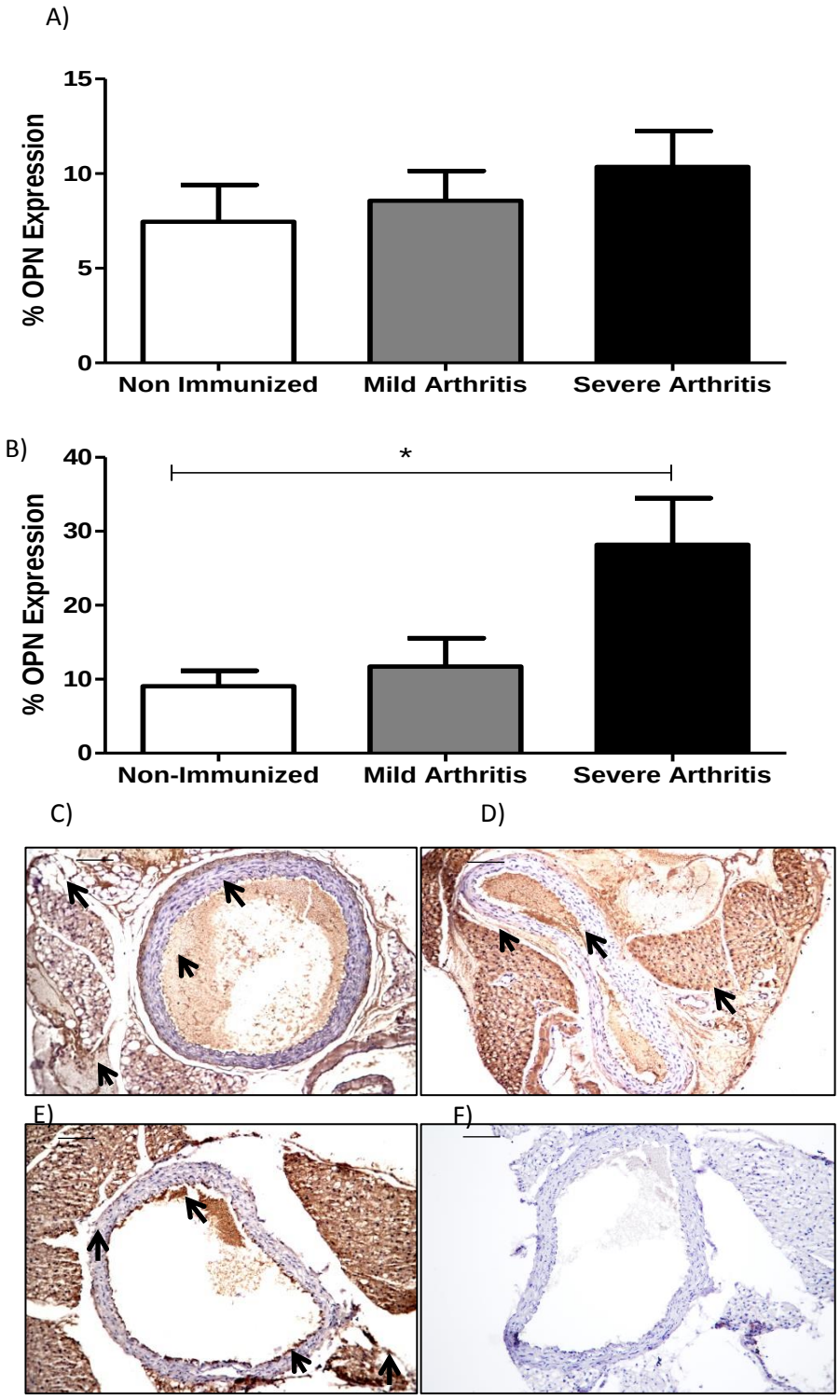

Figure 4.18 - OPN Protein Profile. OPN protein levels determined in the aorta (A) and PVAT (B) of non-immunized, mild and severe arthritic mice. Representative images (x20 magnification) of tissues taken from non-immunized (C) and mild (D), severely (E) arthritic mice and isotype (F) are shown. Scale Bars represent 0.2µm. *=p<0.05. Brown staining represents OPN positive cells.

4.3.7 Changes in Structural Components of Aortic Vessel Wall Following Arthritis Onset.

Collagen and Elastin was only investigated in tissues from non-immunized and severely arthritic mice.

There was no change in the percentage of collagen (42.19± 16.34% (N=3) vs. 53.29± 4.37% (N=9)) within the aortic vessel wall compared to non-immunised controls (Figure 4.19A). No correlation was seen between collagen content and either arthritis severity or time with disease (Figure 4.19B).

Elastin content in the aortic vessel wall significantly (p=0.03) increased in the arthritic mice (Figure 4.20A) (32.53± 9.49% (N=3) for control vs. 53.29± 3.63 (N=9) for arthritis). A significant positive correlation between elastin content and time with arthritis (p=0.02, Pearson's R=0.64) was observed (Figure 4.20B).

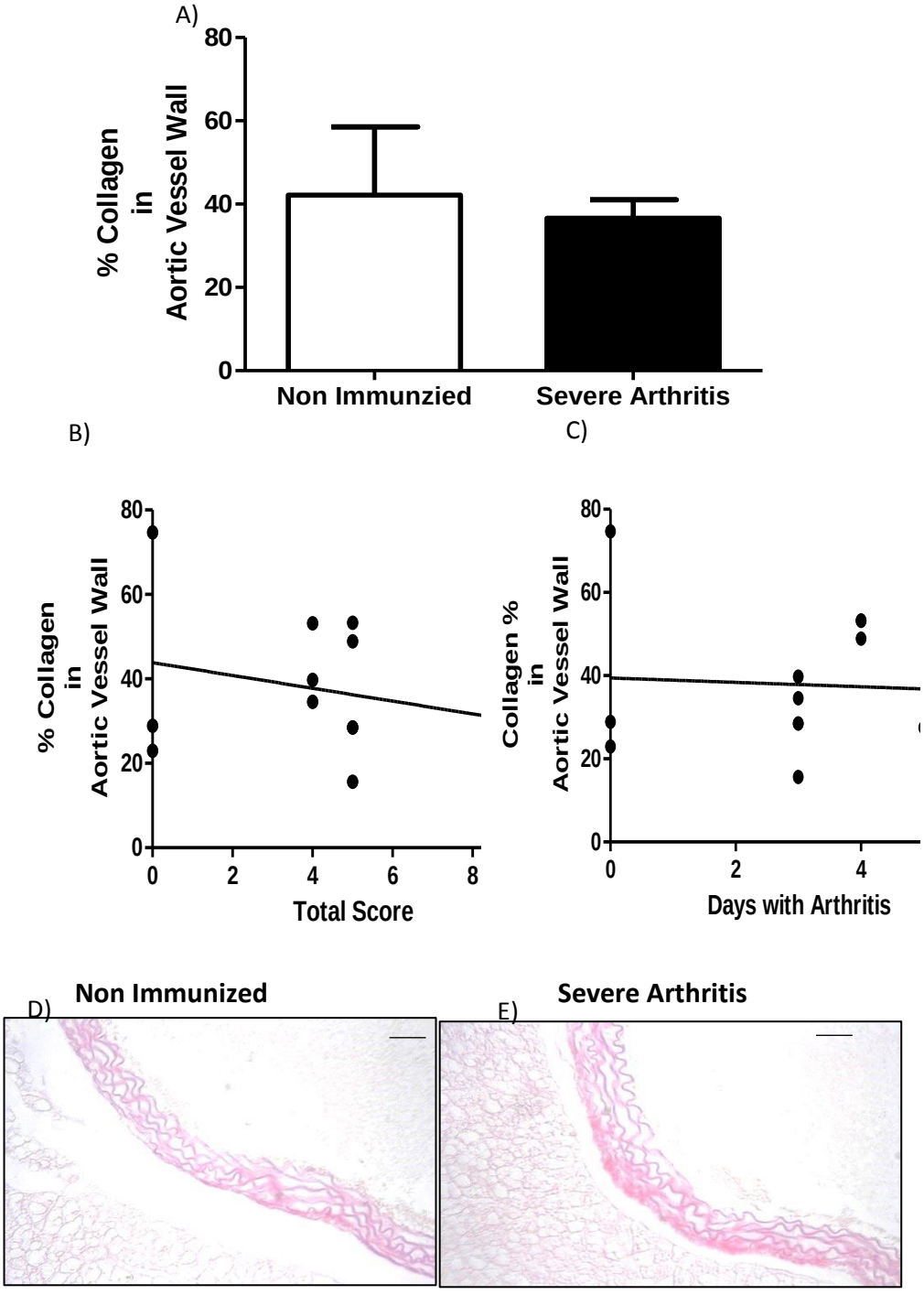

Figure 4.19 - Collagen Content in the Aortic Vessel Wall- The percentage of collagen in the aorta was determined in non-immunized and severely arthritic tissues (A). This was also correlated with worsening arthritis score (B) and time with arthritis (C). Representative images (x40 magnification) show collagen staining in non-immunized (D) and severe arthritic aortae (E). Scale bars represent 0.2µm. Heavy pink staining represents positive collagen filaments.

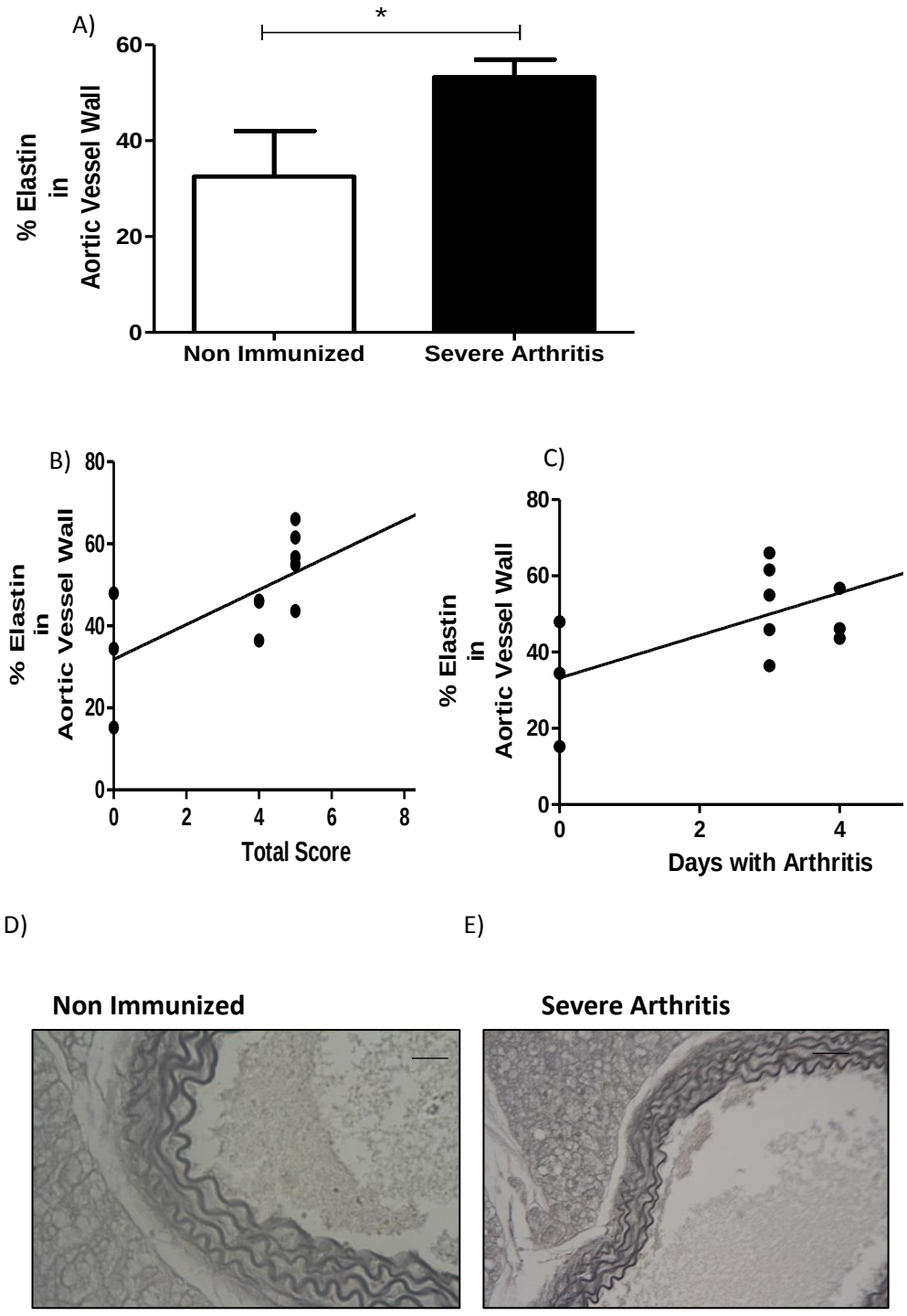

Figure 4.20 - Elastin Content in the Aortic Vessel Wall- The percentage of elastin in the aorta was determined in non-immunized and severely arthritic samples (A). This was also correlated with worsening arthritis score (B) and time with arthritis (C). Representative images (x40 magnification) show elastin staining in non-immunized (D) and severe arthritic aortae (E). Scale bars represent 0.2µm. *=p<0.05. **=p<0.01. Black staining represents Elastin filaments.

4.3.8 Interesting Observations

During a particular experiment, two mice did not reach the severity limit of the protocol and were followed to day 40 with arthritis, at which time they had a total paw score of 7 and 8 respectively. These data were not included in the analysis described above. However, some interesting observations were made when RT-qPCR was carried out on tissues from these animals and the data displayed against that from mice with arthritis for up to 20 days (N=35). Although statistics were not carried out on these data, it is clear that expression of all osteoblast transcription factors; RUNX2, OSX and ATF4 (Figure 4.21A, B and C) were increased with extended time. Similarly, osteoclastogenesis factors; OPG, RANK and RANKL (Figure 4.21D, E and F) were also increased in the day 40 mice. Changes in the osteoclast markers, TRAP, Cathepsin K and Calcitonin Receptor (Figure 4.21 G, H and I) whilst evident, were not as obvious. All apoptosis marker expression was decreased in the older mice (Figure 4.22A, B, C), whereas, mineralization inhibitors MGP and OPN (Figure 4.22D, E) and the mineral marker OCN (Figure 4.22F) were increased.

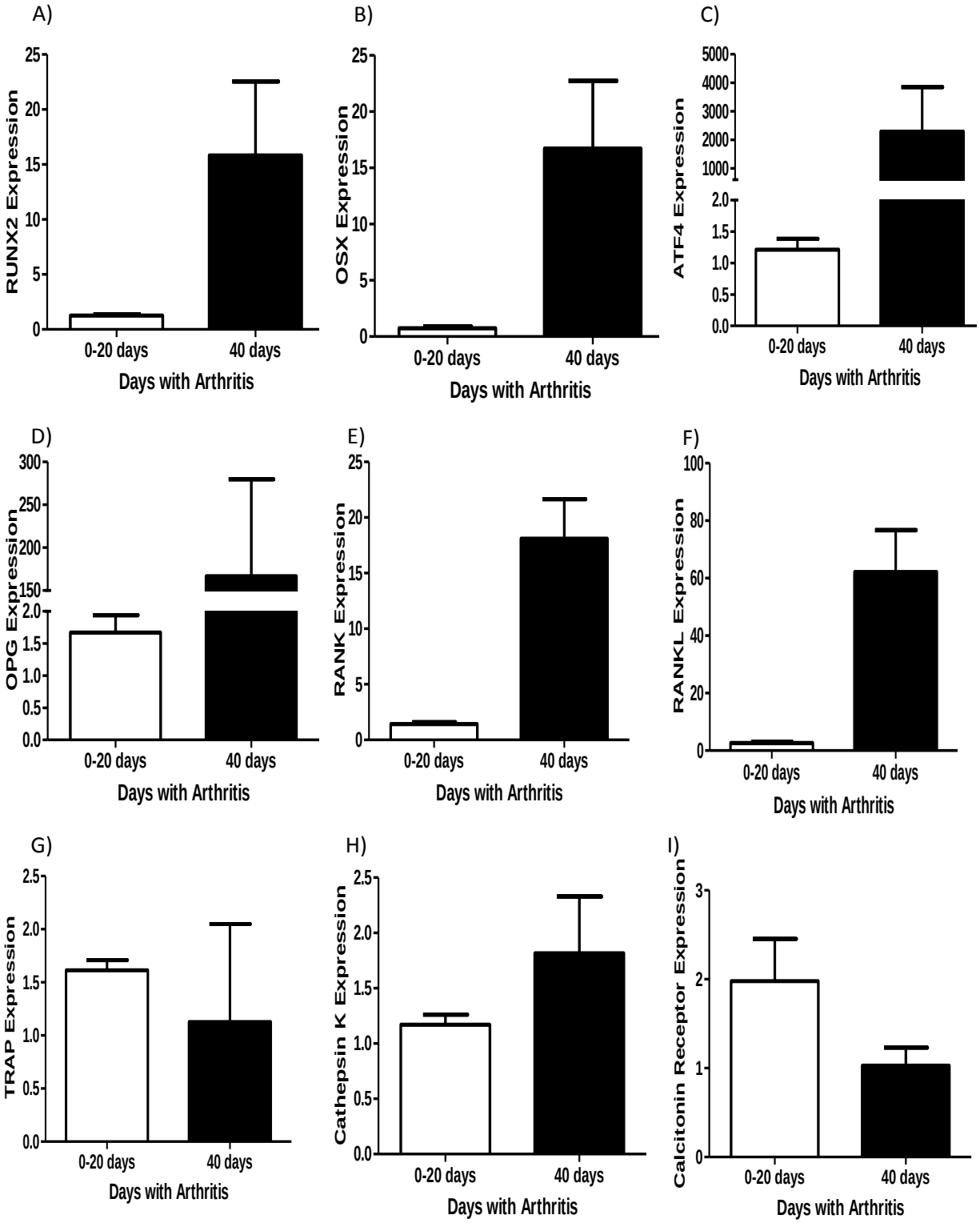

Figure 4.21- Osteoblast and Osteoclast Factors. Expression of markers of: Osteoblast transcription; RUNX2 (A), OSX (B) and ATF4 (C), Osteoclastogenesis; OPG (D), RANK (E) and RANKL (F) and Osteoclasts; TRAP (G), Cathepsin K (H) and Calcitonin Receptor (I) in tissues from older day 40 mice displayed against that from mice with arthritis for up to 20 days. No statistical tests were carried out.

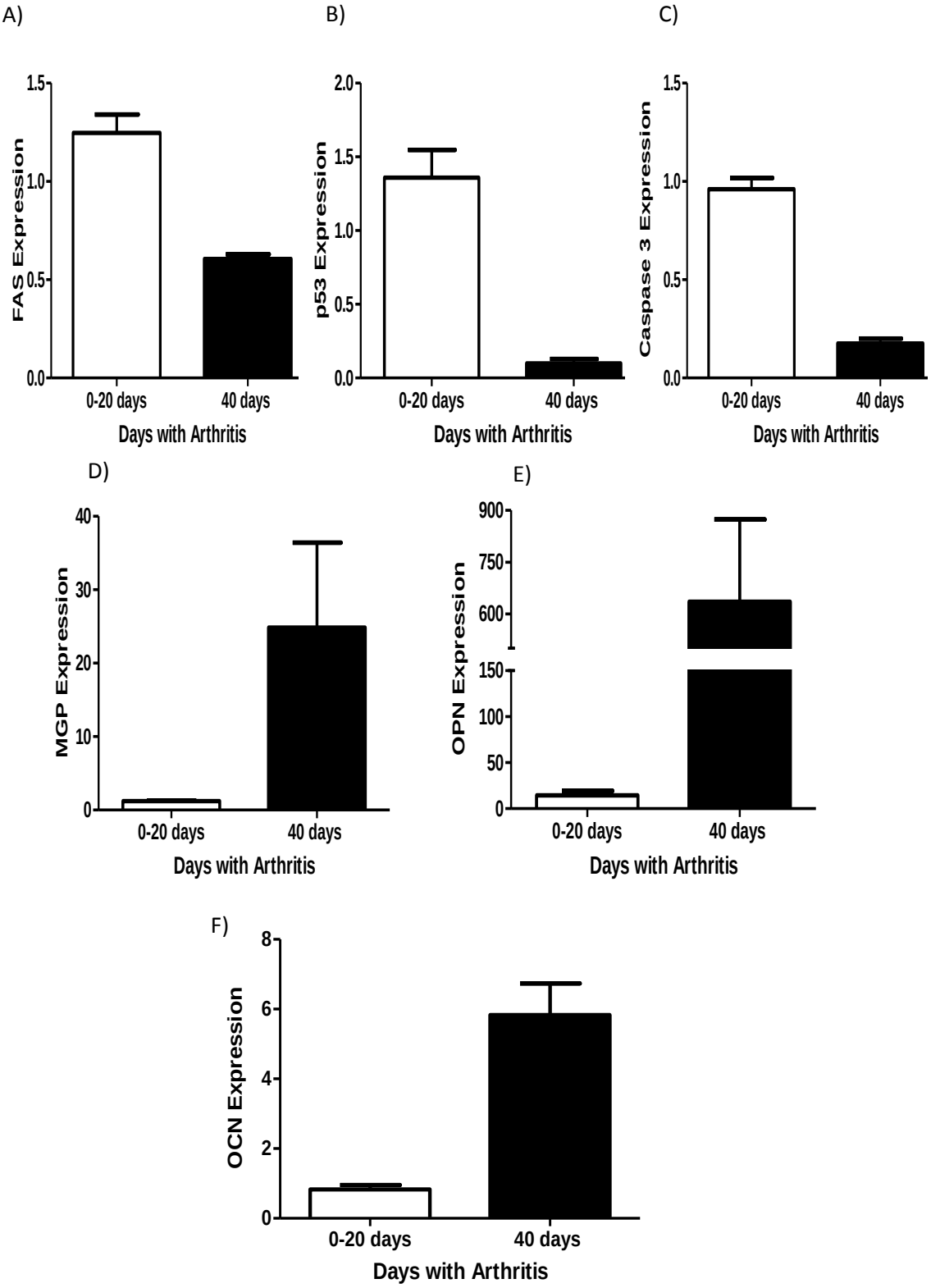

Figure 4.22- Apoptosis and Mineralization Factors. Expression of markers of: Apoptosis; FAS (A), p53 (B) and Caspase 3 (C), Mineralization inhibition; OPN (D), and MGP (E) and Osteocalcin (F), in tissues from older day 40 mice displayed against that from mice with arthritis for up to 20 days. No statistical tests were carried out.

4.4 Discussion

A potential role for vascular calcification in the contractile dysfunction observed in mCIA was investigated for the first time in these experiments. The expression profiles of osteoblast transcription factors were determined to establish whether VSMCs had gained an osteogenic-like phenotype. While no significant changes were observed between control and diseased tissues, the very fact that they were present is noteworthy. Indeed, this suggests that while they do not seem to be driving calcification in this relatively acute model of inflammatory arthritis, they certainly have the potential to do so. The relationship of these transcription factors and the interplay between them during physiological bone formation has been well characterised (Komori, 2006). However, although they have been identified as important in the vascular calcification process, their relationship in this context is ill defined. Unlike RUNX2 and OSX, ATF4 was significantly increased over time with arthritis. One possible explanation relates to ATF4 being a multipurpose transcription factor. For example, ATF4 has been implicated in endoplasmic reticulum stress-mediated apoptosis, a process indicative of vascular calcification (Duan *et al*, 2013). Moreover, the knock down of ATF4 has been shown to reduce endoplasmic reticulum stress mediated apoptosis, blocking vascular calcification via negative regulation of the osteoblast phenotypic switch of VSMCs (Duan *et al*, 2003). This may explain why levels of ATF4 were significantly increased unlike both RUNX2 and OSX expression. In order to determine whether ATF4 is playing a role outside of the osteoblast, further investigations, in particular more localised immunostaining, are warranted.

Interestingly, when OPG levels were low in control and severe arthritis, although not statistically significant, RANKL levels were increased. That the opposite trend was observed in mild disease supports these changes as being pathophysiologically relevant. Importantly this shows a balanced relationship between the two proteins, and one that can change in response to the local environment (Geusens, 2012). When this relationship becomes unbalanced, in favour of RANKL, we would expect osteoclast activity to be favoured (Boyce and Xing, 2008).

Static expression of osteoclast markers; TRAP, Cathepsin K and Calcitonin Receptor coupled with increased RANK expression suggests that there is another cell within the vasculature, other than the osteoclast capable of producing RANK. To this end, macrophages have been described to express RANK (Kido *et al*, 2005), and previous data described in this thesis (Chapter 2) shows an expression profile for F4/80 positive macrophages that matches that for RANK described here. While macrophages can differentiate into osteoclasts under the right environmental conditions (Udagawa *et al*, 1990), it is important to note that RANK is involved in a number of other homeostatic functions, such as, remodelling, repair and immune function. Recently, a study has shown that macrophages within aneurysmal arteries differentiate in to osteoclasts (Takei *et al*, 2016). These macrophages were shown to express a number of osteoclast markers, including TRAP. The study goes on to demonstrate that these markers were not expressed on macrophages within non-diseased aortic tissue. During this study

osteoclastogensis was initiated by the activation of NF-κβ (Takei *et al*, 2016). We therefore suggest the expression profile of RANK in the aorta and PVAT was indicative of the presence of macrophages with the capability to differentiate into osteoclasts within this region.

Although no difference in the number of TRAP positive cells was observed in the aortic vessel wall and surrounding PVAT between control and arthritic mice, for the first time TRAP+ cells were identified in these tissues. While TRAP can be expressed on activated macrophages as well as on osteoclasts (Janckila *et al,* 2007; Takei *et al*, 2016), the pattern of TRAP staining does not fit with that observed for macrophages, or any other inflammatory marker studied in similar tissues in this thesis (Chapter 2). Previous studies by Takei *et al*, suggest that TRAP is only expressed on macrophages that within diseased tissue, however, TRAP+ cells have not previously been examined in the aorta following inflammatory arthritis. Therefore to determine if the TRAP+ staining seen in figure 4.16 is truly representative of osteoclasts or of macrophages, dual colour staining would be required.

When looking at the impact of calcification inhibitors during arthritis the results were surprising. There was no change in MGP gene expression or protein levels, following arthritis onset or during time with arthritis. Previous studies have demonstrated that MGP is expressed in normal vessels, albeit at low levels (Canfield *et al*, 2000). The results presented in Figure 4.8 support this observation for our model, and also show that MGP gene expression was much lower than OPN gene expression in all groups with a 20 fold less expression level in comparison to OPN.

OPN gene expression increased in relation to time and OPN protein levels increased in the PVAT of severely arthritic mice. A similar trend of increased OPN protein was seen in the aortic wall. Increased OPN has been shown previously in the apolipoprotein$^{-/-}$ mouse model of atherosclerosis (Liou *et al*, 2005). However, OPN regulation is complex, it can be cleaved proteolytically by MMP-9 (Lindsey et al, 2015) and unlike most inhibitors does not necessarily decrease to allow calcification to occur. Indeed, OPN may also be involved in other cellular processes. For example, full length OPN is implicated in cell attachment and migration (Scatena *et al*, 2007), while processed OPN is known to be pro-inflammatory (Sharif *et al*, 2009), pro-angiogenic (Hamada *et al*, 2004) and pro-osteogenic (Egusa *et al*, 2009). This suggests the importance of differentiating between the types of OPN present within the aortic vessel wall and PVAT. Moreover, it would be beneficial to co-stain for MMPs and OPN in mCIA given that OPN has previously been associated with increased MMP-9 (Lai *et al*, 2006). That increased MMP-9 was seen in the PVAT of mCIA animals (Chapters 2 and 3) emphasises this point.

Pro-inflammatory OPN is found to be enriched at sites of calcification (Breyne *et al*, 2010), going some way to explaining both increased inflammatory cells and increased OPN in the aorta and PVAT during mCIA. However, this creates a dilemma in which it is difficult to gauge if increased OPN is acting beneficially to reduce calcification or adversely in driving inflammation. Despite mechanisms being unclear, normal blood vessels lack OPN expression and it only appears under pathological conditions (Speer *et*

al, 2002) thus confirming the importance of the observations made in the aorta and PVAT of mCIA animals.

Whether initiation of vascular calcification is triggered by the presence of extracellular, matrix vesicles has been a long-standing question for debate. Recent evidence suggests that vesicles produced from VSMCs and macrophages are mediators in calcification of the vasculature leading to diseases such as atherosclerosis (Krohn *et al*, 2016). However, the underlying mechanisms explaining how these vesicles drive calcification remain elusive. They are produced from the budding of cells such as VSMC, chondrocytes and osteoblasts (Proudfoot *et al*, 2000), and are thought to be remnants of apoptotic cells. This study shows no change in apoptosis markers; FAS and p53, either with severity or over time, suggesting no increase in the number of apoptotic cells. Moreover, Caspase 3 was significantly down regulated as previously observed in a breast cancer model where it provided a cell survival mechanism (Devarajan *et al*, 1987). This may be important when considering why we see increased total cell number (previously described in Chapters 2 and 3). The lack of change in apoptosis markers suggests that apoptopic/matrix vesicles are not being produced in order to initiate vascular calcification in mCIA at this time point. The data here does not conclude a role for apoptosis in vascular calcification. In mCIA it is more likely that vascular dysfunction is driven by inflammatory changes at the level of the blood vessel.

Changes to arterial elasticity, compliance and pulse wave velocity are associated with increased CVD risk and are often due to modifications of collagen and elastin fibres (Chow *et al*, 2013). In mCIA little change to collagen is observed with arthritis onset, increased severity or over time. This suggests that pulse wave velocity has not yet been altered within the aorta. If it was increased it would be expected that collagen would be recruited to the region in order to support the extra tension (Cecelja and Chowienczyk, 2012). While some clinical studies show that calcification is associated with decreased or disrupted collagen production (Rodriguez *et al*, 2014), it would not seem to be the case here. It is possible that although the overall amount of collagen in the aortic vessel wall was broadly unchanged, the highly organised collagen fibres may be dysregulated. Further in depth analysis would be required to determine normal organised structure and whether this has been altered within the arthritic animals.

Perhaps a more important observation is, the significantly increased percentage of elastin within the aortic vessel wall with onset, increasing severity and time with arthritis. From the literature it is very common for the percentage of elastin to decrease for example, with age (Tsamis *et al*, 2012) and in aortic aneurysm (Iribarren-Marin *et al*, 2011). Therefore, this increase in elastin is interesting and is more indicative of a fibrosis-like phenotype (Cantor *et al*, 2002). Vascular fibrosis involves proliferation of VSMCs, accumulation of ECM and is a highly inflammatory process. Whether fibrosis is the cause of the vascular dysfunction in this model, or whether it goes hand in hand with calcification, is still a question for debate. However, it certainly serves as an alternative explanation for the increased total cell counts observed in chapters (2 and 3), but requires far more in depth investigations for confirmation.

The data shown in Figure 4.21 and 4.22 show would seem to indicate that time with arthritis is very important in terms of triggering vascular calcification. While it is not supported by statistical analysis and scrutiny, the data does serve as a basis for the direction of future studies. What we are seeing in this model so far is highly likely to reflect the very earliest pathological changes associated with increased vascular inflammation. The early window on disease provided by mCIA is paramount since in human RA this stage is often missed due to a long diagnosis time. That the 2 mice described in these data sets only reached scores of 7 and 8, 40 days post arthritis onset provided an unusual opportunity to determine the role of time with arthritis as opposed to severity. These animals were thought to more similarly mirror human disease as they had a steady, slow progressing disease.

In these mice the osteoblast transcription factors appear vastly increased, suggesting a likely osteogenic switch in smooth muscle cell phenotype (Steitz *et al*, 2001). The biggest of the increases was seen in ATF4 gene expression and is in line with the data described earlier where ATF4 was expressed at higher levels than RUNX2 and OSX. This may support ATF4 potentially playing more than one role in the initiation of vascular calcification. The increase in all osteoblast transcription factors within the aorta has not previously been described during mCIA. In terms of future studies it would be exciting to determine the impact of long term inflammatory arthritis on the downstream mediators of osteoblast transcription.

The osteoclastogenesis markers were also increased in the 40 day animals. RANKL was elevated to a similar extent as RUNX2 suggesting that osteogenic VSMC switching may be occurring, and the altered cells are now capable of expressing RANKL. However, this increase in gene expression could also be related to an increase in macrophages as earlier discussed. In order to determine whether this was the case further analysis of macrophage numbers within the aorta and PVAT of animals with longer term mCIA is required. That OPG is also increased, suggests a potential counteracting mechanism being initiated within the aorta. To definitively establish whether the RANK/RANKL/OPG pathway is driving osteoclastogenesis, further analysis of the TRAP positive osteoclasts is also warranted.

If these data in Figure 4.21 and 4.22 represents an increase in osteoblast-like cells, then a complementary increase in mineral markers would be expected. To the contrary, both mineralization inhibitors, OPN and MGP are increased. Again, there is much debate as to whether these inhibitors increase or decrease prior to calcification. Further studies using an adapted protocol that allows long term arthritis to be investigated more thoroughly will allow the confirmation of this process.

That the described markers are apparently increased in longer term compared to short term arthritis would suggest that although vascular calcification is not driving the contractile dysfunction seen in mCIA in the short term, the changes to the vessel are indicative that calcification will occur later in the time course of the disease.

4.5 Conclusion

Early arthritis data confirms that vascular calcification is not the underlying cause of vascular dysfunction seen in the mCIA model. The presence of both osteoclast and osteoblast-like cells has been confirmed in the thoracic aorta and surrounding PVAT, however, they are not initiating calcification at this point in the mCIA model. Apoptosis cannot be confirmed as an initiator of vascular calcification. However, the changes to the vessel are indicative that calcification can occur and that this may take some time, as shown by the longer term animals. Excitingly, the results gained from looking at elastin percentage suggest a fibrosis-like phenotype, associated with high inflammatory state within the aorta and surrounding PVAT. This change in vessel elasticity is likely to impact on vessel constriction and thus may be the underlying cause of contractile dysfunction seen in this mCIA model. Further experiments with a longer-term mCIA model will throw light on these questions.

Chapter 5 - Contractile Dysfunction in a Long Term mCIA Model: Role of Medial Calcification and/or Structural Changes

5.1 Introduction

As RA develops into the chronic disease stages, large joints become affected and patients suffer with pain swelling and stiffness. One of the striking observations with RA is its ability to regress and relapse over time. This means patients have periods of high inflammation along with periods of remission. While the changes in the joints are characteristic of RA, it is also important to consider the systemic impact of the inflammatory burden over time. Some RA patients can suffer symptoms of the disease for over half of their lifetime, and it is not surprising that they develop inflammation-associated co-morbidities in the long term. Because ethical issues prevent detailed human studies regarding pathological mechanisms, the current gold standard animal model, mCIA, is often used as a surrogate. While this provides a great opportunity to investigate the very first changes occurring around disease onset, the timeline for studying disease activity is conversely limited. The "norm" in this model is for mice to become arthritic inside approximately 5 days and for severe arthritis to develop within 10 days. Home Office project licence restraints prevent further use of the mice once the arthritis severity limit maximum has been reached. As such adaptations must be made to the mCIA protocol to allow us to investigate long term disease and the effects of sustained systemic inflammation.

RA differs to other autoimmune diseases, including diabetes mellitus and systemic lupus erythematosus, which are associated with peaks of disease activity early in life. As a chronic inflammatory disease RA has a clear link with the aging population and age acts as a major risk factor for both its onset and development (Larbi *et al*, 2008). Whether the onset of RA is triggered by an aging immune system, and time is an important factor in RA pathology, remains open to question. An interesting possibility is that a difference exists between the chronological and biological ages of RA patients. Indeed, it has been demonstrated that RA patients have difficulty in regenerating their immune systems, more specifically T-cell populations, suggesting they have an older biological age than anticipated by their age in years (Jendro *et al*, 1995). The impact of immune system aging in this patient population could go some way to explaining the increased risk of co-morbidity, specifically CVD (Crowson *et al*, 2010). Indeed, that accelerated immune aging has been demonstrated in coronary artery disease patients who do not have an inflammatory disease would seem to support this hypothesis (Liuzzo *et al*, 1999). In fact, RA is now considered as an independent risk factor for CVD.

A key co-morbidity associated with RA, vascular calcification, is also linked with an aging population, in fact it has been suggested that the majority of individuals aged over 60 exhibit progressively enlarging calcium deposits in their major arteries (Allison *et al*, 2004). Such pathology is often associated with decreased aortic elasticity, impairing vascular function and ultimately leading to increased morbidity and mortality (Wayhs *et al*, 2002). In studies that examine the calcium content of the thoracic aorta in different age groups, both intimal and medial calcium concentrations are significantly increased over time (Elliot and McGarth, 1994). The study also demonstrated that calcium was most markedly increased in the medial layers encompassing the elastin rich region of

the vessel wall. Such changes to the vasculature are now considered common and the concept of an aged vascular phenotype is widely accepted (Matsumoto *et al*, 2007). However, little data exists as to how RA and vascular calcification are connected over time. The previous chapter demonstrated the importance of time with arthritis in the expression of calcification mediators within the thoracic aorta and PVAT. This coupled with the knowledge of RA progression and vascular calcification in the aging population justifies looking at mCIA over a longer time period in aging mice. An aim of this chapter is to use the mCIA model to further investigate this question.

In large arteries such as the aorta, elasticity and compliance are essential for vessel function. Stiffening of the aorta and other large elastic arteries is a hallmark of vascular aging. When stiffening occurs there is dysregulation of haemodynamics within the vessel and this often is the underlying cause of hypertension (Wallace *et al*, 2007). Pulse wave velocity can be measured in humans and is representative of vessel elasticity. It has been shown that this measurement is highly predicative of CVD. Importantly, arterial stiffness has been shown to occur independently of atherosclerosis and is a useful prognostic tool in CV pathology (Cecelja and Chowienczyk, 2016).

The changes seen during aging to structural proteins such as collagen and elastin are well established (Panwar *et al*, 2015). Aging drives an increase in collagen content, increased collagen cross linking and associated elastin fragmentation leading to a decrease in total elastin content (Jani and Rajkumar, 2006). Other associated structural changes in the aortic vessel wall during aging include altered endothelial function, dysregulation of wall thickness and stiffening of the vessel (Toda, 2012). Therefore, if these changes are seen in the general population it is likely that long periods of systemic inflammation will enhance them and may explain the increased CV risk in the RA patient cohort.

This chapter shows the experimental approach used to determine whether vascular calcification and/or structural changes occurred over time with arthritis. This chapter details methodology, results and discussion under the following objectives:

Hypothesis: Long term arthritis is associated with vascular calcification and structural changes to the aorta

- To investigate if long term arthritis drives medial calcification
- To establish a role for Osteoblast/ Osteoclast like cells in the vasculature of long term mCIA mice
- To determine if apoptosis occurring more readily in long term disease
- To understand differences due to age not disease status
- To determine if changes in density and structure of ECM components such as Collagen and Elastin are worse effected during long term mCIA

5.2 Methods

Methods described in the previous chapters (2 and 4) may still apply here. Rt-qPCR (4.2.9), TRAP staining (4.4), MGP Immunohistochemsitry (4.5), Elastin (4.6) and Collagen (4.7) staining have been previously described in detail.

Long Term Arthritis Type II Collagen Solution

The type II chick collagen (Sigma, C9301) solution was prepared by dissolving 10mg in 5mls of 10mM acetic acid (the latter made by adding 50µl of 1M acetic acid stock to 4950µl of dH_2O). Collagen was dissolved by stirring overnight at 4^oC.

Type II collagen Immunization Emulsion

The immunization emulsion to initiate mCIA was made by combining equal volumes of the type II collagen and CFA solutions as described in Chapter 2.

5.2.1 Induction of Long Term mCIA

The induction protocol for mCIA has been previously described in Chapter 2. To induce "long term" arthritis the only difference was the use of the new modified immunization emulsion (described above) and disease activity was monitored up to day 40 following arthritis onset. All non-immunized controls were age matched.

Following 40 days with arthritis mice were killed as previously described (Chapter 2) and samples were collected for RT-qpCR, histology, immumohistochemistry and myography as in Chapter 2.

5.2.2 Time Matched mCIA studies

Long term mCIA was also induced in 8 further mice. This experiment was time matched to the short term protocol used in the previous chapters of this thesis (Chapter 2, 3 and 4). This experiment was used to determine the impact of changing the collagen emulsion on structural read outs from the thoracic aorta.

5.2.3. Statistics

Statistics used in this chapter are the same as those described previously in section 2.2.7.3. All RT-qPCR data were analysed for the impact of arthritis severity on factor expression. Comparison of Non-Immunized and long term arthritis was compared using Student's *t*-test. $P<0.05$ was considered significant.

5.3 Results

100% of DBA/1 mice developed arthritis 34 days into the protocol (Figure 5.1). This is compared with 100% incidence in the "short term" protocol by day 31 (Figure 2.5). Weight decreased at the point of arthritis onset but did not differ significantly over time (Figure 5.2 A). Both paw diameter and paw score showed trends of increase over time with arthritis (Figure 5.2 B, C respectively). However, peaks in both measurements were between days 30 and 40.

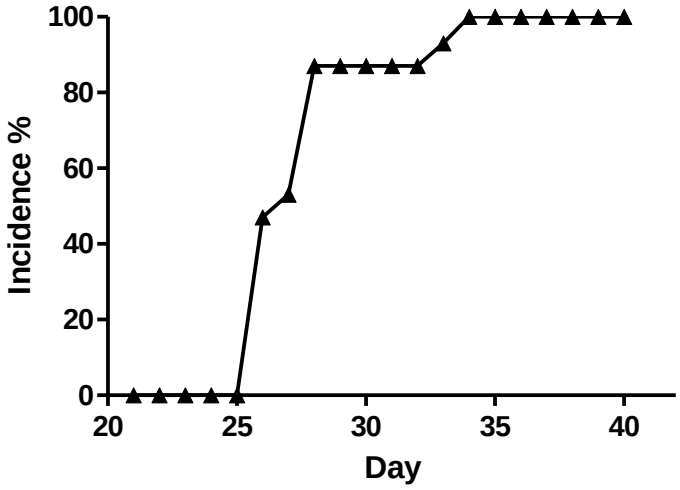

Figure 5.1 – Arthritis Incidence in Long Term mCIA. Graph represents percentage of animals with arthritis at each day following booster immunization on day 21. Data represent one experiment where 8 DBA/1 mice were used.

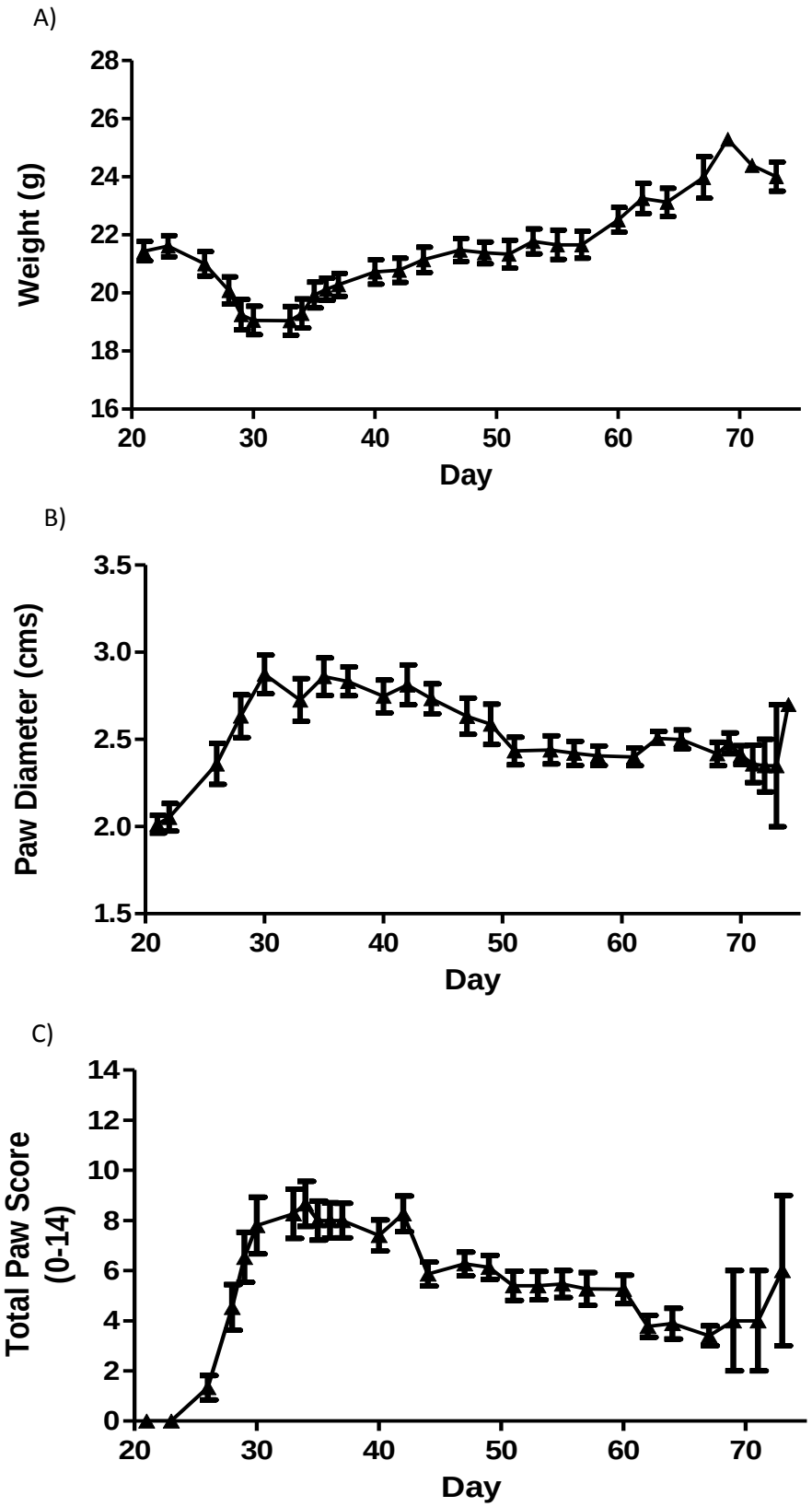

Figure 5.2 - Long Term Arthritis Induction. The graphs represent weight (A), paw diameter (B) and total paw score (C) from a long term arthritis experiment with 8 DBA/1 mice.

5.3.2 Long Term Arthritis is not associated with Changes in Osteoblast and Osteoclast Activity in the Vasculature

The expression of osteoblast transcription factors RUNX2 (Figure 5.3A), OSX (Figure 5.3B) and ATF4 (Figure 5.3C) were analysed in PVAT-intact aortic sections from non-immunised and long term arthritic mice. There was an observable but not significant increase for all transcription factors following arthritis; RUNX2 (2.55 ± 0.62 (N=4) vs. 5.17 ± 1.33 (N=8)), OSX (2.66 ± 1.78 (N=4) vs. 5.33 ± 1.30 (N=8)), ATF4 (0.99 ± 0.34 vs. 2.76 ± 1.38 (N=8).

The expression of osteoclastogenesis markers OPG (Figure 5.4A), RANK (Figure 5.4B) and RANKL (Figure 5.4C) were also analysed in these tissues. No significant change was seen in OPG expression (0.63 ± 0.23 (N=4) vs. 0.86 ± 0.23 (N=8) respectively). The picture was similar for RANK (1.09 ± 0.27 (N=4) vs. 1.22 ± 0.19 (N=8)) and RANKL (3.79 ± 1.93 (N=4) vs. 6.73 ± 1.81 (N=8)) expression.

Compared to non-immunised controls, no distinct changes in the osteoclast markers TRAP (Figure 5.5A), Cathepsin K (Figure 5.5B) and Calcitonin Receptor (Figure 5.5C) were observed in long term arthritis. TRAP (1.06 ± 0.12 (N=4) vs. 1.80 ± 0.31 (N=8)), Cathepsin K (1.19 ± 0.32 (N=4) vs. 1.46 ± 0.28 (N=8)) and Calcitonin Receptor (7.36 ± 3.71 (N=4) vs. 13.55 ± 3.99 (N=8)).

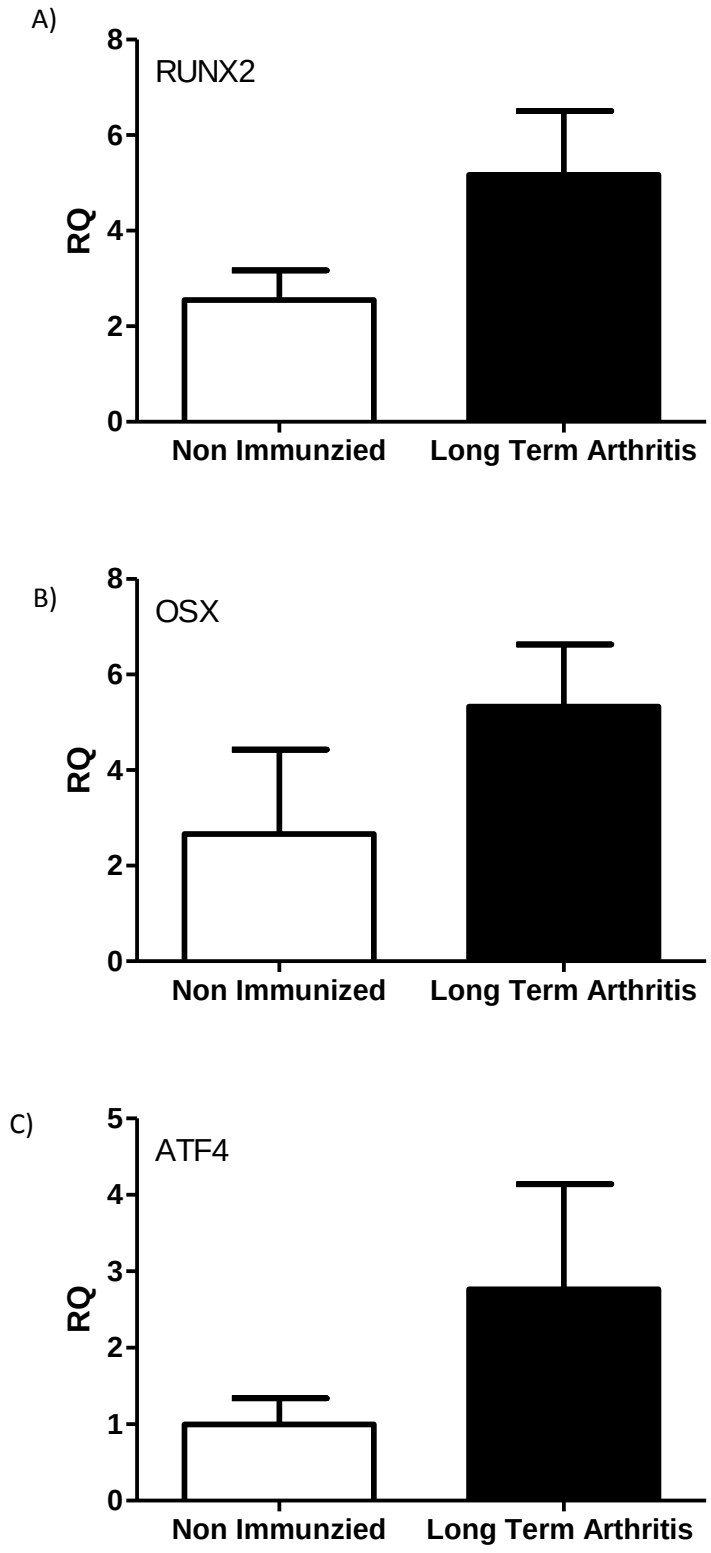

Figure 5.3 - Osteoblast Transcription Factors. Expression of osteoblast transcription factors RUNX2 (A), OSX (B) and ATF4 (C) were determined in non-immunized and long term arthritic PVAT-intact aorta.

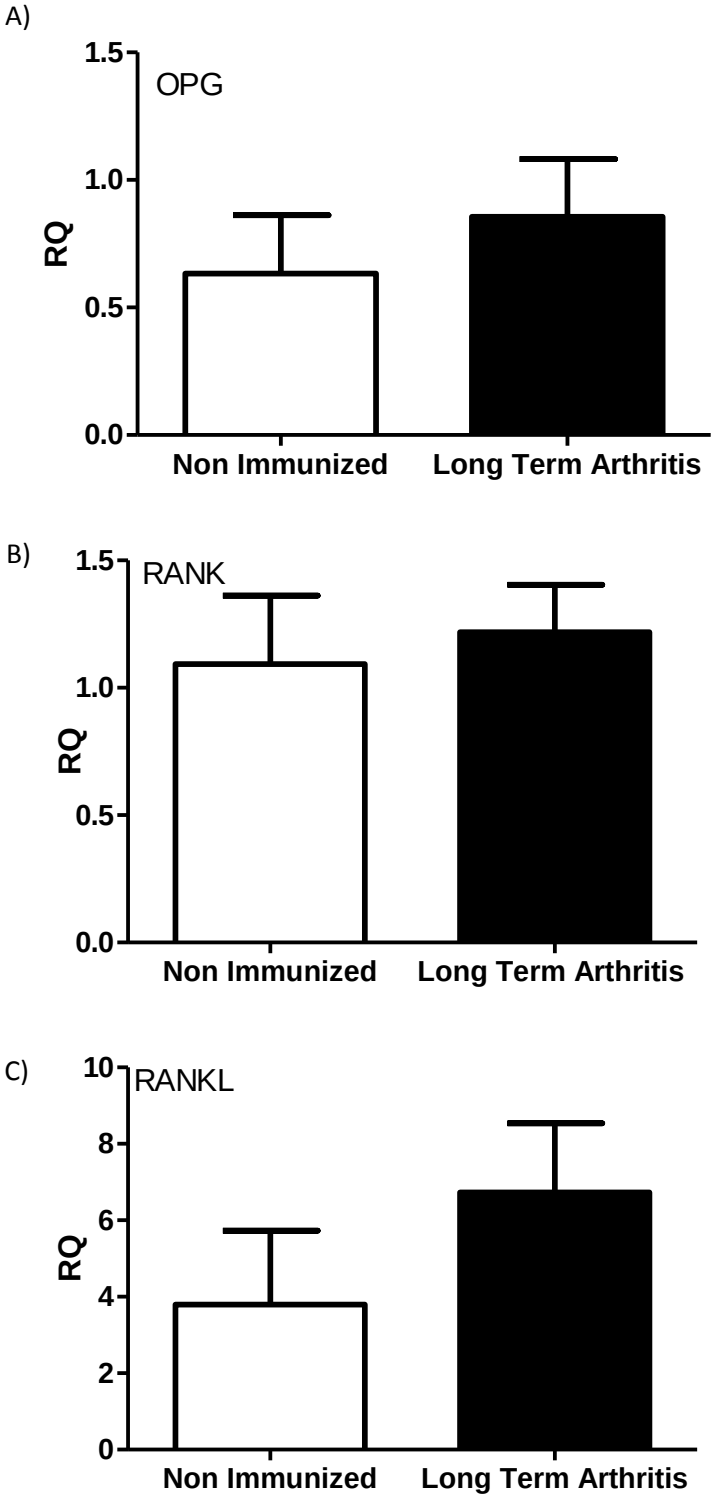

Figure 5.4 – Osteoclastogenesis Factors. Expression of osteoclastogenesis factors OPG (A), RANK (B) and RANKL (C) were determined in non-immunized and long term arthritic PVAT-intact aorta.

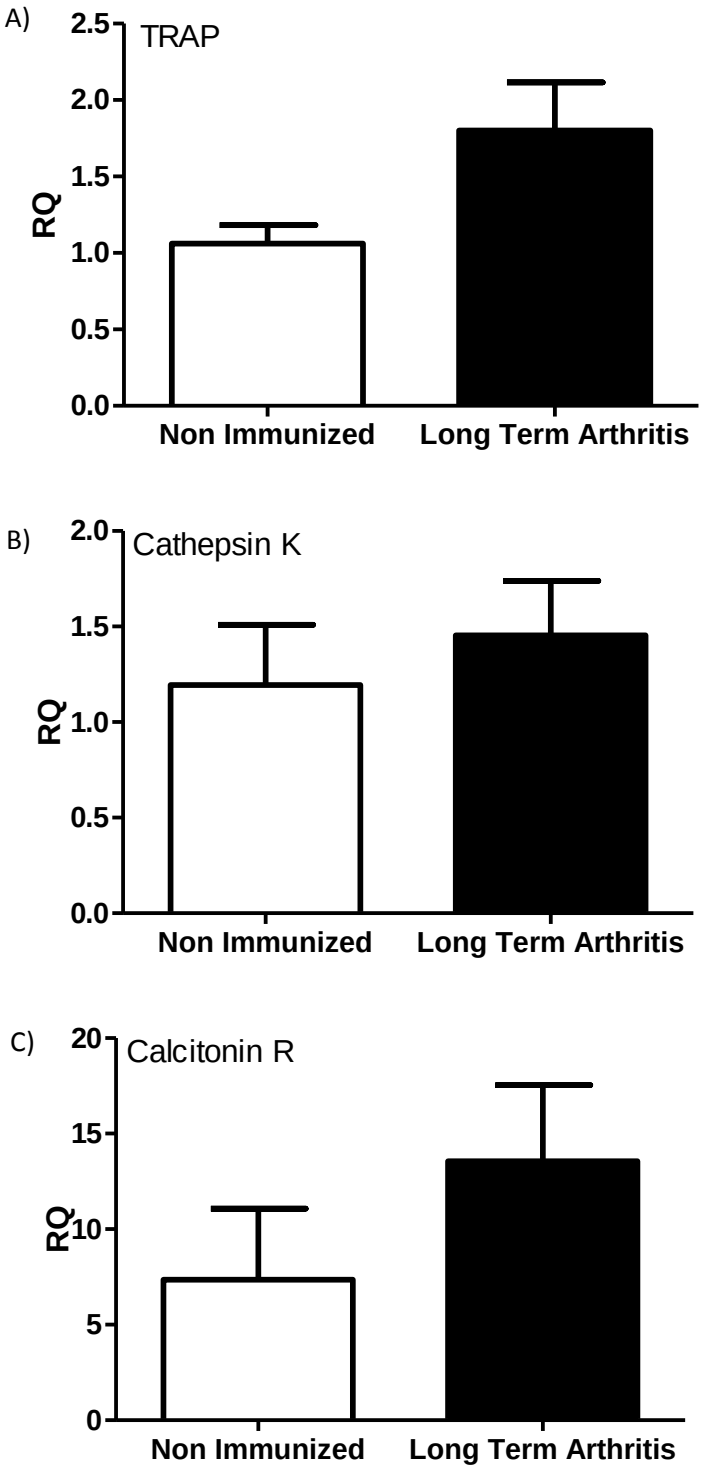

Figure 5.5 – Osteoclast Markers. Expression of Osteoclast markers TRAP (A), Cathepsin K (B) and Calcitonin Receptor (C) were determined in non-immunized and long term arthritic PVAT-intact aorta.

5.3.3. Mechanisms for Initiating Mineralization are not Altered During Long Term Arthritis

The expression of mineralization inhibitors MGP (Figure 5.6A) and OPN (Figure 5.6B) were also investigated. MGP remained constant during long term arthritis (1.79 ± 0.40 (N=4) vs. 1.82 ± 0.28 (N=8)). Similarly, OPN also remained constant (2.80 ± 1.14 (N=4) vs. 7.31 ± 1.84 (N=8)).

Expression of apoptosis markers; FAS (Figure 5.7A), p53 (Figure 5.7B) and Caspase 3 (Figure 5.7C) were determined. No significant differences were observed; FAS ((1.12 ± 0.12 (N=4) vs. 0.96 ± 0.24 (N=8)), p53 (0.32 ± 0.23 (N=4) vs. 0.17 ± 0.11 (N=8)) and Caspase 3(0.80 ± 0.26 (N=4) vs. 1.32 ± 0.43 (N=8)).

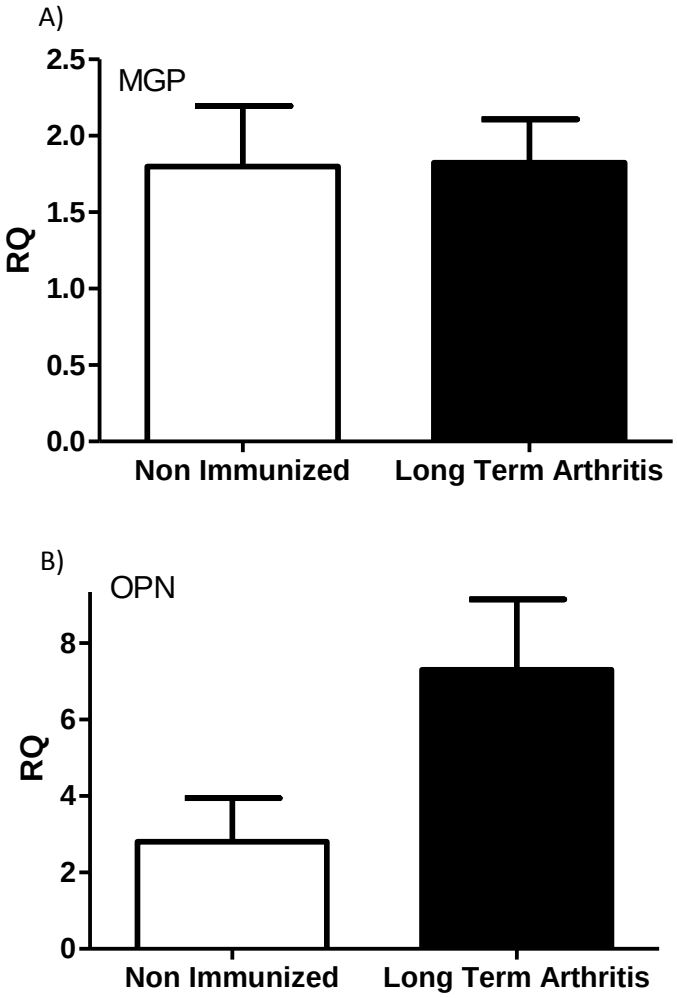

Figure 5.6 - Mineralization Inhibitors. Expression of mineralization inhibitors; MGP (A) and OPN (B) were determined in non-immunized and long term arthritic PVAT-intact aorta.

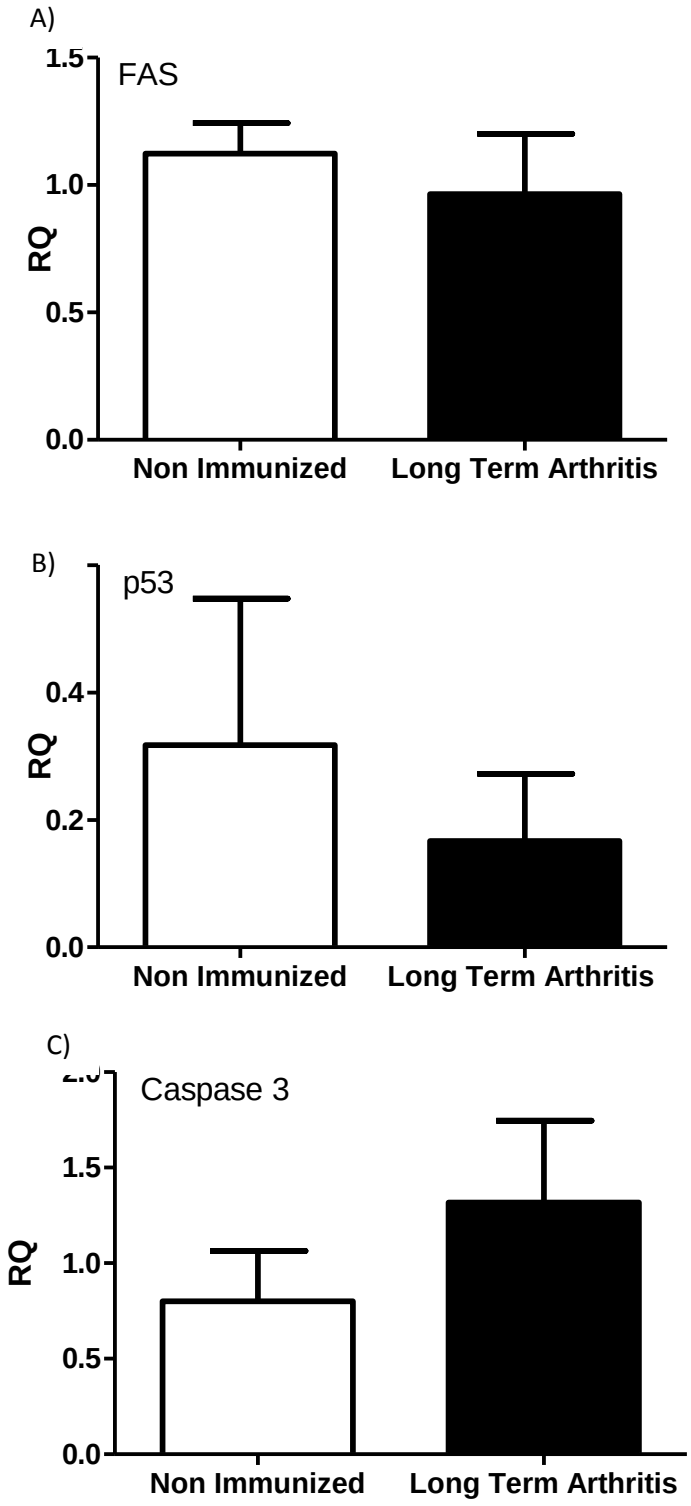

Figure 5.7 - Apoptosis Markers. Expression of osteoclast markers FAS (A), p53 (B) and Caspase 3 (C) were determined in non-immunized, long term arthritic PVAT-intact aorta.

5.3.4 Age Associated Changes to the Vasculature

When a comparison was made between parameters of the non-immunized controls discussed in Chapter 4 (approx. 12 weeks old) and those described in this long term chapter (approx. 18 weeks old) (ie. purely investigating the effect of ageing on normal mice) some interesting observations were uncovered (Figure 5.8). While expression of the majority of markers analysed remained unchanged, some increased with age. Expression of the osteoclast markers TRAP (3.71 ± 0.21 (N=11) vs. 5.24 ± 0.17 (N=4)) and Calcitonin Receptor (13.44 ± 0.43 (N=11) vs. 17.70 ± 0.98 (N=4)) and apoptosis marker Caspase 3 (8.11 ± 0.22 (N=11) vs. 9.67 ± 0.57 (N =4)) were significantly (p=0.0011, 0.0005 and 0.0077 respectively) increased in the older mice.

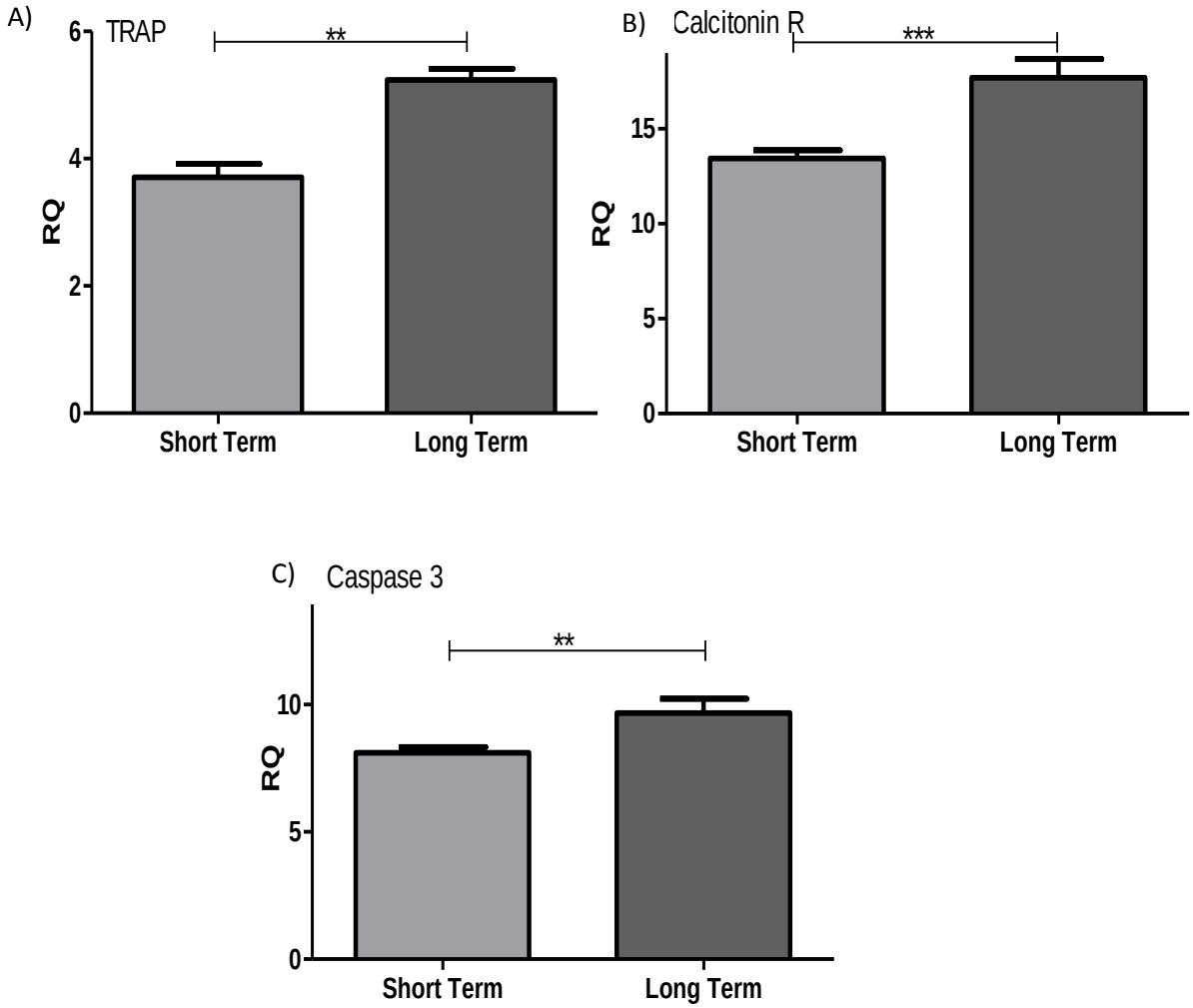

Figure 5.8– Short and Long Term Non-Immunized Comparison. Changes in expression of factors TRAP (A), Calcitonin Receptor (B) and Caspase 3 (C) were determined in short and long term non-immunized control thoracic aorta and PVAT. **=p<0.01, ***=p<0.001

5.3.5 TRAP Positive cell Number Does Not Change Following Long Term Arthritis in the Aorta or PVAT

When the number of TRAP positive cells was counted in both the aorta (3.20 ± 1.28 (N=5) vs. 1.71 ± 0.29 (N=7), Figure 5.9A) and PVAT (6.80 ± 1.46 (N=5) vs. 5.28 ± 1.67 (N=7), Figure 5.9B) there were no significant differences between long term non immunized and arthritic mice. A further comparison between the short term model described in the previous chapter and the long term controls discussed here (Figure 5.9C) revealed that the number of TRAP positive cells was significantly ($p=0.014$) up regulated with age (0.50 ± 0.29 (N=4) vs. 3.75 ± 1.49 (N=4)).

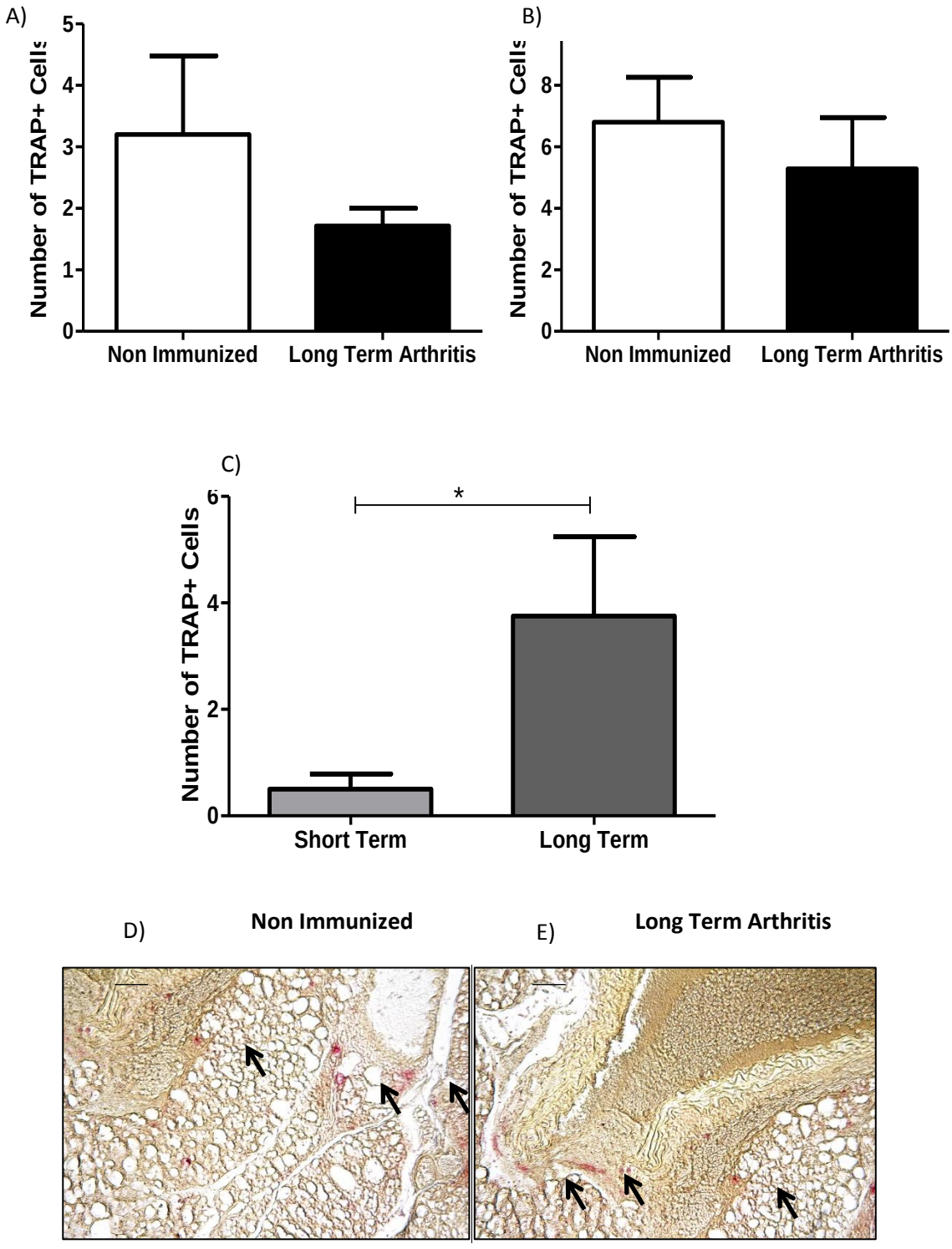

Figure 5.9- TRAP Protein Expression Profile. TRAP expression was determined in the aorta (A) and PVAT (B) of non-immunized and long term arthritic mice. TRAP positive cells were compared for non-immunized controls from short and long term studies (C). Representative images (x40 magnification) represent aorta and PVAT of non-immunized (D) and arthritic (E) mice. Scale Bars represent 0.25µm. *=$p<0.05$. TRAP positive cells are red.

5.3.6 MGP Expression was not Altered Following Long Term Arthritis

When the percentage of MGP protein expression was determined in the aorta (0.56±0.44 (N=4) vs. 16.21±6.24 (N=7)) and surrounding PVAT (16.10±7.32 (N=4) vs. 9.66±1.58 (N=7)) there was no significant difference following onset of long term arthritis (Figure 5.10).

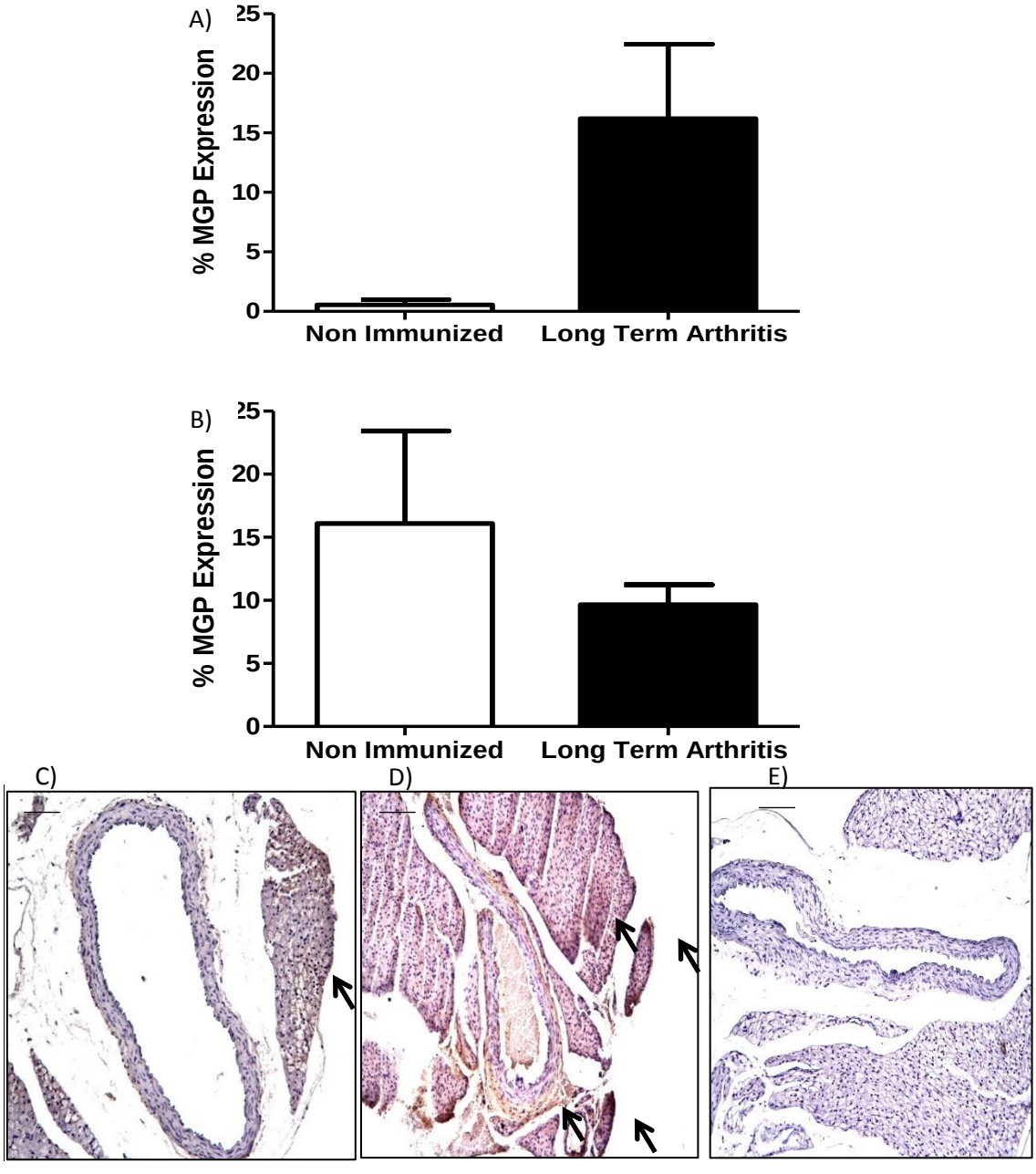

Figure 5.10- MGP Expression Profile. MGP expression was determined in the aorta (A) and PVAT (B) of non-immunized and long term arthritic mice. Representative images (x10 magnification) represent aorta and PVAT of non-immunized (C) long term arthritic mice (D) and isotype (E). Scale Bars represent 0.2µm.

5.3.7 Collagen is decreased in the Aortic Vessel Wall Following Long Term Arthritis

Following long term arthritis there was a significant (p=0.0018) decrease in the aortic content of collagen in comparison to controls (45.50± 3.74% (N=8) vs 72.11± 4.84% (N=4)) (Figure 5.11).

Elastin content in the aortic vessel wall did not change following long term arthritis (42.78 ± 4.25% (N=8) vs 49.44± 8.88% (N=4)) (Figure 5.12). However, it was also noted that the filaments of elastin in the long term arthritis aortas had numerous straightened repeats in comparison to the control aorta.

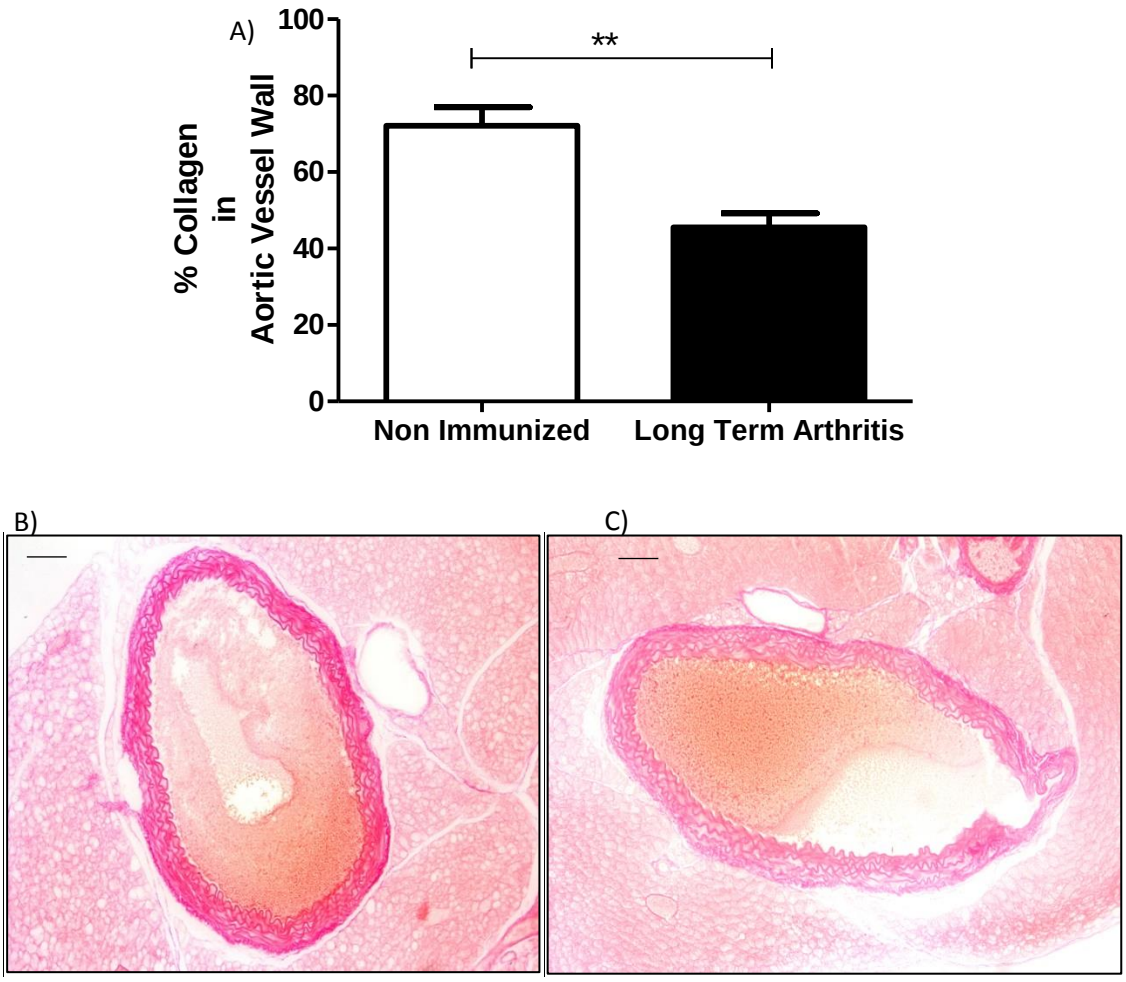

Figure 5.11- Collagen Content in the Aortic Vessel Wall. The percentage of collagen in the aorta was determined in non-immunized and long term arthritis aortae (A). Representative images (x10 magnification) show collagen staining in non-immunized (B) and severe arthritic aortae (C). Scale bars represent 0.2µm. **p=<0.01

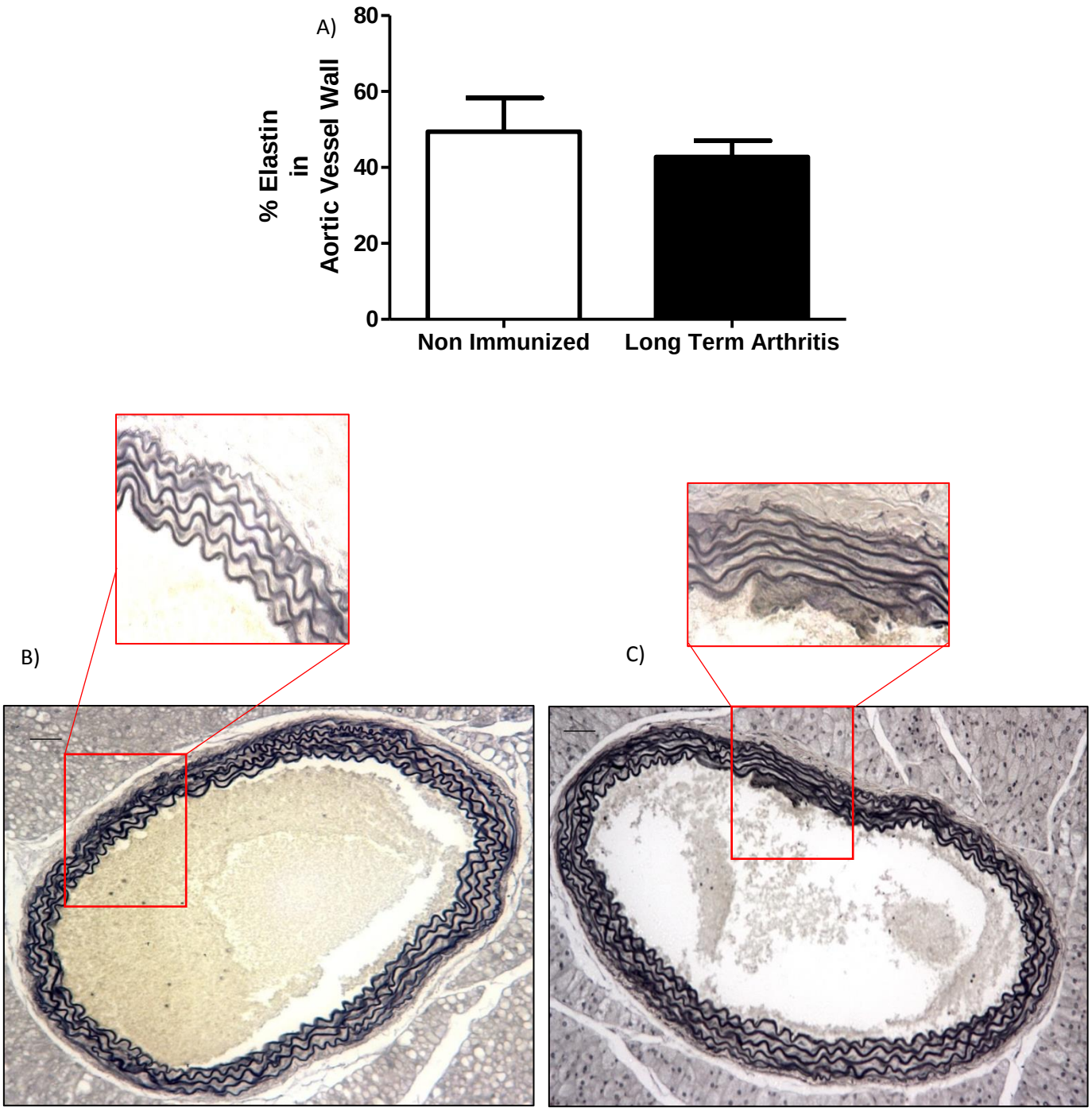

Figure 5.12- Elastin Content in the Aortic Vessel Wall. The percentage of elastin in the aorta was determined in non-immunized and long term arthritis aortae (A). Representative images (X10, X40 magnification) show elastin staining in non-immunized (c) and severe arthritic aortae (D). Scale bars represent 0.2µm. Images are magnified for areas shown in red.

5.3.8 There is No Difference in the Constriction Response to 5HT between Control and Long Term Arthritis Animals.

Vascular constriction responses to 5HT were measured in PVAT-intact and -denuded tissues from non-immunized control and long term arthritic mice. In non-immunised controls, a significantly (P=0.0029) higher maximal constriction response (Figure 5.13A) was observed in the presence of PVAT compared to PVAT-denuded tissues. The PVAT similarly (P=0.0001) altered the constriction responses in tissues from long term arthritic animals (Figure 5.13 B).

Maximal constriction responses remained comparable between intact (Figure 5.13C, 5.94 ± 0.44 mN (N=6) vs. 6.63 ± 0.34 mN (N=6)) and PVAT-denuded (Figure 5.13D 4.00 ± 0.24 (N=6) vs. 4.16 ± 0.21 mN (N=6)) tissues from non-immunized and long term arthritic aorta respectively.

There were no differences between half maximal constriction values in any of the comparisons.

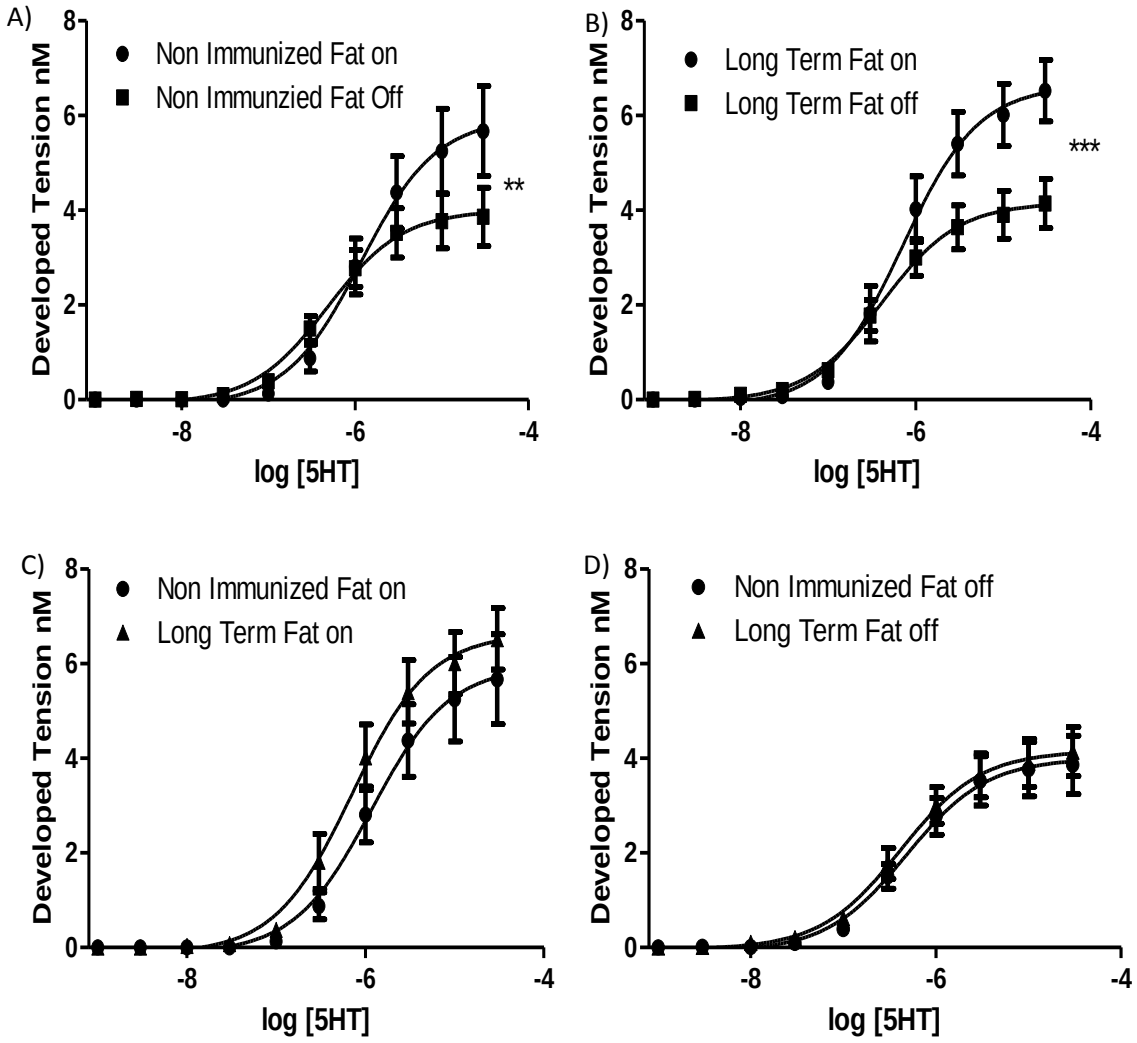

Figure 5.13- Comparison of Constriction Response Curves in Isolated Aortic Rings from Non Immunized and Long Term Arthritic Mice. Constriction responses to 5-HT were determined for PVAT-intact and -denuded tissues from both non-immunized controls (A) and long term arthritic mice (B). The PVAT-intact (C) and -denuded (D) constriction responses for non-immunized controls and arthritic rings were also compared. **=p<0.01, ***=p<0.001

5.3.9 Long Term Arthritis Protocol Reduces Constriction Response Early in the Time Course

Vascular constriction response to 5-HT was measured in PVAT-intact and -denuded tissues from non-immunized control and time matched arthritic animals (animals induced with the long term protocol for a short time period). PVAT had no impact on the maximal constriction response of non-immunized controls (Figure 5.14A). In time matched arthritic animals, a significantly (P=0.0095) higher maximal response (Figure 5.14B) was observed in the presence of PVAT compared to PVAT-denuded tissues.

Maximal constriction response was significantly (P=0.049 and P=0.018) higher in non-immunized aortic rings compared to time matched arthritis aortic rings for both PVAT-intact (5.413 ± 0.37 (N=5) vs. 4.334 ± 0.28 mN (N=5)) (Figure 5.14C) and PVAT-denuded aortic rings (4.349 ± 0.36 (N=4) vs. 3.123 ± 0.22 mN (N=5)) (Figure 5.14 D).

There were no differences between half maximal constriction response values in any of the comparisons.

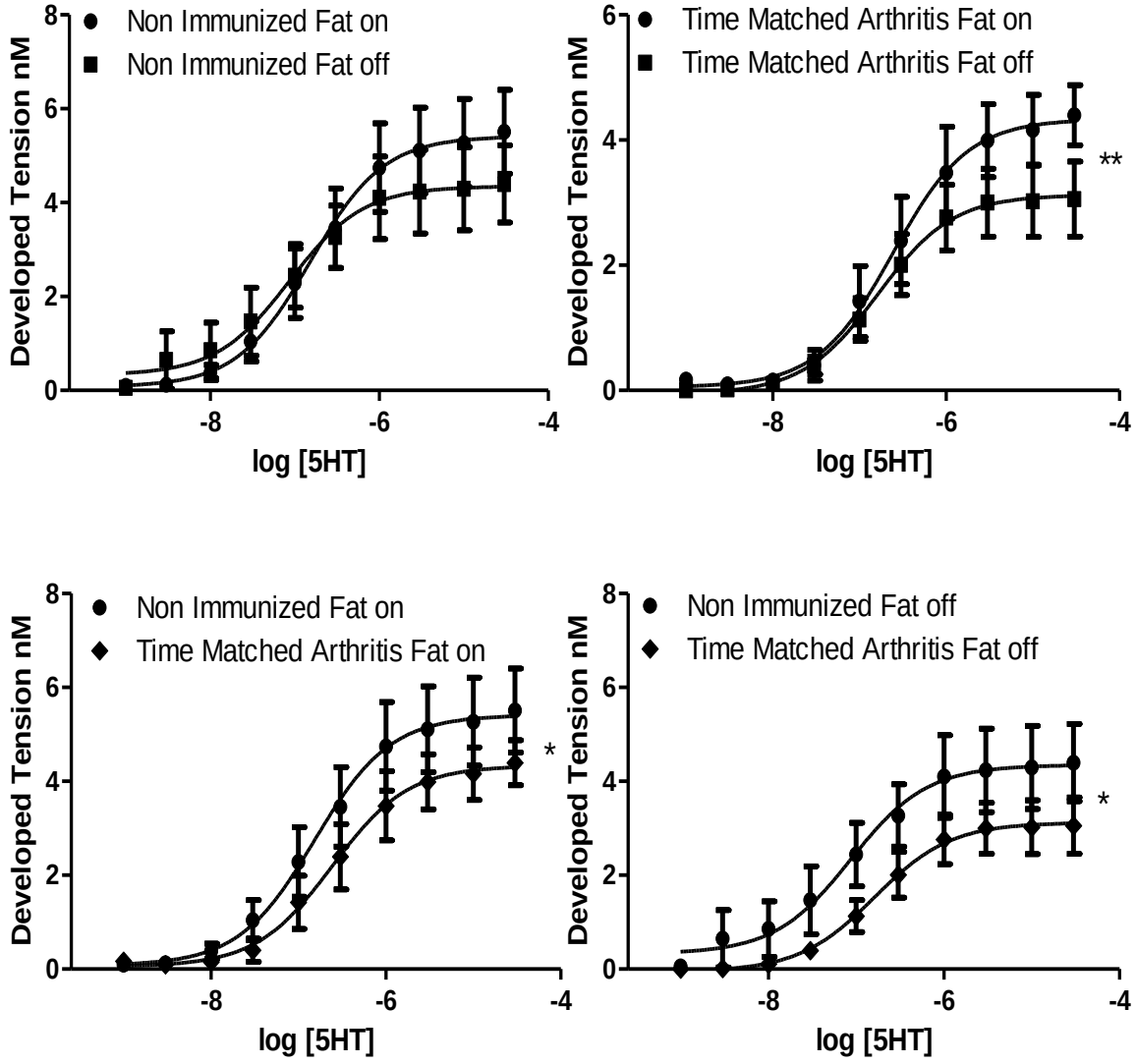

Figure 5.14- Comparison of Constriction Response Curves in Aortic Rings from Non-Immunized and Time Matched Arthritis Mice. Constriction responses to 5-HT were determined for PVAT-intact and -denuded tissues from mice that were non-immunized controls (A) and time matched arthritis mice (B). The PVAT-intact (C) and denuded (D) constriction responses for non-immunized controls and arthritic rings were also compared *=p<0.05, **=p<0.01.

5.3.10 Collagen and Elastin are not Impacted in Time Matched Arthritis.

The percentage of collagen in the aortic vessel wall remained constant (33.60 ± 0.50% (N=3) vs. 44.98 ± 8.11% (N=5)) (Figure 5.15). Elastin percentage also remained constant (63.60 ± 9.35% (N=3) vs. 50.16 ± 7.35% (N-5)) (Figure 5.16).

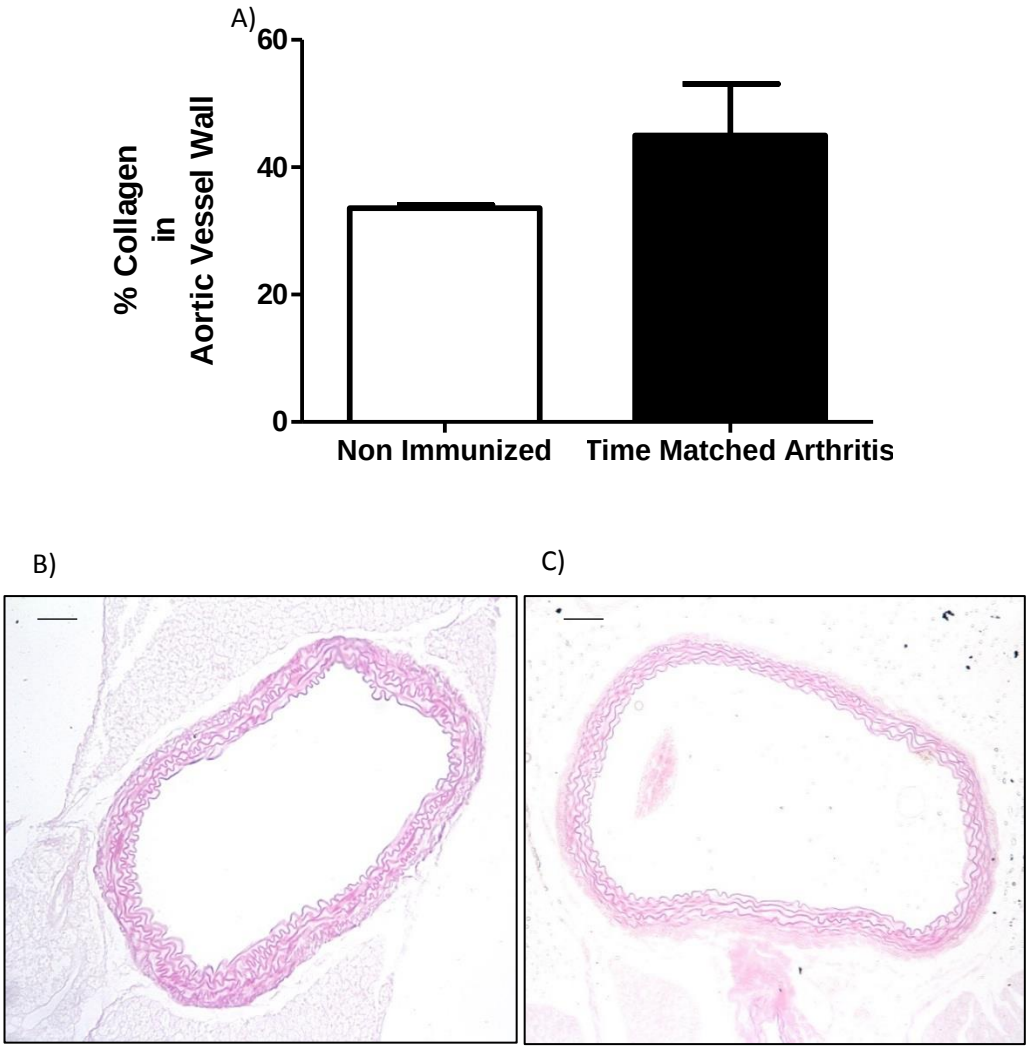

Figure 5.15- Collagen Content in the Aortic Vessel Wall. The percentage of collagen in the aorta was determined in non-immunized and time matched arthritis aortae (A). Representative images (X10 Magnification) show collagen staining in non-immunized (c) and time matched arthritic aortae (D). Scale bars represent 0.2µm.

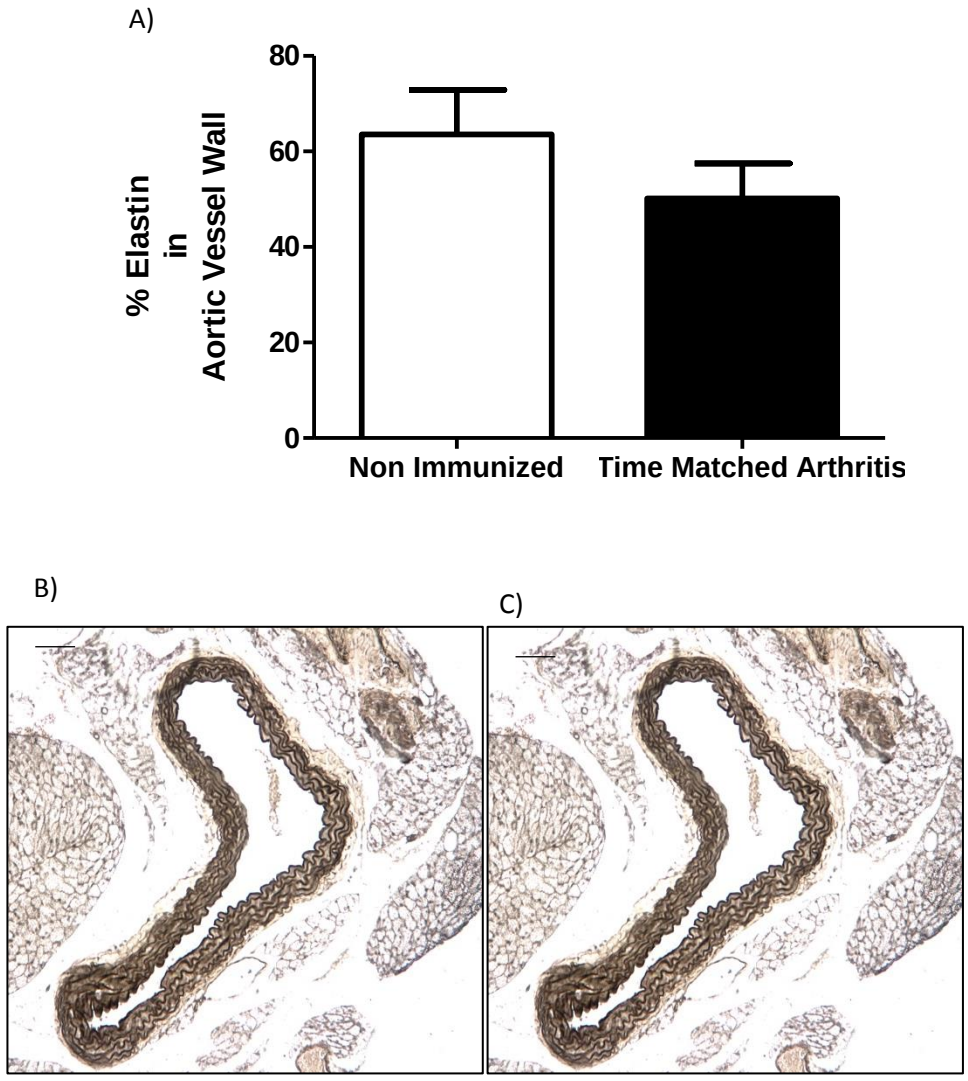

Figure 5.16- Elastin Content in the Aortic Vessel Wall. The percentage of elastin in the aorta was determined in non-immunized and time matched arthritis aortae (A). Representative images (X10 Magnification) show elastin staining in non-immunized (c) and time matched arthritic aortae (D). Scale bars represent 0.2µm.

5.4 Discussion

The adapted mCIA protocol has not previously been studied. As such, the onset and severity of disease constitute important initial findings. As incidence reached 100% the adapted model is suggested as a potential refinement to the current gold standard model. However, total paw score in this model only reached a maximum of 8, whereas in that described previously in this thesis the arthritis severity was reaching 10. The adapted protocol therefore represents a model of inflammatory arthritis with more similarities to human RA given the extended time course. If this was to be used as a refinement protocol, then further work is required to determine collagen antibody titres and histological arthritis index to provide mechanistic understanding.

Long term disease shows trends of increased gene expression of osteoblast transcription factors, osteoclastogenesis proteins and osteoclast markers. Importantly, protein levels themselves have not been measured in this system. Although gene expression is indicative of protein production, protein levels may or may not be impacted due to the changes observed in gene expression. In order to conclude these changes have altered protein expression, levels of these proteins would need to be determined by immunohistochemistry, western blot or flow cytometry. Despite reports of increased aortic common osteoblast transcription factors in the literature in vascular calcification, it is for the first time that increases in these factors have been associated with inflammatory arthritis. However, it is still unclear as to the cause and effect relationship between expression profiles of such bone-related transcription factors and calcification. For example, in models of chronic kidney disease it has been shown that vascular calcification is caused by both osteoblast-like differentiation of VSMCs (Demer and Tintut, 2008) and increased calcium and phosphate levels (Moe and Chen, 2008). Nevertheless, the increase seen in this study, however slight, is indicative of a progressively calcifying phenotype.

A number of calcification mediators have been investigated in both early and late stage vascular disease. Specifically, the expression of RUNX2 and RANKL was found to be increased in aortic explants from patients with aortic stenosis and correlated with stenosis severity in later, advanced disease (Nagy *et al*, 2013). This suggests that the osteoblast and osteoclastogenesis factors may not become prominent until later in the disease process. Interestingly the same study demonstrated a relationship between TRAP expression and vascular disease. In plasma samples and explanted aortic valves, TRAP levels correlated with aortic stenosis and expression was increased in calcified regions of the aortic valve (Nagy *et al*, 2013). Following a multivariable analysis, TRAP expression was associated with stenosis severity in early disease stages, suggesting that it could be an early indicator of calcification in our model of arthritis.

Mechanisms of vascular calcification in inflammatory arthritis are currently elusive. Chronic kidney disease (CKD) is routinely used as a pathological reference point to determine mechanisms that may be implicit for the development of vascular calcification and its associated morbidity and mortality (Paloian *et al*, 2016). CKD has

provided the insight that calcification can occur due to changes in the relationship between pro and anti-calcific factors. This is coupled with a number of knock out models, including MGP (Luo *et al*, 1997), OPG (Bucay *et al*, 1998), β-glucosidase (Spicer et al, 1989) and carbonic anhydrase (Thornell *et al*, 1997) that demonstrate an increased susceptibility to calcification. However, this extensive list only serves to suggest the diversity and variety of possible mechanisms that are likely to be involved in vascular calcification. When we look at the findings of this chapter in relation to these models, it is surprising that MGP gene expression did not change in long term arthritis. Conversely, when the MGP protein levels were determined, although not significant, there was a clear increase during long term arthritis. Such an increase in MGP has previously been related to vascular calcification in CKD (Jono *et al*, 2006). Given that MGP acts as an inhibitor of vascular mineralization (Schurgers *et al*, 2008), this may well represent a protective mechanism in our model. What we do not know is why there is more protein in the face of steady state gene expression, and indeed whether the increased protein is active. While this observation supports the presence of mechanisms that could drive arterial stiffening and deposition of calcium in our model, further detailed investigations, beyond the scope of the current study, are required.

The increase in OPN gene expression that we see in long term arthritis, although not significant, suggests it is also an important mediator in this model. Like MGP, OPN inhibits calcification but it also works to promote dissolution of calcification by physically blocking hydroxyapatite crystal growth (Steiz *et al*, 2002). The increase in this inhibitor suggests it as a further protective mechanism within the vessel wall. Indeed, it is likely that both MGP and OPN work in unison in inhibiting calcification. This is highlighted by the $OPN^{-/-}MGP^{-/-}$ mouse having accelerated and enhanced vascular calcification when compared to the $OPN^{+/+}MGP^{-/-}$ mouse (Speer *et al*, 2002). That an increased presence of OPN is associated with the up regulation of osteoclast formation and function (Lund *et al*, 2009), markers of which are elevated in these data described above, identifies it as a potential target for further in depth studies in the CVD related to arthritis.

Interestingly, changes in expression profiles of TRAP, Calcitonin Receptor and Caspase 3 were altered over time in the non-immunized controls. This was unexpected but does imply the importance of simply aging on the mouse vasculature. Increased TRAP and Calcitonin Receptor gene expression and TRAP protein levels suggest an increase in osteoclasts in aged animals. In normal physiology bone mass is reduced over time due to an excess of resorption that is not balanced by new bone formation (Chung *et al*, 2014). Moreover, it is likely that such age-associated changes are due to the generation of osteoclasts (Chung *et al*, 2014). The novel findings from the present studies suggest that this is not only the case in bone but also more systemically in the vasculature. Such a process would contribute to, and in part explain, the aged vascular phenotype and increased prevalence of vascular calcification seen in the aging population.

Calcification is a pathological process and alters the arrangement and structure of the aortic vessel wall. Importantly, extracellular matrix components, specifically collagen and elastin, can become dysregulated and dysfunctional. For example, while elastin is one of the most stable proteins, it can be degraded by a number of enzymes known as

elastases. These are aggressive enzymes and are most abundant during aging and following disease onset. As a consequence, elastin fragmentation is a pathological hallmark of these processes (Baud *et al*, 2013). It has been suggested that such degradation of elastin filaments initiates the production of factors such as OPN and Alkaline Phosphatase (Persey and D'Haese, 2009). This is a potential explanation for the dysregulation of elastin filaments seen in long term mCIA (Figure 6.13). The normal wave-like appearance of elastin filaments is lost following long term arthritis and large repeats of straightened filaments are noted. This theory would also explain the trend of increase in OPN production and sheds some light as to why this inhibitor is up regulated opposed to MGP. Elastin filaments themselves are capable of driving calcification, due to them containing a number of calcium binding sites (Urry, 1971). In fact, elastin filaments have been shown *in vitro* to calcify in the absence of cells (Price *et al*, 2006). The literature also confirms that in fact the presence of calcified elastin fibres can drive osteoblast-like behaviour of VSMCs (Simionescu *et al*, 2005), suggesting a causative relationship between elastin deregulation and vascular calcification. The differentiation of VSMCs then produces increased levels of matrix metalloproteinase 2, a well-recognised collagenase enzyme that degrades collagen within the aorta. Further work would be required to determine whether MMP-2 was the driving force behind decreased collagen content of the aortic vessel wall in the mCIA model. For example, zymography could be used to determine the levels of pro and active MMP-2 in aortic samples following collagen degradation.

When constriction response curves were analysed for the long term arthritis model, major differences were observed compared to the short term model discussed in the previous chapters. Significantly it would appear that PVAT plays a protective role in long term disease (Figure 6.14) that is not evident in short term mCIA. This role is similar to that described previously in the arthritic $DR3^{-/-}$ studies (Chapter 3). The ability of PVAT to potentiate vasoconstriction has been described previously in metabolic syndrome where the PVAT is unable to reduce the vascular constriction response (Chang *et al*, 2012). However, it is still a question for debate in this model whether the vasorelaxation impact of PVAT is dampened, or whether inflammation drives a positive vasoconstrictive phenotype within the PVAT. The production of adipokines, such as angiotensin II and leptin, by PVAT are also associated with vasoconstriction. These findings not only highlight that the role of PVAT is not as simple as first anticipated, but also how disease can cause changes in PVAT function in relation to aortic vessel constriction.

Despite the altered role of PVAT described above, there was no difference between non immunized and long term disease constriction responses in fat-denuded tissues. This was surprising for two reasons: Firstly, vascular dysfunction is a prominent characteristic of short term "acute" disease. Secondly, long term disease is associated with changes in both collagen and elastin. It is possible that the inflammation associated with long term arthritis is diminished and although changes to collagen and elastin, vascular dysfunction in the long term mCIA model may never exist. Conversely in the short term

model, inflammation and changes to structural proteins lead to vascular dysfunction. Only additional experiments would allow us to investigate this further and there are no other reports in the literature that would give us any clues. Further studies would include the characterisation of the inflammatory makeup of the aortic vessel wall during long term mCIA.

It is evident that a big issue with the gold standard mCIA model is that it does not truly represent the recurring and remising RA disease seen in humans. The latter is characterised by flares and remissions that would be accompanied by reflective bouts of systemic inflammation. As such the human vasculature would consistently be subjected to periods of exposure to circulating inflammatory cells and mediators. Conversely, in the long term mCIA model there is no induction of inflammation after day 21, meaning that the majority of mice in this cohort have gone 50 days without repeated inflammatory stimuli. To explore this issue further, the long term protocol was induced in a further group of mice but was time matched to the arthritis described in the previous chapters. This allowed us to determine the importance of time with arthritis as well as severity of disease. From figure 6.15 we can see that mCIA onset decreased the vascular constriction response in both PVAT-intact and -denuded blood vessels during the early disease time point but not during long term disease. Here we can see the importance of time in our model and it suggests that use of the mCIA model is problematic when looking at long term disease in relation to cardiovascular outcomes. However, it also emphasises how essential this model is when investigating the earliest, and probably most important, changes in vascular function following the onset of inflammatory arthritis.

5.5 Conclusion

The findings in this chapter have highlighted that vascular calcification is not driving vascular dysfunction seen in mCIA, regardless of the time with arthritis and has emphasised the importance of inflammation in this model. Vascular dysfunction seems reliant on the initial burst of systemic inflammation seen in the gold standard mCIA model and although osteoblast and osteoclasts are present in the vasculature they were not significantly up regulated in long term arthritis. Changes to collagen and elastin are likely to be associated with high levels of inflammation within the aortic vessel wall and thus are potentially contributing to irreversible long term vessel damage. However, more work is required to fully understand the activation of inflammatory pathways in the vessel wall and that contribute to the changes seen within the aorta and surrounding PVAT. Thus moving forward in this thesis the role of inflammasome complexes will be determined in relation to mCIA and contractile dysfunction. Activation of the infllammasome is associated with early inflammatory cells, such as macrophages, and thus is a potential driver for the early changes seen during mCIA.

Chapter 6 – The Role of AIM2 Inflammasome Activation in Vascular Dysfunction during Inflammatory Arthritis

6.1 Introduction

Inflammasomes are integral to the innate immune response, reacting to the presence of pathogens, dead cells and irritants. They function to activate the immune response and have key inflammatory roles including pyroptosis, a distinct type of programmed cell death (Mariathasan *et al*, 2004). Ultimately, protein oligomerization drives the activation of caspase-1, which in turn enhances cytokine maturation, specifically of Interleukin-1β (IL-1β) and Interleukin-18 (IL-18) (Martinon *et al*, 2002). In recent years inflammasomes have been widely studied and a number of different protein families are now known to be involved in their activation. The two main types are Nod-Like Receptors (NLRs) and Absent In Melanoma 2 (AIM2)-like receptors (Sharma *et al,* 2016).

The work described in this chapter focuses on the role of the AIM2 inflammasome in both inflammatory arthritis and vascular function. AIM2 binds directly to double-stranded DNA via its hematopoietic interferon-inducible nuclear (HIN) protein domain and in turn this action displaces the pyrin (PYD) protein domain preventing auto-inhibition (Jin *et al*, 2012). The displacement of PYD allows recruitment of adaptor protein apoptosis-associated speck-like protein containing CARD (ASC) (Hornung *et al*, 2009). A PYD-PYD interaction between AIM2 and ASC then drives nucleation of ASC and allows transformation of ASC into its prion form (Jin *et al*, 2013). Prion-like filaments of pro-caspase-1 then begin to form from the ASC filaments, activating caspase-1 (Lu *et al*, 2014).

Inappropriate sensing of host nucleic acids plays a significant role in the pathology associated with auto immune disease (Baccala *et al*, 2007). In inflammatory arthritis knocking out AIM2 has been shown to attenuate disease, both in terms of clinical and histological scores (Baum *et al*, 2015). Moreover, it is proposed that AIM2 is involved in the recognition of endogenous DNA in arthritis and as such is an important pattern recognition receptor in the disease (Jakobs *et al*, 2015). However, in this study AIM2 deficiency did not seem to impact systemically, for example, it had no effect on anti-citrillunated protein antibodies. This suggests that tissue destruction in inflammatory arthritis is governed locally and is not just a secondary outcome of increased systemic pro-inflammatory cytokines (Jakobs *et al*, 2015). The Authors suggest that ablation of AIM2 did not ameliorate all aspects of disease because of its lack of expression on non-myeloid cells, which would include the vasculature.

In contrast, a further study demonstrated that AIM2 was not only present in healthy vascular cells, but also found within pathologic macrovascular tissue (Hakimi *et al*, 2014). That both pro-inflammatory cytokines TNF-α and IFN-ϒ and double stranded DNA were found co-localised with AIM2, and identified as potential triggers for its expression, indicate a potential role for this protein in CVD. The present study will be the first to investigate this action of AIM2 in mCIA.

The study of Hakimi and colleagues was the first of its kind to examine the role of AIM2 in vascular function. A further study has also indicated that AIM2 plays a role in macrophage DNA sensing (Burckstummer *et al*, 2009). Other studies show that by knocking out AIM2 using short interfering RNAs that both inflammasome and pyroptosome activation are reduced (Fernandes-Alnemri *et al*, 2007). Given the number of macrophages is increased in the aorta during mCIA suggests AIM2 could be involved in the increased inflammatory state within the vessel wall.

Recent studies have been carried out using the now commercially available novel inhibitor of the inflammasome complexes, cytokine release inhibitory drug 3 (CRID3) (Coll *et al*, 2015; Ozaki *et al*, 2015). This drug has been shown to effectively block the inflammasome in autoimmune diseases such as, encephalomyelitis, an animal model of multiple sclerosis. In this model IL-1β production was reduced following dosing of CRID3 at 10mg/kg on day 0 and every other day post induction (Coll *et al*, 2015). The successful use of this treatment in inflammatory conditions and the implication of AIM2 in CVD suggest it as a potential therapeutic for our model.

The experiments in this chapter were used to determine the relationship between inflammatory arthritis and AIM2 expression within the vasculature. The expression of AIM2 and its downstream inflammasome mediators will be assessed in both the thoracic aorta and the surrounding PVAT. Protein levels of AIM2 and Caspase-1 were also determined via immunohistochemistry. Finally, the therapeutic potential of AIM2 inhibition, using CRID3 was investigated. This chapter details methodology, results and discussion under the following objectives and hypothesis:

Hypothesis: AIM2 inflammasome activation drives the vascular dysfunction associated with mCIA.

- To determine the presence of AIM2 and its downstream inflammasome mediators; Caspase-1, IL-1 and IL-18, in the healthy and diseased mCIA vasculature.
- To investigate the therapeutic potential of AIM2 inhibition in terms of both arthritis severity and the associated vascular dysfunction.

6.2 Methods

New methods relevant to the work discussed in this chapter are described below, previous methods detailed in Chapter 2 and 3 also apply here, specifically mCIA induction, Immunohistochemistry and RT-qPCR.

6.2.1 Inflammasome qPCR primer sequences

Table 6.1- Primer Sequences for Inflammsome Mediators

Name	Forward Sequence	Reverse Sequence
AIM2	ACAAAGTGCGAGGAAGGAGA	TCACTCCACACTTTTCATGTCA
Caspase-1	ACGCCATGGCTGACAAGATCCTG	GGTCCCGTGCCTTGTCCATAGC
IL1	CAACCAACAAGTGATATTCTCCAT	GGGTGTGCCGTCTTTCATTA
IL18	GCCATGTCAGAAGACTTGCGT	GTACAGTGAAGTCGGCCAAAGTT

6.2.2. PVAT Isolation

In the same way as previously described (section 4.2.2) for thoracic aorta and PVAT samples, the PVAT was isolated from non-immunized and arthritic mice and stored for later qPCR analysis.

6.2.3 Immunohistochemistry Antibodies

Table 6.2- Inflammasome Antibody Suppliers

Antibody	Supplier
AIM2	Abcam (ab93015)
Caspase-1	Abcam (ab1872)

6.2.4 CRID3 Preparation

5mg of CRID3 was dissolved in 1ml of dH_2O. CRID3 was required at 10mg/kg. 400µl of CRID3 was dissolved in 600µl of PBS. 100µl was given to each mouse.

6.2.5 AIM2 and Caspase 1 Immunohistochemistry

Immunohistochemsitry was carried out in order to determine the presence and location of AIM2 and Caspase-1 within the thoracic aorta and surrounding PVAT. General Immunohistochemistry protocols were used as described previously in Section 2.2.6. Specific Antibodies (Table 6.1), concentrations and reagents are described below in Table 6.2.

Table 6.3 – Inflammasome Specific Antibody Reagents and Concentrations

Reagent	AIM2	Caspase-1
Wash Buffer	TBS Tween	TBS Tween
Serum Block	Goat	Goat
Primary Antibody	Rabbit Anti Mouse AIM2 (5ug/ml)	Rabbit Anti Mouse Caspase-1 (0.39ug/ml)
Isotype	Rabbit IgG (5ug/ml)	Rabbit IgG (0.39ug/ml)
Secondary Antibody	Goat Anti Rabbit IgG (1µg/ml)	Goat Anti Rabbit IgG (1µg/ml)

6.2.6 CRID3 mCIA Therapy

As previously described in Chapter 2, mCIA was induced following the standard protocol. Briefly, DBA/1 mice were immunized using the intra-dermal route with a total of 100 µl of immunization emulsion (Section 2.2.1.1). Immunizations of 50 µl were administered at multiple adjacent sites right laterally at the base of the tail. This was termed day 0. Following intradermal injections each treatment group mouse was given 100µl of 10mg/kg CRID3 (see section 6.2.1.2) via intraperitoneal (I.P.) injection. Control mice were given 100µl I.P. of PBS while non-immunized animals received no I.P. injection.

For the following 20 days health status was monitored. At day 20 animals were given Temgesic in their drinking water, which was subsequently changed on a daily basis. On day 21 all immunized mice were given an identical booster intradermal injection as administered on day 0. Mice in treatment and control groups also received CRID3 or PBS via I.P. injection on day 21 and every other day until experimental end point. Concurrently, from day 21 mice were weighed daily, hind paws were measured and paw scores manually scored.

6.2.7. Statistics

Statistics used in this chapter are the same as those described in Section 2.2.7.3. RT-qPCR data are compared by Student's *t*-test. Immunohistochemistry is analysed by one-way ANOVA with a Bon-Ferroni post-test. RMAX and EC50 of vascular constriction response curves are almost analysed using Student's *t*-test. Significance is determined as $p<0.05$.

6.3 Results

6.3.1 Onset of mCIA is associated with Changes in AIM2 Inflammasome Mediators within PVAT-Intact Aorta

Gene expression of AIM2 (Figure 6.1A) within the PVAT-intact aorta and PVAT showed a fivefold increase, approaching significance (p=0.07) following arthritis onset (1.98 ± 0.97 (N=2) vs. 9.67 ± 2.11 (N=3)). Caspase-1 (Figure 6.1B) gene expression also increased threefold, however, not significantly (3.37 ± 2.37 (N=2) vs. 8.64 ± 1.73 (N=3)). IL-1 (Figure 6.1C) gene expression was significantly (p=0.017) increased following onset of mild arthritis (1.43 ± 0.43 (N=2) vs. 4.76 ± 0.48 (N=3)). IL-18 (Figure 6.1D) gene expression remained constant (1.06 ± 0.09 (N=2) vs. 1.22 ± 0.49 (N=3)).

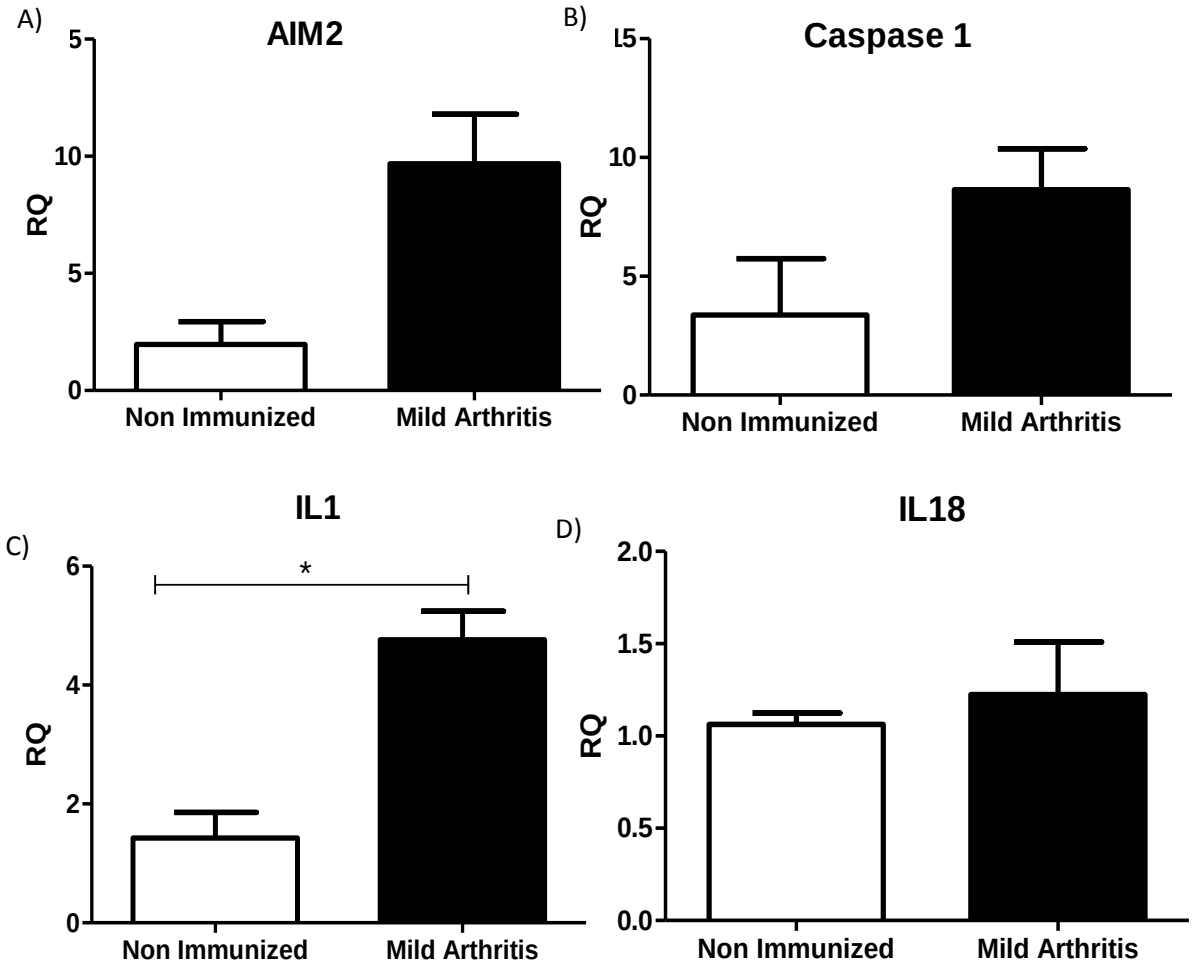

Figure 6.1- Inflammasome Mediators during mCIA. Expression of AIM2 (A), Caspase-1 (B), IL-1 (C) and IL-18 (D) were determined in non-immunized and mildly arthritic PVAT-intact aorta. *=p<0.05.

6.3.2 PVAT Expression of AIM2 Inflammasome Mediators.

In PVAT alone, gene expression of AIM2 (Figure 6.2A) was significantly (p=0.04) decreased during mCIA (1.09 ± 0.13 (N=2) vs. 0.37 ± 0.17 (N=2)). Caspase-1 (Figure 6.2B) remained constant during (0.86 ± 0.14 (N=2) vs. 0.61 ± 0.10 (N=2)), IL-1 (Figure 6.2C) expression significantly (p=0.01) increased (1.04 ± 0.04 (N=2) vs. 4.05 ± 0.30 (N=2)) and IL-18 (Figure 6.2D) remained constant (0.79 ± 0.21 (N=2) vs. 0.61 ± 0.15 (N=2)).

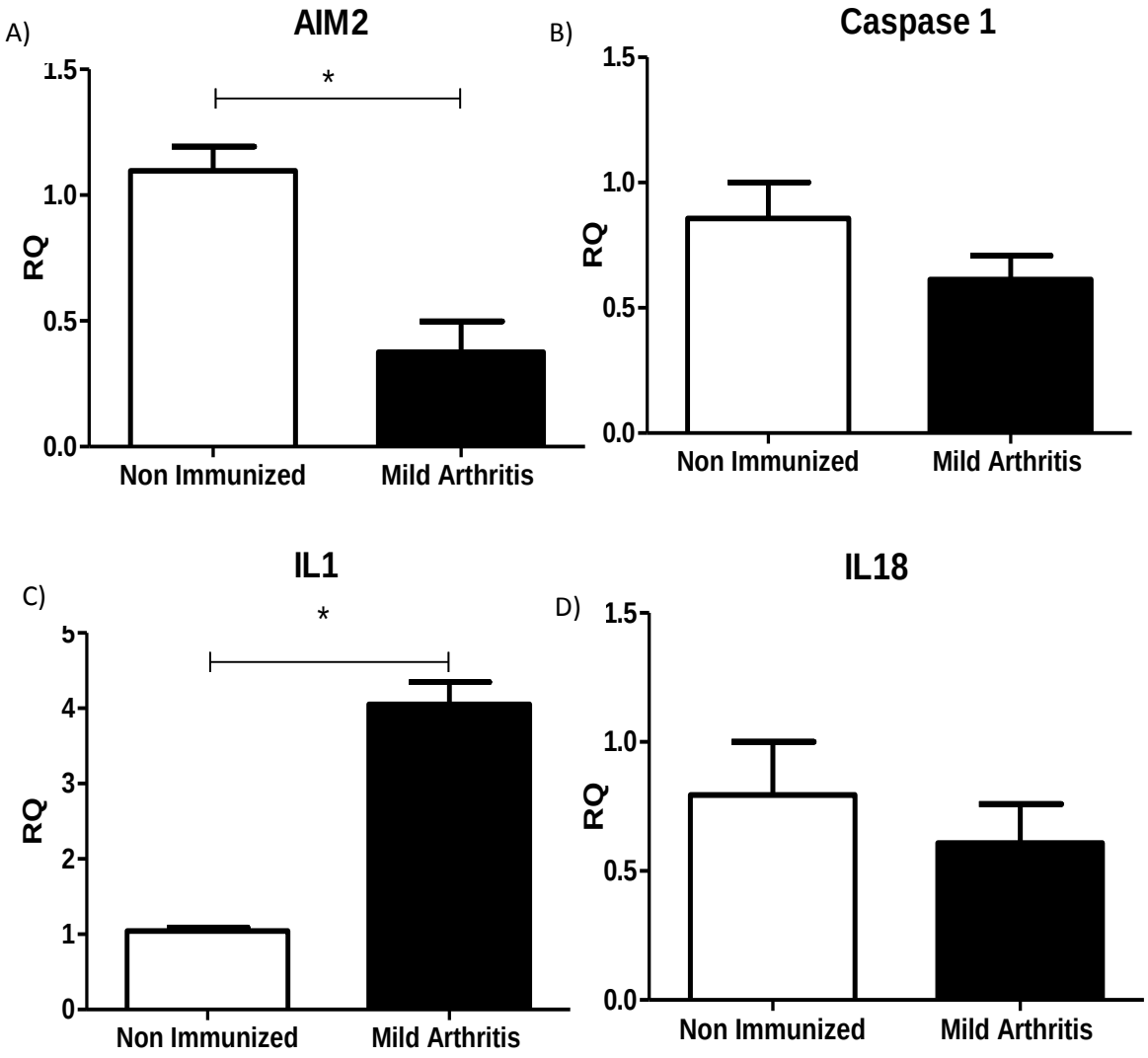

Figure 6.2- Inflammsome Markers in the PVAT alone during mCIA. Expression of AIM2 (A), Caspase-1 (B), IL-1 (C) and IL-18 (D) were determined in non-immunized and mildly arthritic PVAT samples. *=p<0.05.

6.3.3 The Shift in Expression Profiles during mCIA

The expression profiles of inflammasome mediators changes between both healthy and diseased animals and tissue location (Table 6.3). Gene expression for each mediator was determined for the aorta alone by deducting PVAT only RQ values from PVAT-intact aortic values. Values for aorta and PVAT alone were then determined as percentages of the total expression value shown in the PVAT-intact aortic samples. These values provide an estimation of gene expression within the aorta in order to allow comparisons to be made.

Firstly, AIM2 gene expression is equal from both the aorta and the PVAT in healthy animals (50 vs. 50%). However, in disease, firstly the expression increases fivefold and secondly the majority of the AIM2 gene expression comes directly from the aorta, with very little coming from the PVAT (90 vs. 10%). In healthy animals the expression profile of Caspase-1 differs to that of AIM2, with a higher percentage of gene expression being present in the aorta when compared to the PVAT (74 vs. 26%). In disease expression of caspase-1 doubles and the majority of expression, similarly to AIM2 is from the aorta (93 vs. 7%). The opposite trend is seen for IL-1 expression with the PVAT providing the majority of the expression in healthy animals (27 vs. 73%). In disease there is a threefold increase in expression however the majority of expression remains within the PVAT (15 vs. 85%). In healthy animals IL-18 gene expression profile is similar to that of IL-1 with the majority coming from the PVAT (25 vs. 75%). Although expression remains constant during the onset of mCIA the expression profiles shift, with equal IL-18 expression from both the aorta and PVAT (50 vs. 50%).

Table 6.4- Comparison of Gene Expression Profiles between non-immunized and mildly arthritic animals.

	PVAT-Intact Aorta (RQ)		**PVAT Alone (RQ)**	
	Non Immunized	Mild Arthritis	Non Immunized	Mild Arthritis
AIM2	1.97	9.67	1.09	0.37
Caspase-1	3.37	8.64	0.86	0.61
IL-1	1.43	4.76	1.04	4.05
IL-18	1.06	1.22	0.79	0.61
	Expression from Aorta %		**Expression from PVAT %**	
	Non Immunized	Mild Arthritis	Non Immunized	Mild Arthritis
AIM2	45%	96%	55%	4%
Caspase-1	74%	93%	26%	7%
IL-1	27%	15%	73%	85%
IL-18	25%	50%	75%	50%

6.3.4 AIM2 Protein Remains Constant in Arthritis.

Immunohistochemistry identified AIM2 in the aorta and PVAT of non-immunized, mild and severely arthritic animals (Figure 6.3). There was no change in the aorta (A) (7.13 ± 0.87 (N=4) vs. 10.26 ± 4.01 (N=4) vs. 5.74 ± 1.41% (N=4) or PVAT (B) (10.42 ± 1.84 vs. 15.10 ± 3.20 vs. 13.81 ± 5.21%).

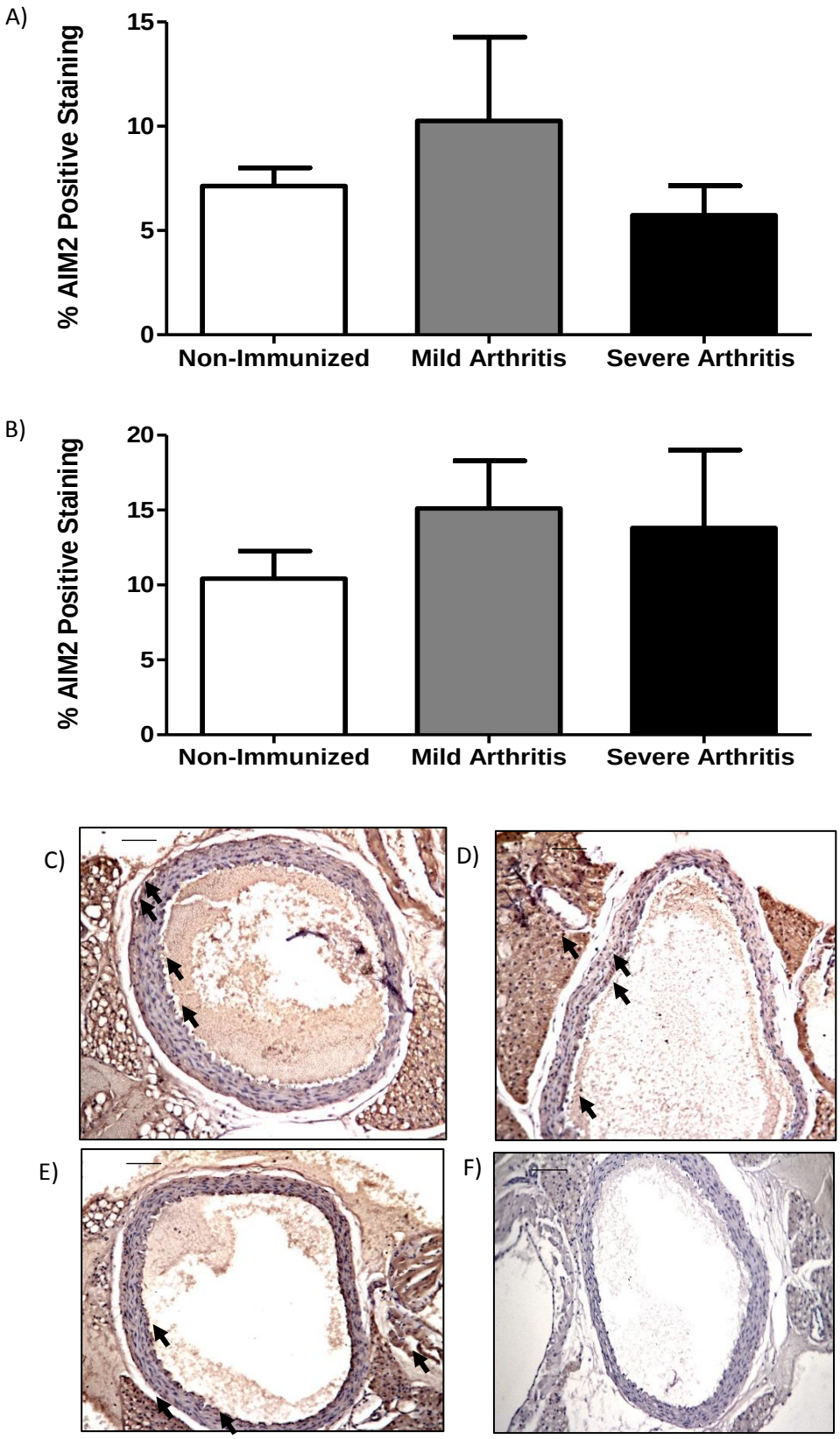

Figure 6.3 – AIM2 Protein Identification. AIM2 protein was identified in the aortic vessel wall (A) and surrounding PVAT (B). Representative images (x20 magnification) in non-immunized controls (C), mild arthritis (D) severe arthritis (E) and isotype (F) thoracic aorta and PVAT samples. Scale bars represent 0.2µm.

6.3.5 Caspase-1 Protein Remains Constant in Arthritis.

Caspase 1 protein remained constant in the aorta (7.57 ± 3.1 (N=4) vs. 9.43 ± 3.0 (N=4) vs. 4.56 ± 2.1% (N=3)) and in the PVAT (22.61 ± 11.6 vs. 23.58 ± 4.7 vs. 37.07 ± 4.2%) between non-immunized, mild and severely arthritic animals.

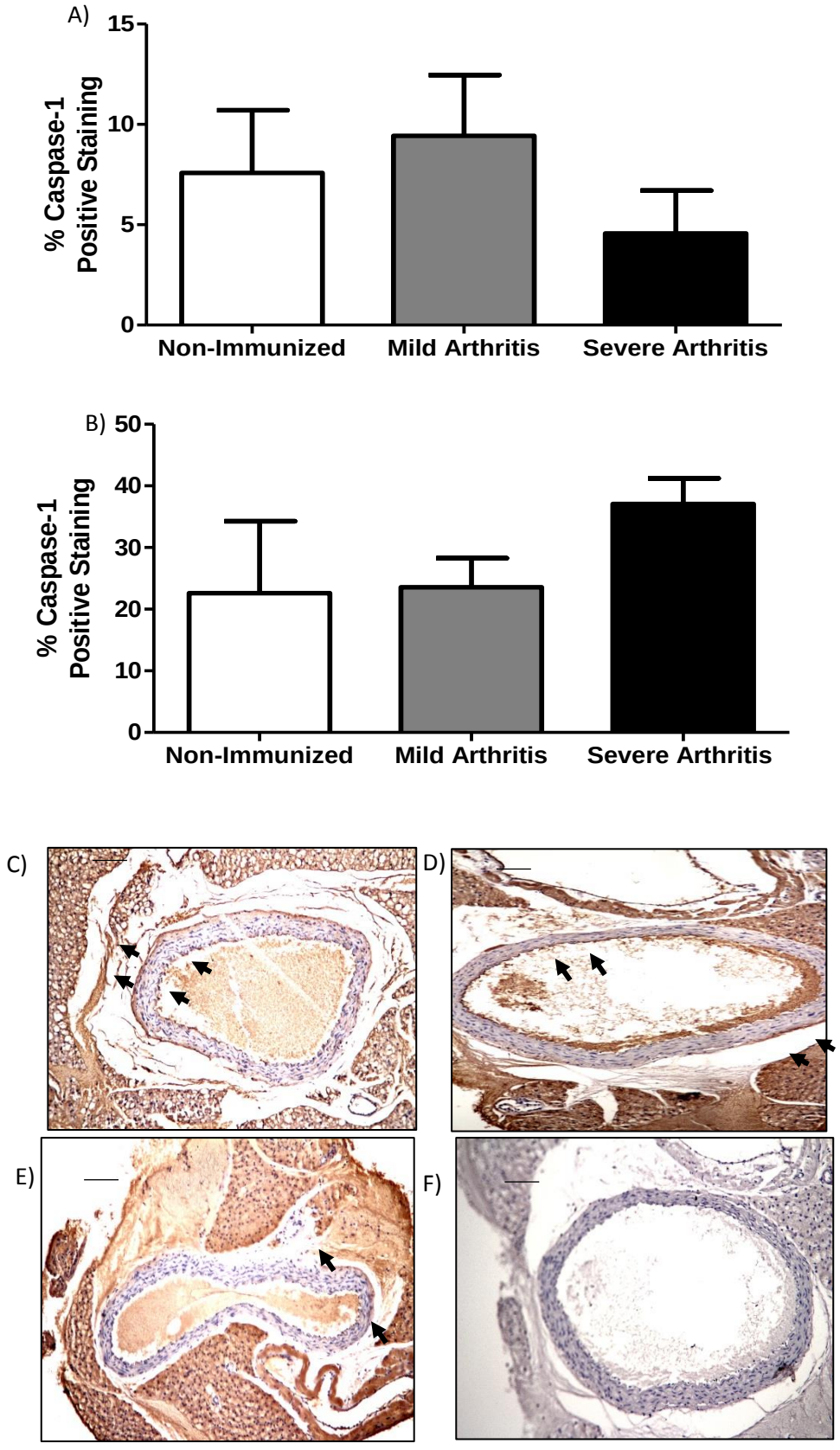

Figure 6.4 – Caspase-1 Protein Identification. Caspase-1 protein was identified in the aortic vessel wall (A) and surrounding PVAT (B). Representative images (x20 magnification) in non-immunized controls (C), Mild arthritis (D) severe arthritis (E) and isotype (F) thoracic aorta and PVAT samples. Scale bars represent 0.2µm.

6.3.6 CRID3 Treatment Does Not Reduce mCIA Onset.

Onset of mCIA was similar in both PBS and CRID3 treated groups, with 100% incidence of arthritis being reached by day 26 in both groups (Figure 6.5A). Animals from both groups lost weight during the course of mCIA (Figure 6.5B) and had comparable total paw scores throughout the experimental time course (Figure 6.5C). The CRID3 treatment group showed significantly (P=0.03) increased paw diameter over the time course with arthritis in comparison to the PBS treated group (Figure 6.5Dz).

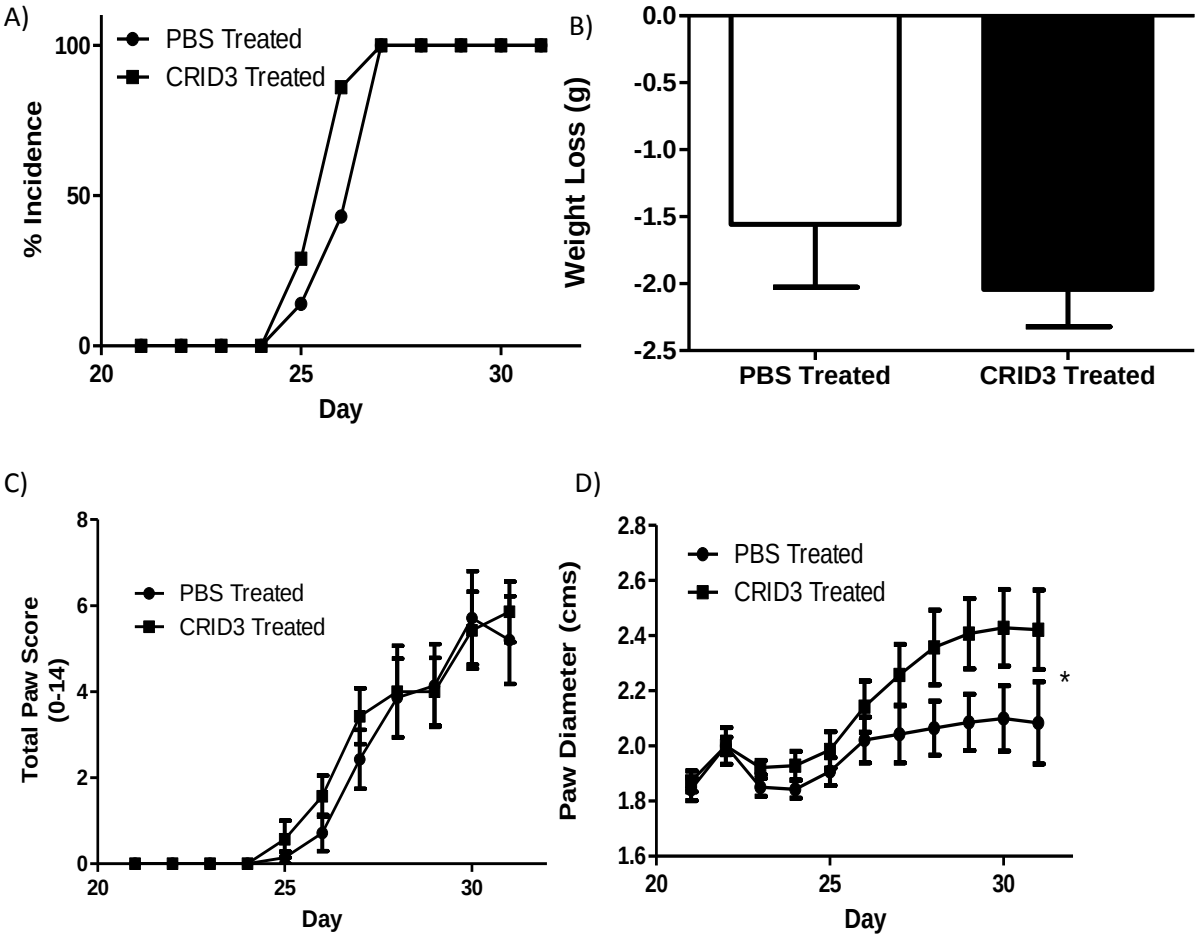

Figure 6.5- Arthritis Induction in PBS and CRID3 Treated DBA/1 Mice. mCIA was induced in 100% of PBS (N=8) and CRID3 (N=8) treated mice (A). Weight (B), Total Paw Score (C) and Paw Diameter (D) were measured over a 32-day time course. *=$p<0.05$.

6.3.7 CRID3 Reduces Vascular Dysfunction during mCIA.

The vascular constriction response was analysed in PVAT intact and PVAT denuded vessels from non-immunized, PBS and CRID3 treated animals, (Figure 6.6). In non-immunized control animals (Figure 6.6 (A)) the presence of PVAT significantly ($p=0.02$) decreased the maximal constriction response in comparison to the PVAT denuded constriction response (4.96 ± 0.45 (N=4) vs. 6.59 ± 0.26 mN (N=4)). However, the presence of PVAT did not alter the half maximal constriction response in this group (-6.82 ± 0.27 vs. -7.13 ± 0.12mN). PVAT had no impact on maximal constriction (Figure 6.6 (B)) (3.54 ± 0.21 (N=4) vs. 3.21 ± 0.22mN (N=4)) or half maximal constriction responses (-6.28 ± 0.13 vs. -6.77 ± 0.18) in PBS treated animals. However, in CRID3 treated animals (Figure 6.6 (C)) PVAT significantly ($p=0.004$) reduced the maximal constriction response (3.81 ± 0.17 (N=4) vs. 4.88 ± 0.16mN (N=4)) and ($p=0.001$) the half maximal constriction response (-6.29 ± 0.10 vs. -7.10 ± 0.10mN), dextrally shifting the concentration response curve.

When the PVAT-denuded constriction responses were compared for non-immunized, PBS treated and CRID3 treated animals, interesting observations were made (Figure 6.7 (A)). While the maximal constriction response was significantly ($P<0.001$) reduced in both the PBS and CRID3 treated groups compared to non-immunized controls, the CRID3 treatment group was significantly ($p<0.01$) higher than the PBS treated group. Half maximal constriction responses are comparable between the three groups.

When PVAT intact constriction responses were compared between the three groups (Figure 6.7 (B)), there was little change in either half maximal constriction or maximal constriction responses.

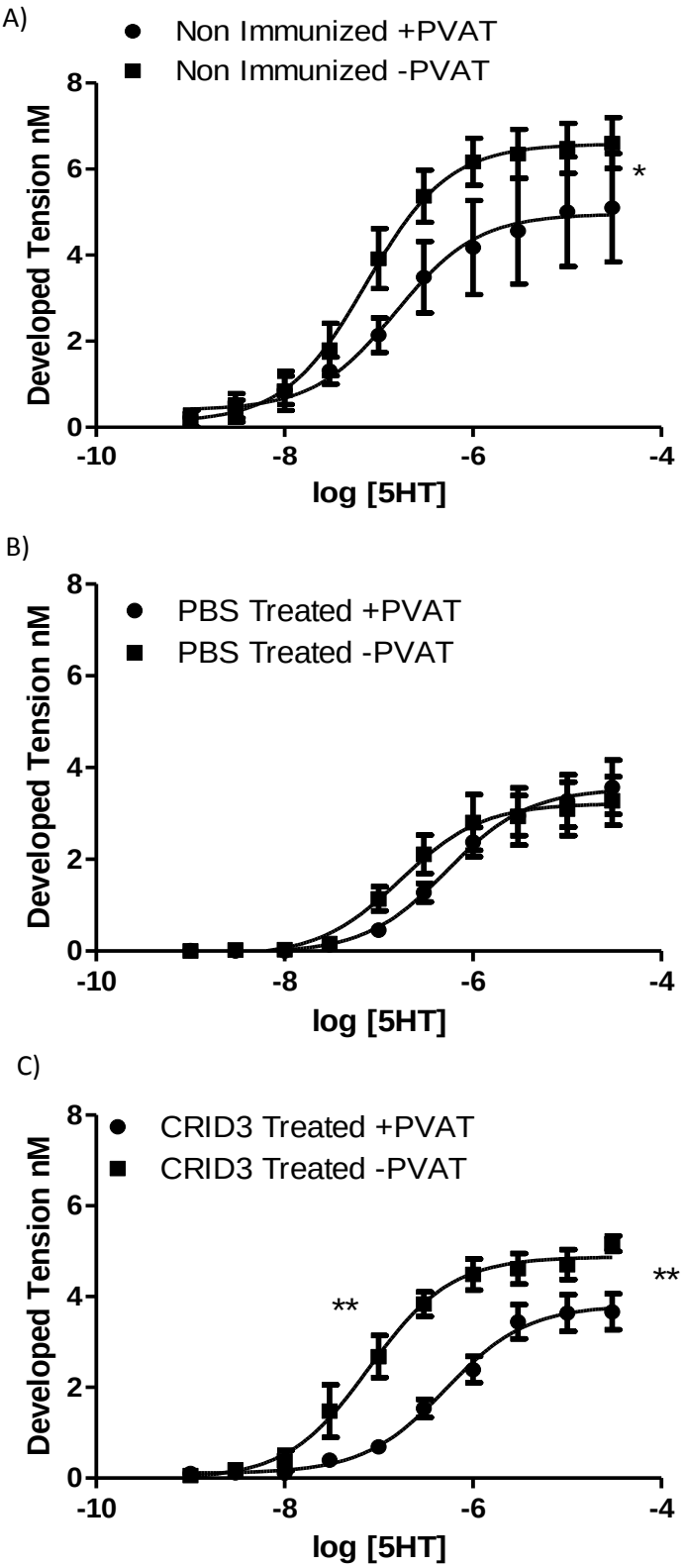

Figure 6.6- The Impact of PVAT on Constriction Response Curves. Constriction responses to 5HT were determined in PVAT intact and PVAT denuded aortic rings for non-immunized (A), PBS treated (B) and CRID3 treated (C) animals. *=p<0.05, **=p<0.01.

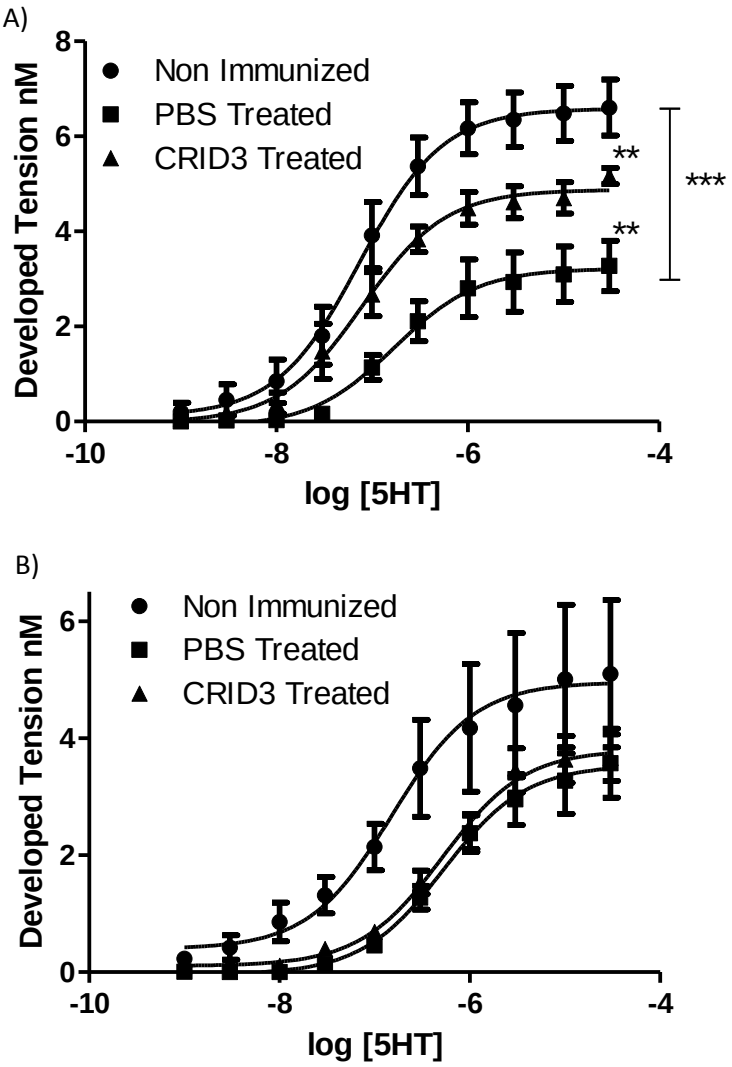

Figure 6.7- The Impact of Treatment on Constriction Response Curves. Constriction responses to 5HT were determined in PVAT denuded (A) and PVAT intact (B) aortic rings for non-immunized, PBS treated and CRID3 treated animals. **=p<0.01, ***=p<0.001.

6.4 Discussion

Inflammasome mediators, AIM2, Caspase-1 and IL-1 were all increased in the aorta and PVAT of mildly arthritic mice. As a pilot study, used to determine the presence of AIM2 in the aorta and PVAT, the N numbers here were low, drastically decreasing the power of the statistical comparisons. Nevertheless, this is the first report showing AIM2 to be increased in the aorta during inflammatory arthritis. Previous studies have shown AIM2 is present in VSMCs during atherosclerosis and that AIM2 activation is inducible by inflammatory factors (Hakimi *et al*, 2013). As such there is great potential for AIM2 to be activated and subsequently contribute to the vascular dysfunction seen in the mCIA model

These RT-qPCR data show that when comparing healthy and diseased tissues, gene expression of AIM2 and its downstream mediators is different in the two situations. Caspase-1, IL-1 and IL-18 are shifted between the aorta itself and the surrounding PVAT. Both AIM2 and Caspase-1 gene expression increase following onset of mCIA, the location of gene expression also changes. In healthy animals 45% of AIM2 and 74% of Caspase-1 expression arises from the aorta. Following disease onset the aorta produces over 90% of both AIM2 and Caspase-1 expression. This suggests that the trigger for AIM2 inflammasome activation is mainly focussed within the aortic vessel wall itself. Of course the aorta and PVAT are in close proximity and work in unison to maintain vascular function. It is suggested that activation occurs primarily in the aorta due to its exposure to circulating factors capable of AIM2 activation. The importance of interplay between the aorta and PVAT has previously been discussed, these results add to the findings that both aorta and PVAT play a role in vascular constriction response and changes to either region may lead to dysfunction.

The increased gene expression of AIM2 and Caspase-1 in mild disease shows a similar trend to that of macrophage infiltration into the aortic vessel wall during mCIA described in Chapter 2. Many studies have now shown that AIM2 is a double stranded DNA sensor present in macrophages (Burckstummer *et al*, 2009; Fernandes-Alnemri *et al*, 2009; Hornung *et al*, 2009). Data in this thesis shows that both macrophages and AIM2 are up regulated specifically in the aortic region of mCIA mice. As these mice have vascular dysfunction it is likely that AIM2 activation in macrophages is the mechanism driving the dysfunction. Given that AIM2 is an IFN inducible factor (Choubey *et al,* 2008) and IFN-ϒ is associated with inflammatory arthritis, it is possible that this cytokine is involved in the increased AIM2 gene expression. It is also known that increased IFN-ϒ production alone can result in the development of systemic auto-immunity, suggesting its importance in driving inflammatory diseases such as RA. Therefore, there is significant potential for IFN-ϒ to trigger activation of AIM2 within macrophages in the aorta and drive vascular dysfunction. Further studies are required to prove this.

The use of diarysulfonylurea-containing compounds, known as cytokine release inhibitory drugs (CRID), inhibits the post translational processing of IL-1β (Baldwin *et al*, 2015). More specifically CP-456,773 (CRID3) blocks the AIM2 inflammasome pathway *in*

vitro (Coll and O'Neil, 2013). Interestingly CRID3 was shown to inhibit the production of IL-1β by stimulated bone marrow derived macrophages and the processing of pro-caspase-1 and pro-IL-1 into their active forms. However, in the present study CRID3 failed to prevent the inflammatory progression of mCIA, which goes against what we expected given the previous literature on this compound. The question remains as to why inhibiting the AIM2 inflammasome did not impact on arthritis in our model.

In previous studies CRID3 was found to have no impact on the ability of macrophages to produce TNF-α (Perregaux *et al*, 2001; Laliberte *et a*l, 2003). This cytokine is considered to be pivotal in RA pathology, correlating with the number of bone erosions and extent of inflammation (Husby *et al*, 1988), and is a significant therapeutic target in human disease (Fox *et al*, 2000). It is therefore logical to conclude that if CRID3 is not capable of reducing TNF-α production; it may not be a surprise that arthritis onset and progression was not altered in the treatment group.

As described above, CRID3 has also been shown to reduce IL-1β production in a model of arthritis (Coll *et al*, 2015). As with TNF-α, IL-1β is a pivotal cytokine in both the onset and progression of inflammatory arthritis (Finnegan and Doodes, 2008). Indeed IL-1 blockade has been used as a potential therapeutic strategy in human disease. For example a recombinant form of the IL-1 receptor was somewhat effective in systemic onset juvenile idiopathic arthritis, although it required administration by daily injection (Correll and Binstadt, 2013). This would suggest that inhibition of IL-1 in this way has very short term effects (Burger *et al*, 2006). This could potentially explain why blocking IL-1 activation by CRID3 every other day does not impact on arthritis onset in our model.

Surprisingly, although there was no overall impact on arthritis onset in the CRID3 treated group, increased paw swelling over time was observed. Explanations for this rather spurious affect can only be postulated. It is possible that CRID3 inhibition of Caspase-1 activation prevents the macrophage from carrying out pryoptosis. Lack of macrophage driven cell death and thus accumulation of macrophages is likely to occur in the diseased joints as there is no clearing mechanism. The accumulation of dead or dying cells therefore will drive a further inflammatory response, attracting more inflammatory cells to the region.

For the first time this chapter describes the impact of blocking the downstream mediators of the AIM2 inflammasome prevented decreased vascular constriction response in comparison to PBS treated controls. However, this is not the first time in which the inflammasome has been suggested as the potential candidate driving both vascular injury and atherosclerosis. Previous studies show downstream mediators of AIM2 are present at the site of vascular injury and are involved in the early inflammatory response following injury (Usui, 2012). Atherosclerosis has also previously been associated with inflammasome activation. Many studies have shown that IL-1β is a pro-atherogenic cytokine and have suggested that the infammasome accelerates atherosclerosis (Kirii *et al*, 2003; Tedgui and Mallat, 2006). In terms of inflammatory arthritis this is the first time the inflammasome has been related to vascular dysfunction and inhibition of AIM2 improves vascular function. This is an exciting prospect for RA

patients who are twice as likely as the general population to suffer a CV event. Further work would be required to optimise dosing regime and optimal drug concentration.

6.5 Conclusion

CRID3 treatment shows potential to work as a successful therapeutic in the treatment of vascular dysfunction. Further work is required in order to determine firstly an appropriate dose and secondly the specific underlying mechanisms by which CRID3 works to alter vascular constriction responses. A question for the future would be whether blocking Caspase-1 and IL-1 maturation with CRID3 (or similar) could be used in combination with IL-6 or TNF inhibitors currently used to treat inflammatory arthritis. It would be expected that this poly-therapy could successfully treat inflammatory arthritis, whilst protecting the vascular system from dysfunction.

Chapter 7 - General Discussion

Prior to the work carried out in this thesis, it was known that mCIA was characterised by aortic contractile dysfunction (Reynolds et al, 2012). It was suggested that this dysfunction was associated with increased MMP-9 levels, however, the source of the latter and the inflammatory state of the vessel was unknown. This thesis has further characterised the aortic vessel wall and closely associated PVAT with regard to contractile function and inflammatory, structural and calcification mediators. As such inflammatory cells were found to be increased within both the aorta and surrounding PVAT, suggesting a global impact of systemic inflammation associated with inflammatory arthritis. In particular F4/80+ macrophages were identified as the increased cellular population, the first time such an observation has been associated with the mCIA vasculature. Numerous studies have identified a role for macrophages in the progression of vascular disease (Frantz et al, 2014; Shirai et al, 2015), key features being the versatility and plasticity of these immune cells. At present we can only speculate as to the roles of macrophages in arthritis-associated vascular dysfunction. Further functional studies could be carried out to determine the specific types of macrophages increased in the aorta and the roles they play. For example, it is known that there are many types of macrophages, including both pro and anti-inflammatory and classified as M1 or M2 macrophages respectively. M1 macrophages inhibit cell proliferation and cause tissue damage whilst M2 macrophages promote cell proliferation and tissue repair (Mills, 2012). It is key in future studies to investigate the impact of the specific macrophage subset that is increasing in number since their potential role is highly variable dependent on their type. This for example could include examining M1 macrophage driven nitric oxide production or M2 macrophage mediated ornithine production (Mills, 2012).

The importance of increased macrophage numbers within the mCIA vasculature is emphasised by it being one of the earliest changes in this tissue. Therefore, it is a potential key identifying factor that could be used in the RA patient cohort to determine early indicators of vascular dysfunction. While this is obviously very difficult, in order for it to be beneficial, techniques and/or probes would need to be developed to identify macrophages *in situ* in the wall of the aorta, or indeed other vascular beds. A potential methodology would be to radiolabel a compound/antibody that has high specificity for F4/80, so that when injected into the patient, together with novel imaging technology, macrophages could be identified. Recent real time imaging platforms have been identified in order to measure macrophage phagocytosis (Kapellos et al, 2016). This technique combines pH-dependent dye particle labelling, along with the acquisition of images in real time and operator independent image analysis. In order for this to be successful it would be imperative for it to be applied as close to RA diagnosis as possible, thus providing the patient with the earliest opportunity to begin preventative measures to reduce the risk of CV outcomes.

Macrophage expression was also associated with increased DR3 expression and increased MMP-9 within the PVAT specifically. Macrophages and DR3 have previously been linked in vascular disease (McLaren et al, 2010). This study suggests the association between the two is not unique to atherosclerosis, but is important in inflammation in general. Data in this thesis has shown for the first time that DR3 ablation reduces both

onset and severity of mCIA. As such this supports data shown in the AIA model of arthritis (Bull et al, 2008) and together these studies highlight a critical role for DR3 in the pathogenesis of joint damage during inflammatory arthritis.

Initially the findings from $DR3^{-/-}$ studies suggested that DR3 ablation was protective against arthritic disease. However, when vascular function was determined in these animals, constriction responses were further dysfunctional. This suggested that DR3 was protective in maintaining a normal level of vascular constriction. Whether RA-associated CVD is coupled to decreased expression of DR3 within the human vasculature is unknown. To throw light on this question it would be possible to determine DR3 levels in RA patient blood samples by either ELISA or flow cytometry and correlate these two measures of vascular function. While DR3 has previously been associated with inflammatory disease protection in the ulcerative colitis cohort (Gomez-Garcia et al, 2007), the studies presented here are the first to target its role in the vascular constriction response. In doing so they have provided a conundrum in that DR3 ablation is beneficial in mCIA prevention, and would likely impact human RA similarly, however co-morbidities were exacerbated. Further studies would be required to determine whether the benefit to the joint was substantial enough to outweigh the potential CVD risks. One way in which this could be investigated would be to specifically target DR3 ablation to the joint. This would demonstrate if local inhibition of the target pathway had a different impact on total pathology in comparison to systemic inhibition.

It was hypothesised in this thesis that the onset of vascular calcification was responsible for the contractile dysfunction seen in mCIA. However, studies in animals with short term mCIA showed that calcification was not initiated, as measured by a number of primary calcification markers. Nevertheless, the studies did suggest the presence of osteoblast transcription markers, osteoclastogenesis markers and TRAP positive cells. Importantly these cells have not previously been identified within the aorta during mCIA and their presence alone highlights that calcification has the potential to occur in this tissue. That fact that calcification was not demonstrated is most likely due to the very early window in disease through which our snapshot on this process was taken. As emphasised throughout this thesis, RA is a long term condition that tends to get worse with time, transitioning from simple flu-like symptoms to a severely debilitating disease of the joints. However, the early time point provided by the mCIA model represents a time when changes are beginning in the aortic vessel, potentially allowing therapeutics to be developed for early intervention and slowing progression of vascular changes in arthritic patients. If time had permitted I would have determined the protein levels of all potential calcification markers and mediators. This is important as gene expression may change independently of protein levels. Although gene expression profiles will give some idea of the effect disease has on message production, it does not determine whether the protein has been made or activated. For enzymes such as TRAP, enzymatic analysis assays could be carried out in order to determine activity. To determine activity of such proteins as osteoblast transcription factors, the differentiation of VSMC could be investigated.

Calcification studies provided the basis for examining the impact of longer term arthritis on this process within the thoracic aorta. Although little statistical significance was seen in the expression of key mineralization mediators, important data came to light suggesting the impact of aging on calcification. Most interestingly expression of osteoclast mediators; TRAP and Calcitonin Receptor were significantly increased in aged control animals. In humans, arteries calcify with age and this process is often accelerated by vascular pathologies, such as atherosclerosis (Kieffer et al, 2000). Data presented here suggests that the aging mouse is indeed beginning to show signs of calcification. The long term mCIA model provided a reduced insult to the animals and further lenghtier modifications to the gold standard mCIA model are like to throw more light on this process. Currently due to severity limits in the mCIA protocol this cannot be carried out. However, these described data allow conclusions to be drawn, in particular that calcification in short or long term arthritis does not drive the observed contractile dysfunction. Rather, the latter would seem to be driven by increases in inflammatory pathways and/or a consequence of early changes in structural proteins such as collagen and elastin. It would be interesting to induce arthritis in aged mice and determine whether the aged vascular phenotype per se is a risk factor for CVD. In reality the long term model requires detailed characterisation given the change in arthritis induction protocol, particularly with regard to antibody production, inflammatory mediators, and impact at both the joint and systemically. It is imperative to determine whether dysfunction was not seen in this model due to lower systemic impact before it can be used as a successful refinement to the current mCIA protocol.

Changes to the structural proteins collagen and elastin are apparent in the thoracic aorta during mCIA. Both suffer some sort of dysregulation, however, the structure of the elastin filaments themselves appear to be the most impacted. The usual arrangement of elastin involves a number of repeated wave-like filaments. However, during mCIA the elastin filaments themselves appear to be straightened. With progressing arthritis severity, the number of straightened repeated filament regions appears to be increased. However, in order to characterise these straightened regions a computer algorithm would be required that could specifically identify straight lines amongst wavy lines. This would provide a measure for elastin dysfunction within the thoracic vessel wall. If a numerical value could be given to the dysfunction it could be correlated with arthritis severity to analyse this dysfunction and throw light on important correlations.

The inflammasome complexes have been linked previously with many inflammatory conditions. However, their role in the progression of arthritis and its prevention has not been investigated in detail. While the AIM2 inflammasome has been associated with both RA (Jakobs et al, 2015) and CVD (Garg, 2011) independently, the underlying mechanisms contecting the two remain elusive. Our studies show interesting observations with regard to the AIM2 pathway during mCIA, and suggest that in some way this inflammasome plays a role in the progression of inflammatory arthritis. However, when AIM2 was inhibited, an effect on either arthritis progression or severity was absent, in fact animals in the AIM2 treatment group showed an increase in paw swelling in comparison to non-treated animals. This was an unexpected finding and there are a number of potential reasons that may explain this observation. For example,

it could be that swelling is protective, in terms of the inflammatory response and in the clearing of pathogens. Moreover, there could be an association between AIM2 and macrophage cell death, which if prevented could escalate the inflammatory response. A "hyper" activated state could recruit further inflammatory cells to the region where they are not necessarily required. Further in depth studies would be required to determine the cause of this swelling. This would require assessing joints for arthritis index as shown in the earlier chapters of this thesis (Chapter 3), in which the actual severity of arthritis is determined in terms of bone and cartilage destruction, inflammatory infiltrate and synovial hyperplasia. F4/80 staining could also be carried out in order to determine whether macrophage numbers are increased within the joint. Lastly, ex vivo studies could look at the impact of AIM2 inhibition on macrophage migration and whether the latter in increased or prevented.

Excitingly, blocking AIM2 improved vascular constriction response in comparison to non-treated animals. This confirmed the involvement of the AIM2 inflammasome within the vascular constriction response, identifying it as a potential target in the treatment of RA associated CVD. That the constriction response was not restored to the level of non-immunized controls suggests that the dose of CRID3 may not be optimal. In order to confirm if this is the case, RT-qPCR and complimentary immunohistochemistry is required to determine levels of AIM2 and its downstream mediators in the thoracic aortas of treated and non-treated animals. This will give us a much better idea of the correct CRID3 dose to use. The impact of AIM2 blockade on the structural proteins has not currently been investigated. Given the changes observed in relation to collagen and elastin within the aortic vessel wall, it is imperative to investigate the effect of treatment on these parameters.

A potential outcome from this thesis could involve a combination therapy. If optimization of CRID3 treatment is successful, it could be used in conjunction with a current RA treatment. This combination would impact on both the progression of RA and the associated CV risk. It is possible that inhibition of the AIM2 inflammasome right from the point of RA diagnosis could prevent the earliest changes to the aortic vessel wall and ameliorate CVD in the RA cohort. Secondly AIM2 blockade could be used in conjunction with a drug that inhibits DR3. The latter has proven beneficial in a number of mouse models of inflammatory arthritis (Bull et al, 2008; Wang et al, 2014; Collins et al, In Press) and targeted inhibition might prove to be very useful in the human population. It is likely that selective blockade of DR3 in the joint would be more successful in treating RA since systemic DR3 ablation may have a negative impact on the vasculature.

This thesis has highlighted a number of novel data points, however, it does have a number of strengths and weaknesses that should be considered. This thesis has characterised the inflammatory cell content of the aortic vessel wall for the first time during arthritis and has shown important early changes that might precede CVD. However, not all early immune cells were investigated, for example both B and T cells could be vital within the progression of vascular disease. The impact of ablating DR3 was shown in mCIA was also characterised for the first time and a role for DR3 in arthritis

progression identified. Although a large number of calcification mediators were investigated, there are a number of important factors that have not been evaluated, including proteins such as bone morphogenic protein 2. It also must be considered that these RT-qPCR data are representative of the aorta and PVAT. Although this gives an idea of the tissue as a whole, it would be useful to investigate specifically the changing expression levels in the aorta alone. Moreover, RT-qPCR data does not highlight the end point change in protein levels. Although these data are indicative of what might happen downstream to proteins, their location and activity remains unknown. Blocking AIM2 produced exciting results in terms of vascular function, however, follow up experiments to determine protein levels and to optimise dosing would be required in the future.

7.1 Conclusion

The work completed in this thesis has allowed the following 5 major conclusions to be drawn. Firstly, inflammatory arthritis drives an increase in systemic inflammation as represented by increased inflammatory cells, namely, macrophages within the wall of the thoracic aorta and in the surrounding PVAT. DR3 has been shown to be involved in both arthritis induction and within the arthritic constriction response, where it works to maintain a healthy constriction potential. Vascular calcification was not responsible for the dysfunction seen in the arthritic constriction response in either short or long term mCIA. However, the contractile phenotype seen in the mCIA model was associated with changes in structural proteins of the ECM, specifically, elastin filaments. Lastly, the AIM2 infammasome was implicated in the arthritic vascular constriction response. Blockade of this inflammatory pathway using a novel inhibitor CRID3 worked to successfully restore some vascular constriction potential and following optimization poses as a potential therapeutic intervention to help treat CV disease in the RA cohort.

8. References

Agabiti-Rosei C, De Ciuceis C, Rossini C, Porteri E, Rodella LF, Withers SB, Heagerty AM, Favero G, Agabiti-Rosei E, Rizzoni D, Rezzani R. Anticontractile activity of perivascular fat in obese mice and the effect of long-term treatment with melatonin. J Hypertens. 2014. 32(6):1264-74

Aiba Y and Nakamura M. The Role of TL1A and DR3 in Autoimmune and Inflammatory Diseases. Mediators of Inflammation. 2013.

Akishima Y, Akasaka Y, Ishikawa Y. Role of macrophage and smooth muscle cell apoptosis in association with oxidized low-density lipoprotein in the atherosclerotic development. Mod Pathol. 2005. 18:365–373.

Allison MA, Criqui MH, Wright CM. Patterns and risk factors for systemic calcified atherosclerosis. Arterioscler Thromb Vasc Biol. 2004; 24: 331–336.

Asquith D, Miller AM, McInnes IB, Liew FY. Animal models of rheumatoid arthritis. European Journal of Immunology. 2009

Baccala R, Hoebe K, Kono DH, Beutler B, Theofilopoulos AN. TLR-dependent and TLR-independent pathways of type I interferon induction in systemic autoimmunity. Nat Med. 2007. 13(5):543-51.

Balcombe JP, Barnard ND, Sandusky C: Laboratory routines cause animal stress. Contemporary Topics in Laboratory Animal Science. 2004, 43 (6): 42-51.

Baldwin AG, Brough D, and Freeman S. Inhibiting the Inflammasome, A chemical perspective. J Med Chem. 2015. 59(5); 1691-1710.

Bamias G, Martin C, III, Marini M, Hoang S, Mishina M, Ross WG, Sachedina MA, Friel CM, Mize J, Bickston SJ, et al. Expression, localization, and functional activity of TL1A, a novel Th1-polarizing cytokine in inflammatory bowel disease. J. Immunol. 2003;171:4868–4874

Baud S, Duca L, Bochicchio B, Brassart B, Belloy N, Pepe A, Dauchez M, Martiny L, Debelle L. Elastin peptides in aging and pathological conditions. Biomol Concepts. 2013.4(1):65-76.

Baum R, Sharma S, Carpenter S, Li QZ, Busto P, Fitzgerald KA, Marshak-Rothstein A and Gravallese EM. Cutting Edge: AIM2 and Endosomal TLRs Differentially Regulate Arthritis and Autoantibody Production in DNase II–Deficient Mice. J Immunol. 2015. 194(3); 873-877

Bendele AM. Animal models of rheumatoid arthritis. Musculoskel Neuron Interact. 2001; 1(4):377-385

Bennett BJ, Scatena M, Kirk EA, Rattazzi M, Varon RM, Averill M, Schwartz SM, Giachelli CM, Rosenfeld ME. Osteoprotegerin inactivation accelerates advanced atherosclerotic lesion progression and calcification in older ApoE$^{-/-}$ mice. Arterioscler Thromb Vasc Biol. 2006. 26:2117–2124.

Bennett; Macrophages; Cause or Cure in atherosclerosis Heart Metab. 2013. 60:5-8

Bennett BJ, de Aguiar Vallim TQ, Wang Z, Shih DM, Meng Y, Gregory J, Allayee H, Lee R, Graham M, Crooke R, Edwards PA, Hazen SL, Lusis AJ. Trimethylamine-N-oxide, a metabolite associated with atherosclerosis, exhibits complex genetic and dietary regulation. Cell Metab. 2013 Jan 8;17(1):49-60.

Benoit JN and Taylor MS. Vascular reactivity following ischemia/reperfusion. Frontiers in Bioscience2. 1997. e28-33

Berry CL, Looker T, Germain J. The growth and development of the rat aorta. I. Morphological aspects. J Anat. 1972;113:1–16

Berry CL, Sosa-Melgarejo JA, Greenwald SE. The relationship between wall tension, lamellar thickness, and intercellular junctions in the fetal and adult aorta: its relevance to the pathology of dissecting aneurysm. J Pathol. 1993;169:15–20

Besch EL, Chou BJ: Physiological responses to blood collection methods in rats. Proceedings of the Society for Experimental Biology and Medicine. 1971. 138 (3): 1019

Beutler BA. The role of tumor necrosis factor in health and disease. J Rheumatol Suppl. 1999. 57:16–21

Billiau A, Matthys P. Collagen-induced arthritis and related animal models: How much of their pathogenesis is auto-immune, how much is auto-inflammatory? Cytokine & Growth Factor Reviews. 2011. V22, 5–6, 339–344

Boisvert WA, Rose DM, Johnson KA, Fuentes ME, Lira SA, Curtiss LA, Terkeltaub RA. Up-Regulated Expression of the CXCR2 Ligand KC/GRO-α in Atherosclerotic Lesions Plays a Central Role in Macrophage Accumulation and Lesion Progression. Am J Pathol. 2006. 168(4): 1385–1395

Borysenko CW, García-Palacios V, Griswold RD, Li Y, Iyer AK, Yaroslavskiy BB, Sharrow AC, Blair HC. Death receptor-3 mediates apoptosis in human osteoblasts under narrowly regulated conditions. J Cell Physiol. 2006 Dec;209(3):1021-8.

Bostrom K, Watson KE, Horn S, Wortham C, Herman IM, Demer LL. Bone morphogenetic protein expression in human atherosclerotic lesions. J Clin Invest. 1993. 91:1800–1809.

Bouloumié A1, Sengenès C, Portolan G, Galitzky J, Lafontan M. Adipocyte produces matrix metalloproteinases 2 and 9: involvement in adipose differentiation. Diabetes. 2001. Sep;50(9):2080-6.

Boyce BF and Xing L. Biology of RANK, RANKL, and osteoprotegerin Arthritis Res Ther. 2007. 9 Suppl 1:S1

Brackertz D, Mitchell GF and Mackay IR. Antigeninduced arthritis in mice I. Induction of arthritis in various strains of mice. Arthritis Rheum. 1977. 20:841-850

Bradley JR. TNF-mediated inflammatory disease. J Pathol. 2008. 214(2):149-60.

Brand DD, Latham KA, Rosloniec EF. Collagen-induced arthritis. Nature Protocols 2. 2007. 1269 – 1275.

Brew and Nagase. The tissue inhibitors of metalloproteinases (TIMPs): An ancient family with structural and functional diversity. Biochim Biophys Acta. 2010 Jan; 1803(1): 55–71.

Breyne J, Juthier F, Corseaux D, Marechaux S, Zawadzki C, Jeanpierre E, Ung A, Ennezat PV, Susen S, Van Belle E, Le Marec H, Vincentelli A, Le Tourneau T, Jude. Atherosclerotic-like process in aortic stenosis: activation of the tissue factor-thrombin pathway and potential role through osteopontin alteration. Atherosclerosis. 2010;213:369–376

Brindle. A transcriptional regulator of osteogenesis expressed in calcifying atherosclerotic plaque. Cardiovascular Research 52. 2001. 178–180

Brown AP, Dinger N, Levine BS: Stress produced by gavage administration in the rat. Contemporary Topics in Laboratory Animal Science. 2000. 39 (1): 17-21.

Bucay N, Sarosi I, Dunstan CR, Morony S, Tarpley J, Capparelli C, Scully S, Tan HL, Xu W, Lacey DL. Osteoprotegerin-deficient mice develop early onset osteoporosis and arterial calcification. Genes Dev. 1998. 12:1260–1268

Bull, MJ, Williams AS, Mecklenburgh Z, Calder CJ, Twohig JP, Elford C, Evans BA, Rowley TF, Slebioda TJ, Taraban VY. The Death Receptor 3-TNF-like protein 1A pathway drives adverse bone pathologyin inflammatory arthritis. J. Exp. Med. 2008. 205: 2457–2464.

Burckstummer T, Baumann C, Bluml S, Dixit E, Durnberger G, Jahn H et al. An orthogonal proteomic-genomic screen identifies AIM2 as a cytoplasmic DNA sensor for the inflammasome. Nat Immunol. 2009. 10: 266–27

Burger D, Dayer JM, Palmer G, Gabay C. Is IL-1 a good therapeutic target in the treatment of arthritis? Best Pract Res Clin Rheumatol. 2006. 20(5):879-96.

Burstone MS. Histochemical demonstration of acid phosphatase activity in osteoclasts. J Histochem Cytochem. 1959. 7:39–41

Butcher MJ, Galkina EV. Phenotypic and functional heterogeneity of macrophages and dendritic cell subsets in the healthy and atherosclerosis-prone aorta. Front Physiol. 2012. 19;3:44.

Canfield AE, Doherty MJ, Wood AC, Farrington C, Ashton B, Begum N, Harvey B, Poole A, Grant ME, Boot-Handford RP. Role of pericytes in vascular calcification: a review. Z Kardiol. 2000. 89 Suppl 2:20-7.

Cantor JO, Keller S, Mandl I, Turino GM. Increased synthesis of elastin in amiodarone-induced pulmonary fibrosis. Oncogene. 2002. 12;21(57):8843-51.

Cassatella MA, Pereira-da-Silva G, Tinazzi I, Facchetti F, Scapini P, Calzetti F, Tamassia N, Wei P, Nardelli B, Roschke V, Vecchi A, Mantovani A, Bambara LM, Edwards SW, Carletto A. Soluble TNF-like cytokine (TL1A) production by immune complexes stimulated monocytes in rheumatoid arthritis. J Immunol. 2007 Jun 1;178(11):7325-33.

Cavallini, O. Lovato, A. Bertolaso. The TNF-family cytokine TL1A inhibits proliferation of human activated B cells. PloS One. 2013. v8(4)

Cecelja M and Chowienczyk P. Role of arterial stiffness in cardiovascular disease. JRSM Cardiovasc Dis. 2012 Jul; 1(4)

Cecelja M, Chowienczyk P. Molecular Mechanisms of Arterial Stiffening. Pulse (Basel). 2016. 4(1):43-8.

Chang L, Villacorta L, Li R, Hamblin M, Xu W, Dou C, Zhang J, Wu J, Zeng R, Chen YE. Loss of perivascular adipose tissue on peroxisome proliferator-activated receptor-γ deletion in smooth muscle cells impairs intravascular thermoregulation and enhances atherosclerosis. Circulation. 2012. 126(9):1067-78.

Chatterjee TK, Stoll LL, Denning GM. Proinflammatory phenotype of perivascular adipocytes: influence of high-fat feeding. Circ. Res. 2009;104:541–549

Chen, Jin M, Yang F, Zhu J, Xiao Q and Zhang L. Matrix Metalloproteinases: Inflammatory Regulators of Cell Behaviors in Vascular Formation and Remodeling. Mediators of Inflammation. 2013.

Cheng XW, Huang Z, Kuzuya M, Okumura K, Murohara T. Cysteine Protease Cathepsins in Atherosclerosis-Based Vascular Disease and Its Complications. Hypertension. 2011; 58: 978-986

Chinnaiyan AM, O'Rourke K, Yu GL. Signal transduction by DR3, a death domain-containing receptor related to TNFR-1 and CD95. Science. 1996. 274:990–2

Cho A and Michael A. Reidy Matrix Metalloproteinase-9 Is Necessary for the Regulation of Smooth Muscle Cell Replication and Migration After Arterial Injury Circulation Research. 2002. 91**:** 845-851

Choubey D, Deka R, Ho SM. Interferon-inducible IFI16 protein in human cancers and autoimmune diseases. Front Biosci. 2008. 1;13:598-608.

Chow MJ, Choi M, Yun SH, Zhang Y. The effect of static stretch on elastin degradation in arteries. PLoS One. 2013. 16;8(12):e81951.

Cleveland Ihle. Contenders in FasL/TNF death signalling. Cell. 1995. V81(4).

Coll R, Robertson AAB, Chae JJ, Higgins SC, Munoz-Planillo R, Inserra MC, Vetter I, Dungan LS, Monks BG, Stutz A, Croker DE, Butler MS, Haneklaus M, Sutton CE, Nunez G, Latz E, Kastner DL, Mills KHG, Masters SL, Schroder K, Cooper MA, O'Neil LAJ. A small molecule inhibitor of the NLRP3 inflammasome for the treatment of inflammatory disease. Nature Medicine. 2015. 21; 248-255.

Collins FL , Williams JO, Bloom AC, Stone MD, Choy E, Wang ECY, and Williams AS. Death Receptor 3 (TNFRSF25) Increases Mineral Apposition by Osteoblasts and Region Specific New Bone Formation in the Axial Skeleton of Male DBA/1 Mice. Journal of Immunology Research. 2015.

Collins FL, Williams JO, Bloom AC, Jordan L, Stone MD, McCabe LR, Wang ECY and Williams AS. CCL3 and MMP-9 are Downstream Effectors of DR3/TL1A Pathway-Dependent Osteoclast Function and Systemic Bone Loss [Accepted Bone 2017; Awaiting Press]

Correll CK and Binstadt BA. Advances in the pathogenesis and treatment of systemic juvenile idiopathic arthritis. Paediatric Research. 2014. 75; 176-183.

Crowson CS, Liang KP, Therneau TM, Kremers HM, Gabriel SE. Could accelerated aging explain the excess mortality in patients with seropositive rheumatoid arthritis? Arthritis Rheum. 2010 Feb;62(2):378-82.

Cypess, A M.D, Lehman S, Williams G, Tal I, Rodman D, Goldfine AB, Kuo FC, Palmer EL, Tseng Y, Doria A, Kolodny GM, and Kahn CR. Identification and Importance of Brown Adipose Tissue in Adult Humans. N Engl J Med. 2009; 360:1509-1517

Davies MR, Hruska KA. Pathophysiological mechanisms of vascular calcification in end-stage renal disease. Kidney Int. 2001. 60(2):472-9.

Demer LL, Tintut Y. Vascular Calcification: Pathobiology of a Multifaceted Disease. Circulation. 2008. 117:2938–2948.

Deryugina E, Zajac E, Juncker-Jensen A, Kupriyanova TA, Welter L, and Quigley JP. Tissue-Infiltrating Neutrophils Constitute the Major *In Vivo* Source of Angiogenesis-Inducing MMP-9 in the Tumor Microenvironment. Neoplasia. 2014. 16(10): 771–788.

Devarajan E, Sahin AA, Chen JS, Krishnamurthy RR, Aggarwal N, Brun AM, Sapino A, Zhang F, Sharma D, Yang XH, Tora AD, Mehta K. Down-regulation of caspase 3 in breast cancer: a possible mechanism for chemoresistance. J Lab Clin Med. 1987.109(4):480-5.

Dingemans KP, Teeling P, Lagendijk JH, Becker AE. Extracellular matrix of the human aortic media: an ultrastructural histochemical and immunohistochemical study of the adult aortic media. Anat Rec. 2000. 258:1–14

Dombrowski, Y., Peric, M., Koglin, S., Kammerbauer, C., Goss, C., Anz, D., Simanski, M. Cytosolic DNA triggers inflammasome activation in keratinocytes in psoriatic lesions. Sci. Transl. Med. 2011. 3: 82ra38

Duan XH, Chang JR, Zhang J, Zhang BH, Li YL, Teng X, Zhu Y, Du J, Tang CS, Qi YF. Activating transcription factor 4 is involved in endoplasmic reticulum stress-mediated apoptosis contributing to vascular calcification. Bone. 2003. 32(6):621-9.

Duque GA and Descoteaux A. Macrophage Cytokines: Involvement in Immunity and Infectious Diseases. Front Immunol. 2014; 5: 491.

Edwards, D. R., Beaudry, P. P., Laing, T. D., Kowal, V., Leco, K. J., Leco, P. A., and Lim, M. S. The role of tissue inhibitors of metalloproteinases in tissue remodelling and cell growth. Int. J. Obesity Relat. Metab. Disord. 1996. 20, Suppl. 3, S9–S15

Egusa H, Kaneda Y, Akashi Y, Hamada Y, Matsumoto T, Saeki M, Thakor DK, Tabata Y, Matsuura N, Yatani H. Enhanced bone regeneration via multimodal actions of synthetic peptide SVVYGLR on osteoprogenitors and osteoclasts. Biomaterials. 2009. 30:4676–4686

Elliott RJ, McGrath LT. Calcification of the human thoracic aorta during aging. Calcif Tissue Int. 1994. 54(4):268-73.

Escalante A, Haas RW, del Rincon I: Paradoxical effect of body mass index on survival in rheumatoid arthritis: role of comorbidity and systemic inflammation. Arch Intern Med. 2005. 165:1624–1629.

Fang FC, Vazquez-Torres A. Nitric oxide production by human macrophages: there's NO doubt about it. American Journal of Physiology - Lung Cellular and Molecular Physiology. 2002. V282(5)L941-L943

Fang, L., B. Adkins, V. Deyev, and E. R. Podack. Essential role of TNF receptor superfamily 25 (TNFRSF25) in the development of allergic lung inflammation.J. Exp. Med. 2008. 205: 1037–1048.

Fantin A1, Vieira JM, Gestri G, Denti L, Schwarz Q, Prykhozhij S, Peri F, Wilson SW, Ruhrberg C. Tissue macrophages act as cellular chaperones for vascular anastomosis downstream of VEGF-mediated endothelial tip cell induction. Blood. 2010. 5;116(5):829-40.

Feldmann M, Maini RN. TNF defined as a therapeutic target for rheumatoid arthritis and other autoimmune diseases. Nat Med. 2003. 9:1245–50

Fernandes-Alnemri T. The pyroptosome: a supramolecular assembly of ASC dimers mediating inflammatory cell death via caspase-1 activation. Cell Death Differ. 2007. 14:1590–1604

Finnegan A and Doodes PD. Pathways for interleukin-1-driven arthritis. Arthritis Rheum. 200. 58(11):3283-5. doi: 10.1002/art.23952.

Firestein G S, Zvaifler N J. How important are T cells in chronic rheumatoid synovitis? II. T cell-independent mechanisms from beginning to end. Arthritis Rheum. 2002. 46 : 298

Forsyth, Hamdy M. Aly, Richard F. Neville, Anton N. Sidawy. Proliferation and extracellular matrix production by human infragenicular smooth muscle cells in response to interleukin-1β Journal of Vascular Surgery.1997. V26(6)1002–1008.

Fox DA. Cytokine blockade as a new strategy to treat rheumatoid arthritis: inhibition of tumor necrosis factor. Arch Intern Med. 2000. 28;160(4):437-44.

Frantz S and Nahrendorf M. Cardiac macrophages and their role in ischaemic heart disease. Cardiovasc Res. 2014. 102(2): 240–248.

Galis ZS, Johnson C, Godin D, Magid R, Shipley JM, Senior RM and Ivan E. Targeted Disruption of the Matrix Metalloproteinase-9 Gene Impairs Smooth Muscle Cell Migration and Geometrical Arterial Remodeling. Circ Res. 2002. 91:852-859

Gao YJ. Dual modulation of vascular function by perivascular adipose tissue and its potential correlation with adiposity/lipoatrophy-related vascular dysfunction. Current Pharm. Des. 2007. 13:2185–2192.

Gao YJ, Lu C, Su LY, Sharma AM, Lee RMKW. Modulation of vascular function by perivascular adipose tissue: the role of endothelium and hydrogen peroxide. Br. J. Pharmacol. 2007. 151:323–331

Garg NJ. Inflammasomes in cardiovascular diseases. Am J Cardiovasc Dis. 2011. 1(3):244-54.

Ge, Sanders AJ, Ye L and Jiang WG. Aberrant expression and function of death receptor-3 and death decoy receptor-3 in human cancer. Exp Ther Med. 2011. 2(2): 167–172.

Gerrity RG. The role of the monocyte in atherogenesis: I: transition of blood-borne monocytes into foam cells in fatty lesions. Am J Pathol. 1981. 103:181–190

Geusens P. The role of RANK ligand/osteoprotegerin in rheumatoid arthritis. Ther Adv Musculoskelet Dis. 2012. 4(4):225-33.

Giles J T, Szklo M, Post W, Petri M, Blumenthal RS, Lam G, Gelber AC, Detrano R, Scott WW, Kronmal RA, and Bathon JM. Coronary arterial calcification in rheumatoid arthritis: comparison with the Multi-Ethnic Study of Atherosclerosis Arthritis. Res Ther. 2009; 11(2): R36

Gleissner CA, Shaked I, Little KM and Ley K. CXCL4 induces a unique transcriptome in monocyte-derived macrophages. J Immunol. 2010. 184(9): 4810–4818.

Godson C, Mitchell S, Harvey K, Petasis NA, Hogg N, Brady HR. Cutting edge: Lipoxins rapidly stimulate nonphlogistic phagocytosis of apoptotic neutrophils by monocyte-derived macrophages. J Immunol. 2000. 164:1663–1667.

Golub E and Boesze-Battaglia K. The role of alkaline phosphatase in mineralization. Curr Opin Orthop. 2013 18:444–448.

Gómez-García M, Oliver J, Márquez A, Mendoza JL, López-Nevot MA, Fernández-Arquero M, González-Escribano MF, Díaz-Rubio M, de la Concha EG, Urcelay E, Martín J, Martínez A. Strong protective effect of DR3 against ulcerative colitis in the Spanish population. Am J Gastroenterol. 2007. 102(12):2762-6.

Griendling KK, Rittenhouse SE, Brock TA, Ekstein LS, Gimbrone MA, Alexander RW. Sustained formation of diacylglycerol from inositol phospholipids in angiotensin II stimulated vascular smooth muscle. J Biol Chem. 1986. 261:5901-6

Grimaldo S, Tian F, Li LY. Sensitization of endothelial cells to VEGI-induced apoptosis by inhibiting the NF-kappaB pathway. Apoptosis. 2009.14:788–95

Grivennikov SI, Greten FR, and Karin M. Crosstalk between sentinel and helper macrophages permits neutrophil migration into infected uroepithelium. Cell. 2010. 19; 140(6): 883–899.

Gruber BL, Sorbi D, French DL, Marchese MJ, Nuovo GJ, Kew RR, Arbeit LA. Markedly elevated serum MMP-9 (gelatinase B) levels in rheumatoid arthritis: a potentially useful laboratory marker. Clin Immunol Immunopathol. 1996. 78(2):161-71.

Guicciardi M E and Gores GJ. Life and death by death receptors. FASEB J. 2009 Jun; 23(6): 1625–1637.

Gunnett, Berg DJ, Faraci FM. Vascular Effects of Lipopolysaccharide Are Enhanced in Interleukin-10–Deficient Mice. Stroke. 1999; 30: 2191-2196

Guo H, Callaway JB and Ting J. Inflammasomes: mechanism of action, role in disease, and therapeutics. Nature Medicine. 2015. 21, 677-687

Hakimi M, Peters A, Becker A, Böckler D, Dihlmann S. Inflammation-related induction of absent in melanoma 2 (AIM2) in vascular cells and atherosclerotic lesions suggests a role in vascular pathogenesis. Vasc Surg. 2014. 59(3):794-803.

Hamada Y, Yuki K, Okazaki M, Fujitani W, Matsumoto T, Hashida MK, Harutsugu K, Nokihara K, Daito M, Matsuura N,Takahashi. Osteopontin-derived peptide SVVYGLR induces angiogenesis in vivo. Dent Mater J. 2004. 23:650–655

Harkness ML, Harkness RD, McDonald DA. The collagen and elastin content of the arterial wall in the dog. Proc R Soc Lond B Biol Sci. 1957. 146:541–551.

Hattersley G and Chambers TJ. Calcitonin Receptors as Markers for Osteoclastic Differentiation: Correlation between Generation of Bone-Resorptive Cells and Cells that Express Calcitonin Receptors in Mouse Bone Marrow Cultures. Endocrinology. 1989.

Hayman AR, Jones SJ, Boyde A, Foster D, Colledge WH, Carlton MB, Evans MJ, Cox TM. Mice lacking tartrate-resistant acid phosphatase (Acp 5) have disrupted endochondral ossification and mild osteopetrosis. Development. 1996. 122:3151–3162

He Y, de Castro LF, Shin MH, Dubois W, Yang HH, Jiang S, Mishra PJ, Ren L, Gou H, Lal A, Khanna C, Merlino G, Lee M, Robey PG, and Huang J. p53 Loss Increases the Osteogenic Differentiation of BMSCsStem Cells. 2015. 33(4): 1304–1319.

Henderson B, Thompson RC, Hardingham T, Lewthwaite J. Inhibition of interleukin-1-induced synovitis and articular cartilage proteoglycan loss in the rabbit knee by recombinant human interleukin-1 receptor antagonist. Cytokine. 1991. 3:246-249

Hochberg MC, Johnston SS, John AK. The incidence and prevalence of extra-articular and systemic manifestations in a cohort of newly-diagnosed patients with rheumatoid arthritis between 1999 and 2006. *Curr Med Res Opin.* 2008. 24:469-80.

Hofbauer LC, Schoppet M. Clinical implications of the osteoprotegerin/RANKL/RANK system for bone and vascular diseases. JAMA. 2004. 292:490–495

Hornung, V. AIM2 recognizes cytosolic dsDNA and forms a caspase-1-activating inflammasome with ASC. Nature. 2009. 458, 514–518.

Hume. The Many Alternative Faces of Macrophage Activation. Front Immunol. 2015; 6: 370.

Husby G, Williams RC Jr. Synovial localization of tumor necrosis factor in patients with rheumatoid arthritis. J Autoimmun. 1988. 1(4):363-71.

Iafolla M. Rheumatoid arthritis and atypical cardiovascular disease Inflammation changing the clinical presentation. Can Fam Physician. 2013. 59(5): 505-509.

Idelevich A, Rais Y, Ornan EM. Bone Gla protein increases HIF-1α-dependent glucose metabolism and induces cartilage and vascular calcification. Arterioscler Thromb Vasc Biol. 2011;31:e55–e71.

Italiani P and Boraschi D. From Monocytes to M1/M2 Macrophages: Phenotypical vs. Functional Differentiation. Front Immunol. 2014. 5: 514.

Iribarren-Marín AM, Carnerero-Herrera V, Domínguez-Pérez A, González-Martín R. Acute Aortic Syndrome and Rheumatoid Arthritis. Rev Esp Cardiol. 2011;64:246-7 - Vol. 64 Num.03

Izumi Y, Hayashi M, Morimoto R, Cheng XW, Wu H, Ishii H, Yasuda Y, Yoshikawa D, Izawa H, Matsuo S, Oiso Y, Murohara T. Impact of circulating cathepsin K on the coronary calcification and the clinical outcome in chronic kidney disease patients. Heart Vessels. 2016. 31(1):6-14.

Jakobs C, Perner S, Hornung V. AIM2 Drives Joint Inflammation in a Self-DNA Triggered Model of Chronic Polyarthritis. PLoS One. 2015. 26;10(6):e0131702.

Janckila AJ, Slone SP, Lear SC, Martin A, Yam LT. Tartrate-resistant acid phosphatase as an immunohistochemical marker for inflammatory macrophages. Am J Clin Pathol. 2007. 127(4):556-66.

Jani B and C Rajkumar. Ageing and vascular ageing. Postgrad Med J. 2006. 82(968): 357–362.

Jendro MC, Ganten T, Matteson EL, Weyand CM, Goronzy JJ. Emergence of oligoclonal T cell populations following therapeutic T cell depletion in rheumatoid arthritis. Arthritis Rheum. 1995. 3

Jin T, Guo F, Kim S, Howard A, Zhang YZ. X-ray crystal structure of TNF ligand family member TL1A at 2.1A. Biochem Biophys Res Commun. 2007. 7;364(1):1-6. Epub 2007 Oct 1.

Jin, T., Perry, A., Jiang, J., Smith, P., Curry, J. A., Unterholzner, L., Jiang, Z. Structures of the HIN domain: DNA complexes reveal ligand binding and activation mechanisms of the AIM2 inflammasome and IFI16 receptor. Immunity 2012. 36: 561–571.

Johnson R, Jane A. Leopold, Joseph Loscalzo. Vascular Calcification Pathobiological Mechanisms and Clinical Implications. Circulation Research. 2006. 99: 1044-1059

Jones L and George Y. Shinowara serum inorganic phosphate and “alkaline” phosphatase activity in hypophysectomized rats. OJ Pathology. 1941.

Jono S, Shioi A, Ikari Y, Nishizawa Y. Vascular calcification in chronic kidney disease. J Bone Miner Metab. 2006. 24(2):176-81.

Kaden JJ, Dempfle CE, Grobholz R, Fischer CS, Vocke DC, Kilic R, Sarikoc A, Pinol R, Hagl S, Lang S, Brueckmann M, Borggrefe M. Inflammatory regulation of extracellular matrix remodeling in calcific aortic valve stenosis. Cardiovasc Pathol. 2005. 14:80–87

Kadl A, Meher AK, Sharma PR, Lee MY, Doran AC, Johnstone SR, Elliott MR, Gruber F, Han J, Chen W, Kensler T, Ravichandran KS, Isakson BE, Wamhoff BR, Leitinger N. Identification of a novel macrophage phenotype that develops in response to atherogenic phospholipids via Nrf2. Circ Res. 2010. 17;107(6):737-46.

Kanbe N1, Tanaka A, Kanbe M, Itakura A, Kurosawa M, Matsuda H. Human mast cells produce matrix metalloproteinase 9. Eur J Immunol. 1999. 29(8):2645-9.

Kang YJ, Kim WJ, Bae HU, Kim DI, Park YB, Park JE, Kwon BS and Lee WH. Involvement of TL1A and DR3 in induction of pro-inflammatory cytokines and matrix metalloproteinase-9 in atherogenesis. Cytokine. 2005. 29(5):229-235.

Kapellos, Taylor L, Lee H, Cowley SA, James WS, Iqbal AJ, Greaves DR. A novel real time imaging platform to quantify macrophage phagocytosis. Biochemical Pharmacology. 2016 V116 (15) 107-119

Kapustin AM, and Shanahan CM. Novel Vascular Metabolic and Osteoinductive Factor? Arteriosclerosis, Thrombosis, and Vascular Biology. 2011. 31: 2169-2171

Kavanaugh A, Lipsky PE. Rheumatoid arthritis. In: Rich RR, Schwartz BD, Fleisher TA, Shearer WT, Strober W (eds) Clinical immunology: principles and practice. 1996.

Kawashima M and Miossec P. Effect of treatment of rheumatoid arthritis with infliximab on IFN gamma, IL4, T-bet, and GATA-3 expression: link with improvement of systemic inflammation and disease activity. Ann Rheum Dis. 2005. 64(3):415-8.

Keffer J, L Probert, H Cazlaris, S Georgopoulos, E Kaslaris, D Kioussis, and G Kollias Transgenic mice expressing human tumour necrosis factor: a predictive genetic model of arthritis. EMBO J. 1991 10(13): 4025–4031

Kelly C and Hamilton J. What kills patients with rheumatoid arthritis? Rheumatology (Oxford). 2007. 46(2):183-4.

Kido S, Inoue D, Hiura K, Javier W, Ito Y, Matsumoto T. Expression of RANK is dependent upon differentiation into the macrophage/osteoclast lineage: induction by 1alpha,25-dihydroxyvitamin D3 and TPA in a human myelomonocytic cell line, HL60. Journal of Biomedical Science. 2005. V12 (6) 869-880

Kieffer P, Robert A, Capdeville-Atkinson C, Atkinson J, Lartaud-Idjouadiene I. Age-related arterial calcification in rats. Life Sci. 2000. 5;66(24):2371-81.

Kinne RW, Bräuer R, Stuhlmüller B, Palombo-Kinne E, and Burmester G. Macrophages in rheumatoid arthritis Arthritis Res. 2000. 2(3): 189–202.

Kirii H, Niwa T, Yamada Y, Wada H, Saito K, Iwakura Y, Asano M, Moriwaki H, Seishima M. Lack of interleukin-1beta decreases the severity of atherosclerosis in ApoE-deficient mice. Arterioscler Thromb Vasc Biol. 2003. 1;23(4):656-60. Epub 2003 Feb 27

Kitson J, Raven T, Jiang YP, et al. A death-domain-containing receptor that mediates apoptosis. Nature. 1996. 384:372–5

Klaus S. Functional differentiation of white and brown adipocytes. Bioessays. 1997. 19(3):215-23.

Klaus L, Miller YI and Hedrick CC**.** Monocyte and Macrophage Dynamics during Atherogenesis. Arterioscler Thromb Vasc Biol. 2011. 31(7): 1506–1516.

Komori. Regulation of Osteoblast Differentiation by Transcription Factors. Journal of Cellular Biochemistry. 2006. 99:1233–1239

Krans B; Mayo Clinic. RA Can Drastically Impact Heart. October 2013

Krieger-Brauer and Kather H. Human fat cells possess a plasma membrane-bound H2O2-generating system that is activated by insulin via a mechanism bypassing the receptor kinase. J Clin Invest. 1992. 89(3): 1006–1013.

Krohn JB, Hutcheson JD, Martínez-Martínez E, Aikawa E. Extracellular vesicles in cardiovascular calcification: expanding current paradigms. J Physiol. 2016. 1;594(11):2895-903.

Kruidering M, Evan GI. Caspase-8 in apoptosis: the beginning of "the end"? IUBMB Life. 2000. 50(2):85-90.

Lacolley P, Regnault V, Nicoletti A, Li Z, Michel JB. The vascular smooth muscle cell in arterial pathology: a cell that can take on multiple roles. Cardiovasc Res. 2012.

Lai CF, Seshadri V, Huang K, Shao JS, Cai J, Vattikuti R, Schumacher A, Loewy AP, Denhardt DT, Rittling SR, Towler DA. An osteopontin-NADPH oxidase signaling cascade promotes pro-matrix metalloproteinase 9 activation in aortic mesenchymal cells. Circ Res. 2006. 98:1479–1489

Laliberte RE, Perregaux DG, Hoth LR, Rosner PJ, Jordan CK, Peese KM, Eggler JF, Dombroski MA, Geoghegan KF, Gabel CA. Glutathione s-transferase omega 1-1 is a target of cytokine release inhibitory drugs and may be responsible for their effect on interleukin-1beta posttranslational processing. J Biol Chem. 2003. 9;278(19):16567-78. Epub 2003 Mar 6.

Larbi A, Fulop T, Pawelec G. Immune receptor signaling, aging and autoimmunity. Adv Exp Med Biol. 2008. 640:312–324

Lavrik I N, Mock T, Golks A, Hoffmann J C, Baumann S, Krammer P H. CD95 stimulation results in the formation of a novel death effector domain protein-containing complex. J Biol Chem. 2008. 283:26401–26408

Lee HY1, Després JP, Koh KK. Perivascular adipose tissue in the pathogenesis of cardiovascular disease. Atherosclerosis. 2013. 230(2):177-84.

Lehman SJ, Massaro JM, Schlett CL, O'Donnell CJ, Hoffmann U, Fox CS. Peri-aortic fat, cardiovascular disease risk factors, and aortic calcification: the Framingham Heart Study. Atherosclerosis. 2010. 210:656–661

Lengner CJ, Steinman HA, Gagnon J, Smith TW, Henderson JE, Kream BE. Osteoblast differentiation and skeletal development are regulated by Mdm2-p53 signaling. J Cell Biol. 2006. 172:909–921

Lepage, Marcoux M and Tremblay A. Serum osteocalcin or bone Gla-protein, a biochemical marker for bone metabolism in horses: differences in serum levels with age. Can J Vet Res. 1990. 54(2): 223–226.

Lepidi S, Kenagy RD, Raines EW, Chiu ES, Chait A, Ross R, Clowes AW. MMP9 production by human monocyte-derived macrophages is decreased on polymerized type I collagen. J Vasc Surg. 2001. 34(6):1111-8

Li KL, Chen J, Li ZH, Zhao L, He YN. p53 negatively regulates the osteogenic differentiation of vascular smooth muscle cells in mice with chronic kidney disease. Cardiovasc J Afr. 2012. 12;23(6):e1-9.

Lin TC, Li CY, Tsai CS, Ku CH, Wu CT, Wong CS, Ho ST. Neutrophil-mediated secretion and activation of matrix metalloproteinase-9 during cardiac surgery with cardiopulmonary bypass. Anesth Analg. 2005. 100(6):1554-60.

Lindsey ML, Zouein FA, Tian Y, Padmanabhan Iyer R, de Castro Brás LE. Osteopontin is proteolytically processed by matrix metalloproteinase 9. Can J Physiol Pharmacol. 2015. 93(10):879-86.

Liou YM, L.Y. Chang, J.M. Liaw, M.J. Jiang Osteopontin gene expression in the aorta and the heart of propylthiouracil-induced hypothyroid mice. 2005

Liu C, Li XX, Gao W, Liu W, Liu DS. Progranulin-derived Atsttrin directly binds to TNFRSF25 (DR3) and inhibits TNF-like ligand 1A (TL1A) activity. PLoS One. 2014. 20;9(3):e92743.

Liu T, Lin J, Ju T, Chu L, Zhang L. Vascular smooth muscle cell differentiation to an osteogenic phenotype involves matrix metalloproteinase-2 modulation by homocysteine. Mol Cell Biochem. 2015. 406(1-2):139-49.

Liuzzo G, Biasucci LM, Gallimore JR, Caligiuri G, Buffon A, Rebuzzi AG, Pepys MB, Maseri A. Enhanced inflammatory response in patients with preinfarction unstable angina. J Am Coll Cardiol. 1999. 15;34(6):1696-703.

Lohn M, Dubrovska G, Lauterbach B, Luft FC, Gollasch M, Sharma A. Periadventitial fat releases a vascular relaxing factor. The FASEB Journal. 2002. V16 (9)1057-1063

Lu A, Wu H. Structural mechanisms of inflammasome assembly. FEBS J. 2015. 282(3):435-44.

Lubberts E and van den Berg WB. Cytokines in the Pathogenesis of Rheumatoid Arthritis and Collagen-Induced Arthritis Madame Curie Bioscience Database [Internet]. Austin (TX): Landes Bioscience; 2000-2013. Available from: http://www.ncbi.nlm.nih.gov/books/NBK6288

Lund SA, Giachelli CM, and Scatena M. The role of osteopontin in inflammatory processes. J Cell Commun Signal. 2009. 3(3-4): 311–322.

Luo. Spontaneous calcification of arteries and cartilage in mice lacking matrix GLA protein. Nature. 1997. 386 (6620) pp. 78–81

Ma Z, Wang B, Wang M, Sun X, Tang Y, Li M, Li F, Li X. TL1A increased IL-6 production on fibroblast-like synoviocytes by preferentially activating TNF receptor 2 in rheumatoid arthritis. Cytokine. 2016. 83:92-8.

Man SM, Karki R, Kanneganti TD. AIM2 inflammasome in infection, cancer, and autoimmunity: Role in DNA sensing, inflammation, and innate immunity. Eur J Immunol. 2016. 46(2):269-80.

Mariathasan S, Newton K, Monack DM, Vucic D, French DM, Lee WP, Roose-Girma M, Erickson S, Dixit VM. Differential activation of the inflammasome by caspase-1 adaptors ASC and Ipaf. Nature. 2004. 8;430(6996):213-8.

Marsters SA, Sheridan JP, Donahue CJ, Pitti RM, Gray CL, Goddard AD, Bauer KD, Ashkenazi A. Apo-3, a new member of the tumor necrosis factor receptor family, contains a death domain and activates apoptosis and NF-kappa B. Current Biology. 1996. ***6*** *(12): 1669–76*

Massy ZA, Mentaverri R, Mozar A, Brazier M, Kamel S. The pathophysiology of vascular calcification: are osteoclast-like cells the missing link? Diabetes Metab. 2008. 34 Suppl 1:S16-20.

Martinon F, Burns K, Tschopp J. The inflammasome: a molecular platform triggering activation of inflammatory caspases and processing of proIL-beta. Mol Cell. 2002. 10(2):417-26.

Matsumoto T, Baker DJ, d'Uscio LV, Mozammel G, Katusic ZS, van Deursen JM. Aging-associated vascular phenotype in mutant mice with low levels of BubR1. Stroke. 2007. 38(3):1050-6.

Matulevicius, Rohatgi A ,Khera A, Das SR, Owens A, Ayers CR, Timaran CH, Rosero EB, Drazner MH, Peshock, de Lemos DA. The association between plasma caspase-3, atherosclerosis, and vascular function in the Dallas Heart Study. Apoptosis. 2008. V13 (10) pp 1281–1289.

Meylan, Arianne C. Richard, and Richard M. Siegel TL1A and DR3, a TNF-family ligand-receptor pair that promotes lymphocyte costimulation, mucosal hyperplasia and autoimmune inflammation. Immunol Rev. 2011. 244(1)

McInnes and Schett. Cytokines in the pathogenesis of rheumatoid arthritis. Nat Rev Immunol. 2007. V 7 (6) 429–442

McLaren JE, Calder CJ, McSharry BP, Sexton, K, Salter RC, Singh NN, Wilkinson GWG, Wang ECY, and Ramj DP. The TNF-Like Protein 1A–Death Receptor 3 Pathway Promotes Macrophage Foam Cell Formation In Vitro. J Immunol. 2010. 15; 184(10): 5827–5834

Miao C and Li Z. The role of perivascular adipose tissue in vascular smooth muscle cell growth. Br J Pharmacol. 2012. 165(3): 643–658

*M*ichel JB, Thaunat O, Houard X, Meilhac O, Caligiuri G, Nicoletti A. Topological determinants and consequences of adventitial responses to arterial wall injury. Arterioscler Thromb Vasc Biol 2007. 27:1259-1268

Michel JB, Li Z, Lacolley P. Smooth muscle cells and vascular diseases Cardiovascular research.2012.

Migone TS1, Zhang J, Luo X, Zhuang L, Chen C, Hu B, Hong JS, Perry JW, Chen SF, Zhou JX, Cho YH, Ullrich S, Kanakaraj P, Carrell J, Boyd E, Olsen HS, Hu G, Pukac L, Liu D, Ni J, Kim S, Gentz R, Feng P, Moore PA, Ruben SM, Wei P. TL1A is a TNF-like ligand for DR3 and TR6/DcR3 and functions as a T cell costimulator. Immunity. 2002. 16(3):479-92.

Miller.' Arterial calcification: Conscripted by collagen. Nature Materials 15. 2016, 257-258.

Mills CD. M1 and M2 Macrophages: Oracles of Health and Disease. Crit Rev Immunol. 2012. 32(6):463-88.

Mizobuchi M, Towler D and Slatopolsky E. Vascular Calcification: The Killer of Patients with Chronic Kidney Disease. JASN July 2009. v20 (7) 1453-1464

Moe and Chen NX. Mechanisms of Vascular Calcification in Chronic Kidney Disease. JASN. 2008. V19 (2) 213-216

Moore JP, Vinh A, Tuck KL, Sakkal S, Krishnan SM, Chan CT, Lieu M, Samuel CS, Diep H, Kemp-Harper BK, Tare M, Ricardo SD, Guzik TJ, Sobey CG, Drummond GR. M2 macrophage accumulation in the aortic wall during angiotensin II infusion in mice is associated with fibrosis, elastin loss, and elevated blood pressure. Am J Physiol Heart Circ Physiol. 2015. 309(5):H906-17.

Murray and Wynn TA. Protective and pathogenic functions of macrophage subsets. Nat Rev Immunol. 2011. 14; 11(11): 723–737.

Murshed, Schinke, McKee, Karsenty. Extracellular matrix mineralization is regulated locally; different roles of two gla-containing proteins. The Journal of Cell Biology. 2004. 165 625–630

Nagata S. Apoptosis by death factor. Cell. 1997. 88:355–365

Nagy E, Eriksson P, Yousry M, Caidahl K, Ingelsson E, Hansson GK, Franco-Cereceda A, Bäck M. Valvular osteoclasts in calcification and aortic valve stenosis severity. Int J Cardiol. 2013. 3;168(3):2264-71.

Nakashima K, Zhou X, Kunkel G, Zhang Z, Deng JM, Behringer RR, de Crombrugghe B. The novel zinc finger-containing transcription factor osterix is required for osteoblast differentiation and bone formation. Cell. 2002. 108*:* 17*–29*

National Rheumatoid Arthritis Society. The economic burden of Rheumatoid Arthritis. 2010.

Nava E, Llorens S. The paracrine control of vascular motion. A historical perspective. Pharmacol Res. 2016. 12;113(Pt A):125-145.

Netea MG, van de Veerdonk FL, van der Meer JWM, Dinarello CA and Joosten LAB. Inflammasome-Independent Regulation of IL-1-Family Cytokines. Annual Review of Immunology. 2015 V33;49-77.

Ohsima S, Saeki Y, Mima T, Sasai M, Nishoka K, Nomura S, Kopfs M, Katada Y, Tanaka T, Seumura M and Kishimoto T. Interleukin 6 plays a key role in the development of antigen-induced arthritis (rheumatoid arthritisyproinflammatory cytokine). Proc. Natl. Acad. Sci. USA. 1998. V95 8222–8226.

Olfe, Domanska G, Schuett C and Kiank C.' Different stress-related phenotypes of BALB/c mice from in-house or vendor: alterations of the sympathetic and HPA axis responsiveness. BMC Physiology. 2010. V10 (2).

Orange JS, Levy O, Geha RS. Human disease resulting from gene mutations that interfere with appropriate nuclear factor-kappaB activation. Immunological reviews. 2005. 203:21-37

Ospelt and Gay. Epigenic epidemiology of inflammation and rheumatoid arthritis. 2012

Owen MK, Witzmann FA, McKenney ML, Lai X, Berwick ZC, Moberly SP, Alloosh M, Sturek M, Tune JD. Perivascular adipose tissue potentiates contraction of coronary vascular smooth muscle: influence of obesity. Circulation. 2013. 2;128(1):9-18

Ozaki E, Campbell M and Doyle SL. Targeting the NLRP3 inflammasome in chronic inflammatory diseases: current perspectives. J Inflamm Res. 2015; 8: 15–27.

Paccou J, Brazier M, Mentaverri R, Kamel S, Fardellone P, Massy ZA. Vascular calcification in rheumatoid arthritis: prevalence, pathophysiological aspects and potential targets. Atherosclerosis. 2012. 224(2):283-90.

Paloian NJ, Leaf E and Giachelli C. Osteopontin protects against high phosphate induced nephrocalcinosis and vascular calcification. Kidney International. 2016. V89(5): 1027-1036

Panwar P, Lamour G, Mackenzie NC, Yang H, Ko F, Li H, Brömme D. Changes in Structural-Mechanical Properties and Degradability of Collagen during Aging-associated Modifications. J Biol Chem. 2015. 18;290(38):23291-306.

Park, **Lo Y**, Lin S, Wang L, **Yang JK** and **Wu H.** The Death Domain Superfamily in Intracellular Signaling of Apoptosis and Inflammation. Annu Rev Immunol. 2007. 25: 561–586.

Permana PA, Menge C, Reaven PD. Macrophage-secreted factors induce adipocyte inflammation and insulin resistance. Biochemical and Biophysical Research Communications. 2006. V341(2)507–514

Perregaux DG, McNiff P, Laliberte R, Hawryluk N, Peurano H, Stam E, Eggler J, Griffiths R, Dombroski MA, Gabel CA. Identification and characterization of a novel class of interleukin-1 post-translational processing inhibitors. J Pharmacol Exp Ther. 2001.299(1):187-97.

Persy V and D'Haese P. Vascular calcification and bone disease: the calcification paradox. Trends Mol Med. 2009. 15:405–416

Peters MJ, van Halm VP, Voskuyl AE, Smulders YM, Boers M, Lems WF, Visser M, Stehouwer CD, Dekker JM, Nijpels G, Heine R, Dijkmans BA, Nurmohamed MT. Does rheumatoid arthritis equal diabetes mellitus as an independent risk factor for cardiovascular disease? A prospective study. Arthritis Rheum. 2009. 15;61(11):1571-9.

Plenge RM. Rheumatoid arthritis genetics: 2009 update. *Curr Rheumatol Rep.* 2009. 11:351-6.

Pobezinskaya, Choksi S, Morgan MJ, and Liu Z. The Adaptor Protein TRADD is Essential for TL1A/DR3 Signaling. J Immunol. 2011. 186(9): 5212–5216.

Porter and Jänicke RU. Emerging roles of caspase-3 in apoptosis cell death and differentiation. 1999

Price PA, Si Chan W, Jolson DM, Williamson MK. The Elastic Lamellae of Devitalized Arteries Calcify When Incubated in Serum: Evidence for a Serum Calcification Factor. Arteriosclerosis, Thrombosis, and Vascular Biology. 2006. 26:1079–1085

Proudfoot D and Shanahan CM. Biology of calcification in vascular cells: intima versus media. Herz. 2001. 26(4):245-51.

Raffetto JD, Khalil RA. Matrix metalloproteinases and their inhibitors in vascular remodeling and vascular disease. Biochem Pharmacol. 2008. 15;75(2):346-59.

Rashid T, Jayakumar KS, Binder A, Ellis S, Cunningham P, Ebringer A. Rheumatoid arthritis patients have elevated antibodies to cross-reactive and non cross-reactive antigens from Proteus microbes. Clin Exp Rheumatol. 2007. 25(2):259-67.

Reinholt, Hultenby K, Oldberg A, Heinegård D. Osteopontin – a possible anchor of osteoclasts to bone. Proceedings of the National Academy of Sciences of the United States of America. 1990. V87(12) 4473–4475

Reynolds SL, Williams AS, Williams H, Smale S, Stephenson HJ, Amos N, George SJ, O'Donnell VB and Lang D. Contractile, but not endothelial, dysfunction in early inflammatory arthritis a possible role for matrixmetalloproteinase-9. British Journal of Pharmacology. 2012.167(3): 505–514.

Rodriguez KJ, Piechura LM, Porras AM, Masters KS. Manipulation of valve composition to elucidate the role of collagen in aortic valve calcification. BMC Cardiovasc Disord. 2014. 1;14:29.

Ruan C, Ge Q, Li Y, Li X, Chen D, Ji K, Wu Y, Sheng L, Yan C, Zhu D, Gao P. Complement-Mediated Macrophage Polarization in Perivascular Adipose Tissue Contributes to Vascular Injury in Deoxycorticosterone Acetate–Salt Mice. Biol. 2015. 35:598-606.

Sattar N, McCarey DW, Capell H, McInnes IB: Explaining how "high-grade" systemic inflammation accelerates vascular risk in rheumatoid arthritis. Circulation. 2003. 108:2957–2963.

Sausbier M, Schubert R, Voigt V, Hirneiss C, Pfeifer A, Korth M, Kleppisch T, Ruth P, Hofmann F. Mechanisms of NO/cGMP-Dependent Vasorelaxation. Circulation Research. 2000. 87: 825-830

Scatena, Liaw L, Giachelli CM. Osteopontin: a multifunctional molecule regulating chronic inflammation and vascular disease. Arteriosclerosis, Thrombosis, and Vascular Biology. 2007. V27 (11) 2302–2309

Schafer C, Heiss A, Schwarz A, Westenfeld R, Ketteler M, Floege J, Muller-Esterl W, Schinke T, Jahnen-Dechent W. The serum protein alpha 2-Heremans-Schmid glycoprotein/fetuin-A is a systemically acting inhibitor of ectopic calcification. The Journal of Clinical Investigation. 2003. 112; 357-366.

Schiwon M, Weisheit C, Franken L, Gutweiler S, Dixit A, Thiebes S, Quast T, Fuhrmann M, Opdenakker G, Bernhagen J, Bucala R, Panzer U, Kolanus W, Gröne H, Knolle PA, Kurts C and Engel DR. Crosstalk between Sentinel and Helper Macrophages Permits Neutrophil Migration into Infected Uroepithelium. Cell. 2014. V156(3) 456-468.

Schneider P, Holler N, Bodmer J L, Hahne M, Frei K, Fontana A, Tschopp J. Conversion of membrane-bound Fas(CD95) ligand to its soluble form is associated with downregulation of its proapoptotic activity and loss of liver toxicity. J Exp Med. 1998. 187:1205–1213

Schoppet M and Shanahan CM. Role for alkaline phosphatase as an inducer of vascular calcification in renal failure? Kidney Int. 2008. 73(9):989-91.

Schroeder TM, Jensen ED, Westendorf JJ. Runx2: a master organizer of gene transcription in developing and maturing osteoblasts. Birth Defects Res C Embryo Today. 2005. 75(3):213-25.

Schurgers LJ, Cranenburg EC, Vermeer C. Matrix Gla-protein: the calcification inhibitor in need of vitamin K. Thromb Haemost. 2008. 100(4):593-603.

Scott DL, Coulton BL, Symmons DPM, Popert AJ. Long-term outcome of treating rheumatoid arthritis: results after 20 years. Lancet. 1987. 329 1108–1111.

Scott DL, Wolfe F, Huizinga TW. Rheumatoid arthritis. Lancet. 2010. 25;376(9746):1094-108

Screaton, Xu XN, Olsen AL. "LARD: a new lymphoid-specific death domain containing receptor regulated by alternative pre-mRNA splicing," Proceedings of the National Academy of Sciences of the United States of America. 1997. V94 (9) 4615–4619.

Seki, Uzuki M, Ohmoto H, Yoshino K, Maeda S, Kokubun S, Sakurai M, Sawai T. Matrix metalloproteinase 9 (MMP-9) in patients with rheumatoid arthritis. Japanese Journal of Rheumatology. 1997. V7(3)197–209

Shanahan CM, Weissberg PL and Metcalfe JC. Isolation of gene markers of differentiated and proliferating vascular smooth muscle cells. Circulation Research. 1993. 73:193-204.

Shanahan CM, Crouthamel MH, Kapustin A, Giachelli CM. Arterial calcification in chronic kidney disease: key roles for calcium and phosphate. Circulation Res. 2011. 2;109(6):697-711.

Shao, Cheng SL, Sadhu J, and Towler DA. Inflammation and the Osteogenic Regulation of Vascular Calcification: A Review. Perspective Hypertension. 2010. 55(3): 579–592.

Sharif SA, Du X, Myles T, Song JJ, Price E, Lee DM, Goodman SB, Nagashima M, Morser J, Robinson WH, Leung L . Thrombin-activatable carboxypeptidase B cleavage of osteopontin regulates neutrophil survival and synoviocyte binding in rheumatoid arthritis. Arthritis Rheum. 2009. 60:2902–2912

Sharma N, Jha S. NLR-regulated pathways in cancer: opportunities and obstacles for therapeutic interventions. Cell Mol Life Sci. 2016. 73(9):1741-64.

Shaw PJ, McDermott MF, and Kanneganti TD. Inflammasomes and autoimmunity. Trends Mol Med. 2011. 17(2): 57–64.

Shawky A. Atherosclerosis. 2015. Avaliable at http://slideplayer.com/slide/8073072/

Shih DQ, Barrett R, Zhang X, Yeager N, Koon HW, Phaosawasdi P, Song Y, Ko B, Wong MH, Michelsen KS, Martins G, Pothoulakis C, Targan SR. Constitutive TL1A (TNFSF15) expression on lymphoid or myeloid cells leads to mild intestinal inflammation and fibrosis. PLoS One. 2011. 11;6(1):e16090.

Shih, Zheng L, Zhang X, Zhang H, Kanazawa Y, Ichikawa R, Wallace KL, Chen, J, Pothoulakis C, Koon HW and Targan SR. Inhibition of a novel fibrogenic factor Tl1a reverses established colonic fibrosis. Mucosal Immunol. 2014. 7(6):1492-503

Shirai, Hilhorst M, Harrison DA, Goronzy JJ, and Weyand CM. Macrophages in Vascular Inflammation – From Atherosclerosis to Vasculitis Autoimmunity. 2015. 48(3): 139–151.

Shroff, Long DA and Shanahan CM. Mechanistic Insights into Vascular Calcification in CKD. JASN. 2013. V24 (2)179-189

Simionescu A, Philips K, Vyavahare N. Elastin-derived peptides and TGF-β1 induce osteogenic responses in smooth muscle cells. Biochemical and Biophysical Research Communications. 2005. 334:524–532.

Simonet WS, Lacey DL, Dunstan CR. Osteoprotegerin: a novel secreted protein involved in the regulation of bone density. Cell. 1997. 89:309–319

Singh R. The role of Death Receptor 3 in allergic lung inflammation. PhD Thesis, Cardiff University. 2014.

Smolen JS, Steiner G. Therapeutic strategies for rheumatoid arthritis. Nat Rev Drug Discov. 2003. 2 473-88.

Solomon DH, Goodson NJ, Katz JN, Weinblatt ME, Avorn J, Setoguchi S, Canning C and Schneeweiss S. Patterns of cardiovascular risk in rheumatoid arthritis. Ann Rheum Dis. 2006. 65(12): 1608–1612.

Soltis E and Cassis L. Influence of perivascular adipose tissue on rat aortic smooth muscle responsiveness. Clin. Exp. Hypertens. A. 1991. 13:277–296

Speer MY, McKee MD, Guldberg RE, Liaw L, Yang HY, Tung E, Karensty G, Giachelli CM. Inactivation of ostepontin gene enhances vascular calcification of matrix gla protein deficient mice. Evidence of OPN as an inducible inhibitor of calcification in vivo. J Exp Med. 2002. 196: 1047-1055

Spicer SS, Lewis SE, Tashian RE, Schulte BA. Mice carrying a CAR-2 null allele lack carbonic anhydrase II immunohistochemically and show vascular calcification. Am J Pathol. 1989. 134(4):947-54.

Stanley ER, Chen DM, Lin HS. Induction of macrophage production and proliferation by a purified colony stimulating factor. Nature. 1978. 13;274(5667):168-70.

Stein M, Keshav S, Harris N, Gordon S. Interleukin 4 potently enhances murine macrophage mannose receptor activity: a marker of alternative immunologic macrophage activation. J Exp Med. 1992. 1;176(1):287-92.

Steitz SA, Speer MY, Curinga G, Yang HY, Haynes P, Aebersold R, Schinke T, Karsenty G, Giachelli CM. Smooth muscle cell phenotypic transition associated with calcification: upregulation of Cbfa1 and downregulation of smooth muscle lineage markers. Circ Res. 2001. 7;89(12):1147-54

Steiz SA, Speer M, and Giachelli C. Osteopontin inhibits mineral deposition and promotes regression of ectopic calcification. Am J Path. 2002. 161(6); 2035-2046

Suresh E. Diagnosis of early rheumatoid arthritis: what the non-specialist needs to know. J R Soc Med. 2004. 97(9): 421–424.

Svensson, Jirholt J, Holmdahl R, Jansson L. B cell-deficient mice do not develop type II collagen-induced arthritis (CIA) Clin. Exp. Immunol. 1998. 111;521–526

Szasz T and Webb RC. Perivascular adipose tissue: more than just structural support. Clin Sci (Lond). 2012. 122(1): 1–12.

Takedatsu, Michelsen HKS, Wei B, Landers CJ, Thomas LS, Dhall D, Braun J, and Targan SR. TL1A (TNFSF15) regulates the developmentof chronic colitis by modulating both T-helper 1 and T-helper 17 activation. Gastroenterology. 2008. 135: 552–567.

Takei Y, Tanaka T, Kent KC, Yamanouchi D. Osteoclastogenic Differentiation of Macrophages in the Development of Abdominal Aortic Aneurysms. Arterioscler Thromb Vasc Biol. 2016. 36(9):1962-71.

Takeuchi O, Akira S. Pattern recognition receptors and inflammation. Cell. 2010. 19;140(6):805-20.

Tanaka T, Doi H, Yoshida CA, Shimizu T, Matsui H, Yamazaki M, Akiyama H, Kawai-Kowase K, Iso T, Komori T, Arai M, and Kurabayashi M. Runx2 Represses Myocardin-Mediated Differentiation and Facilitates Osteogenic Conversion of Vascular Smooth Muscle Cells. Mol Cell Biol. 2008.28(3): 1147–1160.

Tang W, Lu Y, Tian QY, Zhang Y, Guo FJ. The growth factor progranulin binds to TNF receptors and is therapeutic against inflammatory arthritis in mice. Science. 2011. 332: 478–484.

Tedgui A, Mallat Z. Cytokines in atherosclerosis: pathogenic and regulatory pathways. Physiol Rev. 2006. 86(2):515-81.

Terato, Hasty KA, Reife RA, Cremer MA, Kang AH, Stuart JM. Induction of arthritis with monoclonal antibodies to collagen. J. Immunol. 1992. 148;2103–2108

Thornberry NA, Bull HG, Calaycay JR, Chapman KT, Howard AD, Kostura MJ, Miller DK, Molineaux SM, Weidner JR, Aunins J. A novel heterodimeric cysteine protease is required for interleukin-1β processing in monocytes. Nature. 1992. 356:768–774

Thornell L, Carlsson L, Li Z, Mericskay M, Paulin D. Null mutation in the desmin gene gives rise to a cardiomyopathy. J Mol Cell Cardiol. 1997. (0)

Tintut Y, Patel J, Parhami F, Demer LL. Tumor necrosis factor-alpha promotes in vitro calcification of vascular cells via the cAMP pathway. Circulation. 2000. 21;102(21):2636-42

Toda N. Age-related changes in endothelial function and blood flow regulation. Pharmacol Ther. 2012. 133(2):159-76.

Towler DA. Oxidation, inflammation, and aortic valve calcification peroxide paves an osteogenic path. J Am Coll Cardiol. 2008. 52:851–854

Tsamis, Krawiec JT and Vorp DA. Elastin and collagen fibre microstructure of the human aorta in ageing and disease: a review. J R Soc Interface. 2013. 6; 10(83).

Udagawa 1990 mac to oc

Urry DW. Neutral Sites for Calcium Ion Binding to Elastin and Collagen: A Charge Neutralization Theory for Calcification and Its Relationship to Atherosclerosis. Proceedings of the National Academy of Sciences. 1971;68:810–814

Usui F, Shirasuna K, Kimura H, Tatsumi K, Kawashima A, Karasawa T, Hida S, Sagara J, Taniguchi S, Takahashi M. Critical role of caspase-1 in vascular inflammation and development of atherosclerosis in Western diet-fed apolipoprotein E-deficient mice. Biochem Biophys Res Commun. 2012. 24;425(2):162-8.

van den Berg WB, Joosten LA, van Lent PL. Murine antigen-induced arthritis. Methods Mol Med. 2007. 136:243-53

Vattikuti R, Towler DA. Osteogenic regulation of vascular calcification: an early perspective. Am J Physiol Endocrinol Metab. 2004. 286(5):E686-96.

Verhagen SN, Buijsrogge MP, Vink A, van Herwerden LA, van der Graaf Y, Visseren FL. Secretion of adipocytokines by perivascular adipose tissue near stenotic and non-stenotic coronary artery segments in patients undergoing cabg. Atherosclerosis. 2014. 233:242–247

Verlohren S., Dubrovska G, Tsang SY, Essin K, Luft FC, Huang Y, Gollasch M. Visceral periadventitial adipose tissue regulates arterial tone of mesenteric arteries. Hypertension. 2004 V44;271–276

Vladimer GI, Marty-Roix R, Ghosh S, Weng D, and Lien E. Inflammasomes and host defenses against bacterial infections. Curr Opin Microbiol. 2013. 16(1): 23–31.

Wada T, McKee MD, Steitz S, Giachelli. CM Calcification of vascular smooth muscle cell cultures: inhibition by osteopontin. Circ Res. 1999. 5;84(2):166-78.

Wallace SM, McEniery CM, Maki-Petaja KM, Booth AD, Cockcroft JR. Isolated systolic hypertension is characterized by increased aortic stiffness and endothelial dysfunction. Hypertension. 2007. 50:228–233

Wang X, Univeristy of Toronto Canada, Thesis. 2006

Wang, Luo J and He S. Induction of MMP-9 release from human dermal fibroblasts by thrombin: involvement of JAK/STAT3 signaling pathway in MMP-9 release BMC. Cell Biology. 2007. **8**:14

Wang,K.-H. Yiu,M.-Y. Mok,G. C. Ooi,P.-L. Khong,K.-F. H. Mak,C.-P. Lau,K.-F. LAM,C.-S. Lau,H.-F. Tse Prevalence and extent of calcification over aorta, coronary and carotid arteries in patients with rheumatoid arthritis. Journal of internal medicine. 2009. 1365-2796

Wang ECY. On death receptor 3 and its ligands…Immunology. 2012. 137(1): 114–116.

Wang ECY, Newton Z, Hayward OA, Clark SR, Collins F, Perks WV, Singh RK, Twohig JP, Williams AS. Regulation of early cartilage destruction in inflammatory arthritis by death receptor 3. Arthritis Rheumatol. 2014. 66(10):2762-72.

Waring P, Müllbacher A. Cell death induced by the Fas/Fas ligand pathway and its role in pathology. Immunol Cell Biol. 1999. 77(4):312-7.

Wayhs R, Zelinger A, Raggi P. High coronary artery calcium scores pose an extremely elevated risk for hard events. J Am Coll Cardiol. 2002; 39: 225–230.

Webster and Crowe SM. Matrix metalloproteinases, their production by monocytes and macrophages and their potential role in HIV-related diseases. Journal of Leukocyte Biology. 2006. V80(5)1052-1066

Weisser SB, McLarren KW, Kuroda E, Sly LM. Generation and characterization of murine alternatively activated macrophages. Methods Mol Biol. 2013. 946:225-39.

Wellen K.E, Hotamisligil GS. Obesity-induced inflammatory changes in adipose tissue. J Clin. Invest. 2003. V112;1785-1788

Wen L, Zhuang L, Luo X, Wei P. TL1A-induced NF-kappaB activation and c-IAP2 production prevent DR3-mediated apoptosis in TF-1 cells. J Biol Chem. 2003. 278:39251–39258

Woessner, J. F. Matrix metalloproteinases and their inhibitors in connective tissue remodeling. FASEB J. 1991. 5, 2145–2154

Wooley PH, Luthra HS, Stuart JM, David CS. Type II collagen-induced arthritis in mice. I. Major histocompatibility complex (I region) linkage and antibody correlates. J Exp Med. 1981. 1;154(3):688-700

World Health Organization. Fact Sheet. June 2015.

http://www.genecards.org/cgi-bin/carddisp.pl?gene=TNFRSF25

Xue M, McKelvey K, Shen K, Minhas N, March L, Park SY, Jackson CJ. Endogenous MMP-9 and not MMP-2 promotes rheumatoid synovial fibroblast survival, inflammation and cartilage degradation. Rheumatology (Oxford). 2014. 53(12):2270-9.

Yabluchanskiy A, Ma Y, Iyer RP, Hall ME, Lindsey ML. Matrix metalloproteinase-9: Many shades of function in cardiovascular disease. Physiology (Bethesda). 2013. 28(6):391-403.

Yuan XJ, Tod ML, Rubin LJ, Blaustein MP. NO hyperpolarizes pulmonary artery smooth muscle cells and decreases the intracellular Ca2+ concentration by activating voltage-gated K+ channels. Proc Natl Acad Sci U S A. 1996. 17;93(19):10489-94.

Zebboudj AF, Shin V, Boström K. Matrix GLA protein and BMP-2 regulate osteoinduction in calcifying vascular cells. J Cell Biochem. 2003. 1;90(4):756-65.

Zhang, Wang X and Fahmi H. "Role of TL1A in the pathogenesis of rheumatoid arthritis," Journal of Immunology. 2009. V183(8)5350–5357, 2009

Ziółkowska H, Okarska-Napierała M, Stelmaszczyk-Emmel A, Górska E, Zachwieja K, Zurowska A, Szczepańska M, Grenda R, Tkaczyk M, Makulska I, Zajączkowska MM, Roszkowska-Blaim M. Serum fibroblast growth factor 23 and calcium-phosphorus metabolism parameters in children with chronic kidney disease - preliminary report. Dev Period Med. 2014. 18(2):194-202.